

AD617064

WL TR-64-64

WL
TR
64-64

A STUDY OF THE BEHAVIOR OF THICK CYLINDRICAL SHELLS

by

Dale R. Carver
Edwin R. Chubbuck
Robert L. Thoms
Louisiana State University
Baton Rouge, La
Contract No. AF 29(601)-5836

TECHNICAL REPORT NO. WL TR-64-64

242-P
22

COPY	OF	
PRINT COPY		\$. 6.00
MICROFICHE		\$. 1.50



Research and Technology Division
AIR FORCE WEAPONS LABORATORY
Air Force Systems Command
Kirtland Air Force Base
New Mexico

JUN 23 1965

April 1965

TISA 2

ARCHIVE COPY

Research and Technology Division
AIR FORCE WEAPONS LABORATORY
Air Force Systems Command
Kirtland Air Force Base
New Mexico

When U. S. Government drawings, specifications, or other data are used for any purpose other than a definitely related Government procurement operation, the Government thereby incurs no responsibility nor any obligation whatsoever, and the fact that the Government may have formulated, furnished, or in any way supplied the said drawings, specifications, or other data, is not to be regarded by implication or otherwise, as in any manner licensing the holder or any other person or corporation, or conveying any rights or permission to manufacture, use, or sell any patented invention that may in any way be related thereto.

This report is made available for study with the understanding that proprietary interests in and relating thereto will not be impaired. In case of apparent conflict or any other questions between the Government's rights and those of others, notify the Judge Advocate, Air Force Systems Command, Andrews Air Force Base, Washington, D. C. 20331.

DDC release to OTS is authorized.

A STUDY OF THE BEHAVIOR OF THICK CYLINDRICAL SHELLS

by

Dale R. Carver
Edwin R. Chubbuck
Robert L. Thoms
Louisiana State University
Baton Rouge, La
Contract AF 29(601)-5836

April 1965

FOREWORD

This is the final report on a study entitled "An Investigation of Thick Shell Behavior," sponsored by the Air Force Weapons Laboratory, Kirtland Air Force Base, New Mexico, under Contract AF 29(601)-5836, Project 5710, Program Element 7.60.06.01.5, and performed by the Engineering Mechanics Department, Louisiana State University, Baton Rouge, Louisiana. This research was funded by the Defense Atomic Support Agency under Subtask 13.158. Inclusive dates of research were 4 February 1963 to 4 February 1964. The report was submitted for publication 11 March 1965 by the project officer, Lt Joe E. Johnson, AFWL (WLDC).

Section I, an analysis of the static and dynamic behavior of thick rings or long cylindrical shells based upon the Winkler theory of curved beams, is primarily the work of Dr. Dale R. Carver, Professor and Head of Engineering Mechanics, and Project Director.

Section II, an analysis of and computer program for the computation of stresses and displacements in statically loaded thick rings based upon the complex variable technique of the theory of elasticity, is the work of Dr. Edwin R. Chubbuck, Professor of Engineering Mechanics.


Dr. Robert L. Thoms, Associate Professor of Engineering Mechanics, presents in Section III an analysis of capped thick cylindrical shells under radially symmetrical static loads using finite-difference methods and Southwell stress functions.


Mr. David McGill served as checker and did a major portion of the programming.

The cooperation of members of the L.S.U. Computer Center, particularly that of Larry Morton, Jerry Malone, and Byron Haas, is gratefully acknowledged.

This technical report has been reviewed and is approved.


JOE E. JOHNSON
Lt USAF
Project Officer


THOMAS J. LOWRY, JR.
Colonel USAF
Chief, Civil Engineering
Branch


JOHN W. KODIS
Colonel USAF
Chief, Development Division

ABSTRACT

This report describes three approaches to the problem of predicting stresses and displacements in thick cylindrical shells. Section I is an analysis of a ring or segment of an infinitely long thick cylindrical shell based upon the simplifying assumptions of the Winkler curved beam theory. Dynamic loading of thick rings is treated in Chapter 2 of Section I. Section II consists of a static analysis of the thick-walled circular cylinder (or ring) by the elasticity approach developed by N. I. Muskhelishvili. Shear and radial stresses on the inner boundary, outer boundary, or both boundaries constitute the loading. A rather complete theoretical development is followed by a computer program and instructions for its use. Section III presents an analysis of static stresses in axially loaded thick-walled cylinders with end caps. This axisymmetric elasticity problem is solved by finite difference techniques and Southwell stress functions. Cylinders with one end closed by either a flat or a hemispherical cap are analyzed and an example worked for each case. Cylinders with both ends capped are analyzed in the final portion of the report.

This page intentionally left blank.

CONTENTS

SECTION I

A STUDY OF THE BEHAVIOR OF THICK CYLINDRICAL SHELLS USING WINKLER CURVED BEAM THEORY

	<u>PAGE</u>
STATIC LOADING	
General	1
The Strain Energy Expression	3
The Equations of Equilibrium	6
Complete Ring with Radial Loads	8
The Complete Ring with Tangential Loads	12
Example Problems	18
Radial Displacements due to Radial Loads	20
Computer Program for Radial Displacements due to Radial Loads	23
Radial Displacements due to Tangential Loads	24
Computer Program for Radial Displacements due to Tangential Loads	27
DYNAMIC LOADING	30
Free Vibrations	32
Generalized Coordinates and the Lagrangian	34

Contents (cont'd)

	<u>PAGE</u>
Generalized Forces	36
Applications	38
REFERENCES	44
 SECTION II 	
STRESSES AND DISPLACEMENTS IN A CIRCULAR CYLINDER FOR DISTRIBUTED LOADS APPLIED PERPENDICULARLY TO CYLINDER AXIS	
INTRODUCTION	45
THEORETICAL DEVELOPMENT	
FUNDAMENTAL EQUATIONS	47
SERIES SOLUTION FOR STRESSES AND DISPLACEMENTS	50
REPRESENTATION OF σ_r AND $\tau_{r\theta}$ ON BOUNDARIES BY COMPLEX FOURIER SERIES	67
REPRESENTATION OF COEFFICIENTS OF $\phi(z)$ AND $\psi(z)$ IN TERMS OF LOADING COEFFICIENTS	77
FINAL EXPRESSIONS FOR STRESSES AND DISPLACEMENTS USING NO NEGATIVE SUBSCRIPTS	82
THE COMPUTER PROGRAM AND ITS USE	
GENERAL	93
THE PROGRAM PROPER	94
INPUT PARAMETERS AND DATA	115

Contents (Cont'd)

	<u>PAGE</u>
OUTPUT RESULTS	122
EXAMPLE PROBLEM	125
REFERENCES	132
 SECTION III 	
STRESSES IN THICK-WALLED CYLINDERS WITH CAPPED ENDS	
Introduction	133
THE FINITE DIFFERENCE METHOD AND SOUTHWELL STRESS FUNCTIONS	
Difference Equations in Cylindrical Coordinates	135
Boundary Conditions for Cylindrical Regions	137
Conditions on the Axis of Revolution	138
Difference Equations in Spherical Coordinates	140
Juncture of Cylindrical and Hemispherical Regions	141
APPLICATIONS TO CYLINDERS WITH ONE END CAPPED	
Cylinder with a Flat Cap	144
Cylinder with a Hemispherical Cap	147
ANALYSIS OF CYLINDERS WITH BOTH ENDS CAPPED	
Cavities in Axisymmetric Solids	151
Determination of Ψ on an Inner Boundary	151
Summary	155
REFERENCES	156

Contents (Cont'd)

	<u>PAGE</u>
APPENDIX A--DEVELOPMENT OF FINITE DIFFERENCE EQUATIONS FOR SOUTHWELL STRESS FUNCTIONS IN SPHERICAL COORDINATES	157
APPENDIX B--COMPUTER PROGRAMS	167

LIST OF TABLES

<u>TABLE</u>		<u>PAGE</u>
I	INFLUENCE TABLE FOR MOMENT, SHEAR AND THRUST DUE TO RADIAL LOADS	11
	INFLUENCE TABLES FOR MOMENT, SHEAR AND THRUST DUE TO TANGENTIAL LOADS	
II	M, N, and Q at $\theta = +0$ Due to T at α . $h/a = 1/3$	14
III	M, N, and Q at $\theta = +0$ Due to T at α . $h/a = 1/4$	15
IV	M, N, and Q at $\theta = +0$ Due to T at α . $h/a = 1/5$	16
V	M, N, and Q at $\theta = +0$ Due to T at α . $h/a = 1/8$	17

SYMBOLS

Section I

A	area of ring cross section
α	an angle
a	radius of the centroidal surface
β	an angle
c	distance from the centroidal surface to the outer surface
ϵ	an infinitesimal quantity
E	Young's modulus
e_{θ}	tangential strain
E_k	kinetic energy
F_n, \bar{F}_n	generalized forces
h	thickness of ring
i	integer subscript
I	moment of inertia of cross section with respect to the centroidal axis
I'	$I' = I/a^2 A$
J	the third moment of the cross section with respect to the centroidal axis
J'	$J' = J/a^3 A$
M	bending moment

n	integer denoting mode of vibration
η	a virtual displacement
N	force normal to a cross section
p	dimensionless circular frequency; ω , the circular frequency equals $\frac{p}{a} e/p$
q_n, \bar{q}_n	generalized coordinates
R	radial force
R_0	outer radius
R_i	inner radius
ρ	mass per unit volume
$T, t(\theta)$	tangential loads
t	time
μ	Poisson's ratio
v	tangential displacement of centroidal surface
$v(z)$	tangential displacement of particle a distance z from centroidal surface
V	strain energy
w	radial displacement of centroidal surface
$w(z)$	radial displacement of a particle z distance from the centroidal surface. $w(z)$ assumed equal to w .
ω	circular frequency
x, y, z	rectangular coordinates

Section II

A_k	real constants
A'_k	$=\eta_k+i\zeta_k$ = complex Fourier coefficient determined by loading an inner boundary
A''_k	$=\rho_k+i\nu_k$ = complex Fourier coefficient determined by loading on outer boundary
\underline{A}'_k	$= A'_k$ for negative k
\underline{A}''_k	$= A''_k$ for negative k
$a_k = \alpha_k + i\beta_k$	complex constants
$a'_k = \gamma_k + i\delta_k$	complex constants
\bar{a}_{-1}	complex conjugate of a_{-1}
\underline{a}_k	a_k for negative $k = \underline{\alpha}_k + i\underline{\beta}_k$
α'_{-k}	α'_k for negative $k = \underline{\gamma}_k + i\underline{\delta}_k$
α_k	real part of a_k
$\underline{\alpha}_k$	α_k for negative k
β_k	imaginary part of a_k
$\underline{\beta}_k$	β_k for negative k
∇^4	biharmonic operator
δ_k	imaginary part of a'_k
$\underline{\delta}_k$	δ_k for negative k
η_k	real part of A_k
$\underline{\eta}_k$	η_k for negative k
e	base for natural logarithms

γ_k, γ'_k	complex constants
$\bar{\gamma}'$	complex conjugate of γ'
γ_k	real part of a'_k
$\underline{\gamma}_k$	γ_k for negative k
i	$\sqrt{-1}$
Im	imaginary part of
κ	a Lamé' constant = $3-4\sigma$ for plane stress or $\frac{3-\sigma}{1+\sigma}$ for plane strain
L_1	inner boundary
L_2	outer boundary
m	number of interior holes
M	one less than number of equal subdivisions of circle for theoretical part; for computer part $M =$ number equal subdivisions
μ	a Lamé' constant = shear modulus; same as G in engineering usage
n	division point number
ν_k	imaginary part of A'_k
$\underline{\nu}_k$	ν_k for negative k
$\phi(z), \psi(z)$	undetermined stress functions of complex variable z
$\bar{\phi}(z)$	complex conjugate of $\phi(z)$
$\phi'(z)$	$\frac{d\phi(z)}{dz}$

$\varphi(z)$	$\int \phi(z) dz$
$\varphi'(z)$	$\frac{d\varphi(z)}{dz} = \phi(z)$
$\bar{\varphi}'(z)$	complex conjugate of $\varphi'(z)$
$\psi(z)$	$\int \Psi(z) dz$
$\varphi^*(z), \psi^*(z)$	holomorphic (analytic) functions of z
ρ_k	real part of A_k''
$\underline{\rho}_k$	ρ_k for negative k
R_1	radius of inner boundary
R_2	radius of outer boundary
r	distance from origin; a polar coordinate
Re	real part of
S	region between outer and inner boundaries
σ_r	radial stress
σ_θ	tangential stress
$(\sigma_{r_n})_{L_2}^F$	radial stress on outer boundary (L_2) for "far" point at division point n
$(\sigma_r)_n^{L_2}$	linearly distributed radial stress on outer (L_2) boundary between θ_n and θ_{n+1}
$\tau_{r\theta}$	shear stress
θ	angle from base line; a polar coordinate
θ_n	θ at division point n
u	radial displacement; + outward

v	tangential displacement; + in direction of increasing θ
$[u+iv]_{L_k}$	increase in $(u+iv)$ from one traverse
z	$= x+iy =$ complex variagle in Cartesian coordinates $= re^{i\theta} =$ complex variable in polar coordinates
\bar{z}	$= x-iy =$ complex conjugate of z in Cartesian coordinates $= re^{-i\theta} =$ complex conjugate of z in polar coordinates
z_k	complex coordinates of any point in k^{th} hole
ζ_k	imaginary part of A'_k
$\underline{\zeta}_k$	ζ_k for negative k

Section III

φ, ψ	Southwell stress functions
(r, z, θ)	cylindrical coordinates
$\sigma_r, \sigma_\theta, \sigma_z, \tau_{zr}$	stresses for cylindrical coordinates
ν	Poisson's ratio
E	Young's modulus of elasticity
n	direction normal to the boundary
s	arc length along the boundary
α	angle between n and the r axis
h	grid spacing
σ_{pr}	boundary stress component in r direction
σ_{pz}	boundary stress component in z direction
(u, v)	displacement in (r, z) directions respectively
(R, Θ, θ)	spherical coordinates

$\sigma_R, \sigma_\theta, \sigma_\theta$ normal stresses for spherical coordinates
 η incremental angle
 h grid spacing along R axis
 $()_{N,S,E,W,P}$ values of functions at nodal points defined by
subscript

SECTION I

A STUDY OF THE BEHAVIOR OF THICK CYLINDRICAL SHELLS USING WINKLER CURVED-BEAM THEORY

CHAPTER 1

STATIC LOADING OF THICK CIRCULAR ARCHES AND SHELLS

Note: The analysis which follows is written to pertain directly to a circular arch with a plane of symmetry and loaded symmetrically such that it deforms in its original plane. The analysis is immediately adaptable to a unit length of a long cylindrical shell undergoing plane strain.

General

In the analysis of curved beams or segments of long cylindrical shells, simplifying assumptions as to the geometry of deformation are ordinarily made. These assumptions allow one to obtain relatively simple expressions for the stresses and deformations resulting from loads. For design purposes the theory has the advantage that the significant quantities, normal force, shearing force and bending moment are easily computed.

The theory, commonly referred to as the Winkler curved-beam theory, is well known. It predicts tangential stresses with remarkable accuracy except in the neighborhoods of concentrated loads¹. There the more powerful methods of the theory of elasticity are necessary to determine the stresses. The advantages in the use of the theory are its simplicity and immediate applicability to design; one disadvantage is that, as in straight-beam theory, radial stresses are completely disregarded.

It is the purpose of this discussion to develop and present in a usable form the portions of the theory of interest to the designer.

We consider first a segment of a ring with constant curvature which is symmetrical with respect to its center plane ($x = 0$) in Fig. 1).

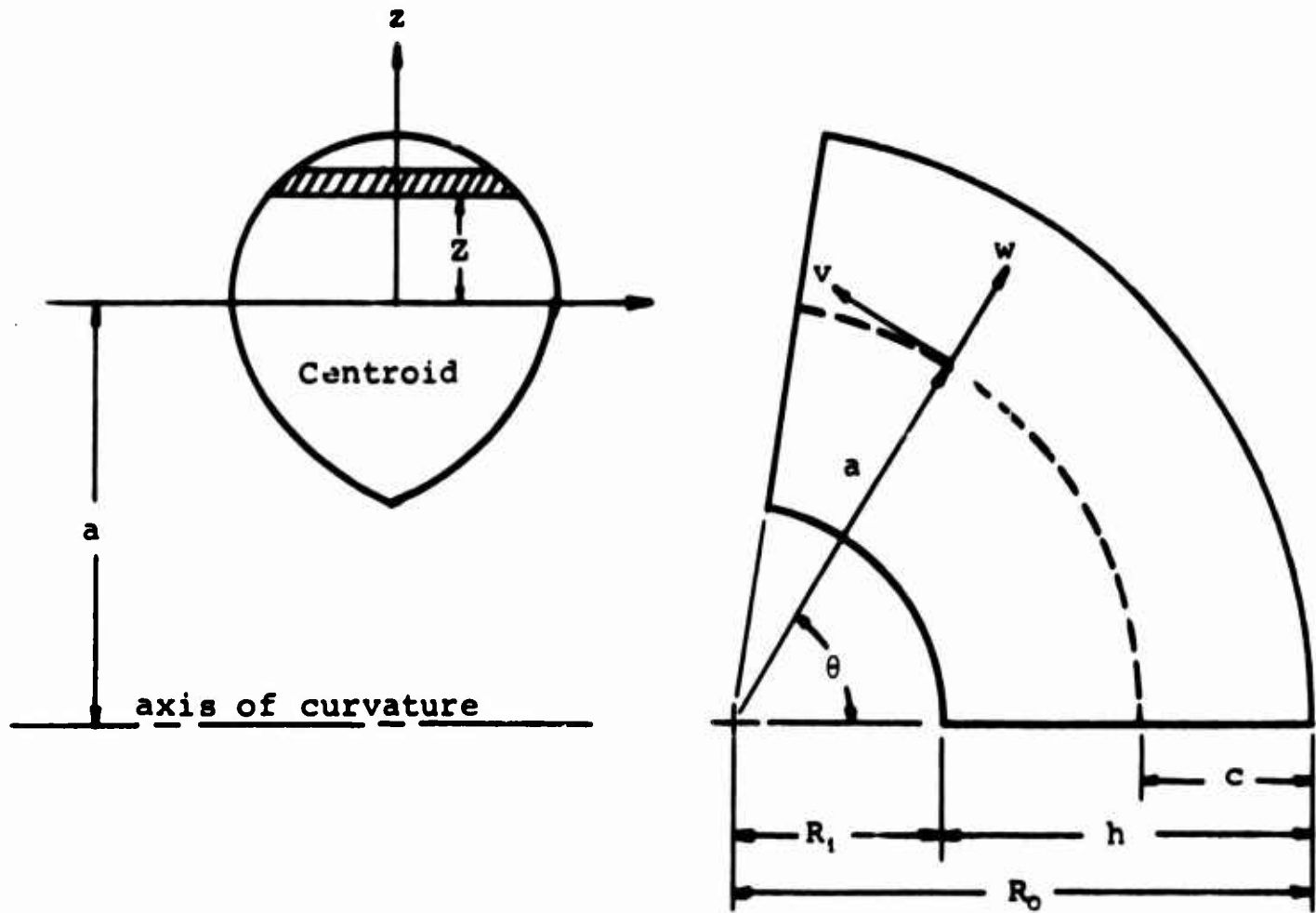


Figure 1. Section of curved beam showing coordinates and dimensions.

The usual assumptions of beam theory are made. Referring to Fig. 1, these are:

- (a) Hooke's law is valid.
- (b) σ_r is negligible.
- (c) The effect of radial strain upon the strain due to bending is negligible.
- (d) Sections normal to the original centroidal surface before deformation are normal to the new centroidal surface after deformation.
- (e) Displacements are small and in the plane of the arch.

The Tangential Strain

The tangential and radial displacement components of particles on the centroidal surface are denoted by v and w respectively. w

is positive in the direction of positive z (outward) and v is positive in the direction of increasing θ . It can be shown² that the assumptions lead to the following expressions for $v(z)$ and e_θ , the tangential displacement of a particle and the tangential strain of an element at a distance z from the centroidal surface:

$$v(z) = \frac{v(a+z)}{a} - \frac{z}{a} \frac{dw}{d\theta} \quad (1-1)$$

$$e_\theta = \frac{1}{a} \frac{dv}{d\theta} - \frac{z}{a(a+z)} \frac{d^2w}{d\theta^2} + \frac{w}{a+z}$$

The radial displacement, $w(z)$, of a particle a distance z from the centroidal surface is taken equal to the radial displacement of the corresponding particle on the centroidal surface; i.e. $w(z) = w$.

The Strain Energy Expression

The strain energy per unit volume is $\frac{1}{2} \sigma_\theta e_\theta$, or, for the arch, $\frac{Ee_\theta^2}{2}$ in which E is Young's modulus. (For the plane strain problem, the strain energy density is $\frac{\sigma_\theta e_\theta}{2}$ or $\frac{Ee_\theta^2}{2(1-\mu^2)}$ in which μ is Poisson's ratio. The strain energy, V , of a portion of the arch which subtends the angle α is

$$V = \frac{E}{2} \int_0^\alpha \int_A e_\theta^2 (a+z) dAd\theta \quad (1-2)$$

Substituting the expression for e_θ from Eq. (1-1) into Eq. (1-2) and integrating over the area,

$$V = \frac{AE}{2a} \int_0^\alpha \left[\left(\frac{dv}{d\theta} + w \right)^2 + Z \left(w + \frac{d^2w}{d\theta^2} \right)^2 \right] d\theta \quad (1-3)$$

In this expression A is the area of the beam cross section and Z , the section constant of curved beam theory, is defined by the equivalent expressions

$$Z = - \frac{1}{A} \int_A \frac{zdA}{a+z} ; Z = \frac{1}{Aa} \int \frac{z^2 dA}{a+z} ; Z = \frac{a}{A} \int \frac{dA}{a+z} - 1 \quad (1-4)$$

The section constant Z is dimensionless and very small. For rings with geometry such that $a \gg z$, the z in the denominator of the second of equation (1-4) can be disregarded in comparison to a and

$$Z \approx I/a^2 A,$$

in which I is the moment of inertia of the cross section with respect to the x axis. Evaluation of Z for a curved beam of rectangular cross section and a mean radius to thickness ratio of 3 reveals that $Z \approx .009$. As the mean radius to thickness ratio increases Z approaches zero.

Equation (1-3) gives the strain energy of a curved beam segment as a function of its configuration as defined by the displacement components v and w of particles on the centroidal surface. These displacements are of course functions of θ ; i.e., $v = v(\theta)$ and $w = w(\theta)$.

For complete rings and statically indeterminate arches it is convenient to have the strain energy expressed as an integral in terms of the normal force $N(\theta)$ and the bending moment $M(\theta)$. In this form Castigliano's theorem may be used to evaluate redundant forces and moments and to compute deflections.

The normal force $N(\theta)$ is defined to be positive when it is tensile and the bending moment $M(\theta)$ is taken as positive when it tends to straighten the arch. Thus

$$N(\theta) = \int_A \sigma_\theta dA = E \int_A e_\theta dA = \frac{EA}{a} \left[\frac{dv}{d\theta} + w + Z \left(w + \frac{d^2 w}{d\theta^2} \right) \right] \quad (1-5)$$

$$M(\theta) = - \int_A \sigma_\theta z dA = - E \int_A e_\theta z dA = AEZ \left(w + \frac{d^2 w}{d\theta^2} \right) \quad (1-6)$$

Expressing Eq. (1-3) in terms of $N(\theta)$ and $M(\theta)$ by means of Eqs. (1-5) and (1-6),

$$v = \frac{1}{2EA} \int_0^\alpha \left\{ a \left[N(\theta) - \frac{M(\theta)}{a} \right]^2 + \frac{M^2(\theta)}{aZ} \right\} d\theta \quad (1-7)$$

As the radius, a , becomes infinite this expression becomes

$$v = \frac{1}{2} \int_0^L \left(\frac{N^2}{AE} + \frac{M^2}{EI} \right) ds,$$

the usual strain energy expression for a loaded straight beam.

The straight beam energy expression is commonly used in arch analysis; equation (1-7) is unquestionably more accurate. Its use is simplified by the fact that the quantity $N(\theta) - \frac{M(\theta)}{a}$ is independent of θ in regions where there are no distributed tangential loads. In the regions between concentrated tangential loads the quantity $N(\theta) - \frac{M(\theta)}{a}$ is a constant. This fact may be verified by statics.

The Equations of Equilibrium

We consider now the portion of a curved beam shown below in Fig. 2. It is loaded at its outer surface by a radial load $q(\theta)$, a tangential load $t(\theta)$ and by the concentrated forces and moment N_e , Q_e and M_e at its free end. The distributed loads are expressed in units of force per unit of arc. The strain energy V and the potential energy of the external loads, Ω , are given below. The total potential energy of the system is designated by U and $U = V + \Omega$. The equilibrium equations are obtained from the principle of stationary potential energy, $\delta U = 0$.

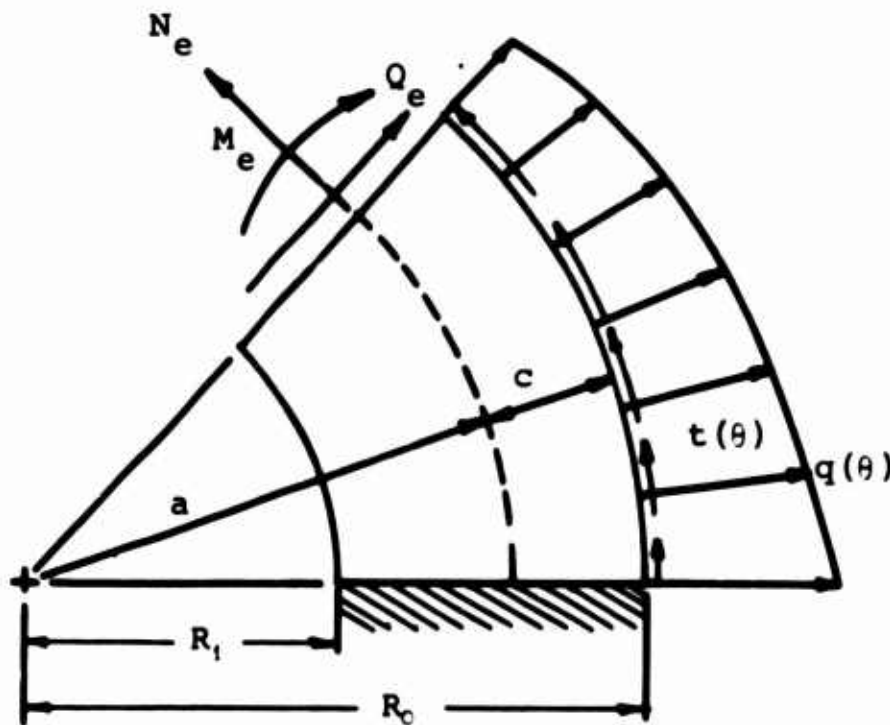


Figure 2. Loaded curved beam section.

$$V = \frac{AE}{2a} \int_0^{\alpha} \left\{ \left(\frac{dv}{d\theta} + w \right)^2 + Z \left(w + \frac{d^2 w}{d\theta^2} \right)^2 \right\} d\theta$$

$$\begin{aligned} \Omega = & - \int_0^{\alpha} \left\{ qw + \frac{R_0}{a} vt - \frac{c}{a} \frac{dw}{d\theta} t \right\} R_0 d\theta - N_e v(\alpha) - Q_e w(\alpha) \\ & - M_e \frac{1}{a} \frac{dw}{d\theta} \Big|_{\theta=\alpha} \end{aligned}$$

$$U = V + \Omega$$

The tangential displacement v is given a virtual displacement $\delta v = \epsilon \eta(\theta)$, consistent with the geometrical boundary conditions, and the corresponding increment in U is computed.

$$\begin{aligned} U + \Delta U = & \frac{AE}{2a} \int_0^{\alpha} \left\{ \left(\frac{dv}{d\theta} + \epsilon \eta' + w \right)^2 + Z \left(w + \frac{d^2 w}{d\theta^2} \right)^2 \right\} d\theta - \int_0^{\alpha} \left\{ qw + \frac{R_0}{a} t (v + \epsilon \eta) \right. \\ & \left. - \frac{c}{a} \frac{dw}{d\theta} t \right\} R_0 d\theta - N_e (v + \epsilon \eta) \Big|_{\theta=\alpha} - Q_e w(\alpha) - M_e \frac{1}{a} \frac{dw}{d\theta} \Big|_{\theta=\alpha} \end{aligned}$$

$$\Delta U = \delta U + O(\epsilon^2)$$

$$\delta U = \frac{AE\epsilon}{a} \int_0^{\alpha} \left(\frac{dv}{d\theta} + w \right) \eta' d\theta - \epsilon \int_0^{\alpha} \frac{R_0^2}{a} t \eta d\theta - N_e \epsilon \eta(\alpha)$$

In this expression and what follows differentiation of η with respect to θ is denoted by η' .

In order for δU to vanish

$$\frac{AE}{a} \left(\frac{d^2 v}{d\theta^2} + \frac{dw}{d\theta} \right) + \frac{R_0^2}{a} t = 0 \quad (1-8)$$

$$\text{and} \quad N_e = \frac{AE}{a} \left(\frac{dv}{d\theta} + w \right) \Big|_{\theta=\alpha} \quad (1-9)$$

The radial displacement w is now varied by $\delta w = \epsilon \eta(\theta)$

$$\begin{aligned}
U + \Delta U &= \frac{AE}{2a} \int_0^\alpha \left\{ \left(\frac{dv}{d\theta} + w + \epsilon \eta \right)^2 + Z \left(w + \epsilon \eta + \frac{d^2 w}{d\theta^2} + \epsilon \eta'' \right)^2 \right\} d\theta \\
&\quad - \int_0^\alpha \left\{ q(w + \epsilon \eta) + \frac{R_0 vt}{a} - \frac{ct}{a} \left(\frac{dw}{d\theta} + \epsilon \eta' \right) \right\} R_0 d\theta \\
&\quad - N_e v(\alpha) - Q_e (w + \epsilon \eta) \Big|_{\theta=\alpha} - \frac{M_e}{a} \left(\frac{dw}{d\theta} + \epsilon \eta' \right) \Big|_{\theta=\alpha}
\end{aligned}$$

$$\begin{aligned}
\delta U &= \frac{AE\epsilon}{a} \int_0^\alpha \left\{ \left(\frac{dv}{d\theta} + w \right) \eta + Z \left(w + \frac{d^2 w}{d\theta^2} \right) \eta + Z \left(w + \frac{d^2 w}{d\theta^2} \right) \eta'' \right\} d\theta \\
&\quad - \int_0^\alpha \left\{ q\epsilon \eta - \frac{ct}{a} \epsilon \eta' \right\} R_0 d\theta - Q_e \epsilon \eta(\alpha) - \frac{M_e}{a} \epsilon \eta'(\alpha)
\end{aligned}$$

For δU to vanish

$$\frac{d^4 w}{d\theta^4} + 2 \frac{d^2 w}{d\theta^2} + w + \frac{1}{Z} \left(\frac{dv}{d\theta} + w \right) - \frac{qR_0 a}{AEZ} - \frac{cR_0}{AEZ} \frac{dt}{d\theta} = 0 \quad (1-10)$$

$$M_e = AEZ \left(w + \frac{d^2 w}{d\theta^2} \right) \Big|_{\theta=\alpha} \quad (1-11)$$

$$Q_e = \frac{ctR_0}{a} \Big|_{\theta=\alpha} - \frac{AEZ}{a} \left(\frac{dw}{d\theta} + \frac{d^3 w}{d\theta^3} \right) \Big|_{\theta=\alpha} \quad (1-12)$$

Equations (1-8) through (1-12) are thus the equilibrium equations and the boundary conditions for the loaded arch.

Equation (1-8) states that

$$\frac{AE}{a} \frac{d}{d\theta} \left(\frac{dv}{d\theta} + w \right) = - \frac{R_0^2 t}{a}$$

If $t \equiv 0$ in a region then $\frac{dv}{d\theta} + w$ is a constant in that region.

From equations (1-5) and (1-6)

$$N(\theta) - \frac{M(\theta)}{a} = \frac{EA}{a} \left(\frac{dv}{d\theta} + w \right)$$

Thus $N(\theta) - \frac{M(\theta)}{a}$ is a constant in regions where there is no tangential load.

Equation (1-9) simply states that the normal force at the end, N_e , equals AE times the strain of the centroidal surface.

The solution to any equilibrium problem of a ring or arch so loaded thus may be obtained by solving for the functions v and w from equations (1-8) and (1-10) subject to the geometrical boundary conditions and the natural boundary conditions given by equations (1-9), (1-11), and (1-12).

The Tangential Stress

Once v and w are known, σ_θ may be computed from $\sigma_\theta = Ee_\theta$ with e_θ given by equation (1-1). It is convenient, however, to have an expression for σ_θ in terms of the normal force and bending moment at any section. $\sigma_\theta = Ee_\theta$ or

$$\begin{aligned}\sigma_\theta &= E \left[\frac{dv}{d\theta} \frac{1}{a} - \frac{z}{a(a+z)} \frac{d^2w}{d\theta^2} + \frac{w}{a+z} \right] \\ &= E \left[\frac{1}{a} \frac{dv}{d\theta} - \frac{z}{a(a+z)} \frac{d^2w}{d\theta^2} + \frac{w}{a+z} - \frac{zw}{a(a+z)} + \frac{zw}{a(a+z)} \right] \\ &= E \left[\frac{1}{a} \frac{dv}{d\theta} + \frac{w}{a} - \frac{z}{a(a+z)} \left(w + \frac{d^2w}{d\theta^2} \right) \right]\end{aligned}$$

From equations (1-5) and (1-6)

$$\sigma_\theta = \frac{1}{A} \left[N(\theta) - \frac{M(\theta)}{a} - \frac{M(\theta)z}{aZ(a+z)} \right] \quad (1-13)$$

The Complete Ring with Radial Loads

We consider now a complete ring loaded at its outer surface by radial and tangential loads whose resultant is zero. Castigliano's theorem and the principle of superposition permit one to determine the normal and shear forces and the bending moment at any section and to analyze deflections.

We consider first the ring shown below loaded by only a concentrated force P at the angle α . P is positive in what follows when as shown.

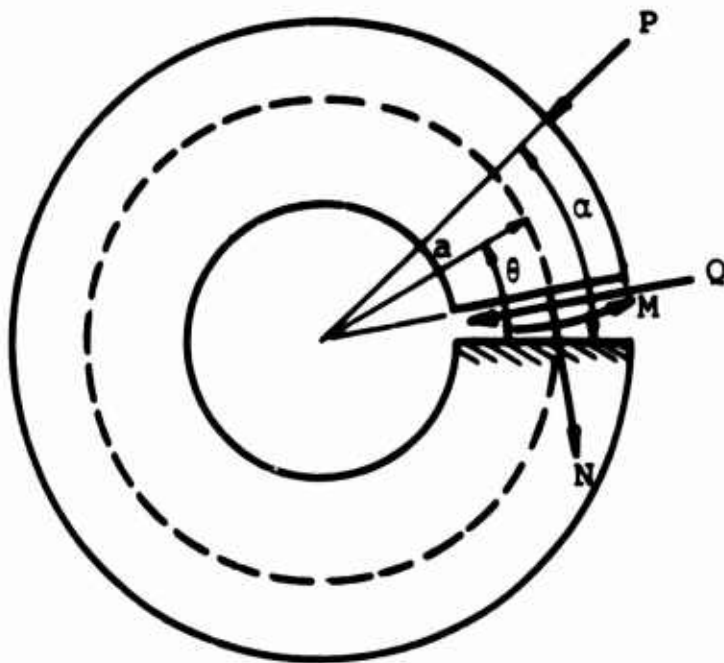


Figure 3. Complete ring fixed at $\theta = 0$ and with radial load at $\theta = \alpha$

The ring is, of course, not in equilibrium under the action of P and, for convenience, we imagine a cross section at $\theta = 0$ to be fixed by external supports. The first problem considered is that of determining the redundant forces and moment N, Q and M at $\theta = +0$ due to P at α . Having these quantities due to a concentrated load at α , they may be determined for any system of concentrated radial loads by superposition. A distributed radial load may be treated by replacing it with an equivalent system of concentrated loads. If the loading system is self equilibrating the external supports required at $\theta = 0$ to maintain equilibrium vanish.

The expressions for $N(\theta)$ and $M(\theta)$ at any angle θ due to P at α are given below.

$$N(\theta) = N \cos \theta - Q \sin \theta \text{ for } 0 < \theta < \alpha$$

$$M(\theta) = M - Na(1 - \cos \theta) - Qa \sin \theta \text{ for } 0 < \theta \leq \alpha$$

$$N(\theta) = N \cos \theta - Q \sin \theta - P \sin(\theta - \alpha) \text{ for } \alpha < \theta \leq 2\pi$$

$$M(\theta) = M - Na(1 - \cos \theta) - Qa \sin \theta - Pa \sin(\theta - \alpha) \\ \text{for } \alpha < \theta \leq 2\pi$$

The strain energy from equation (1-7) is thus

$$V = \frac{1}{2EA} \int_0^\alpha \left\{ a \left(N - \frac{M}{a} \right)^2 + \frac{1}{AZ} [M - Na(1 - \cos \theta) - Qa \sin \theta]^2 \right\} d\theta$$

$$+ \frac{1}{2EA} \int_\alpha^{2\pi} \left\{ a \left(N - \frac{M}{a} \right)^2 + \frac{1}{AZ} [M - Na(1 - \cos \theta) - Qa \sin \theta - Pa \sin(\theta - \alpha)]^2 \right\} d\theta$$

Since there is no displacement or rotation of the cross section upon which M, N and Q act, it follows that

$$\frac{\partial V}{\partial M} = \frac{\partial V}{\partial N} = \frac{\partial V}{\partial Q} = 0$$

Setting these derivatives of V equal to zero and simplifying, one obtains the three influence functions for M, N and Q given below.

$$\frac{M}{Pa} = \left(\frac{\alpha}{2\pi} - 1 \right) \sin \alpha + \frac{(1 - \cos \alpha)}{2\pi(1+Z)}$$

$$\frac{N}{P} = \left(\frac{\alpha}{2\pi} - 1 \right) \sin \alpha \tag{1-14}$$

$$\frac{Q}{P} = -\frac{\sin^3 \alpha}{2\pi} - \left(\pi - \frac{\alpha}{2} + \frac{\sin 2\alpha}{4} \right) \frac{\cos \alpha}{\pi}$$

It is to be noted that N and Q are completely independent of the thickness of the ring. Since Z is very small, M also is essentially unaffected by the thickness to radius ratio. This fact is important since many solutions based on ordinary arch theory exist. They can be used with great accuracy for determining the redundant reactions due to radial loads.

Knowing M, N and Q one may draw complete shear and bending moment diagrams for the ring. Equation (1-13) will give σ_θ at any cross section. Elementary theory is ordinarily used for computing shearing stresses.

To facilitate computation, the table of influence coefficients is presented in Table I which follows.

TABLE I*

M, N, and Q at $\theta = +0$ Due to
P at α

α°	Q/P	N/P	M/Pa
0	-1.00000	.000000	.000000
10	-.985089	-.168825	-.166407
20	-.941922	-.323019	-.313421
30	-.873434	-.458333	-.437011
40	-.783231	-.571367	-.534132
50	-.675431	-.659649	-.602797
60	-.554499	-.721688	-.642110
70	-.425073	-.756975	-.652254
80	-.291797	-.765962	-.634444
90	-.159155	-.750000	-.590845
100	-.031324	-.711250	-.524458
110	.087957	-.652564	-.438975
120	.195501	-.577350	-.338618
130	.288750	-.489417	-.227960
140	.365836	-.392815	-.111740
150	.425604	-.291667	.005320
160	.467617	-.190011	.118700
170	.492123	-.091648	.224244
180	.500000	.000000	.318310
190	.492685	.082001	.397892
200	.472075	.152009	.460721
210	.440421	.208333	.505321
220	.400209	.249973	.531048
230	.354038	.276627	.538085
240	.304499	.288675	.527408
250	.254063	.287128	.500717
260	.204973	.273558	.460350
270	.159155	.250000	.409155
280	.118148	.218846	.350364
290	.083053	.182718	.287439
300	.054499	.144338	.223915
310	.032644	.106395	.163247
320	.017187	.071421	.108656
330	.007409	.041667	.062989
340	.002229	.019001	.028599
350	.000281	.004824	.007241
360	.000000	.000000	.000000

*This table was computed from equations (1-14) with Z set equal to zero.

In the computation of this table, Z was set equal to zero since it is always small in comparison to unity. Unfortunately, when tangential loads are considered, the thickness to radius ratio is of significance and influence tables are necessary for each thickness to radius ratio.

The Complete Ring with Tangential Loads

Referring to Figure (3) and replacing the radial load P at α with a concentrated tangential load T (positive in the direction of increasing θ) at α then

$$N(\theta) = N \cos \theta - Q \sin \theta \text{ for } 0 < \theta < \alpha$$

$$M(\theta) = M - Na(1 - \cos \theta) - Qa \sin \theta \text{ for } 0 < \theta \leq \alpha$$

$$N(\theta) = N \cos \theta - Q \sin \theta - T \cos(\theta - \alpha) \text{ for } \alpha < \theta \leq 2\pi$$

$$M(\theta) = M - Na(1 - \cos \theta) - Qa \sin \theta + Tc + Ta[1 - \cos(\theta - \alpha)] \\ \text{for } \alpha \leq \theta \leq 2\pi$$

The strain energy by equation (1-7) is thus

$$2EAV = \int_0^\alpha \left\{ a \left(N - \frac{M}{a} \right)^2 + \frac{1}{AZ} [M - Na(1 - \cos \theta) - Qa \sin \theta]^2 \right\} d\theta \\ + \int_\alpha^{2\pi} \left\{ a \left[N - \frac{M}{a} - T(1 + c/a) \right]^2 + \frac{1}{AZ} [M - Na(1 - \cos \theta) - Qa \sin \theta \\ + Tc + Ta - Ta \cos(\theta - \alpha)]^2 \right\} d\theta$$

Again, since there is no displacement or rotation of the cross section upon which M, N and Q act

$$\frac{\partial V}{\partial M} = \frac{\partial V}{\partial N} = \frac{\partial V}{\partial Q} = 0.$$

Setting these derivatives of V equal to zero and simplifying

$$\frac{M}{Ta} = \frac{1}{\pi} \left[\frac{Z \sin \alpha}{2(1+Z)} + \frac{c}{a} \sin \alpha + \pi \cos \alpha \right. \\ \left. + \frac{\alpha}{2}(1 - \cos \alpha) - \pi \left(1 + \frac{c}{a}\right) + \frac{c\alpha}{2a} \right]$$

$$\frac{N}{T} = \frac{1}{\pi} \left[\left(\frac{1}{2} + \frac{c}{a} \right) \sin \alpha + (\pi - \alpha/2) \cos \alpha \right] \tag{1-15}$$

$$\frac{Q}{T} = -\frac{1}{\pi} \left(1 + \frac{c}{a}\right) (1 - \cos \alpha) - \left(1 - \frac{a}{2\pi}\right) \sin \alpha$$

The influence tables presented below were computed using $c = \frac{R_0 R_1}{2} = \frac{h}{2}$. Tables are presented for thickness, h , to mean radius, a , ratios of $\frac{1}{3}$, $\frac{1}{4}$, $\frac{1}{5}$, and $\frac{1}{8}$. Linear interpolation may be used with accuracy for intermediate values.

TABLE II

M, N, and Q at $\theta = +0$ Due to
T at α . $h/a = 1/3$

a°	Q/T	N/T	M/Ta
0	.000000	1.000000	-.166667
10	-.174466	.994301	-.167337
20	-.345415	.960066	-.195712
30	-.508086	.899960	-.248320
40	-.658249	.817332	-.321053
50	-.792304	.716071	-.409341
60	-.907369	.600443	-.508326
70	-1.001323	.474925	-.613051
80	-1.072837	.344042	-.718640
90	-1.121362	.212207	-.820464
100	-1.147098	.083570	-.914297
110	-1.150939	-.038105	-.996452
120	-1.134393	-.149557	-1.063881
130	-1.099485	-.248110	-1.114263
140	-1.048656	-.331735	-1.146046
150	-.984637	-.399078	-1.158469
160	-.910338	-.449473	-1.151547
170	-.828729	-.482910	-1.126030
180	-.742723	-.500000	-1.083333
190	-.655081	-.501897	-1.025444
200	-.568318	-.490220	-.954812
210	-.484637	-.466947	-.874223
220	-.405868	-.434310	-.786665
230	-.333441	-.394677	-.695191
240	-.268367	-.350443	-.602785
250	-.211246	-.303915	-.512235
260	-.162290	-.257218	-.426017
270	-.121361	-.212207	-.346203
280	-.088029	-.170394	-.274379
290	-.061630	-.132905	-.211595
300	-.041343	-.100443	-.158341
310	-.026260	-.073284	-.114538
320	-.015461	-.051288	-.079569
330	-.008086	-.033934	-.052322
340	-.003395	-.020374	-.031262
350	-.000818	-.009493	-.014522
360	.000000	.000000	.000000

TABLE III

M, N, and Q at $\theta = +0$ Due to
T at α . $h/a = 1/4$

α°	Q/T	N/T	M/Ta
0	.000000	1.000000	-.125000
10	-.174265	.991998	-.129244
20	-.344615	.955530	-.161119
30	-.506310	.893328	-.217083
40	-.655146	.808807	-.292961
50	-.787567	.705911	-.384121
60	-.900737	.588957	-.485654
70	-.992596	.462462	-.592562
80	-1.061877	.330981	-.699936
90	-1.108099	.198944	-.803129
100	-1.131532	.070509	-.897909
110	-1.133140	-.050568	-.980593
120	-1.114498	-.161043	-1.048154
130	-1.077697	-.258270	-1.098302
140	-1.025233	-.340260	-1.129528
150	-.959888	-.405710	-1.141121
160	-.884612	-.454009	-1.133158
170	-.802405	-.485213	-1.106456
180	-.716197	-.500000	-1.062500
190	-.628756	-.499594	-1.003352
200	-.542592	-.485684	-.931534
210	-.459888	-.460316	-.849904
220	-.382445	-.425785	-.761517
230	-.311653	-.384517	-.669485
240	-.248473	-.338957	-.576846
250	-.193447	-.291452	-.486427
260	-.146724	-.244157	-.400740
270	-.108099	-.198944	-.321871
280	-.077069	-.157333	-.251415
290	-.052904	-.120442	-.190417
300	-.034712	-.088957	-.139346
310	-.021522	-.063124	-.098091
320	-.012358	-.042762	-.065995
330	-.006309	-.027303	-.041892
340	-.002595	-.015838	-.024188
350	-.000617	-.007190	-.010948
360	.000000	.000000	.000000

TABLE IV

M, N, and Q at $\theta = +0$ Due to
T at α . $h/a = 1/5$

α°	Q/T	N/T	M/Ta
0	.000000	1.000000	-.100000
10	-.174144	.990616	-.106373
20	-.344135	.952809	-.140333
30	-.505243	.889350	-.198295
40	-.653284	.803692	-.276047
50	-.784724	.699815	-.368919
60	-.896758	.582065	-.471973
70	-.987360	.454984	-.580184
80	-1.055301	.323144	-.688625
90	-1.100141	.190986	-.792637
100	-1.122192	.062672	-.887986
110	-1.122460	-.058046	-.970992
120	-1.102562	-.167935	-1.038640
130	-1.064624	-.264366	-1.088656
140	-1.011179	-.345375	-1.119558
150	-.945038	-.409689	-1.130667
160	-.869177	-.456730	-1.122094
170	-.786610	-.486595	-1.094695
180	-.700282	-.500000	-1.050000
190	-.612962	-.498213	-.990112
200	-.527157	-.482962	-.917599
210	-.445038	-.456337	-.835359
220	-.368391	-.420670	-.746486
230	-.298580	-.378422	-.654131
240	-.236536	-.332065	-.561360
250	-.182768	-.283974	-.471028
260	-.137384	-.236320	-.385662
270	-.100141	-.190986	-.307363
280	-.070493	-.149496	-.237727
290	-.047668	-.112964	-.177796
300	-.030733	-.082065	-.128027
310	-.018680	-.057028	-.088293
320	-.010496	-.037647	-.057909
330	-.005243	-.023324	-.035679
340	-.002115	-.013116	-.019975
350	-.000496	-.005809	-.008820
360	.000000	.000000	.000000

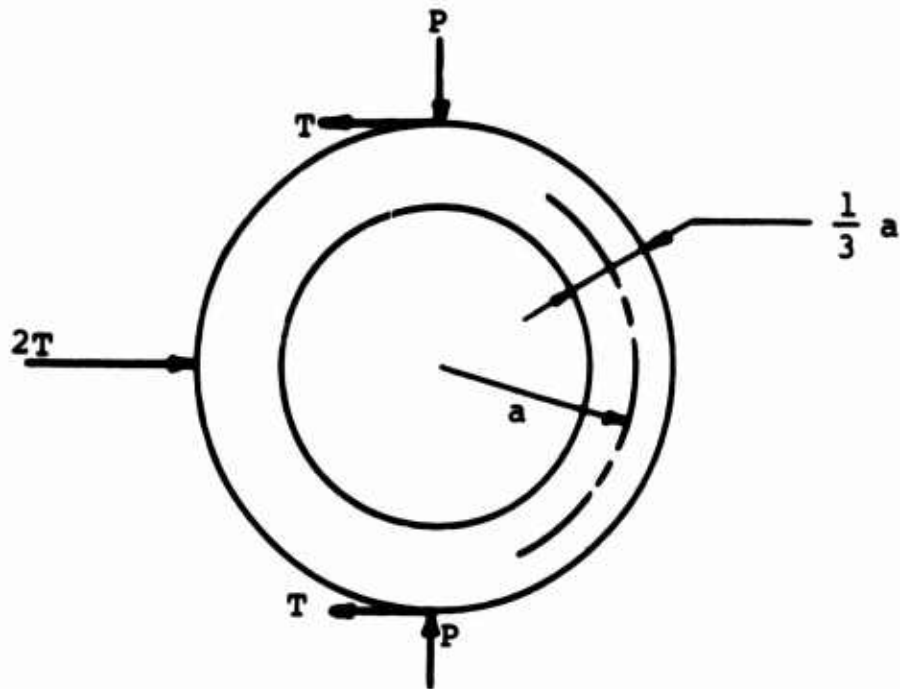
TABLE V

M, N, and Q at $\theta = +0$ Due to
T at α . $h/a = 1/8$

α°	Q/T	N/T	M/Ta
0	.000000	1.000000	-.062500
10	-.173963	.988544	-.072044
20	-.343415	.948726	-.109110
30	-.503644	.883381	-.170051
40	-.650492	.796019	-.250595
50	-.780460	.690671	-.346020
60	-.890790	.571728	-.451341
70	-.979506	.443768	-.561497
80	-1.045437	.311389	-.671533
90	-1.088204	.179049	-.776773
100	-1.108183	.050917	-.872977
110	-1.106441	-.069263	-.956472
120	-1.084657	-.178272	-1.024258
130	-1.045015	-.273510	-1.074090
140	-.990098	-.353048	-1.104523
150	-.922764	-.415657	-1.114922
160	-.846023	-.460813	-1.105454
170	-.762918	-.488668	-1.077033
180	-.676408	-.500000	-1.031250
190	-.589270	-.496140	-.970275
200	-.504003	-.478880	-.896739
210	-.422764	-.450369	-.813603
220	-.347311	-.412997	-.724022
230	-.278970	-.369278	-.631197
240	-.218631	-.321728	-.538242
250	-.166749	-.272757	-.448048
260	-.123375	-.224565	-.363171
270	-.088204	-.179049	-.285727
280	-.060629	-.137741	-.217319
290	-.039814	-.101747	-.158983
300	-.024765	-.071728	-.111159
310	-.014416	-.047884	-.073692
320	-.007704	-.029975	-.045861
330	-.003644	-.017356	-.026424
340	-.001395	-.009033	-.013698
350	-.000315	-.003736	-.005649
360	.000000	.000000	.000000

Example Problems

A. As the first example let us determine the value of M , N and Q at $\theta = 0$ in a ring loaded as shown below:



Ring with concentrated loads

Referring to Table I, M , N and Q due to the load P at 90° are

$$M = -.5908 Pa$$

$$N = -.7500 P$$

$$Q = -.1592 P$$

The values due to $2T$ at 180° are

$$M = 2(.3183) Ta$$

$$N = 2(.0000) T$$

$$Q = 2(.5000) T$$

The values due to P at 270° are

$$M = +.4092 Pa$$

$$N = +.2500 P$$

$$Q = +.1592 P$$

Due to T at 90° from Table II

$$M = -.8205 Ta$$

$$N = +.2122 T$$

$$Q = -1.1214 T$$

Due to -T at 270° from Table II,

$$M = -.3462 (-Ta)$$

$$N = -.2122 (-T)$$

$$Q = -.1214 (-T)$$

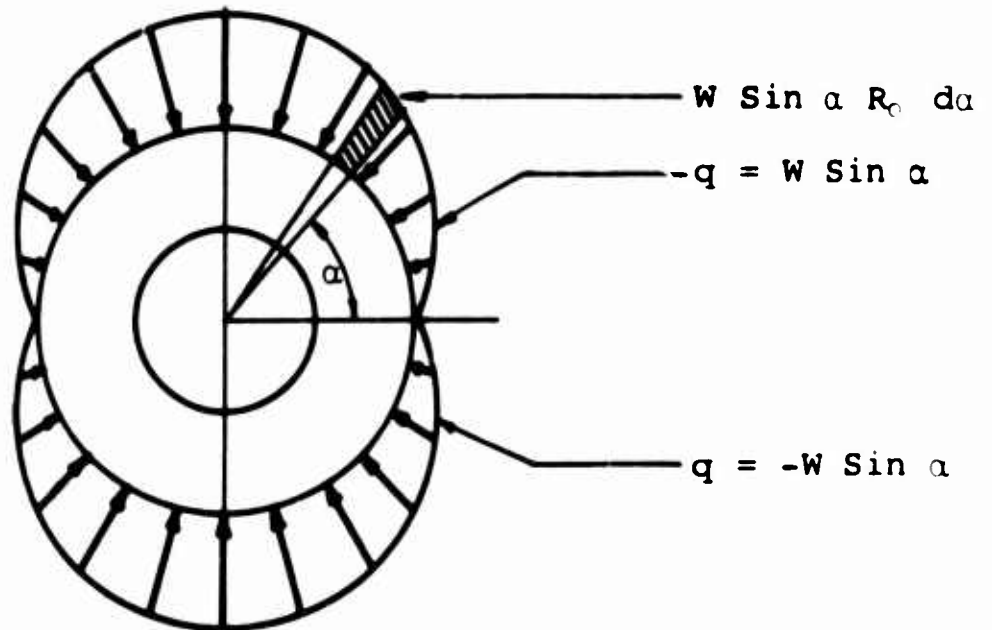
By superposition

$$M = -.1816 Pa + .1623 Ta$$

$$N = -.5P + .4144 T$$

$$Q = 0.$$

B. As a second example, we consider the ring loaded as shown below.



Ring with distributed radial load.

This distributed radial load could be replaced by an equivalent set of concentrated loads and Table I could be used. In this case, however, the loading function is simple and M, N and Q may be easily computed from equations (1-14) by integration. For example, from equation (1-14), neglecting Z,

$$M = Pa \left[\left(\frac{\alpha}{2\pi} - 1 \right) \sin \alpha + \frac{1 - \cos \alpha}{2\pi} \right]$$

Replacing P by $W \sin \alpha R_0 d\alpha$ from 0 to π and by $-W \sin \alpha R_0 d\alpha$ from π to 2π

$$dM = W \sin \alpha R_0 d\alpha a \left[\left(\frac{\alpha}{2\pi} - 1 \right) \sin \alpha + \frac{1 - \cos \alpha}{2\pi} \right]$$

Thus

$$M = WR_0 a \int_0^{\pi} \left[\left(\frac{\alpha}{2\pi} - 1 \right) \sin \alpha + \frac{1 - \cos \alpha}{2\pi} \right] \sin \alpha d\alpha$$

$$- WR_0 a \int_{\pi}^{2\pi} \left[\left(\frac{\alpha}{2\pi} - 1 \right) \sin \alpha + \frac{1 - \cos \alpha}{2\pi} \right] \sin \alpha d\alpha$$

Integrating

$$M = -WR_0 a \left(\frac{\pi}{4} - \frac{2}{\pi} \right).$$

N and Q may be computed in a similar fashion.

Radial Displacements due to Radial Loads

We consider the complete ring shown below, Fig. 4, with a radial load P, taken positive inward as shown, at α , and a concentrated radial load R at β .

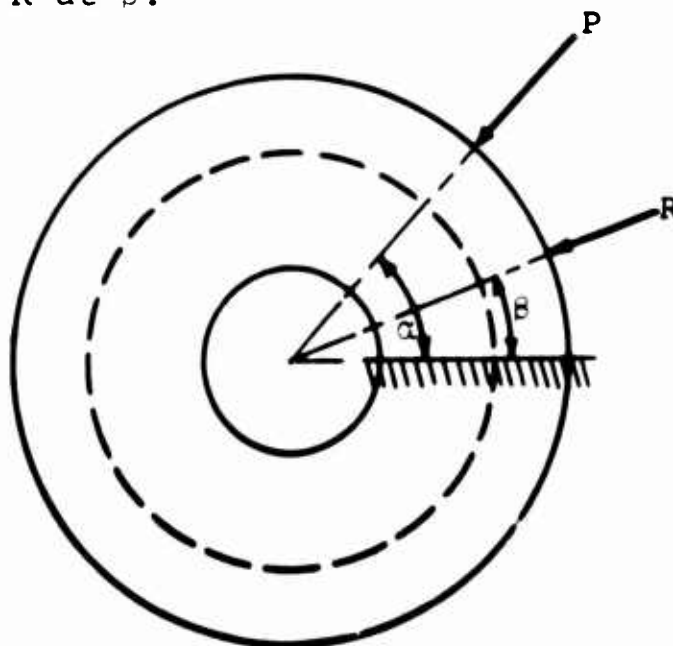


Figure 4. Ring with radial loads at $\theta = \alpha$ and $\theta = \beta$.

M, N and Q are, as before, the redundant reactions at $\theta = +0$.
Then for $\beta \leq \alpha$

$$N(\theta) = N \cos \theta - Q \sin \theta \text{ for } 0 < \theta < \beta$$

$$M(\theta) = M - Na(1 - \cos \theta) - Qa \sin \theta \text{ for } 0 < \theta \leq \beta$$

$$N(\theta) = N \cos \theta - Q \sin \theta - R \sin(\theta - \beta) \text{ for } \beta < \theta < \alpha$$

$$M(\theta) = M - Na(1 - \cos \theta) - Qa \sin \theta - Ra \sin(\theta - \beta) \text{ for } \\ \beta \leq \theta \leq \alpha$$

$$N(\theta) = N \cos \theta - Q \sin \theta - R \sin(\theta - \beta) - P \sin(\theta - \alpha) \text{ for } \\ \alpha < \theta \leq 2\pi$$

$$M(\theta) = M - Na(1 - \cos \theta) - Qa \sin \theta - Ra \sin(\theta - \beta) - Pa \sin(\theta - \alpha) \\ \text{for } \alpha < \theta \leq 2\pi$$

The strain energy is then given by

$$2EAV = \int_0^\beta \left\{ a \left(N - \frac{M}{a} \right)^2 + \frac{1}{AZ} \left[M - Na(1 - \cos \theta) - Qa \sin \theta \right]^2 \right\} d\theta \\ + \int_\beta^\alpha \left\{ a \left(N - \frac{M}{a} \right)^2 + \frac{1}{aZ} \left[M - Na(1 - \cos \theta) - Qa \sin \theta - Ra \sin(\theta - \beta) \right]^2 \right\} d\theta \\ + \int_\alpha^{2\pi} \left\{ a \left(N - \frac{M}{a} \right)^2 + \frac{1}{aZ} \left[M - Na(1 - \cos \theta) - Qa \sin \theta - Ra \sin(\theta - \beta) \right. \right. \\ \left. \left. - Pa \sin(\theta - \alpha) \right]^2 \right\} d\theta$$

The radial deflection, w , at β due to P at α equals $\frac{\partial V}{\partial R} \Big|_{R=0}$;
 $w(\beta, \alpha) = \frac{\partial V}{\partial R} \Big|_{R=0}$.

Performing this differentiation and integration and solving for $\frac{\partial V}{\partial R}$ with R set equal to zero,

$$EAZ w(\beta, \alpha) = (M - Na) (\cos \beta - 1) + (\pi - \beta/2) Na \sin \beta \\ + (\pi - \beta/2) Qa \cos \beta + \frac{Qa}{2} \sin \beta \\ + (\pi - \alpha/2) Pa \cos(\beta - \alpha) + \frac{Pa}{2} \cos \beta \sin \alpha.$$

Substituting for M, N and Q their values from equations (1-14) and simplifying

$$\begin{aligned} \frac{EAZ}{Pa} w(\beta, \alpha) = & \frac{(\cos \alpha - 1)(1 - \cos \beta)}{2\pi(1+Z)} + \frac{\beta}{2\pi} \left(\pi - \frac{\alpha}{2}\right) \cos(\beta - \alpha) \\ & + \frac{\beta}{4\pi} \cos \beta \sin \alpha - \frac{\sin \beta \sin \alpha}{4\pi} - \left(\pi - \frac{\alpha}{2}\right) \frac{\sin \beta \cos \alpha}{2\pi} \end{aligned} \quad (1-16)$$

Equation (1-16) is valid for the radial deflection at β due to a radial load, P, at α with $\beta \leq \alpha$. The computations were repeated for the case in which $\beta \geq \alpha$ and in this case

$$\begin{aligned} \frac{EAZ}{Pa} w(\beta, \alpha) = & \frac{(\cos \beta - 1)(1 - \cos \alpha)}{2\pi(1+Z)} + \frac{\alpha}{2\pi} \left(\pi - \beta/2\right) \cos(\beta - \alpha) \\ & + \frac{\alpha}{4\pi} \cos \alpha \sin \beta - \frac{\sin \beta \sin \alpha}{4\pi} - \left(\pi - \beta/2\right) \frac{\sin \alpha \cos \alpha}{2\pi} \end{aligned} \quad (1-17)$$

Equations (1-16) and (1-17) are the complete influence function for the radial displacement due to radial loads for the entire ring. It is to be noted that $w(\beta, \alpha) = w(\alpha, \beta)$; i.e., if α and β are interchanged in either equation (1-16) or (1-17) the equations become identical. Also, from Fig. 4 it is obvious that $w(\beta, \alpha) = w(2\pi - \beta, 2\pi - \alpha)$.

From equation (1-17) a complete set of influence coefficients with 10° increments and with Z on the right hand side set equal to zero has been computed. By omitting 0° and 360° , this set is a 35 x 35 array, symmetrical with respect to both diagonals.

The following program, written in Fortran II, will generate this matrix. The deflection due to any radial loading may be computed by constructing a column loading matrix and multiplying it by the influence matrix.

```

DIMENSION P(35,35),JJ(35)
DO 1 I=10,180,10
K=I/10
ALPHA=I
ALPHA=ALPHA*.017453293
SA=SINF(ALPHA)
CA=COSF(ALPHA)
IJ=360-I
DO 1 J=I,IJ,10
L=J/10
BETA=J
BETA=BETA*.017453293
SB=SINF(BETA)
CB=COSF(BETA)
COSAB=COSF(ALPHA-BETA)
1 OP(K,L)=- (CB-1.)*(CA-1.)*.15915494+ (.5-BETA*.079577471)*(ALPHA*
1COSAB-SA*CB)+(ALPHA*CA-SA)*SB*.079577471
DO 2 I=1,17
IJ=35-I
K=36-I
DO 2 J=I,IJ
M=36-J
2 P(M,K)=P(I,J)
DO 3 I=2,35
IJ=I-1
DO 3 J=1,IJ
3 P(I,J)=P(J,I)
4 FORMAT(I3,1H0,6X,7F10.6)
5 FORMAT(5H.....)
6 FORMAT(15HBETA . ALPHA ,6(I3,7X),I3)
7 FORMAT(12H ..... )
M1=1
M2=7
DO 9 N=1,5
PUNCH 5
DO 8 I=M1,M2
8 JJ(I)=I*10
PUNCH 6,(JJ(I),I=M1,M2)
PUNCH 7
PUNCH 4,(J,(P(I,J),I=M1,M2),J=1,35)
M1=M2+1
9 M2=M2+7
END

```

Radial Displacements due to Tangential Loads

We now consider the complete ring loaded as shown below in Fig. 5. It carries a concentrated tangential load, T , at the angle α and a concentrated radial load, R , at the angle β with $\alpha \geq \beta$. The radial deflection at β due to T at α equals $\partial V/\partial R$ with R set equal to 0.

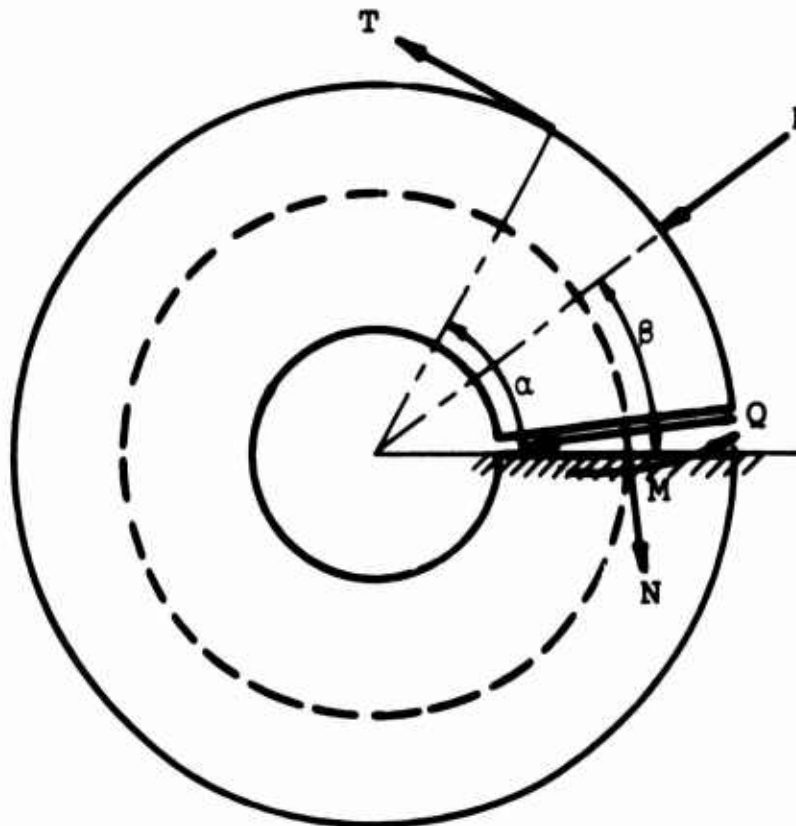


Figure 5. Ring with radial load at β and tangential load at α .

The values of $M(\theta)$ and $N(\theta)$ at any angle θ are as given below.

$$N(\theta) = N \cos \theta - Q \sin \theta \text{ for } 0 < \theta < \beta$$

$$M(\theta) = M - Na(1 - \cos \theta) - Qa \sin \theta \text{ for } 0 < \theta \leq \beta$$

$$N(\theta) = N \cos \theta - Q \sin \theta - R \sin(\theta - \beta) \text{ for } \beta < \theta < \alpha$$

$$M(\theta) = M - Na(1 - \cos \theta) - Qa \sin \theta - Ra \sin(\theta - \beta) \text{ for } \beta \leq \theta \leq \alpha$$

$$N(\theta) = N \cos \theta - Q \sin \theta - R \sin(\theta-\beta) - T \cos(\theta-\alpha) \text{ for } \alpha < \theta \leq 2\pi$$

$$M(\theta) = M - Na(1-\cos\theta) - Qa \sin \theta - Ra \sin(\theta-\beta) + Tc + Ta[1-\cos(\theta-\alpha)] \text{ for } \alpha \leq \theta \leq 2\pi.$$

Then

$$\begin{aligned} 2EAV &= \int_0^\alpha \left\{ a \left(N - \frac{M}{a} \right)^2 + \frac{1}{aZ} \left[M - Na(1-\cos \theta) - Qa \sin \theta \right]^2 \right\} d\theta \\ &+ \int_\alpha^\beta \left\{ a \left(M - \frac{N}{a} \right)^2 + \frac{1}{aZ} \left[M - Na(1-\cos \theta) - Qa \sin \theta - Ra \sin(\theta-\beta) \right]^2 \right\} d\theta \\ &+ \int_\alpha^{2\pi} \left\{ a \left[N - \frac{M}{a} - T \left(1 + \frac{c}{a} \right) \right]^2 + \frac{1}{aZ} \left[M - Na(1-\cos \theta) - Qa \sin \theta \right. \right. \\ &\left. \left. - Ra \sin(\theta-\beta) + Tc + Ta - Ta \cos(\theta-\alpha) \right]^2 \right\} d\theta \end{aligned}$$

Differentiating the above expression for V with respect to R, setting R = 0, substituting the values of M, N and Q from equations (1-15), and simplifying, there results,

$$\begin{aligned} \frac{EAZ}{Ta} \frac{\partial V}{\partial R} \Big|_{R=0} &= \frac{EAZ}{Ta} w(\theta, \alpha) = \left(1 + \frac{c}{a} \right) (1 - \alpha/2\pi) (1 - \cos \beta) \\ &+ \frac{\sin \alpha}{2\pi(1+c/a)} (1 - \cos \beta) + (\pi - \beta/2) \left[\frac{\sin \beta \sin \alpha}{\pi} \left(\frac{1}{2} + c/a \right) \right. \\ &+ \left. (1 - \alpha/2\pi) \sin(\beta - \alpha) - (1 + c/a) (1 - \cos \alpha) \frac{\cos \beta}{\pi} \right] \\ &- (1 + c/a) \left[\frac{\sin \beta}{2\pi} (1 - \cos \alpha) + \cos(\beta - \alpha) - \cos \beta \right] \\ &- (\pi - \alpha/2) \sin(\beta - \alpha) + \frac{\alpha}{4\pi} \sin \beta \sin \alpha. \end{aligned} \tag{1-18}$$

Equation (1-18) is valid for computation of radial deflections at the angle β resulting from a tangential load, T, at the angle α with $\alpha \geq \beta$. The problem was reworked with the loading given in Fig. 5 but with $\beta \geq \alpha$. The final result only is presented here.

$$\begin{aligned}
\frac{EAZ}{Ta} w(\beta, \alpha) = & (\cos \beta - 1) \left[\frac{\alpha}{2\pi} \left(1 + \frac{c}{a}\right) - \frac{\sin \alpha}{2\pi(1+Z)} \right] \\
& - \left(\pi - \frac{\beta}{2}\right) \left[\frac{\cos \beta}{\pi} (1+c/a) (1-\cos \alpha) - \frac{\alpha}{2\pi} \sin(\alpha-\beta) \right] \\
& - \frac{\sin \alpha \sin \beta}{\pi} \left(\frac{1}{2} + c/a\right) - \frac{\sin \beta}{2\pi} (1+c/a) (1-\cos \alpha) \\
& + \frac{\alpha}{4\pi} \sin \beta \sin \alpha \qquad (1-19)
\end{aligned}$$

Equations (1-18) and (1-19) represent the entire influence function for a complete ring carrying tangential loads on its outer surface. In this case $w(\beta, \alpha) \neq w(\alpha, \beta)$ since the radial displacement at β due to a tangential load at α is not equal to the radial displacement at α due to a tangential load at β . There is, however, a different type of symmetry. Consideration of Fig. 5 reveals that $w(\beta, \alpha) = -w(2\pi-\beta, 2\pi-\alpha)$.

The following program, written in Fortran II, will generate a complete set of influence coefficients for radial displacements due to tangential loads for 10° increments. In the program, c was set equal to $h/2$ and h/a may be assigned any value. The matrix is antisymmetrical with respect to its center element, a fact which was used to shorten the program. The value of the radial deflection at each 10° interval may be obtained by constructing a loading column matrix and multiplying it by the influence matrix.

```

DIMENSION P (35, 35) ,JJ (35)
1  READ 8, TOR
   PUNCH 9, TOR
   P (18, 18) = 0.
   CONST = 1. + .5 * TOR
   HALF = (1. + TOR) * .5
   Z = 1. / ((1. / TOR) * LOGF ((2. + TOR) / (2. - TOR)))
   M = 1
   DO 3 I = 10, 340, 10
     IP1 = I + 10
     GO TO 4
2  DO 3 J = IP1, 350, 10
     GO TO 5
3  CONTINUE
     GO TO 6
4  K = I / 10
     I1 = 36 - K
     ALPHA = I
     ALPHA = ALPHA * .017453293
     SA = SIN (ALPHA)
     CA = 1. - COS (ALPHA)
     ALPH2 = ALPHA * .5
     GO TO (2, 5), M
5  L = J / 10
     I2 = 36 - L
     BETA = J
     BETA = BETA * .017453293
     SB = SIN (BETA)
     CB = COS (BETA)
     CB1 = 1. - CB
     CBCA = CB * CA * CONST
     SBSA = SB * SA
     SBMA = SIN (BETA - ALPHA)
     PMB = 3.1415927 - BETA * .5
     OP (K, L) = ((SA * .5 * Z - ALPH2 * CONST) * CB1 + (HALF * SBSA - ALPH2 * SBMA - CBCA) *
     1PMB - (CONST * CA - ALPH2 * SA) * SB * .5) * .31830989
     P (I1, I2) = -P (K, L)
     GO TO (3, 7), M
6  M = 2
     DO 7 I = 10, 170, 10
       J = I
       GO TO 4
7  CONTINUE
8  FORMAT (E15.8)

```

```

9   FORMAT(37HRATIO OF THICKNESS TO MEAN RADIUS IS ,F12.8)
10  FORMAT(5H.....)
11  FORMAT(15HBETA . ALPHA      ,6(I3,7X),I3)
12  FORMAT(12H      ..... )
13  FORMAT(I3,1H0,6X,7F10.6)
    M1=1
    M2=7
    DO 15 N=1,5
    PUNCH 10
    DO 14 I=M1,M2
14  JJ(I)=I*10
    PUNCH 11,(JJ(I),I=M1,M2)
    PUNCH 12
    PUNCH 13,(J,(P(I,J),I=M1,M2),J=1,35)
    M1=M2+1
15  M2=M2+7
    GO TO 1
    END

```

Summary

Deep underground blast-resistant cylindrical structures can be most easily designed by considering static loads which are adjusted by a factor to compensate for dynamic effects. The analysis presented permits one to compute stresses and radial displacements in thick cylindrical shells resulting from any exterior static loading.

CHAPTER 2

DYNAMIC LOADING OF THICK CIRCULAR ARCHES AND SHELLS

Kinetic Energy Expression

The expression for the kinetic energy of an arch segment deforming in its plane is readily obtained by integration. Denoting the kinetic energy by E_k ,

$$E_k = \frac{\rho}{2} \int_0^\alpha \int_A \left\{ \left[\frac{\partial w(z,t)}{\partial t} \right]^2 + \left[\frac{\partial v(z,t)}{\partial t} \right]^2 \right\} (a+z) dA d\theta,$$

in which α is the subtended angle, ρ is the mass per unit volume, and w and v are now functions of time as well as of z .

Substituting for $v(z,t)$ from equation (1-1), letting $w(z,t) = w(t)$ and integrating with respect to z over the area,

$$\begin{aligned} E_k = & \frac{\rho}{2} \int_0^\alpha \left\{ \left[\left(\frac{\partial w}{\partial t} \right)^2 + \left(\frac{\partial v}{\partial t} \right)^2 \right] aA + \frac{I}{a} \left[3 \left(\frac{\partial v}{\partial t} \right)^2 - 4 \frac{\partial v}{\partial t} \cdot \frac{\partial^2 w}{\partial \theta \partial t} + \left(\frac{\partial^2 w}{\partial \theta \partial t} \right)^2 \right] \right. \\ & \left. + \frac{J}{a^2} \left[\left(\frac{\partial v}{\partial t} \right)^2 - 2 \frac{\partial v}{\partial t} \frac{\partial^2 w}{\partial \theta \partial t} + \left(\frac{\partial^2 w}{\partial \theta \partial t} \right)^2 \right] \right\} d\theta \end{aligned} \quad (1-20)$$

In this expression I is the moment of inertia of the cross section with respect to the x axis (Fig. 1), and J is the third moment of the area with respect to the same axis; i.e.,

$$I = \int_A z^2 dA; \quad J = \int_A z^3 dA.$$

J will be zero for cross sections having two axes of symmetry.

Free Vibrations

The equations of motion of a thick circular ring segment deforming in its plane may be obtained readily from Hamilton's principle,

$$\delta \int_0^t (E_k - V) dt = 0.$$

With E_x from equation (1-20) and V from equation (1-3) this becomes

$$\delta \int_0^t \int_0^a \left\{ \frac{\rho a A}{2} \left[\left(\frac{\partial w}{\partial t} \right)^2 + \left(\frac{\partial v}{\partial t} \right)^2 \right] + \frac{\rho I}{2a} \left[3 \left(\frac{\partial v}{\partial t} \right)^2 - 4 \frac{\partial v}{\partial t} \frac{\partial^2 w}{\partial \theta \partial t} + \left(\frac{\partial^2 w}{\partial \theta \partial t} \right)^2 \right] \right. \\ \left. + \frac{\rho J}{2a^2} \left(\frac{\partial v}{\partial t} - \frac{\partial^2 w}{\partial \theta \partial t} \right)^2 - \frac{AE}{2a} \left(\frac{\partial v}{\partial \theta} + w \right)^2 - \frac{AEZ}{2a} \left(w + \frac{\partial^2 w}{\partial \theta^2} \right)^2 \right\} d\theta dt = 0 \quad (1-21)$$

With the notation

$$I' = I/a^2 A \text{ and } J' = J/a^3 A$$

the Euler equations of this integral are

$$(1+3I'+J') \frac{\partial^2 v}{\partial t^2} - (2I'+J') \frac{\partial^3 w}{\partial \theta \partial t^2} - \frac{E}{a^2 \rho} \left(\frac{\partial^2 v}{\partial \theta^2} + \frac{\partial w}{\partial \theta} \right) = 0 \quad (1-22)$$

and

$$\frac{\partial^4 w}{\partial \theta^4} - \frac{\rho a^2}{EZ} (I'+J') \frac{\partial^4 w}{\partial \theta^2 \partial t^2} + 2 \frac{\partial^2 w}{\partial \theta^2} + \frac{\rho a^2}{EZ} \frac{\partial^2 w}{\partial t^2} + w \left(1 + \frac{1}{Z} \right) + \frac{1}{Z} \frac{\partial v}{\partial \theta} \\ + \frac{\rho a^2}{EZ} (2I'+J') \frac{\partial^3 v}{\partial \theta \partial t^2} = 0. \quad (1-23)$$

It should be noted that a solution of equations (1-22) and (1-23) is

$$v = 0$$

$$w = C_1 \sin \frac{t}{a} \sqrt{(1+Z) \frac{E}{\rho}} + C_2 \cos \frac{t}{a} \sqrt{(1+Z) \frac{E}{\rho}} \quad (1-24)$$

in which C_1 and C_2 are arbitrary constants. This solution represents a motion such that the ring remains circular and deforms with time with a circular frequency of

$$\omega_0 = \frac{1}{a} \sqrt{(1+Z) E/\rho}.$$

Thus when $\frac{t}{a} \sqrt{(1+Z) E/\rho}$ increases by an amount of 2π , the ring undergoes one cycle of this motion. The period of this motion is

$$T_0 = \frac{2\pi}{\omega_0} = \frac{2\pi a}{\sqrt{(1+Z) E/\rho}}. \quad (1-25)$$

The duration of a transient load may be conveniently expressed in units of T_0 .

In what follows we will be interested in the complete ring and in motion which is symmetrical at all times to the axis $\theta = 0$; thus we assume the following solution to equations (1-22) and (1-23).

$$w = \text{Cos } n\theta \text{ Sin } \frac{pt}{a} \sqrt{E/\rho} \quad (1-26)$$

$$v = r \text{ Sin } n\theta \text{ Sin } \frac{pt}{a} \sqrt{E/\rho}$$

In equations (1-26) n must be an integer to satisfy the periodicity requirements on v and w , $\frac{p}{a} \sqrt{E/\rho}$ is the circular frequency ω , and r is the ratio of the amplitude of the displacement v to that of w . Substituting equations (1-26) into (1-22) and (1-23)

$$\left[(2I' + J')np^2 - n \right] + r \left[p^2 (1 + 3I' + J') - n^2 \right] = 0 \quad (1-27)$$

$$\left[Z(n^2 - 1)^2 - p^2 + 1 - (I' + J')p^2 n^2 \right] + r \left[n - (2I' + J')p^2 n \right] = 0 \quad (1-28)$$

For equations (1-26) to be a solution to equations (1-22) and (1-23), it is necessary that the determinant of the homogeneous equations (1-27) and (1-28) vanish. Setting this determinant equal to zero yields

$$\begin{aligned} & p^4 \left\{ \frac{n^2}{Z} (I' + J' - I'^2) + (1 + 3I' + J') \cdot \frac{1}{Z} \right\} \\ & - p^2 \left\{ (1 + 3I' + J') \left[(n^2 - 1)^2 + \frac{1}{Z} \right] + \frac{I' + J'}{Z} n^4 - \frac{2}{Z} (2I' + J' - \frac{1}{2}) n^2 \right\} \\ & + n^2 (n^2 - 1)^2 = 0 \end{aligned} \quad (1-29)$$

Equation (1-29) may be used to compute the natural frequencies of vibrations of complete thick rings for each mode, $n=0, 1, 2, \dots, \infty$. For $n=0$ it yields

$$p^2 = 1 + Z$$

the motion described by equations (1-24). For $n=1$ it yields but one value of p^2 ,

$$p^2 = \frac{2}{1 + 4I' + 2J' - I'^2} .$$

For $n \geq 2$, equation (1-29) yields two values of p^2 for each integer n . The higher value represents the dimensionless circular frequency of a deformation which is primarily extensional and the lesser value of p^2 is that of a deformation which is primarily flexural.

Equation (1-29) is rigorously consistent with the Winkler assumptions; it thus includes the effect of "rotary inertia" but not the effect of shearing deformation. Baron³ derived a similar equation for the frequencies of thin rings which accounts for the coupling between the extensional and flexural motions. For thin rings Love⁴ cites the formulas

$$\omega^2 = \frac{AE}{ma^2} (1+n^2)$$

and

$$\omega^2 = \frac{EI}{ma^4} \frac{n^2 (n^2 - 1)^2}{n^2 + 1}$$

for extensional and flexural vibrations respectively. Here ω , A , E , I and n denote the same quantities as in this paper and m is the mass per unit length of centerline. Equation (1-29) includes that of Baron and those cited by Love as special cases.

A review and survey of the implications of the analysis presented is in order. Equations (1-22) and (1-23) are the equations of motion. Solutions of the form of equations (1-26) exist provided equations (1-27) and (1-28) are satisfied. Nontrivial solutions to equations (1-27) and (1-28) exist for each integer value of n provided equation (1-29) is satisfied. For both $n = 0$ and $n = 1$ there is a value of p^2 which satisfies equation (1-29). For $n > 1$ there are two values of p^2 which are roots of equation (1-29). In what follows these two values will be designated as p_n^2 and \bar{p}_n^2 where, arbitrarily, p_n^2 is the lesser and \bar{p}_n^2 is the greater. For each value of p^2 either of equations (1-27) or (1-28) will yield a value of r . For $p^2 = p_n^2$ the value of r will be designated as r_n ; for $p^2 = \bar{p}_n^2$ the value of r will be called \bar{r}_n . For computational purposes the simpler equation for r_n will be used.

$$r_n = \frac{n - (2I' + J')n p_n^2}{p_n^2 (1 + 3I' + J') - n^2} \quad (1-30)$$

In the following analysis, which is meant to pertain to a segment of a long thick cylindrical shell, J' will be set equal to zero and r_n will be given by

$$r_n = \frac{n(1 - 2I' p_n^2)}{p_n^2 (1 + 3I') - n^2}$$

Since the differential equations of motion are linear, solutions may be summed and the resultant normalized expressions for w and v may be written as

$$w = \text{Sin}\bar{\omega}_0 t + \text{Cos}\theta \text{Sin}\bar{\omega}_1 t + \sum_2^{\infty} \text{Cos}n\theta (\text{Sin}\omega_n t + \text{Sin}\bar{\omega}_n t)$$

$$v = \bar{r}_1 \text{Sin}\theta \text{Sin}\bar{\omega}_1 t + \sum_2^{\infty} \text{Sin} n\theta (r_n \text{Sin}\omega_n t - \bar{r}_n \text{Sin}\bar{\omega}_n t).$$

The ω 's in these equations are related to the p 's, of course, by

$$\omega_n = \frac{p_n}{a} \sqrt{E/\rho}$$

and ω_0 and ω_1 are written as $\bar{\omega}_0$ and $\bar{\omega}_1$ so that consistently the $\bar{\omega}_n$'s are the frequencies of the motions which are primarily extensional.

GENERALIZED COORDINATES AND THE LAGRANGIAN FUNCTION

Knowing the modes of vibration and their associated frequencies it is now possible to proceed with the problem of the response of the ring to the time-dependent loads. The generalized coordinates will be designated, following Baron³, by $q_n(t)$ and $\bar{q}_n(t)$ in solutions of the form

$$w = \sum_{n=0}^{\infty} [q_n(t) + \bar{q}_n(t)] \text{Cos} n\theta \tag{1-31}$$

$$v = \sum_{n=1}^{\infty} [r_n q_n(t) + \bar{r}_n \bar{q}_n(t)] \text{Sin} n\theta$$

in which it is understood that $q_0(t) = q_1(t) \equiv 0$.

Substituting the expressions for w and v , equations (1-31), into equation (1-20), letting $\alpha = 2\pi$, and utilizing the orthogonality of the sine cosine set

$$\begin{aligned}
E_k &= \frac{\rho\pi aA}{2} \sum_{n=0}^{\infty} \left\{ [1+r_n^2+3I'r_n^2+4nr_n I'+I'n^2] \left(\frac{\partial q_n}{\partial t}\right)^2 \right. \\
&\quad + 2[1+r_n \bar{r}_n+3r_n \bar{r}_n I'+2(r_n+\bar{r}_n)nI'+I'n^2] \left(\frac{\partial q_n}{\partial t}\right) \left(\frac{\partial \bar{q}_n}{\partial t}\right) \\
&\quad \left. + [1+\bar{r}_n^2+3I'\bar{r}_n^2+4n\bar{r}_n I'+I'n^2] \left(\frac{\partial \bar{q}_n}{\partial t}\right)^2 \right\} \quad (1-32)
\end{aligned}$$

Similarly, from equation (1-3),

$$\begin{aligned}
V &= \frac{EA\pi}{2a} \sum_{n=0}^{\infty} \left\{ [1+n^2 r_n^2+2nr_n+Z(1-n^2)^2] q_n^2 \right. \\
&\quad + 2[1+n^2 r_n \bar{r}_n+(r_n+\bar{r}_n)n+Z(1-n^2)^2] q_n \bar{q}_n \\
&\quad \left. + [1+n^2 \bar{r}_n^2+2n\bar{r}_n+Z(1-n^2)^2] \bar{q}_n^2 \right\} \quad (1-33)
\end{aligned}$$

In equation (1-32) the coefficient of $\frac{\partial q_n}{\partial t} \frac{\partial \bar{q}_n}{\partial t}$ is identically zero. Likewise in equation (1-33), the coefficient of $q_n \bar{q}_n$ is zero. (The proof that these quantities vanish is extremely tedious and is not presented). Thus, in final form,

$$\begin{aligned}
E_k &= \frac{\rho\pi aA}{2} \sum_{n=0}^{\infty} \left\{ [1+r_n^2+3I'r_n^2+4nr_n I'+I'n^2] \left(\frac{\partial q_n}{\partial t}\right)^2 \right. \\
&\quad \left. + [1+\bar{r}_n^2+3I'\bar{r}_n^2+4n\bar{r}_n I'+I'n^2] \left(\frac{\partial \bar{q}_n}{\partial t}\right)^2 \right\} \quad (1-34)
\end{aligned}$$

$$\begin{aligned}
V &= \frac{EA\pi}{2a} \sum_{n=0}^{\infty} [1+n^2 r_n^2+2nr_n+Z(1-n^2)^2] q_n^2 \\
&\quad + [1+n^2 \bar{r}_n^2+2n\bar{r}_n+Z(1-n^2)^2] \bar{q}_n^2 \quad (1-35)
\end{aligned}$$

and L, the Lagrangian function, equals $E_k - V$.

There remains the task of determining the generalized forces corresponding to each q_n and \bar{q}_n . Once this is accomplished, Lagrange's equations may be used to deduce the differential equations which describe each q_n and \bar{q}_n .

GENERALIZED FORCES

The ring shown in Fig. 6 below is considered.

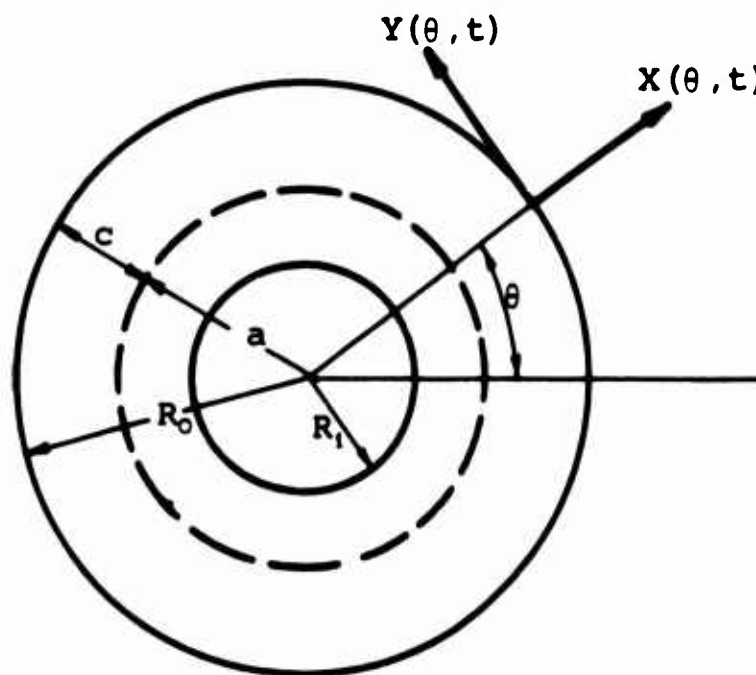


Figure 6. Ring with time-dependent loads.

It is loaded at its outer surface by a radial load, $X(\theta, t)$ and a tangential load $Y(\theta, t)$.

To determine the generalized forces corresponding to q_n and \bar{q}_n , X and Y will first be expanded in even and odd Fourier series, i.e.,

$$X(\theta, t) = \frac{X_0(t)}{r} + \sum_{n=1}^{\infty} X_n(t) \cos n\theta \quad (1-36)$$

$$Y(\theta, t) = \sum_{n=1}^{\infty} Y_n(t) \sin n\theta$$

The virtual work of the external forces X and Y will be designated by δW_e and

$$\delta W_e = \int_0^{2\pi} \left[X\delta w + Y\delta v \right]_{z=c} R_0 d\theta \quad (1-36)$$

When q_n is varied by δq_n , from the first of equations (1-31),

$$\delta w = \delta q_n \cos n\theta$$

From equation (1-1) and equations (1-31)

$$v)_{z=c} = \frac{R_0}{a} v - \frac{c}{a} \frac{\partial w}{\partial \theta}$$

$$\delta v)_{z=c} = \frac{R_0}{a} \delta v - \frac{c}{a} \delta \left(\frac{\partial w}{\partial \theta} \right)$$

$$\delta v)_{z=c} = \left(\frac{R_0}{a} r_n + \frac{cn}{a} \right) \sin n\theta \delta q_n$$

Thus

$$\delta W_e = \pi R_0 \left[X_n(t) + Y_n(t) \left(\frac{R_0}{a} r_n + \frac{cn}{a} \right) \right] \delta q_n$$

and

$$F_n = \pi R_0 \left[X_n(t) + Y_n(t) \left(\frac{R_0}{a} r_n + \frac{cn}{a} \right) \right] \quad (1-37)$$

in which F_n is the generalized force corresponding to q_n .

Similarly the generalized force corresponding to \bar{q}_n is

$$\bar{F}_n = \pi R_0 \left\{ X_n(t) + Y_n(t) \left(\frac{R_0}{a} \bar{r}_n + \frac{nc}{a} \right) \right\} \quad (1-38)$$

The Lagrangian function, L, is now known from equations (1-34) and (1-35)

$$L = E_k - V$$

and the generalized forces from equations (1-37) and (1-38). The Lagrange's equations of motion are thus

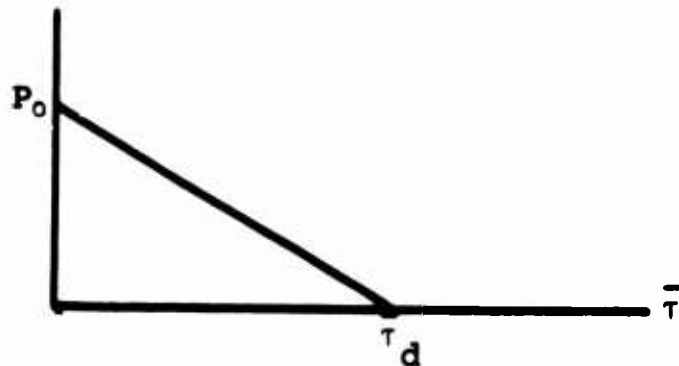
$$\frac{\partial L}{\partial q_n} - \frac{d}{dt} \frac{\partial L}{\partial \dot{q}_n} = -F_n$$

$$\frac{\partial \bar{L}}{\partial \bar{q}_n} - \frac{d}{dt} \frac{\partial \bar{L}}{\partial \dot{\bar{q}}_n} = -\bar{F}_n$$

Application

Two significant problems have been worked⁶.

The first problem considered was that of the thick ring, initially at rest, loaded by a uniform external pressure which varied with time as shown below.



This loading produces, of course, only radial motion. Figure 7 shows the radial displacement w as a function of dimensionless time $\bar{\tau}$ for various values of the dimensionless decay time $\bar{\tau}_d$. $\bar{\tau}$ is the ratio of actual time to the period of the $n = 0$ mode of vibration (equation (1-25)).

The second loading chosen was such as to excite the fundamental bending mode of vibration ($n = 2$), and produce large bending stresses. A radial pressure which varies as $\cos 2\theta$ and linearly with time from P_0 at $\bar{\tau} = 0$ to 0 at $\bar{\tau} = \bar{\tau}_d$ was chosen. The dynamic response of a ring with a thickness to mean radius ratio of one to three to this loading is given in Figures 8, 9, and 10.

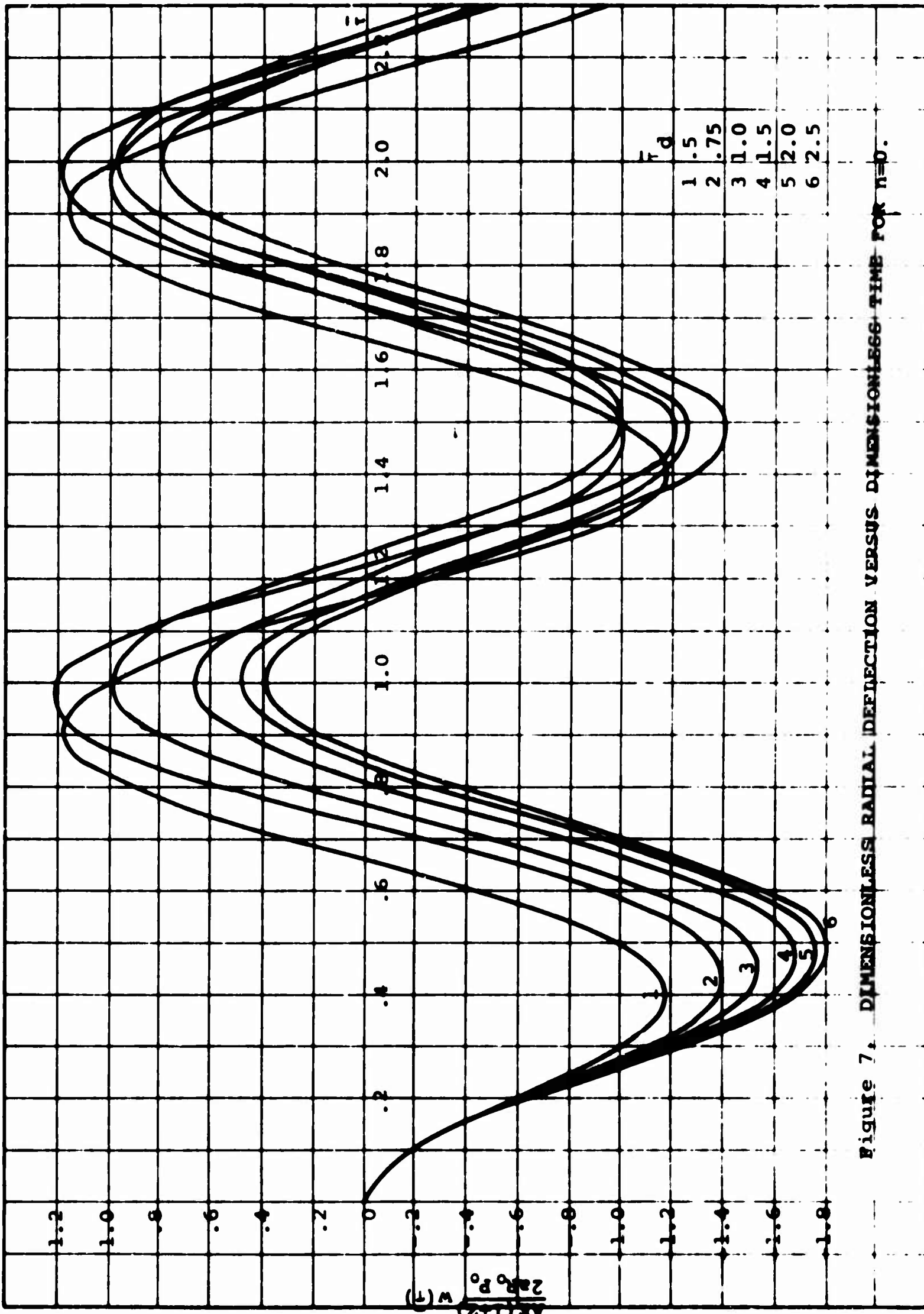


Figure 7. DIMENSIONLESS RADIAL DEFLECTION VERSUS DIMENSIONLESS TIME FOR $n=0$.

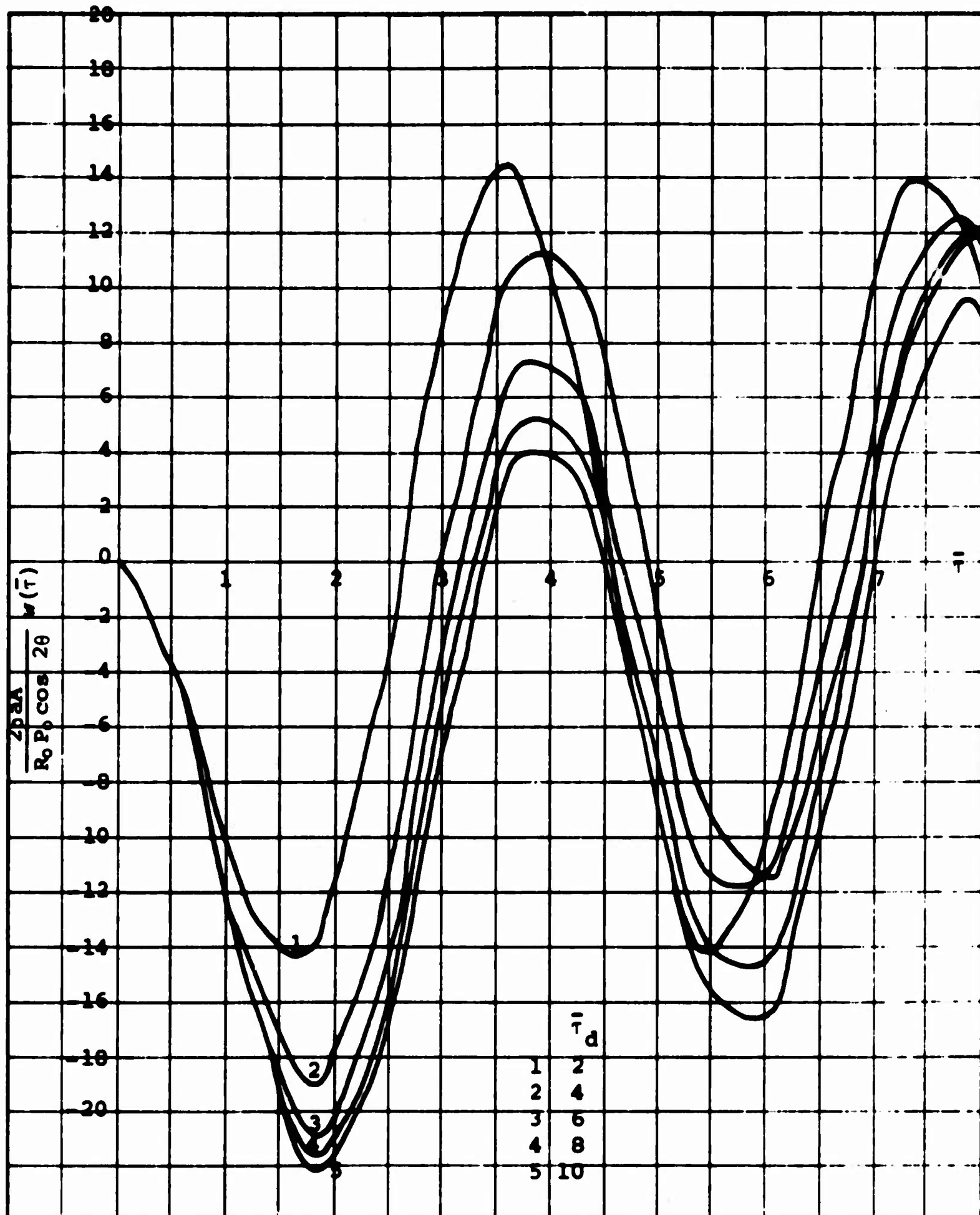
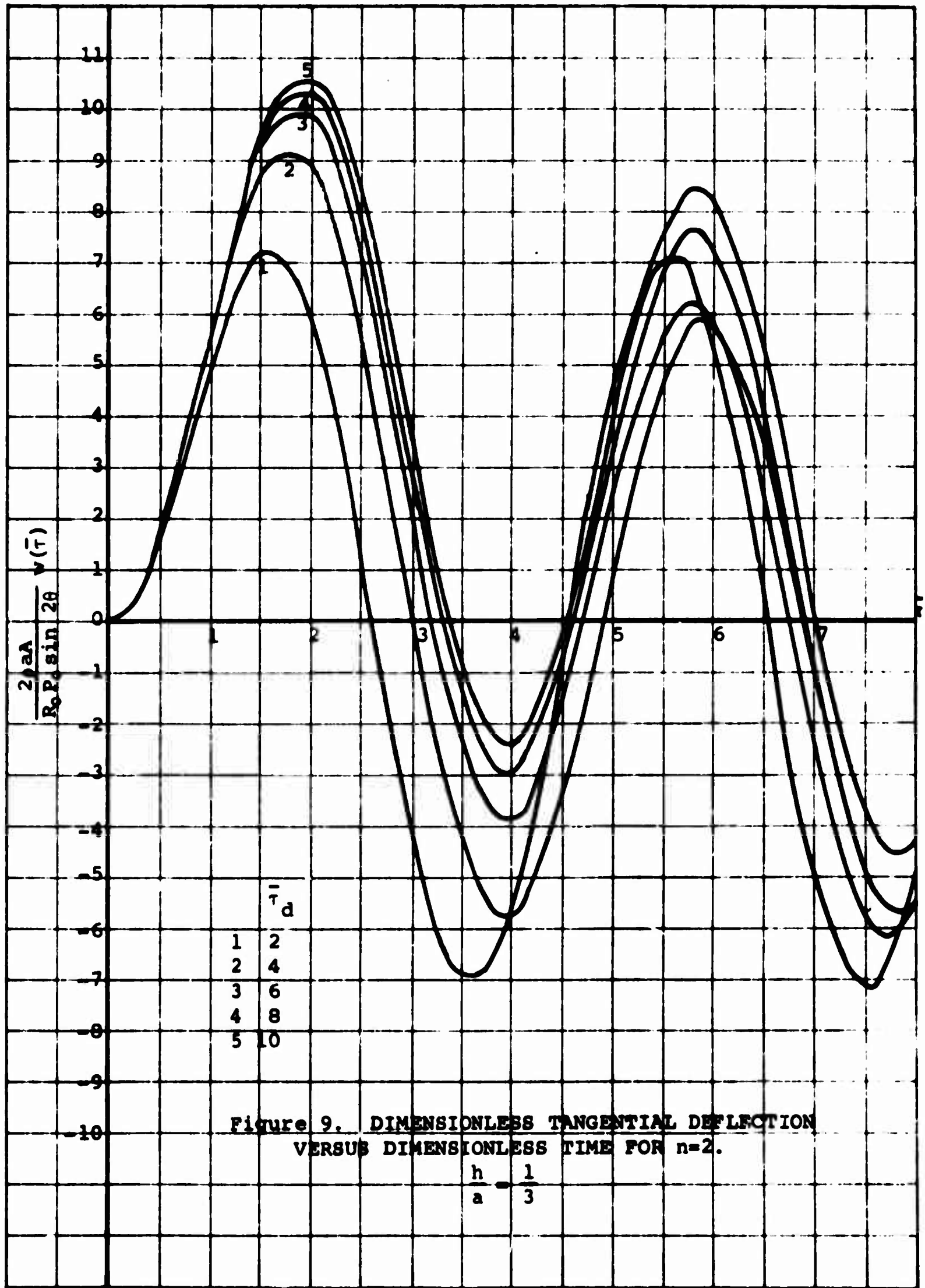


Figure 8. DIMENSIONLESS RADIAL DEFLECTION VERSUS DIMENSIONLESS TIME FOR $n=2$.

$$\frac{h}{a} = \frac{1}{3}$$



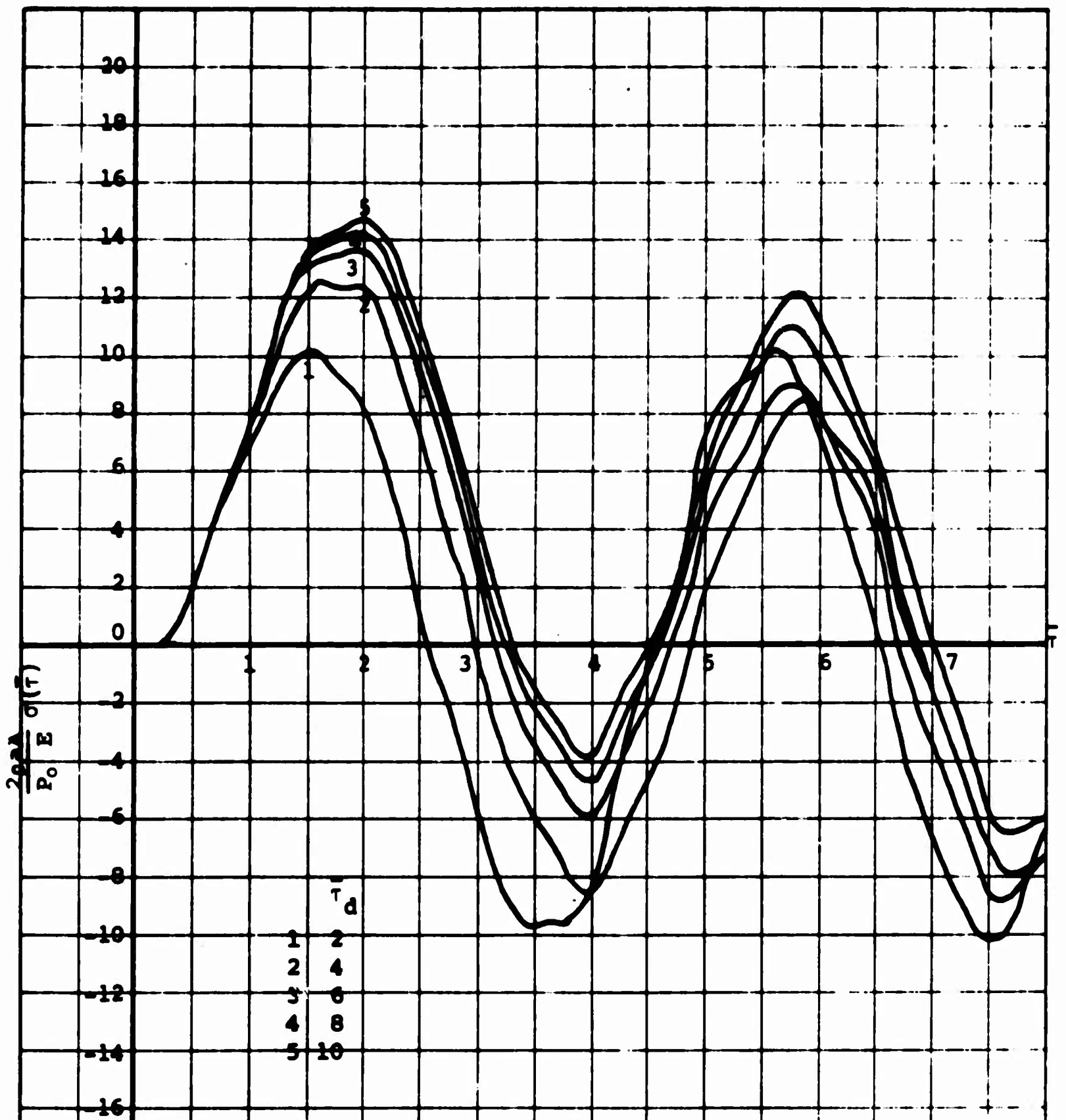


Figure 10. MAXIMUM DIMENSIONLESS TANGENTIAL STRESS
VERSUS DIMENSIONLESS TIME FOR $n=2$.

$$\frac{h}{a} = \frac{1}{3}$$

Conclusions

The analysis presented allows one to predict the response of thick rings to dynamic loads. The theory can be used to determine stresses and displacements in long cylindrical shells imbedded in acoustic or elastic media.

Since experiments in dynamic loading are difficult to perform one can judge a theory only by comparing its predictions with the results of other theories.

Experiments show that the formulas cited by Love (page 37), the work of Baron³, and equation (1-29) all predict the lower flexural natural frequencies of thick and thin rings very accurately.⁶ Since the largest displacements, strains and stresses occur with the lower modes, the work of Baron, though admittedly applicable to thin shells, should yield results applicable with engineering accuracy to thick shells.

REFERENCES

1. S. Timoshenko and J. N. Goodier, Theory of Elasticity, McGraw Hill Book Co., Inc. pp. 121, 122, 1951.
2. W. Flugge, Stresses in Shells, Springer-Verlag, Second Printing, p. 212, 1962.
3. Melvin L. Baron, "The Response of a Cylindrical Shell to a Transverse Shock Wave", Proceedings of the Second U.S. National Conference of Applied Mechanics, A.S.M.E., pp. 201-212, 1954.
4. A. E. H. Love, "A Treatise on the Mathematical Theory of Elasticity", Fourth Edition, Cambridge University Press, pp 452-54, 1927.
5. W. H. Parker, Jr., "Dynamic Response of Thick Rings to Distributed Self-Equilibrating Exterior Loads", M. S. Thesis, Louisiana State University, 1964.
6. Ronald Calvin, "An Experimental Investigation of the Natural Frequencies of Vibrations of Thick Elastic Rings", M. S. Thesis, Louisiana State University, 1964.

SECTION II
STRESSES AND DISPLACEMENTS
IN A
CIRCULAR CYLINDER
FOR
DISTRIBUTED STATIC LOADS APPLIED
PERPENDICULARLY TO CYLINDER AXIS

INTRODUCTION

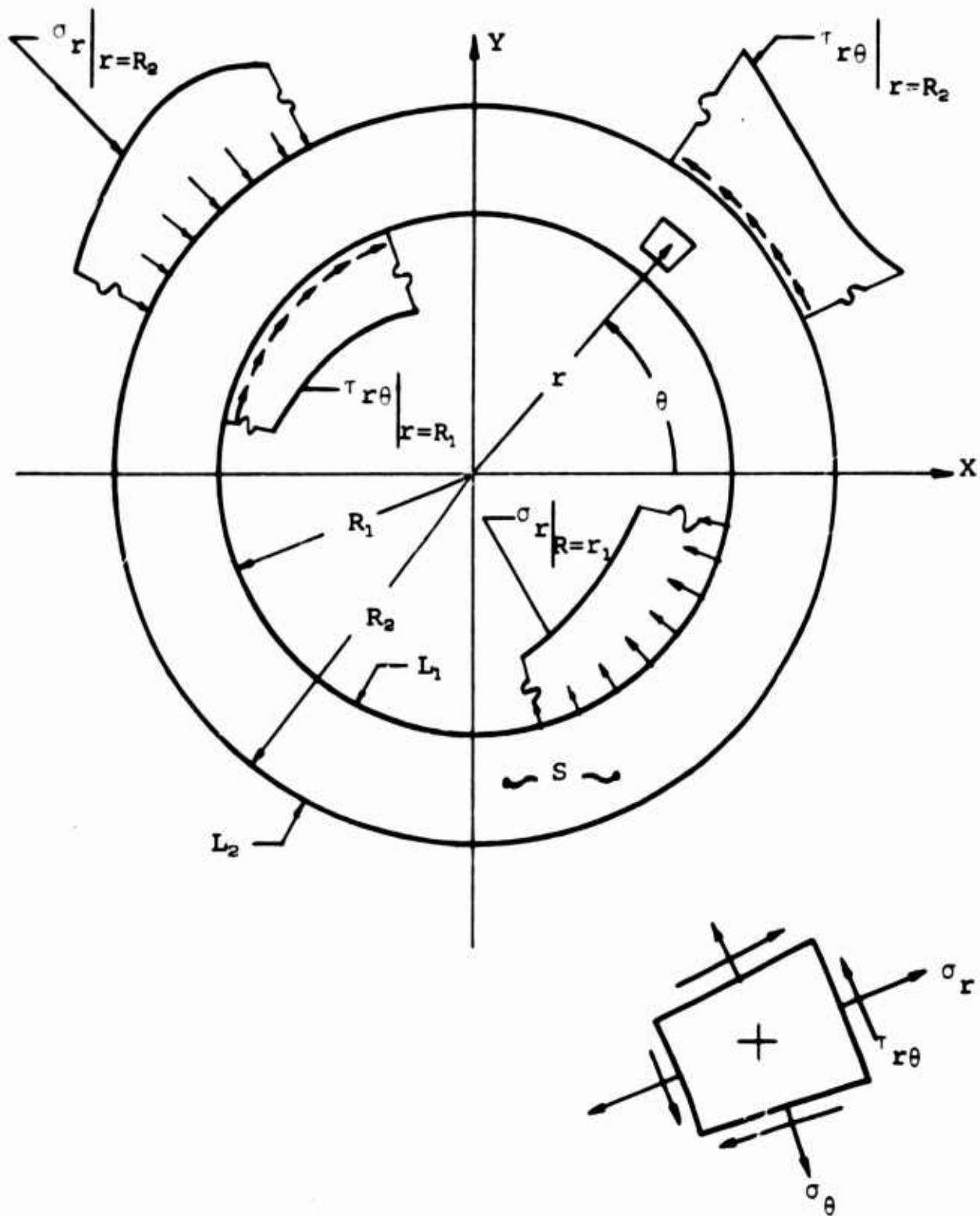
The basic theory of the method of solution used here is described by N. I. Muskhelishvili¹, though he does not claim originality for some of the background work. The procedure is restricted to the solution of plane problems of elasticity and for static cases. The governing differential equation for the plane, static elasticity problem is known as the biharmonic equation, $\nabla^4 \varphi = 0$, where φ is a stress function. It can be shown readily^{1, 2} that an equivalent solution for stresses and displacements can be accomplished by making use of two stress functions of a complex variable. Ultimately these two stress functions are written as Laurent series' for the particular problem of the circular cylinder. Then, with the applied loads expressed as complex Fourier series', coefficients of like terms are matched at the two boundaries, providing sufficient equations to solve for all coefficients.

Figure 11 illustrates a cross section of the circular cylinder with an indication of the loads applied. Both radial and tangential loads may be applied to either or both boundaries; to avoid confusion, only representative separated sections of the distributed loads are shown. The total loading must of course be self-equilibrating in order to have a static problem, but there is no necessity that the loads in each individual boundary have zero resultant. In a later section, a test for force resultant and another for moment resultant are presented; these tests are included in the computer program to ensure that no attempt will be made to solve an improper problem by this procedure.

One precaution regarding loading should be made here; concentrated loads cannot be handled by the computer program as developed; however, a concentrated load can be approximated by a statically equivalent distributed load applied over an arc as small as one subdivision of the ring.

The input to the procedure is in the form of shear and normal stresses on each boundary at any desired number (this number must be divisible by four) of equally spaced (angular spacing) points.

The output produces radial (σ_r), tangential (σ_θ), and shear ($\tau_{r\theta}$) stresses as well as radial (u) and tangential (v) displacements at any desired point of the ring.



Sign Convention for Stresses

Figure 11. Cross section of circular cylinder with portions of distributed loading indicated.

CHAPTER 1

THEORETICAL DEVELOPMENT

FUNDAMENTAL EQUATIONS

Since it is well known that the expression of stresses and displacements for the plane static elasticity problem can be accomplished in terms of two stress functions of a complex variable, we shall not repeat that development but will start with such expressions.

Stresses

For polar coordinates, the three stress components are involved in two equations.

$$\sigma_r + \sigma_\theta = 4 \operatorname{Re} \phi(z) = 2[\phi(z) + \bar{\phi}(z)] \quad (2-1)$$

$$\sigma_\theta - \sigma_r + 2i \tau_{r\theta} = 2[\bar{z}\phi'(z) + \psi(z)]e^{i\theta} \quad (2-2)$$

where

$$i = \sqrt{-1}$$

r, θ = polar coordinates (Fig. 11)

$z = x+iy$ (complex variable in rectangular coordinates)

$= re^{i\theta}$ (complex variable in polar coordinates)

$\bar{z} = x-iy$ (complex conjugate of z in rectangular coordinates)

$= re^{-i\theta}$ (complex conjugate of z in polar coordinates)

Re = real part of

$\phi(z), \psi(z)$ = undetermined stress functions of complex variable z

$\bar{\phi}(z)$ = complex conjugate of $\phi(z)$

$$\phi'(z) = \frac{d\phi(z)}{dz}$$

By subtracting Eq. (2-2) from Eq. (2-1) we obtain a very useful relation which does not contain σ_θ .

$$\sigma_r - i \tau_{r\theta} = \phi(z) + \bar{\phi}(z) - e^{i\theta}[\bar{z}\phi'(z) + \psi(z)] \quad (2-3)$$

Relation Eq. (2-3) is precisely the desired one for expressing the boundary stresses because we see that the radial stress is the real part and the shear stress is the negative of the imaginary part of the right side of Eq. (2-3).

Displacements

Again in polar coordinates, the displacements can be expressed in complex form.

$$2\mu(u+iv) = e^{-i\theta} [\kappa \varphi(z) - z \bar{\varphi}'(z) - \bar{\psi}(z)] \quad (2-4)$$

where

u = radial displacement (+ outward)

v = tangential displacement (+ in direction of increasing θ)

μ = one of the Lamé' constants = shear modulus

σ = Poisson's ratio

$$\varphi(z) = \int \bar{\varphi}(z) dz$$

$$\varphi'(z) = \frac{d\varphi(z)}{dz}$$

$$\bar{\varphi}'(z) = \text{complex conjugate of } \varphi'(z)$$

$$\psi(z) = \int \bar{\psi}(z) dz$$

κ = the other Lamé' constant. $\kappa = 3-4\sigma$ for plane stress,

$\kappa = \frac{3-\sigma}{1-\sigma}$ for plane strain.

We see that, once we have $\varphi(z)$ and $\psi(z)$, the radial displacement is the real part and the tangential displacement is the imaginary part of the right side of Eq. (2-4) after division by 2μ .

Two Relations from Unique Displacements

Since the cross section of the hollow circular cylinder is a multiply connected region, the requirement that displacements be single valued upon traversing a closed contour containing the inner boundary results in two essential relations. In general, it has been demonstrated¹ for multiply connected regions that the functions $\varphi(z)$ and $\psi(z)$ used in Eq. (2-4) can be expressed as

$$\varphi(z) = z \sum_{k=1}^m A_k \ln(z-z_k) + \sum_{k=1}^m \gamma_k \ln(z-z_k) + \varphi^*(z) \quad (a)$$

$$\psi(z) = \sum_{k=1}^m \gamma_k' \ln(z-z_k) + \psi^*(z) \quad (b)$$

where

m = number of interior holes

z_k = any point inside the k th hole

A_k = real constants

γ_k, γ_k' = complex constants

$\varphi^*(z), \psi^*(z)$ = holomorphic (single valued) functions of z

If $\phi(z)$ and $\psi(z)$ from Eqs. (a) and (b) are substituted into Eq. (2-4), we obtain

$$2u \left[u+iv \right]_{L_k'} = 2\pi i e^{-i\theta} \left[(\kappa+1) A_k z + \kappa \gamma_k + \bar{\gamma}_k' \right] \quad (c)$$

where $\left[u+iv \right]_{L_k'}$ = the increase in $(u+iv)$ obtained during one traverse around a closed curve containing the k^{th} hole.

Since we must have single valued displacements, the right side of Eq. (c) must vanish; therefore, it is obviously necessary and sufficient that the two relations of Eq. (d) must hold.

$$A_k = 0, \quad \kappa \gamma_k + \bar{\gamma}_k' = 0 \quad (d)$$

for $k = 1, 2, \dots, m$

In our particular case of the hollow circular cylinder, $m = 1$ (one hole), and we obtain the equations (2-5).

$$A = 0, \quad \kappa \gamma + \bar{\gamma}' = 0 \quad (2-5)$$

where $\bar{\gamma}'$ = complex conjugate of γ'

Since $\phi(z) = \frac{d\phi(z)}{dz}$ and $\psi(z) = \frac{d\psi(z)}{dz}$, we can obtain Eqs. (e) and (f) for our case ($m=1, z_k=0+i0, z=re^{i\theta}$) from Eqs. (a) and (b).

$$\begin{aligned} \phi(z) &= A(1+\ln z) + \frac{\gamma}{z} + \frac{d\phi^*(z)}{dz} \\ &= A \ln z + A + \frac{\gamma}{z} + \frac{d\phi^*(z)}{dz} \\ &= A \ln z + \phi^*(z) \end{aligned} \quad (e)$$

in which $A + \frac{\gamma}{z} + \frac{d\phi^*(z)}{dz}$ is single valued.

$$\psi(z) = \frac{\gamma'}{z} + \frac{d\psi^*(z)}{dz} \quad (f)$$

in which $\frac{\gamma'}{z} + \frac{d\psi^*(z)}{dz}$ is single valued.

Two important observations should be made from Eqs. (e) and (f): (1) $\phi(z)$ and $\psi(z)$ are single valued (since $A \neq 0$), and (2) γ and γ' are the coefficients of z^{-1} in the series expressions for $\phi(z)$ and $\psi(z)$.

Equation (2-5) expresses the two relations referred to in the heading of this paragraph. Actually, since the second relation is in terms of complex constants, Eq. (2-5) gives us three scalar relations.

SERIES SOLUTION FOR STRESSES AND DISPLACEMENTS

Fourier Representation of Loads

Referring to Fig. 11, we will label the inner boundary of radius R_1 as L_1 and the outer boundary of radius R_2 as L_2 . The region between L_1 and L_2 will be called S . It is assumed that the loading for this problem will be given in the form of values of σ_r and $\tau_{r\theta}$ on L_1 and L_2 , either as functions or θ or as values at discrete points. Of course, as mentioned earlier, the ring must be in equilibrium from these loads and the weight of the ring itself is ignored.

We shall represent the stresses acting on L_1 and L_2 by complex Fourier series.

$$\begin{aligned} (\sigma_r - i\tau_{r\theta})_{L_1} &= \sum_{-\infty}^{\infty} A'_k e^{ik\theta} = \sum_{-\infty}^{\infty} (\eta_k + i\zeta_k) e^{ik\theta} \\ (\sigma_r - i\tau_{r\theta})_{L_2} &= \sum_{-\infty}^{\infty} A''_k e^{ik\theta} = \sum_{-\infty}^{\infty} (\rho_k + i\nu_k) e^{ik\theta} \end{aligned} \quad (2-6)$$

where

$A'_k = \eta_k + i\zeta_k$ = complex Fourier coefficient determined by loading on inner boundary.

$A''_k = \rho_k + i\nu_k$ = complex Fourier coefficient determined by loading on outer boundary.

Laurent Series Representation of Complex Stress Functions

Though a digital computer cannot work with complex numbers other than by separation into real and imaginary parts, it will be convenient to continue the development in complex form and separate at the end. A later section deals in detail with the load representation by Fourier series, so for now we will consider the complex Fourier coefficients, A'_k and A''_k , as known. From Eqs. (2-3) and (2-6) we can express the boundary conditions in terms of stress functions $\phi(z)$ and $\psi(z)$.

$$\phi(z) + \bar{\phi}(z) - e^{2i\theta} [\bar{z}\phi'(z) + \psi(z)] = \begin{cases} \sum_{-\infty}^{\infty} A'_k e^{ik\theta} & \text{on } L_1 \\ & (r=R_1) \\ \sum_{-\infty}^{\infty} A''_k e^{ik\theta} & \text{on } L_2 \\ & (r=R_2) \end{cases} \quad (2-7)$$

For reference, one form of equation (e) is repeated here.

$$\phi(z) = A \ln z + \phi^*(z) \quad (\text{repeated}) \quad (e)$$

where

$A = \text{real constant}$

$\phi^*(z) = \text{holomorphic function of } z$

Since $\phi^*(z)$ is holomorphic in S up to and including the boundary, it can be represented by a Laurent series (power series in complex variable).

$$\phi^*(z) = \sum_{-\infty}^{\infty} a_k z^k \quad (g)$$

where

$a_k = \text{complex constant}$

Let us now consider Eq. (2-2). Since the stresses are given by Fourier series, they are holomorphic functions; thus, the right side of Eq. (2-2) must be also. From Eq. (e) we obtain the following:

$$\begin{aligned} \phi'(z) &= \frac{A}{z} + \frac{d\phi^*(z)}{dz} = \frac{A}{z} + \sum_{-\infty}^{\infty} k a_k z^{k-1} \\ \bar{z}\phi'(z) &= A \frac{\bar{z}}{z} + \sum_{-\infty}^{\infty} k a_k \bar{z} z^{k-1} \\ &= A \frac{r e^{-i\theta}}{r e^{i\theta}} + \sum_{-\infty}^{\infty} k a_k r e^{-i\theta} r^{k-1} e^{i(k-1)\theta} \\ &= A e^{-2i\theta} + \sum_{-\infty}^{\infty} k a_k r^k e^{i(k-2)\theta} \end{aligned}$$

Thus, we see that $\bar{z}\phi'(z)$ is holomorphic and for that reason so is $\psi(z)$. Therefore, $\psi(z)$ also can be represented by a Laurent series.

$$\phi(z) = A \ln z + \sum_{-\infty}^{\infty} a_k z^k \quad (2-8)$$

$$\psi(z) = \sum_{-\infty}^{\infty} a'_k z^k$$

Recursion Relations

Recalling Eqs. (2-5) and noting that γ and γ' are the coefficients of z^{-1} in the series representation of $\phi(z)$ and $\psi(z)$ respectively, we see that a_{-1} and a'_{-1} play the same roles in Eqs. (2-8) as do γ and γ' in Eqs. (2-5). We can write Eqs. (2-9) immediately from Eqs. (2-5).

$$A = 0, \quad \kappa a_{-1} + \bar{a}'_{-1} = 0 \quad (2-9)$$

where

$\bar{a}'_{-1} = \text{complex conjugate of } a'_{-1}$

We now substitute the expressions for $\phi(z)$ and $\psi(z)$ from Eqs. (2-8) into (2-7), using $A = 0$, to obtain Eqs. (2-10), two very important relations.

$$\begin{aligned} & \sum_{-\infty}^{\infty} (1-k) a_k r^k e^{ik\theta} + \sum_{-\infty}^{\infty} \bar{a}_k r^k e^{-ik\theta} - \sum_{-\infty}^{\infty} a'_{k-2} r^{k-2} e^{ik\theta} \\ &= \sum_{-\infty}^{\infty} A'_k e^{ik\theta} \quad \text{for } r = R_1 \\ &= \sum_{-\infty}^{\infty} A''_k e^{ik\theta} \quad \text{for } r = R_2 \end{aligned} \tag{2-10}$$

Since Eqs. (2-10) must hold on L_1 and L_2 for any value of $0 \leq \theta \leq 2\pi$, we may equate the coefficients of like powers of $e^{i\theta}$ for $r = R_1$ and for $r = R_2$ to obtain recursion relations for the unknown complex coefficients a_k and a'_k in terms of the known complex coefficients A'_k and A''_k (remember that A'_k and A''_k are the complex Fourier coefficients representing the loading).

Comparing terms independent of θ ($k=0$), we obtain

$$a_0 + \bar{a}_0 - a'_{-2} R_1^{-2} = A'_0$$

from the first of Eqs. (2-10), and

$$a_0 + \bar{a}_0 - a'_{-2} R_2^{-2} = A''_0$$

from the second of Eqs. (2-10). Since a_0 and \bar{a}_0 are complex conjugates, these two relations may be expressed as in Eqs. (2-11).

$$2 \operatorname{Re} a_0 - a'_{-2} R_1^{-2} = A'_0 \tag{2-11}$$

$$2 \operatorname{Re} a_0 - a'_{-2} R_2^{-2} = A''_0$$

Solving Eqs. (2-11) simultaneously, we obtain Eqs. (2-12).

$$\begin{aligned} \operatorname{Re} a_0 &= \frac{R_2^2 A''_0 - R_1^2 A'_0}{2(R_2^2 - R_1^2)} \\ a'_{-2} &= \frac{R_1^2 R_2^2 (A''_0 - A'_0)}{R_2^2 - R_1^2} \end{aligned} \tag{2-12}$$

Let us now assign symbols for the real and imaginary parts of the various coefficients involved here:

$$\begin{aligned} a_k &= \alpha_k + i\beta_k \\ a'_k &= \gamma_k + i\delta_k \\ A'_k &= \eta_k + i\zeta_k \\ A''_k &= \rho_k + i\nu_k \end{aligned} \quad \text{where } k = 0, \pm 1, \dots, \pm \infty$$

Thus, from the first of Eqs. (2-12) we write Eq. (h) which will be used later in making a check for equilibrium.

$$\text{Im}(R_2^2 A_0'' - R_1^2 A_0') = R_2^2 v_0 - R_1^2 \zeta_0 = 0 \quad (\text{h})$$

At this point we may wonder about the contribution of the imaginary part of a_0 ; that is, β_0 . The addition of an imaginary constant to $\psi(z)$ in Eqs. (2-1) and (2-2) leaves the stresses unchanged; therefore, β_0 can be assigned any desired value, say zero.

Equating coefficients of $e^{ik\theta}$ for $k = \pm 1, \pm 2, + \dots \pm \infty$, on $r = R_1$ and on $r = R_2$, we obtain Eqs. (2-13).

$$(1-k) a_k R_1^k + \bar{a}_{-k} R_1^{-k} - a'_{k-2} R_1^{k-2} = A_k' \quad (2-13)$$

$$(1-k) a_k R_2^k + \bar{a}_{-k} R_2^{-k} - a'_{k-2} R_2^{k-2} = A_k''$$

We eliminate a'_{k-2} between Eqs. (2-13) to obtain Eq. (2-14) for $k = \pm 1, \pm 2, + \dots \pm \infty$.

$$(1-k) (R_2^2 - R_1^2) a_k + (R_2^{-2k+2} - R_1^{-2k+2}) \bar{a}_{-k} = A_k'' R_2^{-k+2} - A_k' R_1^{-k+2} \quad (2-14)$$

Now Eq. (2-14) is of the form $A + iB = C + iD$ since a_k, \bar{a}_{-k}, A_k'' , and A_k' are all complex; therefore, $A = C$ and $B = D$. Thus we can write $A - iB = C - iD$; that is, we obtain a valid equation by going to the complex conjugate form of Eq. (2-14). However, in doing so, we obtain a relation in \bar{a}_k and a_{-k} instead of one in a_k and \bar{a}_{-k} . Thus we shall replace k by $-k$ in the conjugate of Eq. (2-14) in order to obtain another equation in the same two unknowns.

$$(R_2^{2k+2} - R_1^{2k+2}) a_k + (1+k) (R_2^2 - R_1^2) \bar{a}_{-k} = \bar{A}_{-k}'' R_2^{k+2} - \bar{A}_{-k}' R_1^{k+2} \quad (2-15)$$

Equations (2-14) and (2-15) can be solved simultaneously for a_k and \bar{a}_{-k} provided the determinant of the coefficient matrix $\neq 0$. We need consider Eqs. (2-14) and (2-15) only for $k = +1, +2, +3, \dots$ since for each of $k = -1, -2, \dots$ we obtain a pair of equations conjugate to each pair for positive k and thus obtain no new information (if we know a_k , we know \bar{a}_{-k}). The determinant of the coefficient matrix is given as Eq. (2-16).

$$\begin{aligned}
D_k &= \begin{vmatrix} (1-k)(R_2^2 - R_1^2) & (R_2^{-2k+2} - R_1^{-2k+2}) \\ (R_2^{2k+2} - R_1^{2k+2}) & (1+k)(R_2^2 - R_1^2) \end{vmatrix} \\
&= (1-k^2)(R_2^2 - R_1^2)^2 - (R_2^{2k+2} - R_1^{2k+2})(R_2^{-2k+2} - R_1^{-2k+2})
\end{aligned} \tag{2-16}$$

From Eq. (2-16) we see that D_k vanishes for $k = 0, \pm 1$; therefore, Eqs. (2-14) and (2-15) must be solved specifically for these values of k . We already have a_0 by the first of Eq. (2-12), so we will need consider Eqs. (2-14) and (2-15) specially only for $k = 1$. Equations (2-17) result from Eqs. (2-14) and (2-15) respectively for $k = 1$.

$$\begin{aligned}
A_1' R_2 - A_1' R_1 &= 0 \\
(R_2^4 - R_1^4) a_1 + 2(R_2^2 - R_1^2) \bar{a}_{-1} &= \bar{A}_{-1}' R_2^3 - \bar{A}_{-1}' R_1^3
\end{aligned} \tag{2-17}$$

We now solve for a_1 and \bar{a}_{-1} by using the second of Eqs. (2-9)

$$\kappa a_{-1} + \bar{a}_{-1} = 0 \tag{j}$$

and the first of Eqs. (2-13) for $k = 1$.

$$\bar{a}_{-1} R_1^{-1} - a_{-1}' R_1^{-1} = A_1' \tag{k}$$

In order to obtain identical unknowns, we take the conjugate of Eq. (k) to obtain Eq. (l).

$$a_{-1} - \bar{a}_{-1}' = \bar{A}_1' R_1 \tag{l}$$

We solve Eqs. (j) and (l) simultaneously for a_{-1} and \bar{a}_{-1}' after which we take the conjugate of \bar{a}_{-1}' .

$$a_{-1} = \frac{\bar{A}_1' R_1}{\kappa + 1} \tag{2-18}$$

$$a_{-1}' = -\frac{\kappa A_1' R_1}{1 + \kappa} \tag{2-19}$$

Since $\bar{a}_{-1} = \frac{A_1' R_1}{\kappa + 1}$ from Eq. (2-18), we can now solve for a_1 from the second of Eq. (2-17).

$$a_1 = \frac{\bar{A}'_1 R_2^3 - \bar{A}'_1 R_1^3}{R_2^3 - R_1^3} - \frac{2 A'_1 R_1}{(R_2^3 + R_1^3)(\kappa + 1)} \quad (2-20)$$

It can be shown that $D_k \neq 0$ for $|k| \geq 2$; and thus, for $k = 2, 3, \dots, \infty$, we solve Eqs. (2-14) and (2-15) simultaneously for a_k and \bar{a}_{-k} . Also notice that $D_k = D_{-k}$.

$$a_k = \frac{(1+k)(R_2^3 - R_1^3)(A'_k R_2^{-k+2} - A'_k R_1^{-k+2}) - (R_2^{-2k+2} - R_1^{-2k+2})(\bar{A}'_{-k} R_2^{k+2} - \bar{A}'_{-k} R_1^{k+2})}{D_k} \quad (2-21)$$

$$\bar{a}_{-k} = \frac{(1-k)(R_2^3 - R_1^3)(\bar{A}'_{-k} R_2^{k+2} - \bar{A}'_{-k} R_1^{k+2}) - (R_2^{2k+2} - R_1^{2k+2})(A'_k R_2^{-k+2} - A'_k R_1^{-k+2})}{D_k} \quad (2-21')$$

Thus, Eqs. (2-18), (2-20), (2-21), and the first of Eqs. (2-12) completely determine all a_k , the coefficients for $\phi^*(z)$.

We now shall determine a'_k , the coefficients of the series for $\psi(z)$. Knowing a_k and \bar{a}_{-k} , either of Eqs. (2-13) may be employed to solve for a'_{k-2} . Using the first of Eqs. (2-13), we obtain Eq. (2-22a) which can be re-indexed and expressed as Eq. (2-22b).

$$a'_{k-2} = (1-k)R_2^3 a_k + \bar{a}_{-k} R_1^{-2k+2} - A'_k R_1^{-k+2} \quad (2-22a)$$

$$\text{for } k = \frac{+}{-} 1, \frac{+}{-} 2, \dots$$

$$a'_k = -(1+k)R_1^3 a_{k+2} + \bar{a}_{-(k+2)} R_1^{-(k+2)} - A'_{k+2} R_1^{-k} \quad (2-22b)$$

$$\text{for } k = 0, \frac{+}{-} 1, \frac{+}{-} 2, \frac{+}{-} 3, \dots$$

Neither Eq. (2-22a) nor Eq. (2-22b) gives the term a'_{-2} , but we already have this from the second of Eqs. (2-12); therefore all coefficients for $\psi(z)$ can be computed. In order to reduce the number of computations, it was decided to let $R_2 = 1$ and R_1 be the appropriate fraction less than one; then the solution for a cylinder with $R_2 \neq 1$ (but geometrically similar) can be readily found by dimensional analysis.

The use of Eq. (2-22a) or Eq. (2-22b) for large k resulted in lack of precision on a'_k because of small differences of large numbers. It can be seen that, since $R_1 < 1$, we have numbers less than unity to large negative powers. Because of this precision trouble, the second of Eqs. (2-13) instead of the first was used

to compute a'_k since it contains only $R_2 = 1$, and therefore no difficulties caused by small differences of large numbers. Equation (2-22c) also gives a'_k , but from the second of Eqs. (2-13).

$$\begin{aligned}
 a'_k &= -(1+k)a_{k+2}R_2^2 + a_{-(k+2)}R_2^{-(2k+2)} - A'_{k+2}R_2^{-k} \\
 &= -(1+k)a_{k+2} + \bar{a}_{-(k+2)} - A'_{k+2} \qquad (2-22c) \\
 &\text{for } k = 0, \pm 1, \pm 2, \pm 3, \dots
 \end{aligned}$$

Summary

Coefficients of $\phi(z)$:

- a_0 Equation (2-12)
- a_1 " (2-20)
- a_{-1} " (2-18)
- a_k (for $k = \pm 2, \pm 3, \dots$) " (2-21)

Coefficients of $\psi(z)$:

- a'_{-1} Equation (2-19) or (2-22c)
- a'_{-2} " (2-12)
- a'_k (for $k = 0, \pm 1, \pm 2, \pm 3, \dots$) " (2-22c)

Equilibrium Verification

Inasmuch as the entire procedure here is restricted to the static case, there are three relations which must be satisfied if the hollow cylinder is to be in equilibrium. With the entire ring as a free body in Fig. 12, we will sum moments about the origin and also sum forces horizontally and vertically.

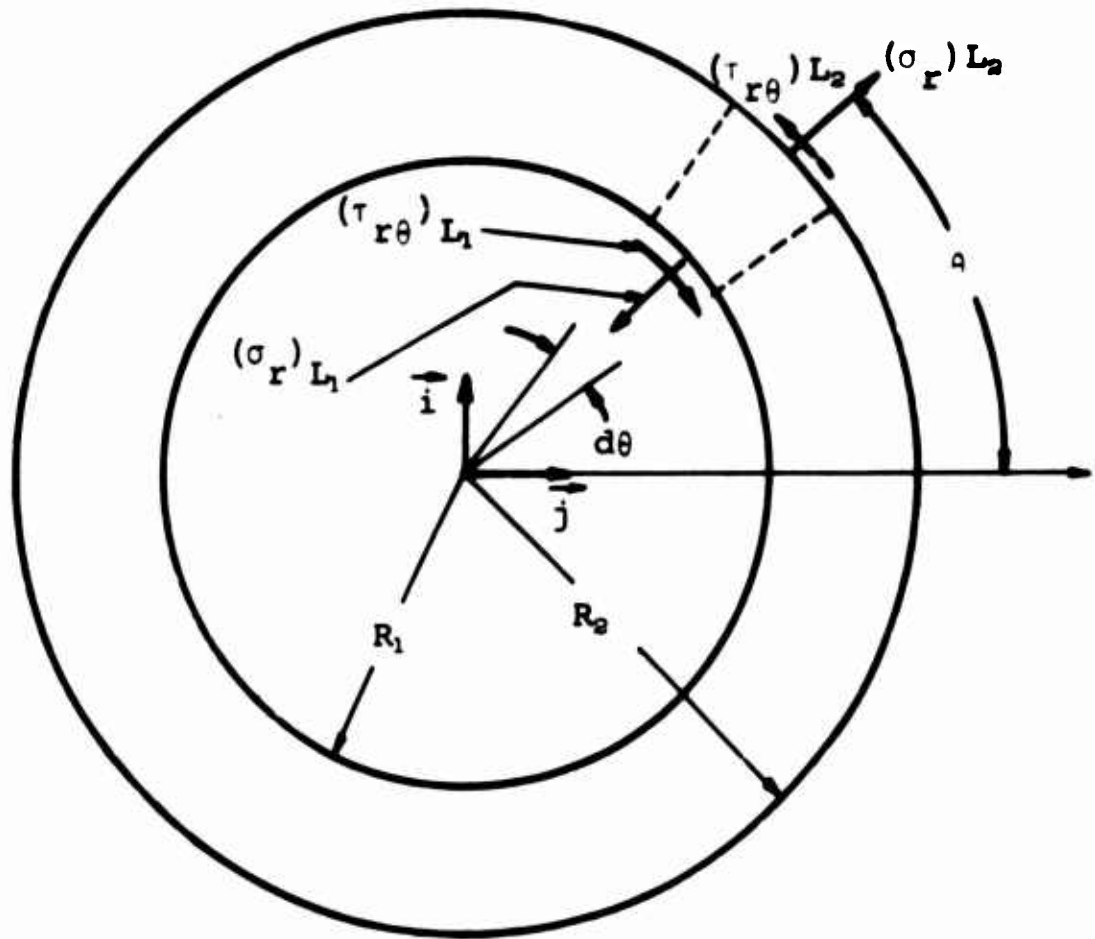


Figure 12. Equilibrium of Entire Hollow Cylinder

$$\sum^{\pm} M_0 = 0 = \int_0^{2\pi} [R_2^2 (\tau_{r\theta})_{L_2} - R_1^2 (\tau_{r\theta})_{L_1}] d\theta$$

From Eqs. (2-6), we may write the following relations after expanding A_k' and A_k'' into real and imaginary parts:

$$(\sigma_r)_{L_1} - i(\tau_{r\theta})_{L_1} = \sum_{-\infty}^{\infty} (\eta_k + i \zeta_k) (\cos k\theta + i \sin k\theta)$$

$$(\sigma_r)_{L_2} - i(\tau_{r\theta})_{L_2} = \sum_{-\infty}^{\infty} (\rho_k + i \nu_k) (\cos k\theta + i \sin k\theta)$$

Thus, we can separate into real and imaginary parts and express σ_r and $\tau_{r\theta}$ on each boundary.

$$(\sigma_r)_{L_1} = \sum_{-\infty}^{\infty} (\eta_k \cos k\theta - \zeta_k \sin k\theta)$$

$$(\tau_{r\theta})_{L_1} = -\sum_{-\infty}^{\infty} (\zeta_k \cos k\theta + \eta_k \sin k\theta)$$

$$(\sigma_r)_{L_2} = \sum_{-\infty}^{\infty} (\rho_k \cos k\theta - \nu_k \sin k\theta)$$

$$(\tau_{r\theta})_{L_2} = -\sum_{-\infty}^{\infty} (\nu_k \cos k\theta + \rho_k \sin k\theta)$$

We now substitute $(\tau_{r\theta})_{L_1}$ and $(\tau_{r\theta})_{L_2}$ into the moment equilibrium equation.

$$\sum M_o = -R_2^2 \sum_{-\infty}^{\infty} \left[\frac{\nu_k}{k} \sin k\theta - \frac{\rho_k}{k} \cos k\theta \right]_0^{2\pi} + R_1^2 \sum_{-\infty}^{\infty} \left[\frac{\zeta_k}{k} \sin k\theta - \frac{\eta_k}{k} \cos k\theta \right]_0^{2\pi}$$

This expression for M identically vanishes term by term except for $k = 0$ which must be handled separately.

$$\sum M_o = -R_2^2 \int_0^{2\pi} \nu_o \, d\theta + R_1^2 \int_0^{2\pi} \zeta_o \, d\theta = 2\pi (R_1^2 \zeta_o - R_2^2 \nu_o) = 0 \quad (2-23a)$$

$$\therefore R_1^2 \zeta_o - R_2^2 \nu_o = 0 \quad (\text{repeated}) \quad (h)$$

We see that the forced condition of Eq. (h) is a consequence of the fact that the entire ring must be in moment equilibrium.

Similarly, the entire ring must be in force equilibrium

$$\begin{aligned} \sum \vec{F} = 0 &= \int_0^{2\pi} \left[(\sigma_r)_{L_2} R_2 - (\sigma_r)_{L_1} R_1 \right] (\vec{i} \cos \theta + \vec{j} \sin \theta) \, d\theta \\ &+ \int_0^{2\pi} \left[(\tau_{r\theta})_{L_2} R_2 - (\tau_{r\theta})_{L_1} R_1 \right] (-\vec{i} \sin \theta + \vec{j} \cos \theta) \, d\theta \end{aligned}$$

Again we substitute the series expressions for stresses.

$$\begin{aligned} \sum \vec{F} &= \int_0^{2\pi} \left\{ \sum_{-\infty}^{\infty} \left[(\rho_k R_2 - \eta_k R_1) \cos k\theta - (\nu_k R_2 - \zeta_k R_1) \sin k\theta \right] \right. \\ &\quad \left. (\vec{i} \cos \theta + \vec{j} \sin \theta) \right\} d\theta \end{aligned}$$

$$- \int_0^{2\pi} \left\{ \sum_{-\infty}^{\infty} \left[(\nu_k R_2 - \zeta_k R_1) \cos k\theta + (\rho_k R_2 - \eta_k R_1) \sin k\theta \right] \right. \\ \left. (-\vec{i} \sin \theta + \vec{j} \cos \theta) \right\} d\theta$$

Now, since $\sin n\theta$ and $\cos n\theta$ comprise a set of orthogonal functions over the range from 0 to 2π , we have only the terms for $k = 1$ and of like kind survive.

$$\sum \vec{F} = 2\pi (\rho_1 R_2 - \eta_1 R_1) \vec{i} - 2\pi (\nu_1 R_2 - \zeta_1 R_1) \vec{j} \equiv 0 \quad (2-23b)$$

$$\rho_1 R_2 - \eta_1 R_1 = 0, \quad \nu_1 R_2 - \zeta_1 R_1 = 0 \quad (\text{repeated}) \quad ((2-17) \text{ first})$$

Thus, we see that the two forced conditions (one from real equality, one from imaginary equality) of Eq. (2-17) are consequences of the necessary force equilibrium of the entire ring.

In the computer program for the solution of this problem, these three verifications are made early in the computation as soon as $\zeta_0, \nu_0, \rho_1, \eta_1, \nu_1$, and ζ_1 are available. Of course, with loading data supplied numerically, we would not expect an exact check; but to some tolerance, these three relations must be satisfied before we have a valid problem for the method.

Stresses in Terms of α, β, γ , and δ

Since a digital computer cannot function directly in terms of complex numbers, we will now express the three stress components in terms of real numbers.

From Eqs. (2-1) and (2-8), we obtain Eq. (2-24) after using $A=0$ in Eq. (2-8).

$$\begin{aligned} \sigma_r + \sigma_\theta &= 2 \left[\phi(z) + \bar{\phi}(z) \right] = 2 \left[\sum_{-\infty}^{\infty} a_k z^k + \sum_{-\infty}^{\infty} \bar{a}_k \bar{z}^k \right] \\ &= 2 \sum_{-\infty}^{\infty} r^k (a_k e^{i k \theta} + \bar{a}_k e^{-i k \theta}) \\ &= 2 \sum_{-\infty}^{\infty} r^k \left[(\alpha_k + i\beta_k) (\cos k\theta + i \sin k\theta) + (\alpha_k - i\beta_k) (\cos k\theta - i \sin k\theta) \right] \\ &= 4 \sum_{-\infty}^{\infty} r^k (\alpha_k \cos k\theta - \beta_k \sin k\theta) \end{aligned} \quad (2-24)$$

We obtain equation (2-25) by using Eqs. (2-2) and (2-8).

$$\begin{aligned}
\sigma_{\theta} - \sigma_r + 2i\tau_{r\theta} &= 2\left[\bar{z} \phi'(z) + \psi(z)\right] e^{s+1\theta} \\
&= 2e^{s+1\theta} \left[\bar{z} \sum_{-\infty}^{\infty} k a_k z^{k-1} + \sum_{-\infty}^{\infty} a'_k z^k \right] \\
&= 2e^{s+1\theta} \left[r e^{-1\theta} \sum_{-\infty}^{\infty} k a_k r^{k-1} e^{i(k-1)\theta} + \sum_{-\infty}^{\infty} a'_k r^k e^{i k \theta} \right] \\
&= 2 \left[\sum_{-\infty}^{\infty} k a_k e^{i k \theta} + \sum_{-\infty}^{\infty} a'_k r^k e^{i(k+s)\theta} \right] \\
&= 2 \sum_{-\infty}^{\infty} r^k \left[k \alpha_k \cos k\theta - k \beta_k \sin k\theta + \gamma_k \cos(k\theta+2\theta) - \delta_k \sin(k\theta+2\theta) \right] \\
&\quad + 2i \sum_{-\infty}^{\infty} r^k \left[k \beta_k \cos k\theta + k \alpha_k \sin k\theta + \delta_k \cos(k\theta+2\theta) + \gamma_k \sin(k\theta+2\theta) \right]
\end{aligned} \tag{2-25}$$

By adding Eq. (2-24) and the real part of Eq. (2-25), we obtain σ_{θ} as given by Eq. (2-26); by subtracting the real part of Eq. (2-25) from Eq. (2-24), we obtain σ_r as given by Eq. (2-27); and the imaginary part of Eq. (2-25) gives $\tau_{r\theta}$ directly in Eq. (2-28).

$$\begin{aligned}
2\sigma_{\theta} &= \sum_{-\infty}^{\infty} \left\{ 4r^k (\alpha_k \cos k\theta - \beta_k \sin k\theta) + 2r^k \left[k \alpha_k \cos k\theta - k \beta_k \sin k\theta \right. \right. \\
&\quad \left. \left. + \gamma_k \cos(k\theta+2\theta) - \delta_k \sin(k\theta+2\theta) \right] \right\}
\end{aligned}$$

or

$$\sigma_{\theta} = \sum_{-\infty}^{\infty} r^k \left[(2+k) (\alpha_k \cos k\theta - \beta_k \sin k\theta) + \gamma_k \cos(k\theta+2\theta) - \delta_k \sin(k\theta+2\theta) \right] \tag{2-26}$$

$$\begin{aligned}
2\sigma_r &= \sum_{-\infty}^{\infty} r^k \left[(4-2k) (\alpha_k \cos k\theta - \beta_k \sin k\theta) - 2\gamma_k \cos(k\theta+2\theta) \right. \\
&\quad \left. + 2\delta_k \sin(k\theta+2\theta) \right]
\end{aligned}$$

or

$$\sigma_r = \sum_{-\infty}^{\infty} r^k \left[(2-k) (\alpha_k \cos k\theta - \beta_k \sin k\theta) - \gamma_k \cos(k\theta+2\theta) + \delta_k \sin(k\theta+2\theta) \right] \tag{2-27}$$

$$\tau_{r\theta} = \sum_{-\infty}^{\infty} r^k \left[k\beta_k \cos k\theta + k\alpha_k \sin k\theta + \delta_k \cos(k\theta + 2\theta) + \gamma_k \sin(k\theta + 2\theta) \right] \quad (2-28)$$

Displacements in Terms of α , β , γ , and δ

We find displacements u and v from the real and imaginary parts respectively of Eq. (2-4).

$$2\mu(u+iv) = e^{-i\theta} \left[\kappa\varphi(z) - z\bar{\varphi}'(z) - \bar{\psi}(z) \right] \quad (\text{repeated}) \quad (2-4)$$

where

$$\begin{aligned} \varphi(z) &= \int \phi(z) dz = \int \left[\phi^*(z) + A \ln z \right] dz = \int \sum_{-\infty}^{\infty} a_k z^k dz \\ &\quad \text{from Eq. (2-8) with } A=0 \\ &= \sum_{-\infty}^{-2} \frac{a_k}{k+1} z^{k+1} + a_{-1} \ln z + \sum_0^{\infty} \frac{a_k}{k+1} z^{k+1} \end{aligned}$$

$$\varphi'(z) = \phi(z) = A \ln z + \sum_{-\infty}^{\infty} a_k z^k = \sum_{-\infty}^{\infty} a_k z^k, \quad \text{since } A = 0$$

$$\bar{\varphi}'(z) = \sum_{-\infty}^{\infty} \bar{a}_k \bar{z}^k = \sum_{-\infty}^{\infty} \bar{a}_k r^k e^{-ik\theta}$$

$$z\bar{\varphi}'(z) = \sum_{-\infty}^{\infty} \bar{a}_k r^{k+1} e^{-i(k-1)\theta}$$

$$\psi(z) = \int \Psi(z) dz = \int \sum_{-\infty}^{\infty} a'_k z^k dz \quad \text{from Eq. (2-8)}$$

$$= \sum_{-\infty}^{-2} \frac{a'_k}{k+1} z^{k+1} + a'_{-1} \ln z + \sum_0^{\infty} \frac{a'_k}{k+1} z^{k+1}$$

$$\bar{\psi}(z) = \sum_{-\infty}^{-2} \frac{\bar{a}'_k}{k+1} \bar{z}^{k+1} + \bar{a}'_{-1} \ln \bar{z} + \sum_0^{\infty} \frac{\bar{a}'_k}{k+1} \bar{z}^{k+1}$$

The above integrations were carried out without including any additive constants because such constants represent rigid-body

motion. That this is so can be seen by observing that the total of such constants in the square brackets of Eq. (2-4) would be of the following form:

$$\begin{aligned}
 (u+iv) &= \frac{e^{-i\theta}}{2\mu} [a'+ib'] = e^{-i\theta} (a+ib) \\
 &\text{due to} \\
 &\text{additive} \\
 &\text{constants} \\
 &\text{in Eq. (2-4)} \\
 &= (a+ib) (\cos \theta + i \sin \theta) \\
 &= a \cos \theta + b \sin \theta + i(b \cos \theta - a \sin \theta)
 \end{aligned}$$

$$u = a \cos \theta + b \sin \theta$$

$$v = -a \sin \theta + b \cos \theta$$

As seen from Fig. 13, these values of u and v are exactly the radial and transverse components of displacement each particle would have if the entire body were rigidly translated by an amount a in the x -direction and an amount b in the y -direction.

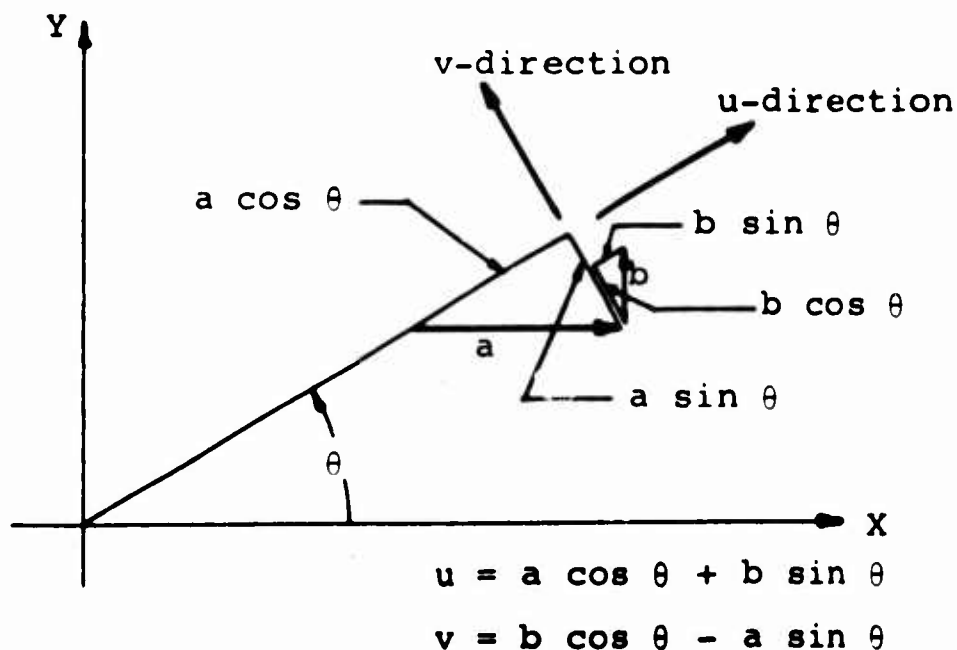


Figure 13. Radial and transverse displacements of a particle due to given Cartesian displacements.

Similarly, we find by Eqs. (2-1) and (2-2) that an addition of an imaginary constant ($i\beta_0$) to $\phi(z)$ leaves the stresses unchanged. This addition of $i\beta_0$ to $\phi(z)$, however, changes $\varphi(z)$ by the amount of $i\beta_0 z$ and changes the displacements as follows:

$$\begin{aligned} (u+iv) &= i \frac{e^{-i\theta}}{2\mu} \kappa\beta_0 z = \frac{\kappa\beta_0}{2\mu} i e^{-i\theta} r e^{i\theta} \\ &\text{due to adding } i\beta_0 \text{ to } \phi(z) \\ &= \Delta\theta i r \end{aligned}$$

$$u = 0, \quad v = \Delta\theta r$$

$$\text{where } \Delta\theta = \frac{\kappa\beta_0}{2\mu} \text{ or } \beta_0 = \frac{2\mu\Delta\theta}{\kappa}$$

However, the displacements $u = 0$ and $v = r\Delta\theta$ are exactly those each particle of a body would receive if the body underwent rigid body rotation by the angle $\Delta\theta$ about an axis through the origin as indicated in Fig. 14. Actually, of course, the displacement $v = r\Delta\theta$ in the instantaneous v -direction is valid only for small $\Delta\theta$. However, the path of a particle is a circular arc of length $r\Delta\theta$ even for large $\Delta\theta$. Thus, the addition of the term $i\beta_0$ to the series for $\phi(z)$ has the effect of a rigid body rotation of the ring about an axis through the origin by an amount $\Delta\theta = \frac{\kappa\beta_0}{2\mu}$.

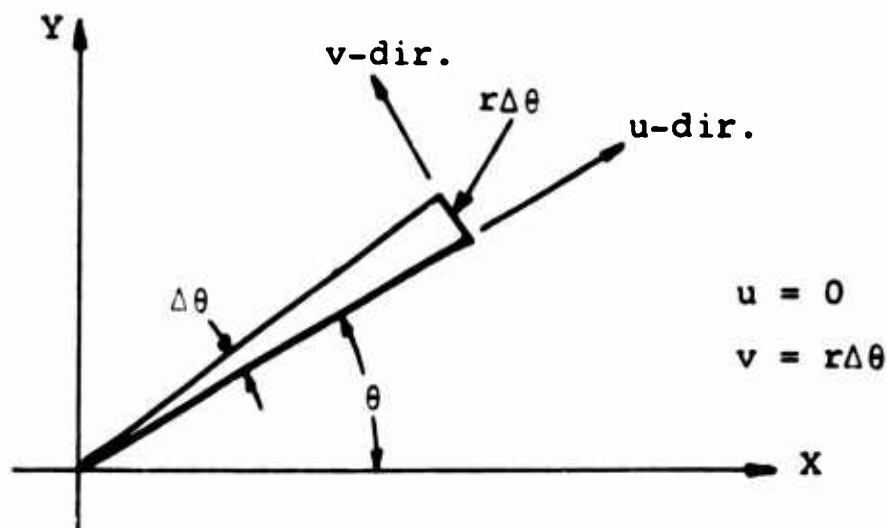


Figure 14. Radial and transverse displacements due to rigid body rotation.

In programming this procedure, these rigid body displacements were left unspecified and thus the computed displacements are "floating." This actually enables one to obtain the displacements in an advantageous form especially for problems of symmetrical loading.

Ignoring these constants of integration in Eq.(2-4) and the term $i\beta_0$ in $\phi(z)$, we obtain a series expression for displacements as given by Eq.(2-4').

$$2\mu(u+iv) = e^{-i\theta} \left[\sum_{-\infty}^{-2} \kappa \frac{a_k}{k+1} z^{k+1} + \kappa a_{-1} \ln z + \sum_0^{\infty} \kappa \frac{a_k}{k+1} z^{k+1} \right. \\ \left. - \sum_{-\infty}^{\infty} \bar{a}_k r^{k+1} e^{-i(k-1)\theta} - \sum_{-\infty}^{-2} \frac{\bar{a}'_k}{k+1} \bar{z}^{k+1} - \bar{a}'_{-1} \ln \bar{z} \right. \\ \left. - \sum_0^{\infty} \frac{\bar{a}'_k}{k+1} \bar{z}^{k+1} \right]$$

$$2\mu(u+iv) = e^{-i\theta} \left[\sum_{-\infty}^{-2} \kappa \frac{a_k}{k+1} r^{k+1} e^{i(k+1)\theta} + \kappa a_{-1} (\ln r + i\theta) \right. \\ \left. + \sum_0^{\infty} \kappa \frac{a_k}{k+1} r^{k+1} e^{i(k+1)\theta} - \sum_{-\infty}^{\infty} \bar{a}_k r^{k+1} e^{-i(k-1)\theta} \right. \\ \left. - \sum_{-\infty}^{-2} \frac{\bar{a}'_k}{k+1} r^{k+1} e^{-i(k+1)\theta} - \bar{a}'_{-1} (\ln r - i\theta) \right. \\ \left. - \sum_0^{\infty} \frac{\bar{a}'_k}{k+1} r^{k+1} e^{-i(k+1)\theta} \right]$$

or

$$2\mu(u+iv) = \sum_{-\infty}^{-2} \kappa \frac{a_k}{k+1} r^{k+1} e^{ik\theta} + e^{-i\theta} \ln r (\kappa a_{-1} - \bar{a}'_{-1}) \\ + \sum_0^{\infty} \kappa \frac{a_k}{k+1} r^{k+1} e^{ik\theta} - \sum_{-\infty}^{\infty} \bar{a}_k r^{k+1} e^{-ik\theta} \\ - \sum_{-\infty}^{-2} \frac{\bar{a}'_k}{k+1} r^{k+1} e^{-i(k+2)\theta} - \sum_0^{\infty} \frac{\bar{a}'_k}{k+1} r^{k+1} e^{-i(k+1)\theta} \\ + i\theta e^{-i\theta} (\kappa a_{-1} + \bar{a}'_{-1}) \quad (2-4')$$

where $(\kappa a_{-1} + \bar{a}'_{-1}) = 0$ by Eq.(2-9).

Finally, we obtain the series solution for u from the real part of Eq.(2-4') and the solution for v from the imaginary part.

$$\begin{aligned}
2\mu u = & \sum_{-\infty}^{-2} \frac{r^{k+1}}{k+1} [\alpha_k \cos k\theta - \beta_k \sin k\theta] + \ln r [(\kappa\alpha_{-1} - \gamma_{-1}) \cos \theta + (\kappa\beta_{-1} - \delta_{-1}) \sin \theta] \\
& + \sum_0^{\infty} \frac{r^{k+1}}{k+1} [\alpha_k \cos k\theta - \beta_k \sin k\theta] - \sum_{-\infty}^{\infty} r^{k+1} [\alpha_k \cos k\theta - \beta_k \sin k\theta] \\
& - \sum_{-\infty}^{-2} \frac{r^{k+1}}{k+1} [\gamma_k \cos(k\theta+2\theta) - \delta_k \sin(k\theta+2\theta)] \\
& - \sum_0^{\infty} \frac{r^{k+1}}{k+1} [\gamma_k \cos(k\theta+2\theta) - \delta_k \sin(k\theta+2\theta)] \tag{2-4a}
\end{aligned}$$

$$\begin{aligned}
2\mu v = & \sum_{-\infty}^{-2} \frac{r^{k+1}}{k+1} [\alpha_k \sin k\theta + \beta_k \cos k\theta] + \ln r [(\kappa\beta_{-1} + \delta_{-1}) \cos \theta + (\gamma_{-1} - \kappa\alpha_{-1}) \sin \theta] \\
& + \sum_0^{\infty} \frac{r^{k+1}}{k+1} [\alpha_k \sin k\theta + \beta_k \cos k\theta] + \sum_{-\infty}^{\infty} r^{k+1} [\alpha_k \sin k\theta + \beta_k \cos k\theta] \\
& + \sum_{-\infty}^{-2} \frac{r^{k+1}}{k+1} [\gamma_k \sin(k\theta+2\theta) + \delta_k \cos(k\theta+2\theta)] \\
& + \sum_0^{\infty} \frac{r^{k+1}}{k+1} [\gamma_k \sin(k\theta+2\theta) + \delta_k \cos(k\theta+2\theta)] \tag{2-4b}
\end{aligned}$$

The form for Eqs. (2-4a) and (2-4b) is obtained using $a_k = \alpha_k + i\beta_k$ and $a'_k = \gamma_k + i\delta_k$.

Since the Fortran system cannot handle negative subscripts for subscripted variables, we will later convert the stress equations (2-26, 2-27, 2-28) and the displacement equations (2-4a, 2-4b) into forms not using negative indices.

Summary

Stresses

σ_θ	Equation (2-26)
σ_r	" (2-27)
$\tau_{r\theta}$	" (2-28)

Displacements

u Equation (2-4a)

v " (2-4b)

The above equations for stress and displacement are in terms of series coefficients α_k , β_k , γ_k , and δ_k which are the real and imaginary parts of coefficients a_k and a'_k . The coefficients a_k and a'_k are in turn expressed in terms of A'_k and A''_k , the Fourier loading coefficients; and these loading coefficients are determined from the distribution of σ_r and $\tau_{r\theta}$ on L_1 and L_2 . Thus, our next task is to develop a useful procedure of determining A'_k and A''_k from the given loading on L_1 and L_2 . The loading on the boundaries may be in graphical or numerical form and the usual formal determination of Fourier coefficients will not suffice.

REPRESENTATION OF σ_r and $\tau_{r\theta}$ ON BOUNDARIES
BY COMPLEX FOURIER SERIES

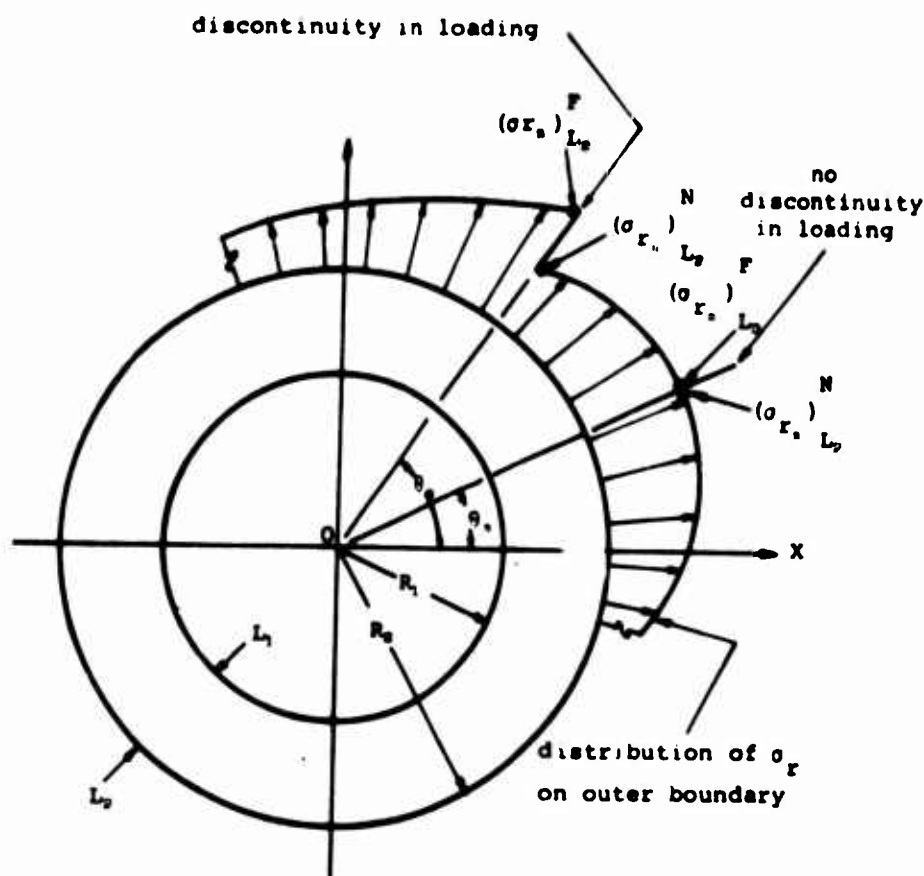


Figure 15. Representative distribution of one of the stresses (σ_r) on one boundary showing the "double value" nomenclature.

Our next task is to spell out a detailed procedure for obtaining the complex Fourier coefficients A_k' and A_k'' in Eqs. (2-6) which are repeated here for convenience.

$$\sigma_r - i\tau_{r\theta} = \sum_{-8}^8 A_k' e^{ik\theta} \text{ on } L_1$$

$$\sigma_r - i\tau_{r\theta} = \sum_{-8}^8 A_k'' e^{ik\theta} \text{ on } L_2$$

(repeated) (2-6)

where

$A'_k = \eta_k + i\zeta_k =$ complex Fourier coefficients on inner boundary.

$A''_k = \rho_k + i\nu_k =$ complex Fourier coefficients on outer boundary.

In the usual manner, we obtain the Fourier coefficients by multiplying both sides of each of Eq. (2-6) by $e^{-in\theta}$ and integrating with respect to θ from 0 to 2π .

$$\int_0^{2\pi} (\sigma_r - i\tau_{r\theta})_{L_1} e^{-in\theta} d\theta = \sum_{k=-\infty}^{\infty} A'_k \int_0^{2\pi} e^{i(k-n)\theta} d\theta = 2\pi A'_k$$

$$\text{since } \int_0^{2\pi} e^{i(k-n)\theta} d\theta = 0 \text{ if } n \neq k \\ = 2\pi \text{ if } n = k$$

$$\therefore A'_k = \frac{1}{2\pi} \int_0^{2\pi} (\sigma_r - i\tau_{r\theta})_{L_1} e^{-ik\theta} d\theta = \frac{1}{2\pi} \int_0^{2\pi} (\sigma_r - i\tau_{r\theta})_{L_1} (\cos k\theta - i\sin k\theta) d\theta$$

$$= \frac{1}{2\pi} \int_0^{2\pi} \left[(\sigma_r \cos k\theta - \tau_{r\theta} \sin k\theta) - i(\tau_{r\theta} \cos k\theta + \sigma_r \sin k\theta) \right]_{L_1} d\theta$$

$$\eta_k = \frac{1}{2\pi} \int_0^{2\pi} (\sigma_r \cos k\theta - \tau_{r\theta} \sin k\theta)_{L_1} d\theta$$

(2-29)

$$\zeta_k = -\frac{1}{2\pi} \int_0^{2\pi} (\tau_{r\theta} \cos k\theta + \sigma_r \sin k\theta)_{L_1} d\theta$$

In similar fashion, we can write expressions for A''_k , ρ_k , and ν_k .

$$A''_k = \frac{1}{2\pi} \int_0^{2\pi} \left[(\sigma_r \cos k\theta - \tau_{r\theta} \sin k\theta) - i(\tau_{r\theta} \cos k\theta + \sigma_r \sin k\theta) \right]_{L_2} d\theta$$

$$\rho_k = \frac{1}{2\pi} \int_0^{2\pi} (\sigma_r \cos k\theta - \tau_{r\theta} \sin k\theta)_{L_2} d\theta$$

(2-30)

$$\nu_k = -\frac{1}{2\pi} \int_0^{2\pi} (\tau_{r\theta} \cos k\theta + \sigma_r \sin k\theta)_{L_2} d\theta$$

In case the loading is given in functional form, the coefficients can be found from Eqs. (2-29) and (2-30) and then read directly into the computer program. A subprogram to compute these coefficients could be used. In general, however, it is anticipated that the loading stresses on the boundaries will be in graphical or numerical form; the remainder of the development of this division will be aimed at obtaining the coefficients ρ , ν , η , ζ for this situation.

A representative distribution of one stress (σ_r) on one boundary is shown in Fig. 15. We will represent the given boundary load stresses as segments of linear functions of θ between equally spaced divisions of the boundaries. These linear functions of θ would be straight lines on a rectangular stress - vs. - θ plot, but do not plot as straight lines on one such as Fig. 15. In order to allow for discontinuities, each load stress on each boundary is assigned two values, a "near" value and a "far" value. These are, of course, the values of the considered stress just prior to and just after the discontinuity respectively. In a symbol such as $(\sigma_r)_{L_2}^F$; n refers to the n^{th} division point of the boundary, L_2 refers to the outside boundary, and F refers to the value of σ_r on the "far" side of the discontinuity. At most division points, there will be no discontinuity and the "near" value of the stress will be equal to the "far" value.

Loading Coefficients for Case where Discontinuities May Exist

For each linear segment of a loading stress, we may express this stress in the form given by Eq. (m).

$$(\sigma_r)_n^{L_2} = (\sigma_r)_{L_2}^F + \frac{\left[(\sigma_r)_{L_2}^N - (\sigma_r)_{L_2}^F \right] (\theta - \theta_n)}{(\theta_{n+1} - \theta_n)} \quad (m)$$

where $(\sigma_r)_n^{L_2} = \sigma_r$ between θ_n and θ_{n+1} on outer boundary at the angle θ .

To reduce writing, we shall develop the expression for ρ_k only and it is understood that we are working only with loading stresses on the outer boundary. From the first of Eqs. (2-30), we express ρ_k by integrating over each segment, one after the other, until the integration around the entire boundary is complete.

$$2\pi\rho_k = \sum_{n=0}^M \int_{\theta_n}^{\theta_{n+1}} \left[(\sigma_r)_{L_2}^n \cos k\theta - (\tau_{r\theta})_{L_2}^n \sin k\theta \right] d\theta \quad (n)$$

where $M+1$ = number of equal subdivisions of the circle.

Into Eq. (n) are now substituted the linear expressions for $(\sigma_r)_{L_2}^n$ and $(\tau_{r\theta})_{L_2}^n$ in the form given by Eq. (m). For convenience, we shall represent σ_r by σ and $\tau_{r\theta}$ by τ ; also we understand that both σ and τ are the loading stresses on L_2 .

$$2\pi\rho_k = \sum_{n=0}^M \int_{\theta_n}^{\theta_{n+1}} \left\{ \left[\sigma_n^F + \left(\frac{\sigma_{n+1}^N - \sigma_n^F}{\Delta\theta} \right) (\theta - \theta_n) \right] \cos k\theta - \left[\tau_n^F + \left(\frac{\tau_{n+1}^N - \tau_n^F}{\Delta\theta} \right) (\theta - \theta_n) \right] \sin k\theta \right\} d\theta$$

where $\theta_{n+1} - \theta_n = \Delta\theta$ since each boundary is divided into $M+1$ equal parts.

$$\begin{aligned} &= \sum_{n=0}^M \int_{\theta_n}^{\theta_{n+1}} \left\{ \left[\sigma_n^F - \theta_n \left(\frac{\sigma_{n+1}^N - \sigma_n^F}{\Delta\theta} \right) \right] \cos k\theta + \left(\frac{\sigma_{n+1}^N - \sigma_n^F}{\Delta\theta} \right) \theta \cos k\theta - \left[\tau_n^F - \theta_n \left(\frac{\tau_{n+1}^N - \tau_n^F}{\Delta\theta} \right) \right] \sin k\theta + \left(\frac{\tau_{n+1}^N - \tau_n^F}{\Delta\theta} \right) \theta \sin k\theta \right\} d\theta \\ &= \sum_{n=0}^M \left\{ \left[\sigma_n^F - \theta_n \left(\frac{\sigma_{n+1}^N - \sigma_n^F}{\Delta\theta} \right) \right] \left[\frac{\sin k\theta}{k} \right]_{\theta_n}^{\theta_{n+1}} + \left(\frac{\sigma_{n+1}^N - \sigma_n^F}{\Delta\theta} \right) \left[\frac{\theta}{k} \sin k\theta + \frac{1}{k^2} \cos k\theta \right]_{\theta_n}^{\theta_{n+1}} \right. \\ &\quad \left. + \left[\tau_n^F - \theta_n \left(\frac{\tau_{n+1}^N - \tau_n^F}{\Delta\theta} \right) \right] \left[\frac{\cos k\theta}{k} \right]_{\theta_n}^{\theta_{n+1}} + \left(\frac{\tau_{n+1}^N - \tau_n^F}{\Delta\theta} \right) \left[\frac{\theta}{k} \cos k\theta - \frac{1}{k^2} \sin k\theta \right]_{\theta_n}^{\theta_{n+1}} \right\} \end{aligned}$$

We now evaluate the above relation for $2\pi\rho_k$ in terms of the indicated limits and then cancel all possible terms.

$$2\pi\rho_k = \frac{1}{k} \sum_{n=0}^M \left\{ \sigma_{n+1}^N \sin k\theta_{n+1} - \sigma_n^F \sin k\theta_n - \frac{1}{k} \left(\frac{\sigma_{n+1}^N - \sigma_n^F}{\Delta\theta} \right) (\cos k\theta_{n+1} - \cos k\theta_n) + \tau_{n+1}^N \cos k\theta_{n+1} - \tau_n^F \cos k\theta_n - \frac{1}{k} \left(\frac{\tau_{n+1}^N - \tau_n^F}{\Delta\theta} \right) (\sin k\theta_{n+1} - \sin k\theta_n) \right\} \quad (p)$$

$$\text{for } k = \pm 1, \pm 2, \dots, \pm\infty$$

By writing out several terms of the above series we see that we can reassemble the terms into a more useful form as given by Eq. (2-31p). Notice that $\sigma_0 = \sigma_{n+1}$ and $\tau_0 = \tau_{n+1}$.

$$\rho_k = \frac{1}{2k\pi} \sum_{n=1}^{M+1} \left[(\sigma_{r_n}^N - \sigma_{r_n}^F) \sin k\theta_n + \left(\frac{\sigma_{r_n}^N + \sigma_{r_n}^F - \sigma_{r_{n-1}}^F - \sigma_{r_{n+1}}^N}{k\Delta\theta} \right) \cos k\theta_n \right] \\ + \frac{1}{2k\pi} \sum_{n=1}^{M+1} \left[(\tau_{r_{\theta_n}}^N - \tau_{r_{\theta_n}}^F) \cos k\theta_n - \left(\frac{\tau_{r_{\theta_n}}^N + \tau_{r_{\theta_n}}^F - \tau_{r_{\theta_{n-1}}}^F - \tau_{r_{\theta_{n+1}}}^N}{k\Delta\theta} \right) \sin k\theta_n \right] \\ \text{for } k = \pm 1, \pm 2, \dots, \pm\infty \quad (2-31p)$$

Since this procedure is designed for use with Fortran programming of digital computers, we must avoid the use of subscripted variables with negative subscripts. Therefore, we shall relabel ρ_k , v_k , η_k , and ζ_k in Eqs. (2-29) and (2-30) for negative k as $\underline{\rho}_k$, \underline{v}_k , $\underline{\eta}_k$, and $\underline{\zeta}_k$. If $-k$ is substituted into Eq. (2-31p) for k , we obtain no change in the first \sum but we obtain a sign change for each part of the second \sum . Therefore, we do not need to compute ρ_k separately; if we represent ρ_k as

$$\rho_k = \sum_{\sigma}^{\rho} + \sum_{\tau}^{\rho}, \quad (k = 1, 2, \dots, \infty)$$

then we will find $\underline{\rho}_k$ by

$$\underline{\rho}_k = \sum_{\sigma}^{\rho} - \sum_{\tau}^{\rho}, \quad (k = 1, 2, \dots, \infty) \quad (2-31\underline{p})$$

We can compute v_k and \underline{v}_k in a very similar manner to that above for ρ_k and $\underline{\rho}_k$ to obtain Eqs. (2-31v) and (2-31\underline{v})

$$\begin{aligned}
v_k &= -\frac{1}{2k\pi} \sum_{n=1}^{M+1} \left[(\tau_{r\theta_n}^N - \tau_{r\theta_n}^F) \sin k\theta_n + \left(\frac{\tau_{r\theta_n}^N + \tau_{r\theta_n}^F - \tau_{r\theta_{n-1}}^F - \tau_{r\theta_{n+1}}^N}{k\Delta\theta} \right) \cos k\theta_n \right] \\
&\quad + \frac{1}{2k\pi} \sum_{n=1}^{M+1} \left[(\sigma_{r_n}^N - \sigma_{r_n}^F) \cos k\theta_n - \left(\frac{\sigma_{r_n}^N + \sigma_{r_n}^F - \sigma_{r_{n-1}}^F - \sigma_{r_{n+1}}^N}{k\Delta\theta} \right) \sin k\theta_n \right] \\
&= -\sum_{\tau}^v + \sum_{\sigma}^v \quad (2-31v)
\end{aligned}$$

$$\underline{v}_k = -\sum_{\tau}^v - \sum_{\sigma}^v \quad (k = 1, 2, \dots, \infty) \quad (2-31\underline{v})$$

The coefficients η , $\underline{\eta}$, ζ , and $\underline{\zeta}$ are computed in exactly the same way except that they are the Fourier coefficients for the inner boundary and thus are computed from the shear and normal loading stresses on L_1 .

$$\begin{aligned}
\eta_k &= \frac{1}{2k\pi} \sum_{n=1}^{M+1} \left[(\sigma_{r_n}^N - \sigma_{r_n}^F) \sin k\theta_n + \left(\frac{\sigma_{r_n}^N + \sigma_{r_n}^F - \sigma_{r_{n-1}}^F - \sigma_{r_{n+1}}^N}{k\Delta\theta} \right) \cos k\theta_n \right] \\
k &= 1, 2, \dots, \infty \\
&\quad + \frac{1}{2k\pi} \sum_{n=1}^{M+1} \left[(\tau_{r\theta_n}^N - \tau_{r\theta_n}^F) \cos k\theta_n - \left(\frac{\tau_{r\theta_n}^N + \tau_{r\theta_n}^F - \tau_{r\theta_{n-1}}^F - \tau_{r\theta_{n+1}}^N}{k\Delta\theta} \right) \sin k\theta_n \right] \\
&= \sum_{\sigma}^{\eta} + \sum_{\tau}^{\eta} \quad (k = 1, 2, \dots, \infty) \quad (2-31\eta)
\end{aligned}$$

$$\underline{\eta}_k = \sum_{\sigma}^{\eta} - \sum_{\tau}^{\eta} \quad (2-31\underline{\eta})$$

$$\begin{aligned}
\zeta_k &= -\frac{1}{2k\pi} \sum_{n=1}^{M+1} \left[(\tau_{r\theta_n}^N - \tau_{r\theta_n}^F) \sin k\theta_n + \left(\frac{\tau_{r\theta_n}^N + \tau_{r\theta_n}^F - \tau_{r\theta_{n-1}}^F - \tau_{r\theta_{n+1}}^N}{k\Delta\theta} \right) \cos k\theta_n \right] \\
k &= 1, 2, \dots, \infty \\
&\quad + \frac{1}{2k\pi} \sum_{n=1}^{M+1} \left[(\sigma_{r_n}^N - \sigma_{r_n}^F) \cos k\theta_n - \left(\frac{\sigma_{r_n}^N + \sigma_{r_n}^F - \sigma_{r_{n-1}}^F - \sigma_{r_{n+1}}^N}{k\Delta\theta} \right) \sin k\theta_n \right] \\
&= -\sum_{\tau}^{\zeta} + \sum_{\sigma}^{\zeta} \quad (2-31\zeta)
\end{aligned}$$

$$\underline{\zeta}_k = - \sum_{\tau} \zeta - \sum_{\sigma} \zeta \quad (k = 1, 2, \dots \infty) \quad (2-31\underline{\zeta})$$

Notice that, if discontinuities are present in the loading stresses, the coefficients diminish as $\frac{1}{k}$. This is a well known result in Fourier analysis.

Loading Coefficients for Case of No Discontinuities

At this point, it should be noted that the first version of the Fortran program was based on the assumption that there were no discontinuities in the loading stresses; for this case, the "near" and "far" values of any loading stress are the same at each division point and we can eliminate the superscripts N and F. Thus, for no loading stress discontinuities we obtain from Eqs. (2-31) the following expressions for ρ , $\underline{\rho}$, ν , $\underline{\nu}$, η , $\underline{\eta}$, ζ , and $\underline{\zeta}$ for $k = 1, 2, 3, \dots \infty$:

$$\begin{aligned} \rho_k &= \frac{1}{2\pi\Delta\theta k^2} \sum_{n=1}^{M+1} (2\sigma_{r_n} - \sigma_{r_{n-1}} - \sigma_{r_{n+1}})_{L_2} \cos k\theta_n \\ &\quad - \frac{1}{2\pi\Delta\theta k^2} \sum_{n=1}^{M+1} (2\tau_{r\theta_n} - \tau_{r\theta_{n-1}} - \tau_{r\theta_{n+1}})_{L_2} \sin k\theta_n \quad (2-31\underline{\rho})' \\ &= \sum_{\sigma} \rho' - \sum_{\tau} \rho' \end{aligned}$$

$$\underline{\rho}_k = \sum_{\sigma} \rho' + \sum_{\tau} \rho' \quad (2-31\underline{\rho})'$$

$$\begin{aligned} \nu_k &= - \frac{1}{2\pi\Delta\theta k^2} \sum_{n=1}^{M+1} (2\tau_{r\theta_n} - \tau_{r\theta_{n-1}} - \tau_{r\theta_{n+1}})_{L_2} \cos k\theta_n \\ &\quad - \frac{1}{2\pi\Delta\theta k^2} \sum_{n=1}^{M+1} (2\sigma_{r_n} - \sigma_{r_{n-1}} - \sigma_{r_{n+1}})_{L_2} \sin k\theta_n \quad (2-31\underline{\nu})' \\ &= - \sum_{\tau} \nu' + \sum_{\sigma} \nu' \end{aligned}$$

$$\underline{v}_k = - \sum_{\tau}' v - \sum_{\sigma}' v \quad (2-31\underline{v})'$$

$$\eta_k = \frac{1}{2\pi\Delta\theta k^2} \sum_{n=1}^{M+1} (2\sigma_{r_n} - \sigma_{r_{n-1}} - \sigma_{r_{n+1}})_{L_1} \cos k\theta_n$$

$$- \frac{1}{2\pi\Delta\theta k^2} \sum_{n=1}^{M+1} (2\tau_{r\theta_n} - \tau_{r\theta_{n-1}} - \tau_{r\theta_{n+1}})_{L_1} \sin k\theta_n \quad (2-31\underline{\eta})'$$

$$= \sum_{\sigma}' \eta - \sum_{\tau}' \eta$$

$$\underline{\eta}_k = \sum_{\sigma}' \eta + \sum_{\tau}' \eta \quad (2-31\underline{\eta})'$$

$$\zeta_k = - \frac{1}{2\pi\Delta\theta k^2} \sum_{n=1}^{M+1} (2\tau_{r\theta_n} - \tau_{r\theta_{n-1}} - \tau_{r\theta_{n+1}})_{L_1} \cos k\theta_n$$

$$- \frac{1}{2\pi\Delta\theta k^2} \sum_{n=1}^{M+1} (2\sigma_{r_n} - \sigma_{r_{n-1}} - \sigma_{r_{n+1}})_{L_1} \sin k\theta_n \quad (2-31\underline{\zeta})'$$

$$= - \sum_{\tau}' \zeta + \sum_{\sigma}' \zeta$$

$$\underline{\zeta}_k = - \sum_{\tau}' \zeta - \sum_{\sigma}' \zeta \quad (2-31\underline{\zeta})'$$

Notice that, for no loading discontinuities, the coefficients diminish as $\frac{1}{k^2}$, this fact is also well known in regard to Fourier series.

Loading Coefficients for k = 0

It is readily seen from Eq. (p) that Eqs. (2-31) and (2-31)' are invalid for k = 0 since k appears in the denominators; this situation was caused by the integration of Eq. (n) with the stresses in the form given by Eq. (m). Therefore, we must handle the zero terms separately beginning with expressions in the form of Eq. (n) for k = 0.

$$\begin{aligned}
 2\pi\rho_0 &= \sum_{n=0}^M \int_{\theta_n}^{\theta_{n+1}} (\sigma_r)_n^{L_2} d\theta \\
 &= \sum_{n=0}^M \int_{\theta_n}^{\theta_{n+1}} \left[\sigma_n^F + \frac{(\sigma_{n+1}^N - \sigma_n^F)}{\Delta\theta} (\theta - \theta_n) \right]_{L_2} d\theta \\
 &= \sum_{n=0}^M \left[\sigma_n^F \theta + \frac{(\sigma_{n+1}^N - \sigma_n^F)}{\Delta\theta} \left(\frac{\theta^2}{2} - \theta_n \theta \right) \right]_{\theta_n}^{\theta_{n+1}} \\
 &= \sum_{n=0}^M \left\{ \sigma_n^F (\theta_{n+1} - \theta_n) + \frac{(\sigma_{n+1}^N - \sigma_n^F)}{\Delta\theta} \left[\frac{\theta_{n+1}^2 - \theta_n^2}{2} - \theta_n (\theta_{n+1} - \theta_n) \right] \right\} \\
 &= \sum_{n=0}^M \sigma_n^F \Delta\theta + \frac{1}{2} (\sigma_{n+1}^N - \sigma_n^F) \Delta\theta \\
 &= \sum_{n=0}^M \frac{(\sigma_n^F + \sigma_{n+1}^N)}{2} \Delta\theta_{L_2}
 \end{aligned}$$

or
$$\rho_0 = \frac{\Delta\theta}{4\pi} \sum_{n=0}^M (\sigma_{r_n}^F + \sigma_{r_{n+1}}^N)_{L_2} \quad (2-31\rho_0)$$

Similarly,

$$\nu_0 = -\frac{\Delta\theta}{4\pi} \sum_{n=0}^M (\tau_{r\theta_n}^F + \tau_{r\theta_{n+1}}^N)_{L_2} \quad (2-31\nu_0)$$

$$\tau_0 = \frac{\Delta\theta}{4\pi} \sum_{n=0}^M (\sigma_{r_n}^F + \sigma_{r_{n+1}}^N)_{L_1} \quad (2-31\tau_0)$$

$$\zeta_0 = -\frac{\Delta\theta}{4\pi} \sum_{n=0}^M (\tau_{r\theta_n}^F + \tau_{r\theta_{n+1}}^N) L_1 \quad (2-31\zeta_0)$$

In case there are no discontinuities, the "near" and "far" values of any loading stress are alike at each division point and we can drop the N and F designation and obtain the following expressions for the zero terms of the loading coefficients:

$$\rho_0 = \frac{\Delta\theta}{2\pi} \sum_{n=0}^M (\sigma_{r_n}) L_2 \quad (2-31\rho_0)'$$

$$\nu_0 = -\frac{\Delta\theta}{2\pi} \sum_{n=0}^M (\tau_{r\theta_n}) L_2 \quad (2-31\nu_0)'$$

$$\eta_0 = \frac{\Delta\theta}{2\pi} \sum_{n=0}^M (\sigma_{r_n}) L_1 \quad (2-31\eta_0)'$$

$$\zeta_0 = -\frac{\Delta\theta}{2\pi} \sum_{n=0}^M (\tau_{r\theta_n}) L_1 \quad (2-31\zeta_0)'$$

REPRESENTATION OF COEFFICIENTS FOR $\phi(z)$ and $\psi(z)$
IN TERMS OF LOADING COEFFICIENTS

Our next task is to express a_k and a'_k , the coefficients in the series' for $\phi(z)$ and $\psi(z)$ respectively, in terms of $\rho_k, \underline{\rho}_k, \nu_k, \underline{\nu}_k, \eta_k, \underline{\eta}_k, \zeta_k,$ and $\underline{\zeta}_k$, which are the Fourier coefficients representing the loading on the boundaries. Since we have found these loading coefficients in the previous paragraph in terms of the given loading stresses, our solution will be formally complete when we obtain a_k and a'_k in terms of $\rho_k, \underline{\rho}_k, \nu_k,$ etc. Again, because the Fortran system cannot allow negative subscripts, we shall formulate all series' and their coefficients to avoid such use. Therefore, we shall employ the following equivalence of symbols:

$$\begin{aligned} A'_{-k} &= \underline{A}'_k = \underline{\eta}_k + i\underline{\zeta}_k \\ A''_{-k} &= \underline{A}''_k = \underline{\rho}_k + i\underline{\nu}_k \\ a_{-k} &= \underline{a}_k = \underline{\alpha}_k + i\underline{\beta}_k \\ a'_{-k} &= \underline{a}'_k = \underline{\gamma}_k + i\underline{\delta}_k \end{aligned}$$

Thus, we must express $\alpha, \beta, \gamma, \delta, \underline{\alpha}, \underline{\beta}, \underline{\gamma}, \underline{\delta}$ in terms of $\rho, \underline{\rho}, \nu, \underline{\nu}, \eta, \underline{\eta}, \zeta, \underline{\zeta}$.

Coefficients of $\phi(z)$

From the first of Eqs. (2-12) and Eq. (h) we obtain α_0 .

$$\alpha_0 = \text{Re } a_0 = \frac{R_2^2 (\rho_0 + i\nu_0) - R_1^2 (\eta_0 + i\zeta_0)}{2(R_2^2 - R_1^2)} = \frac{R_2^2 \rho_0 - R_1^2 \eta_0}{2(R_2^2 - R_1^2)} \quad (2-32a)$$

β_0 = any real number. Values for β_0 produce rigid body rotation (see earlier paragraph on displacements) and will be assigned for convenience after a specific problem is solved on the computer. During computation, $\beta_0 = 0$. (2-32a)'

We obtain α_1 and β_1 from Eq. (2-20) after changing A'_{-1} to \underline{A}'_1 , etc.

$$\begin{aligned}
a_1 &= \alpha_1 + i\beta_1 = \frac{\bar{A}_1' R_2^3 - \bar{A}_1' R_1^3}{R_2^3 - R_1^3} - \frac{2A_1' R_1}{(R_2^2 + R_1^2)(\kappa+1)} \\
&= \frac{R_2^3 (\rho_1 - i\nu_1) - R_1^3 (\eta_1 - i\zeta_1)}{R_2^3 - R_1^3} - \frac{2(\eta_1 + i\zeta_1) R_1}{(R_2^2 + R_1^2)(\kappa+1)} \\
\therefore \alpha_1 &= \frac{R_2^3 \rho_1 - R_1^3 \eta_1}{R_2^3 - R_1^3} - \frac{2\eta_1 R_1}{(R_2^2 + R_1^2)(\kappa+1)} \\
\beta_1 &= \frac{-R_2^3 \nu_1 + R_1^3 \zeta_1}{R_2^3 - R_1^3} - \frac{2\zeta_1 R_1}{(R_2^2 + R_1^2)(\kappa+1)}
\end{aligned} \tag{2-32b}$$

The remainder of the α_k and β_k for $k = 2, 3, \dots, \infty$ are computed from Eq. (2-21) with D_k given by Eq. (2-16).

$$\begin{aligned}
a_k &= \frac{(1+k)(R_2^2 - R_1^2)(A_k' R_2^{-k+2} - A_k' R_1^{-k+2}) - (R_2^{-2k+2} - R_1^{-2k+2})(\bar{A}_k' R_2^{k+2} - \bar{A}_k' R_1^{k+2})}{D_k} \\
&= \frac{(1+k)(R_2^2 - R_1^2)[(\rho_k + i\nu_k)R_2^{-k+2} - (\eta_k + i\zeta_k)R_1^{-k+2}]}{D_k} \\
&\quad - \frac{(R_2^{-2k+2} - R_1^{-2k+2})[(\rho_k - i\nu_k)R_2^{k+2} - (\eta_k - i\zeta_k)R_1^{k+2}]}{D_k} \\
\therefore \alpha_k &= \frac{(1+k)(R_2^2 - R_1^2)(\rho_k R_2^{-k+2} - \eta_k R_1^{-k+2}) - (R_2^{-2k+2} - R_1^{-2k+2})(\rho_k R_2^{k+2} - \eta_k R_1^{k+2})}{D_k} \\
\beta_k &= \frac{(1+k)(R_2^2 - R_1^2)(\nu_k R_2^{-k+2} - \zeta_k R_1^{-k+2}) + (R_2^{-2k+2} - R_1^{-2k+2})(\nu_k R_2^{k+2} - \zeta_k R_1^{k+2})}{D_k}
\end{aligned} \tag{2-32c}$$

We can determine $\underline{\alpha}_1$ and $\underline{\beta}_1$ from Eq. (2-18) and these terms are given below in Eqs. (2-33a)

$$\begin{aligned}
a_{-1} &= \underline{a}_1 = \underline{\alpha}_1 + i\underline{\beta}_1 = \frac{\bar{A}_1' R_1}{\kappa+1} = \frac{(\eta_1 - i\zeta_1) R_1}{\kappa+1} \\
\therefore \underline{\alpha}_1 &= \frac{\eta_1 R_1}{\kappa+1} \\
\underline{\beta}_1 &= \frac{-\zeta_1 R_1}{\kappa+1}
\end{aligned} \tag{2-33a}$$

The remainder of the $\underline{\alpha}_k$ and $\underline{\beta}_k$ for $k = 2, 3, \dots, \infty$ are also obtained from Eqs. (2-21) and (2-16) but with k replaced by $-k$ and utilizing the changed symbols. Note that $D_{-k} = D_k$.

$$\begin{aligned}
 a_{-k} &= \underline{a}_k = \underline{\alpha}_k + i\underline{\beta}_k \\
 &= \frac{(1-k)(R_2^2 - R_1^2)(\underline{A}_k R_2^{k+2} - \underline{A}'_k R_2^{k+2})}{D_k} \\
 &\quad - \frac{(R_2^{2k+2} - R_1^{2k+2})(\bar{A}'_k R_2^{-k+2} - \bar{A}_k R_1^{-k+2})}{D_k} \\
 \underline{\alpha}_k &= \frac{(1-k)(R_2^2 - R_1^2)(\underline{\rho}_k R_2^{k+2} - \underline{\eta}_k R_1^{k+2}) - (R_2^{2k+2} - R_1^{2k+2})(\underline{\rho}_k R_2^{-k+2} - \underline{\eta}_k R_1^{-k+2})}{D_k} \\
 &\hspace{25em} (2-33b) \\
 \underline{\beta}_k &= \frac{(1-k)(R_2^2 - R_1^2)(\underline{\nu}_k R_2^{k+2} - \underline{\zeta}_k R_1^{k+2}) + (R_2^{2k+2} - R_1^{2k+2})(\underline{\nu}_k R_2^{-k+2} - \underline{\zeta}_k R_1^{-k+2})}{D_k}
 \end{aligned}$$

For efficiency of computation, notice the common parts in Eqs. (2-32c) and (2-33b).

Coefficients of $\psi(z)$

We may obtain γ_k and δ_k for $k = 0, 1, 2, \dots, \infty$ from Eq. (2-22b) or Eq. (2-22c). As explained earlier, the use of Eq. (2-22b) resulted in loss of precision; therefore we shall use Eq. (2-22c). In some check problems, it was verified that it makes no difference which one of Eq. (2-22b) or Eq. (2-22c) is used as long as all components are accurately computed.

$$\begin{aligned}
 a'_k &= \gamma_k + i\delta_k = -(1+k)a_{k+2} + \underline{a}_{k+2} - A'_{k+2} \text{ for } k = 0, 1, 2, \dots, \infty \\
 &= -(1+k)(\alpha_{k+2} + i\beta_{k+2}) + (\underline{\alpha}_{k+2} - i\underline{\beta}_{k+2}) - (\rho_{k+2} + i\nu_{k+2})
 \end{aligned}$$

$$\therefore \gamma_k = -(1+k)\alpha_{k+2} + \underline{\alpha}_{k+2} - \rho_{k+2} \hspace{15em} (2-34)$$

$$\delta_k = -(1+k)\beta_{k+2} - \underline{\beta}_{k+2} - \nu_{k+2} \text{ for } k = 0, 1, 2, \dots, \infty$$

We obtain $\underline{\gamma}_1$ and $\underline{\delta}_1$ from Eq. (2-19).

$$a'_{-1} = \underline{a}'_1 = \underline{\gamma}_1 + i\underline{\delta}_1 = -\frac{\kappa A'_1 R_1}{1+\kappa} = -\frac{\kappa(\eta_1 + i\zeta_1)R_1}{1+\kappa}$$

$$\begin{aligned} \therefore \underline{y}_1 &= -\frac{\kappa \eta_0 R_1}{1+\kappa} \\ \underline{\delta}_1 &= -\frac{\kappa \zeta_0 R_1}{1+\kappa} \end{aligned} \quad (2-35a)$$

The second of Eqs. (2-12) gives \underline{y}_2 and $\underline{\delta}_2$.

$$\begin{aligned} a'_{-2} = \underline{a}'_2 &= \underline{y}_2 + i\underline{\delta}_2 = \frac{R_1^2 R_2^2 (A'_0 - A_0')}{R_2^2 - R_1^2} \\ &= \frac{R_1^2 R_2^2}{R_2^2 - R_1^2} (\rho_0 + i\nu_0 - \eta_0 - i\zeta_0) \\ \therefore \underline{y}_2 &= \frac{R_1^2 R_2^2}{R_2^2 - R_1^2} (\rho_0 - \eta_0) \\ \underline{\delta}_2 &= \frac{R_1^2 R_2^2}{R_2^2 - R_1^2} (\nu_0 - \zeta_0) \end{aligned} \quad (2-35b)$$

The remainder of the \underline{y}_k and $\underline{\delta}_k$ are found from Eq. (2-22b) with k replaced by $-k$ and using the change of symbols to eliminate negative subscripts.

$$\begin{aligned} a'_{-k} = \underline{a}'_k &= \underline{y}_k + i\underline{\delta}_k = (k-1)R_1^2 a_{k-2} + \bar{a}_{k-2} R_1^{2k-2} - A'_{k-2} R_1^k \\ &= (k-1)R_1^2 \underline{a}_{k-2} + \bar{a}_{k-2} R_1^{2k-2} - \underline{A}'_{k-2} R_1^k \\ &= (k-1)R_1^2 (\underline{\alpha}_{k-2} + i\underline{\beta}_{k-2}) + (\alpha_{k-2} - i\beta_{k-2}) R_1^{2k-2} - (\underline{\eta}_{k-2} + i\underline{\zeta}_{k-2}) R_1^k \\ \therefore \underline{y}_k &= (k-1)R_1^2 \underline{\alpha}_{k-2} + \alpha_{k-2} R_1^{2k-2} - \underline{\eta}_{k-2} R_1^k \\ \underline{\delta}_k &= (k-1)R_1^2 \underline{\beta}_{k-2} - \beta_{k-2} R_1^{2k-2} - \underline{\zeta}_{k-2} R_1^k \end{aligned} \quad (2-35c)$$

for $k = 3, 4, \dots, \infty$

Again it was found in some check problems that \underline{y}_k and $\underline{\delta}_k$ could be found from Eq. (2-35c) based on Eq. (2-22b) or they could be found from a relation corresponding to Eq. (2-35c) based on Eq. (2-22c); both methods gave the same values for \underline{y}_k and $\underline{\delta}_k$ if the components were accurate. Here, however, it is better to compute with R_1 included because two terms in each of Eq. (2-35c) contain R_1 to positive exponents in k and these two terms become negligible compared to the other term for large k .

All that remains now is to express our stresses and displacements within the ring in terms of series' using no negative subscripts.

**FINAL EXPRESSIONS FOR STRESSES AND DISPLACEMENTS
USING NO NEGATIVE SUBSCRIPTS**

Stresses

From Eqs. (2-26), (2-27), and (2-28) we obtain the three stress components by splitting each series, substituting $-k$ for k in the part summed from $-\infty$ to -1 , and by employing the modified symbols used above to avoid negative subscripts.

$$\begin{aligned} \sigma_{\theta} = & \sum_{k=0}^{\infty} r^k \left[(2+k) (\underline{\alpha}_k \cos k\theta - \underline{\beta}_k \sin k\theta) + \underline{\gamma}_k \cos(k\theta+2\theta) - \underline{\delta}_k \sin(k\theta+2\theta) \right] \\ & + \sum_{k=1}^{\infty} r^{-k} \left[(2-k) (\underline{\alpha}_k \cos k\theta + \underline{\beta}_k \sin k\theta) + \underline{\gamma}_k \cos(2\theta-k\theta) - \underline{\delta}_k \sin(2\theta-k\theta) \right] \end{aligned} \quad (2-36a)$$

$$\begin{aligned} \sigma_r = & \sum_{k=0}^{\infty} r^k \left[(2-k) (\underline{\alpha}_k \cos k\theta - \underline{\beta}_k \sin k\theta) - \underline{\gamma}_k \cos(k\theta+2\theta) + \underline{\delta}_k \sin(k\theta+2\theta) \right] \\ & + \sum_{k=1}^{\infty} r^{-k} \left[(2+k) (\underline{\alpha}_k \cos k\theta + \underline{\beta}_k \sin k\theta) - \underline{\gamma}_k \cos(2\theta-k\theta) + \underline{\delta}_k \sin(2\theta-k\theta) \right] \end{aligned} \quad (2-36b)$$

$$\begin{aligned} \tau_{r\theta} = & \sum_{k=0}^{\infty} r^k \left[k\underline{\beta}_k \cos k\theta + k\underline{\alpha}_k \sin k\theta + \underline{\delta}_k \cos(k\theta+2\theta) + \underline{\gamma}_k \sin(k\theta+2\theta) \right] \\ & + \sum_{k=1}^{\infty} r^{-k} \left[-k\underline{\beta}_k \cos k\theta + k\underline{\alpha}_k \sin k\theta + \underline{\delta}_k \cos(2\theta-k\theta) + \underline{\gamma}_k \sin(2\theta-k\theta) \right] \end{aligned} \quad (2-36c)$$

Displacements

We find displacements from Eqs. (2-4a) and (2-4b) with no negative subscripts by the same sort of substitutions as were done for stresses.

$$\begin{aligned} 2\mu u = & \sum_{2}^{\infty} \frac{r^{1-k}}{1-k} (\underline{\alpha}_k \cos k\theta + \underline{\beta}_k \sin k\theta) + \left[(\kappa \underline{\alpha}_1 - \underline{\gamma}_1) \cos \theta + (\kappa \underline{\beta}_1 + \underline{\delta}_1) \sin \theta \right] \ln r \\ & + \sum_{0}^{\infty} \frac{r^{1+k}}{1+k} (\underline{\alpha}_k \cos k\theta - \underline{\beta}_k \sin k\theta) - \sum_{0}^{\infty} r^{1+k} (\underline{\alpha}_k \cos k\theta - \underline{\beta}_k \sin k\theta) \end{aligned}$$

$$- \sum_1^{\infty} r^{1-k} (\underline{\alpha}_k \cos k\theta + \underline{\beta}_k \sin k\theta) - \sum_2^{\infty} \frac{r^{1-k}}{1-k} [\underline{\gamma}_k \cos(2\theta - k\theta) - \underline{\delta}_k \sin(2\theta - k\theta)]$$

$$- \sum_0^{\infty} \frac{r^{1+k}}{1+k} [\underline{\gamma}_k \cos(k\theta + 2\theta) - \underline{\delta}_k \sin(k\theta + 2\theta)]$$

or

$$2\mu u = [(\kappa \underline{\alpha}_1 - \underline{\gamma}_1) \cos \theta + (\kappa \underline{\beta}_1 + \underline{\delta}_1) \sin \theta] \ln r - \underline{\alpha}_1 \cos \theta - \underline{\beta}_1 \sin \theta$$

$$+ \sum_2^{\infty} r^{1-k} \left(\frac{\kappa - 1 + k}{1-k} \right) (\underline{\alpha}_k \cos k\theta + \underline{\beta}_k \sin k\theta)$$

$$+ \sum_0^{\infty} r^{1+k} \left(\frac{\kappa - 1 - k}{1+k} \right) (\underline{\alpha}_k \cos k\theta - \underline{\beta}_k \sin k\theta)$$

$$- \sum_2^{\infty} \frac{r^{1-k}}{1-k} [\underline{\gamma}_k \cos(k\theta - 2\theta) + \underline{\delta}_k \sin(k\theta - 2\theta)]$$

$$- \sum_0^{\infty} \frac{r^{1+k}}{1+k} [\underline{\gamma}_k \cos(k\theta + 2\theta) - \underline{\delta}_k \sin(k\theta + 2\theta)] \quad (2-37a)$$

$$2\mu v = \sum_2^{\infty} \frac{\kappa r^{1-k}}{1-k} (-\underline{\alpha}_k \sin k\theta + \underline{\beta}_k \cos k\theta) + [(\kappa (\underline{\beta}_1 + \underline{\delta}_1) \cos \theta + (\underline{\gamma}_1 - \kappa \underline{\alpha}_1) \sin \theta] \ln r$$

$$+ \sum_0^{\infty} \frac{\kappa r^{1+k}}{1+k} (\underline{\alpha}_k \sin k\theta + \underline{\beta}_k \cos k\theta) + \sum_0^{\infty} r^{1+k} (\underline{\alpha}_k \sin k\theta + \underline{\beta}_k \cos k\theta)$$

$$+ \sum_1^{\infty} r^{1-k} (-\underline{\alpha}_k \sin k\theta + \underline{\beta}_k \cos k\theta) + \sum_2^{\infty} \frac{r^{1-k}}{1-k} [\underline{\gamma}_k \sin(2\theta - k\theta) + \underline{\delta}_k \cos(2\theta - k\theta)]$$

$$+ \sum_0^{\infty} \frac{r^{1+k}}{1+k} [\underline{\gamma}_k \sin(k\theta + 2\theta) + \underline{\delta}_k \cos(k\theta + 2\theta)]$$

or

$$\begin{aligned}
2\mu v = & \left[(\kappa \underline{\beta}_1 + \underline{\delta}_1) \cos \theta + (\underline{\gamma}_1 - \kappa \underline{\alpha}_1) \sin \theta \right] \ln r + \underline{\beta}_1 \cos \theta - \underline{\alpha}_1 \sin \theta \\
& + \sum_2^{\infty} r^{1-k} \left(\frac{\kappa+1-k}{1-k} \right) (-\underline{\alpha}_k \sin k\theta + \underline{\beta}_k \cos k\theta) \\
& + \sum_0^{\infty} r^{1+k} \left(\frac{\kappa+1+k}{1+k} \right) (\underline{\alpha}_k \sin k\theta + \underline{\beta}_k \cos k\theta) \\
& + \sum_2^{\infty} \frac{r^{1-k}}{1-k} \left[-\underline{\gamma}_k \sin(k\theta - 2\theta) + \underline{\delta}_k \cos(k\theta - 2\theta) \right] \\
& + \sum_0^{\infty} \frac{r^{1+k}}{1+k} \left[\underline{\gamma}_k \sin(k\theta + 2\theta) + \underline{\delta}_k \cos(k\theta + 2\theta) \right] \tag{2-37b}
\end{aligned}$$

In Eqs. (2-36a,b,c) and (2-37a,b) we obtain α and β from Eqs. (32a,b,c); $\underline{\alpha}$ and $\underline{\beta}$ from Eqs. (2-33a,b); γ and δ from Eqs. (2-34); and $\underline{\gamma}$ and $\underline{\delta}$ from Eqs. (2-35a,b,c).

Alternate Forms for Stresses

While Eqs. (2-36) are quite compact in appearance, there are some possible objections to the form of the expressions: (a) the trigonometric functions of θ have three separate values of argument, and (b) the coefficients γ , $\underline{\gamma}$, δ , and $\underline{\delta}$ must be computed and stored.

We would like to have only one value (namely, $k\theta$) of the trigonometric argument in the k^{th} term so that we have a true truncated Fourier series. Such a series forms the most accurate trigonometric series possible for k terms. It would be possible to make large errors if only a part of the Fourier coefficient of the last term were included; this could happen if a large missing part nearly canceled the included part to make a small total coefficient.

The reason we would like to eliminate γ , $\underline{\gamma}$, δ , and $\underline{\delta}$ is to reduce storage and to avoid some possible lack of precision in their computation. If all coefficients are to remain stored (as was done in first Fortran version), this elimination of necessary storage may be important.

Therefore, in Eqs. (2-26), (2-27), and (2-28), we shall re-assemble the various terms so as to have our series' expressed with coefficients of $\sin k\theta$ and $\cos k\theta$; in other words, the stresses themselves are just Fourier series' even though the Fourier coefficients are involved. We shall also express γ , $\underline{\gamma}$, δ , and $\underline{\delta}$ in terms of α , $\underline{\alpha}$, β , $\underline{\beta}$, ρ , $\underline{\rho}$, ν , and $\underline{\nu}$ from Eqs. (2-34) and two relations giving $\underline{\gamma}$ and $\underline{\delta}$ from Eq. (2-22c). These two relations (for $R_2 = 1$) are as follows:

$$\underline{\gamma}_k = (k-1)\underline{\alpha}_{k-2} + \alpha_{k-2} - \underline{\rho}_{k-2} \quad (q)$$

$$\underline{\delta}_k = (k-1)\underline{\beta}_{k-2} - \beta_{k-2} - \underline{\nu}_{k-2} \quad \text{for } k = 3, 4, \dots \infty$$

Omitting considerable algebra, we obtain the stresses from Eqs. (2-36a), (2-36b), and (2-36c) in the above indicated modified form as shown by Eqs. (2-38a), (2-38b), and (2-38c).

$$\begin{aligned} \sigma_\theta = & 2\alpha_0 + \frac{r^{-2}R_1^2(\rho_0 - \tau_0)}{1-R_1^2} \\ & + \left[(3r+r^{-3})\alpha_1 + (r^{-1}+2r^{-3})\underline{\alpha}_1 - \frac{r^{-1}R_1\tau_1}{1+R_1} - r^{-3}\rho_1 \right] \cos \theta \\ & + \left[-(3r+r^{-3})\beta_1 + (r^{-1}+2r^{-3})\underline{\beta}_1 + \frac{r^{-1}R_1\delta_1}{1+R_1} - r^{-3}\underline{\nu}_1 \right] \sin \theta \\ & + \sum_{k=2}^{\infty} \left\{ r^k \left[(2+k-kr^{-2}+r^{-2}+r^{-2k-2})\alpha_k - r^{-2}\rho_k \right] \right. \\ & \quad \left. + r^{-k} \left[(2-k+kr^{-2}+r^{-2}+r^{2k-2})\underline{\alpha}_k - r^{-2}\underline{\rho}_k \right] \right\} \cos k\theta \\ & + \sum_{k=2}^{\infty} \left\{ r^k \left[(-2-k+kr^{-2}-r^{-2}-r^{-2k-2})\beta_k + r^{-2}\nu_k \right] \right. \\ & \quad \left. + r^{-k} \left[(2-k+kr^{-2}+r^{-2}+r^{2k-2})\underline{\beta}_k - r^{-2}\underline{\nu}_k \right] \right\} \sin k\theta \quad (2-38a) \end{aligned}$$

$$\begin{aligned}
\sigma_r &= 2\alpha_0 - \frac{r^{-2} R_1^2 (\rho_0 - \eta_0)}{1 - R_1^2} \\
&+ \left[(r - r^{-3}) \alpha_1 + (3r^{-1} - 2r^{-3}) \underline{\alpha}_1 + \frac{r^{-1} \kappa R_1 \eta_1}{1 + \kappa} + r^{-3} \underline{\rho}_1 \right] \cos \theta \\
&+ \left[-(r - r^{-3}) \beta_1 + (3r^{-1} - 2r^{-3}) \underline{\beta}_1 - \frac{r^{-1} \kappa R_1 \zeta_1}{1 + \kappa} + r^{-3} \underline{\nu}_1 \right] \sin \theta \\
&+ \sum_{k=2}^{\infty} \left\{ r^k \left[(2 - k + \kappa r^{-2} - r^{-2} - r^{-2k-2}) \alpha_k + r^{-2} \rho_k \right] \right. \\
&\quad \left. + r^{-k} \left[(2 + k - r^{-2} - \kappa r^{-2} - r^{2k-2}) \underline{\alpha}_k + r^{-2} \underline{\rho}_k \right] \right\} \cos k\theta \\
&+ \sum_{k=2}^{\infty} \left\{ r^k \left[(-2 + k - \kappa r^{-2} + r^{-2} + r^{-2k-2}) \beta_k - r^{-2} \nu_k \right] \right. \\
&\quad \left. + r^{-k} \left[(2 + k - r^{-2} - \kappa r^{-2} - r^{2k-2}) \underline{\beta}_k + r^{-2} \underline{\nu}_k \right] \right\} \sin k\theta \quad (2-38b)
\end{aligned}$$

$$\begin{aligned}
\tau_{r\theta} &= \frac{r^{-2} R_1^2 (\nu_0 - \zeta_0)}{1 - R_1^2} \\
&+ \left[(r - r^{-3} R_1^4) \beta_1 + (-r^{-1} + 2r^{-3} R_1^2) \underline{\beta}_1 - \frac{r^{-1} \kappa R_1 \zeta_1}{1 + \kappa} - r^{-3} R_1^3 \underline{\zeta}_1 \right] \cos \theta \\
&+ \left[(r - r^{-3} R_1^4) \alpha_1 + (r^{-1} - 2r^{-3} R_1^2) \underline{\alpha}_1 - \frac{r^{-1} \kappa R_1 \eta_1}{1 + \kappa} - r^{-3} R_1^3 \underline{\eta}_1 \right] \sin \theta \\
&+ \sum_{k=2}^{\infty} \left\{ r^k \left[\beta_k (k - \kappa r^{-2} + r^{-2} - r^{-2k-2}) - r^{-2} \nu_k \right] \right. \\
&\quad \left. + r^{-k} \left[\underline{\beta}_k (-k + \kappa r^{-2} + r^{-2} - r^{2k-2}) - r^{-2} \underline{\nu}_k \right] \right\} \cos k\theta
\end{aligned}$$

$$\begin{aligned}
& + \sum_{k=2}^{\infty} \left\{ r^k \left[\alpha_k (k - kr^{-2} + r^{-2} - r^{-2k-2}) - r^{-2} \rho_k \right] \right. \\
& \quad \left. + r^{-k} \left[\underline{\alpha}_k (k - kr^{-2} - r^{-2} + r^{2k-2}) + r^{-2} \underline{\rho}_k \right] \right\} \sin k\theta \quad (2-38c)
\end{aligned}$$

In equations (2-38a, b, c) the value of $R_2 = 1$ has already been used; similarly, computations of α , β , $\underline{\alpha}$, and $\underline{\beta}$ should be done with R_2 set equal to 1.

For efficiency in computation, notice that in Eq.(2-38a) the coefficient of α_k is the negative of the coefficient β_k ; also that the coefficient of $\underline{\alpha}_k$ is the same as that of $\underline{\beta}_k$. These same remarks hold for Eq.(2-38b), and negatively for Eq.(2-38c). In fact, if the coefficient of α_k in Eq.(2-38a) is named XA, then the coefficient of α_k in Eq.(2-38b) is (4-XA); similarly if we label the coefficient of α_k in Eq.(2-38a) as XB, then the coefficient of $\underline{\alpha}_k$ in Eq.(2-38b) is (4-XB).

Alternate Forms for Displacements

For the same reasons as for stresses, we would like to express displacements with only one argument in θ in the general term and also eliminate the use of γ , δ , $\underline{\gamma}$, and $\underline{\delta}$. Again we do this by regrouping the terms of the several series and substituting for γ , δ , $\underline{\gamma}$, $\underline{\delta}$, their values from Eqs.(2-34), (2-35a,b), and (q). From Eqs.(2-37a) and (2-37b), we obtain Eqs.(2-39a) and (2-39b).

$$\begin{aligned}
2\mu u &= r(\kappa-1)\alpha_0 + \frac{r^{-1}R_1^2(\rho_0 - \eta_b)}{1-R_1^2} \\
&+ \left[(\kappa\underline{\alpha}_1 + \frac{\kappa\eta_b R_1}{1+\kappa}) \ln r + r^2 \left(\frac{\kappa-2}{2}\right)\alpha_1 - \underline{\alpha}_1 + \frac{r^{-2}}{2}(2\underline{\alpha}_1 + \alpha_1 - \rho_1) \right] \cos \theta \\
&+ \left[(\kappa\underline{\beta}_1 - \frac{\kappa\zeta_1 R_1}{1+\kappa}) \ln r - \underline{\beta}_1 - \frac{r^{-2}}{2}(2\underline{\beta}_1 - \beta_1 - \underline{\nu}_1) - r^2 \left(\frac{\kappa-2}{2}\right)\beta_1 \right] \sin \theta \\
&+ \sum_{k=2}^{\infty} \left\{ \frac{r^k}{k+1} \left[r(\kappa-1-k) + r^{-1}(1+k) + r^{-2k-1} \right] \alpha_k \right. \\
& \quad \left. + \frac{r^{-k}}{k+1} \left[r(\kappa-1-k) + r^{-1}(1+k) + r^{-2k-1} \right] \underline{\alpha}_k \right\}
\end{aligned}$$

$$\begin{aligned}
& + \frac{r^{-k}}{1-k} \left[r(\kappa-1+k) + (1-k)r^{-1} + r^{2k-1} \right] \underline{\alpha}_k - \frac{r^{-k-1}}{k+1} \underline{\rho}_k + \frac{r^{k-1}}{k-1} \underline{\rho}_k \} \cos k\theta \\
& + \sum_2^{\infty} \left\{ -\frac{r^k}{k+1} \left[r(\kappa-1-k) + (1+k)r^{-1} + r^{-2k-1} \right] \underline{\beta}_k \right. \\
& \left. + \frac{r^{-k}}{1-k} \left[r(\kappa-1+k) + (1-k)r^{-1} + r^{2k-1} \right] \underline{\beta}_k - \frac{r^{-k-1}}{1+k} \underline{\nu}_k - \frac{r^{k-1}}{k-1} \underline{\nu}_k \right\} \sin k\theta
\end{aligned} \tag{2-39a}$$

$$\begin{aligned}
2\mu v & = r(\kappa+1)\beta_0 - \frac{r^{-1}(\nu_0 - \zeta_0)R_1^2}{1-R_1^2} \\
& + \left[(\kappa\underline{\beta}_1 - \frac{\kappa\zeta_1 R_1}{1+\kappa}) \ln r + \underline{\beta}_1 + r^2 \left(\frac{\kappa+2}{2}\right) \beta_1 - \frac{r^{-2}}{2}(2\underline{\beta}_1 - \beta_1 - \underline{\nu}_1) \right] \cos \theta \\
& + \left[-(\kappa\underline{\alpha}_1 + \frac{\kappa\eta_1 R_1}{1+\kappa}) \ln r - \underline{\alpha}_1 + r^2 \left(\frac{\kappa+2}{2}\right) \alpha_1 + \frac{r^{-2}}{2}(2\underline{\alpha}_1 + \alpha_1 - \underline{\rho}_1) \right] \sin \theta \\
& + \sum_2^{\infty} \left\{ \frac{r^k}{1+k} \left[r(\kappa+1+k) + r^{-2k-1} - (1+k)r^{-1} \right] \underline{\beta}_k \right. \\
& \left. + \frac{r^{-k}}{1-k} \left[r(\kappa+1-k) - r^{2k-1} + (1-k)r^{-1} \right] \underline{\beta}_k + \frac{r^{-k-1}}{1+k} \underline{\nu}_k - \frac{r^{k-1}}{k-1} \underline{\nu}_k \right\} \cos k\theta \\
& + \sum_2^{\infty} \left\{ \frac{r^k}{1+k} \left[r(\kappa+1+k) + r^{-2k-1} - (1+k)r^{-1} \right] \underline{\alpha}_k \right. \\
& \left. + \frac{r^{-k}}{1-k} \left[-r(\kappa+1-k) + r^{2k-1} - (1-k)r^{-1} \right] \underline{\alpha}_k - \frac{r^{-k-1}}{1+k} \underline{\rho}_k - \frac{r^{k-1}}{k-1} \underline{\rho}_k \right\} \sin k\theta
\end{aligned} \tag{2-39b}$$

Modified Expressions for Stresses and Displacements to Avoid Overflow of Computer

Because the separate computation of such terms as r^{-k} (a number less than one to a large negative power) resulted in overflows in the computer, it was necessary to modify Eqs. (2-38a,b,c) and (2-39a,b) considerably. Basically, the indicated expressions were

expanded so as to perform algebraically the subtraction of large, approximately equal numbers rather than attempt to do it numerically by computer. Then the various terms in each expression were grouped in such a manner that no single term "ran away". This required a considerable amount of manipulation which will not be repeated here--only the final expressions are shown below. Actually, many individual terms in the expressions below tend to zero as k becomes large, and an underflow condition could result. Underflows were avoided, however, by programming tests prior to calculation--then if the number to be computed would underflow, the number was merely set to zero and not computed.

In the following modified forms for Eqs.(2-38a,b,c) and (2-39a,b), we shall use the following terminology to avoid excessive writing:

$$T1 = 1 + k - R_1^2 - kR_1^2$$

$$T2 = 1 - k - R_1^2 + kR_1^2$$

$$H = k^2 (2R_1^2 - R_1^4 - 1) + R_1^2 (R_1^{2k} - 2)$$

$$T9 = \frac{1}{1 + HR_1^{2k-2}}$$

$$\alpha_k = \left\{ R_1^{2k-2} [\rho_k (T1) - \underline{\rho}_k] - R_1^k [\eta_k (T1) + \underline{\eta}_k R_1^2] + \underline{\eta}_k R_1^{3k} + \underline{\rho}_k \right\} (T9)$$

$$\beta_k = \left\{ R_1^{2k-2} [\nu_k (T1) + \underline{\nu}_k] + R_1^k [-\zeta_k (T1) + \underline{\zeta}_k R_1^2] - \underline{\zeta}_k R_1^{3k} - \underline{\nu}_k \right\} (T9)$$

$$T3 = 2 + k - kr^{-2} + r^{-2}$$

$$T4 = 2 - k + kr^{-2} + r^{-2} + r^{2k-2}$$

$$T5 = \underline{\alpha}_k r^{-k}$$

$$= \left(\frac{R_1}{r}\right)^k \left\{ R_1^{k-2} [(T2) \underline{\rho}_k - \rho_k] - R_1^{2k} [(T2) \underline{\eta}_k + R_1^2 \eta_k] + \eta_k + \rho_k R_1^{3k} \right\} (T9)$$

$$T6 = r^{-k-2} (\alpha_k - \underline{\rho}_k)$$

$$= \left(\frac{R_1}{r}\right)^{k+2} \left\{ R_1^{k-4} [(T1) \rho_k - \underline{\rho}_k - H\underline{\rho}_k] - R_1^{-2} \eta_k (T1) - \underline{\eta}_k + \underline{\eta}_k R_1^{2k-2} \right\} (T9)$$

$$\begin{aligned}
T7 &= r^{-k} \underline{\beta}_k \\
&= \left(\frac{R_1}{r}\right)^k \left\{ R_1^{k-2} \left[(T2) \underline{v}_k - v_k \right] + R_1^{2k} \left[\underline{c}_k R_1^2 - \underline{c}_k (T2) \right] - \underline{c}_k - v_k R_1^{2k} \right\} (T9)
\end{aligned}$$

$$\begin{aligned}
T8 &= r^{-k-2} (-\beta_k - v_k) \\
&= \left(\frac{R_1}{r}\right)^{k+2} \left\{ R_1^{k-4} \left[\underline{v}_k - v_k (T1) - H \underline{v}_k \right] - R_1^{-2} \underline{c}_k (T1) + \underline{c}_k - \underline{c}_k R_1^{2k-2} \right\} (T9)
\end{aligned}$$

$$T10 = k - kr^{-2} + r^{-2}$$

$$T11 = -k + kr^{-2} + r^{-2} - r^{2k-2}$$

$$T12 = \frac{r(\kappa-1-k)}{k+1} + r^{-1}$$

$$T13 = r \frac{(\kappa-1+k)}{k-1} - r^{-1} + \frac{r^{2k-1}}{k-1}$$

$$T14 = r \frac{(\kappa+1+k)}{1+k} - r^{-1}$$

From Eq. (2-38a),

$$\begin{aligned}
\sigma_\theta &= 2\alpha_0 + \frac{r^{-2} R_1^2 (\rho_0 - \eta_0)}{1-R_1^2} \\
&+ \left[(3r + r^{-3}) \alpha_1 + (r^{-1} + 2r^{-3}) \underline{\alpha}_1 - \frac{r^{-1} \kappa R_1 \eta_1}{1+\kappa} - r^{-3} \underline{\rho}_1 \right] \cos \theta \\
&+ \left[-(3r + r^{-3}) \beta_1 + (r^{-1} + 2r^{-3}) \underline{\beta}_1 + \frac{r^{-1} \kappa R_1 \underline{c}_1}{1+\kappa} - r^{-3} \underline{v}_1 \right] \sin \theta \\
&+ \sum_{k=2}^{\infty} \left\{ r^k \left[(T3) \alpha_k - \rho_k r^{-2} \right] + (T4) (T5) + T6 \right\} \cos k\theta \\
&+ \sum_{k=2}^{\infty} \left\{ r^k \left[-(T3) \beta_k + r^{-2} v_k \right] + (T4) (T7) + T8 \right\} \sin k\theta \quad (2-38aa)
\end{aligned}$$

From Eq. (2-38b) ,

$$\begin{aligned}
 \sigma_r = & 2a_0 - \frac{r^{-2} R_1^2 (\rho_0 - \eta_0)}{1-R_1^2} \\
 & + \left[(r - r^{-3}) \alpha_1 + (3r^{-1} - 2r^{-3}) \underline{\alpha}_1 + \frac{r^{-1} \kappa R_1 \eta_1}{1+\kappa} + r^{-3} \underline{\rho}_1 \right] \cos \theta \\
 & + \left[-(r - r^{-3}) \beta_1 + (3r^{-1} - 2r^{-3}) \underline{\beta}_1 - \frac{r^{-1} \kappa R_1 \zeta_1}{1+\kappa} + r^{-3} \underline{\nu}_1 \right] \sin \theta \\
 & + \sum_{k=2}^{\infty} \left\{ r^k \left[(4-T3) \alpha_k + r^{-2} \rho_k \right] + (4-T4) (T5) - T6 \right\} \cos k\theta \\
 & + \sum_{k=2}^{\infty} \left\{ r^k \left[(T3-4) \beta_k - r^{-2} \nu_k \right] + (4-T4) (T7) - T8 \right\} \sin k\theta \quad (2-38bb)
 \end{aligned}$$

From Eq. (2-38c) ,

$$\begin{aligned}
 \tau_{r\theta} = & \frac{r^{-2} R_1^2 (\nu_0 - \zeta_0)}{1-R_1^2} \\
 & + \left[(r - r^{-3} R_1^4) \beta_1 + (-r^{-1} + 2r^{-3} R_1^2) \underline{\beta}_1 - \frac{r^{-1} \kappa R_1 \zeta_1}{1+\kappa} - r^{-3} R_1^2 \underline{\zeta}_1 \right] \cos \theta \\
 & + \left[(r - r^{-3} R_1^4) \alpha_1 + (r^{-1} - 2r^{-3} R_1^2) \underline{\alpha}_1 - \frac{r^{-1} \kappa R_1 \eta_1}{1+\kappa} - r^{-3} R_1^2 \underline{\eta}_1 \right] \sin \theta \\
 & + \sum_{k=2}^{\infty} \left\{ r^k \left[(T10) \beta_k - r^{-2} \nu_k \right] + (T11) (T7) + T8 \right\} \cos k\theta \\
 & + \sum_{k=2}^{\infty} \left\{ r^k \left[(T10) \alpha_k - r^{-2} \rho_k \right] - (T11) (T5) - T6 \right\} \sin k\theta \quad (2-38cc)
 \end{aligned}$$

From Eq. (2-39a) ,

$$\begin{aligned}
2\mu u = & r(\kappa-1)\alpha_0 + \frac{r^{-1}R_1^2(\rho_0-\eta_0)}{1-R_1^2} \\
& + \left[\left(\kappa\underline{\alpha}_1 + \frac{\kappa\eta_1 R_1}{1+\kappa} \right) \ln r - \underline{\alpha}_1 + \frac{r^{-2}}{2}(2\underline{\alpha}_1 + \alpha_1 - \underline{\rho}_1) + r^2 \left(\frac{\kappa-2}{2} \right) \alpha_1 \right] \cos \theta \\
& + \left[\left(\kappa\underline{\beta}_1 - \frac{\kappa\underline{\zeta}_1 R_1}{1+\kappa} \right) \ln r - \underline{\beta}_1 - \frac{r^{-2}}{2}(2\underline{\beta}_1 - \beta_1 - \underline{\nu}_1) - r^2 \left(\frac{\kappa-2}{2} \right) \beta_1 \right] \sin \theta \\
& + \sum_{k=2}^{\infty} \left\{ r^k (T12)\alpha_k - (T13)(T5) + \frac{r^{k-1}\rho_k}{k-1} + \frac{r(T6)}{k+1} \right\} \cos k\theta \\
& + \sum_{k=2}^{\infty} \left\{ -r^k (T12)\beta_k - (T13)(T7) - \frac{r^{k-1}\nu_k}{k-1} + \frac{r(T8)}{k+1} \right\} \sin k\theta
\end{aligned}
\tag{2-39aa}$$

From Eq. (2-39b) ,

$$\begin{aligned}
2\mu v = & r(\kappa+1)\beta_0 - \frac{r^{-1}(\nu_0 - \zeta_0)R_1^2}{1-R_1^2} \\
& + \left[\left(\kappa\underline{\beta}_1 - \frac{\kappa\underline{\zeta}_1 R_1}{1+\kappa} \right) \ln r + \underline{\beta}_1 + r^2 \left(\frac{\kappa+2}{2} \right) \beta_1 - \frac{r^{-2}}{2}(2\underline{\beta}_1 - \beta_1 - \underline{\nu}_1) \right] \cos \theta \\
& + \left[-\left(\kappa\underline{\alpha}_1 + \frac{\kappa\eta_1 R_1}{1+\kappa} \right) \ln r - \underline{\alpha}_1 + r^2 \left(\frac{\kappa+2}{2} \right) \alpha_1 + \frac{r^{-2}}{2}(2\underline{\alpha}_1 + \alpha_1 - \underline{\rho}_1) \right] \sin \theta \\
& + \sum_{k=2}^{\infty} \left\{ r^k (T14)\beta_k + (T13 - \frac{2r\kappa}{k-1})(T7) - \frac{r^{k-1}\nu_k}{k-1} - \frac{r}{k+1}(T8) \right\} \cos k\theta \\
& + \sum_{k=2}^{\infty} \left\{ r^k (T14)\alpha_k - (T13 - \frac{2r\kappa}{k-1})(T5) - \frac{r^{k-1}\rho_k}{k-1} + \frac{r}{k+1}(T6) \right\} \sin k\theta
\end{aligned}
\tag{2-39bb}$$

CHAPTER 2

THE COMPUTER PROGRAM AND ITS USE

General

The FORTRAN II computer program for solution of the thick cylindrical shell by the Muskhelishvili method will be described in such a manner that it can be used by persons quite unfamiliar with the theoretical development.

Basically, the program will yield stresses and displacements at all specified locations in the shell for any specific stress loading on the boundaries. This loading must place the shell in static equilibrium. Only plane problems can be solved; the loading stresses must not vary in the direction of the cylinder axis. Either or both boundaries may be loaded by radial stresses, shear stresses, or by both radial and shear stresses (in any case, overall static equilibrium must exist). There need not be symmetry in any of the loading stresses. The loading stresses may be continuous or discontinuous.

The analysis is based on approximation of the distributed loading stresses by straight line segments between equally spaced points (called division points). Therefore, to prepare a problem to be solved by this program, the ring is first divided angularly into some number (M) of equal parts. Next the numerical value of each loading stress at each division point is divided by the largest absolute value of any stress on any boundary. These stress ratios at each division point are the loading stress inputs to the program. Also, the program takes the outer radius to be unity and any other radius as the geometrically similar fraction thereof. Thus, there is a bit of dimensional analysis in first reducing the actual problem to proper computational form and then interpreting the results in terms of the actual problem. In all that follows here we are referring to these "reduced" or "program" stresses and dimensions.

THE PROGRAM PROPER

Brief Functional Outline

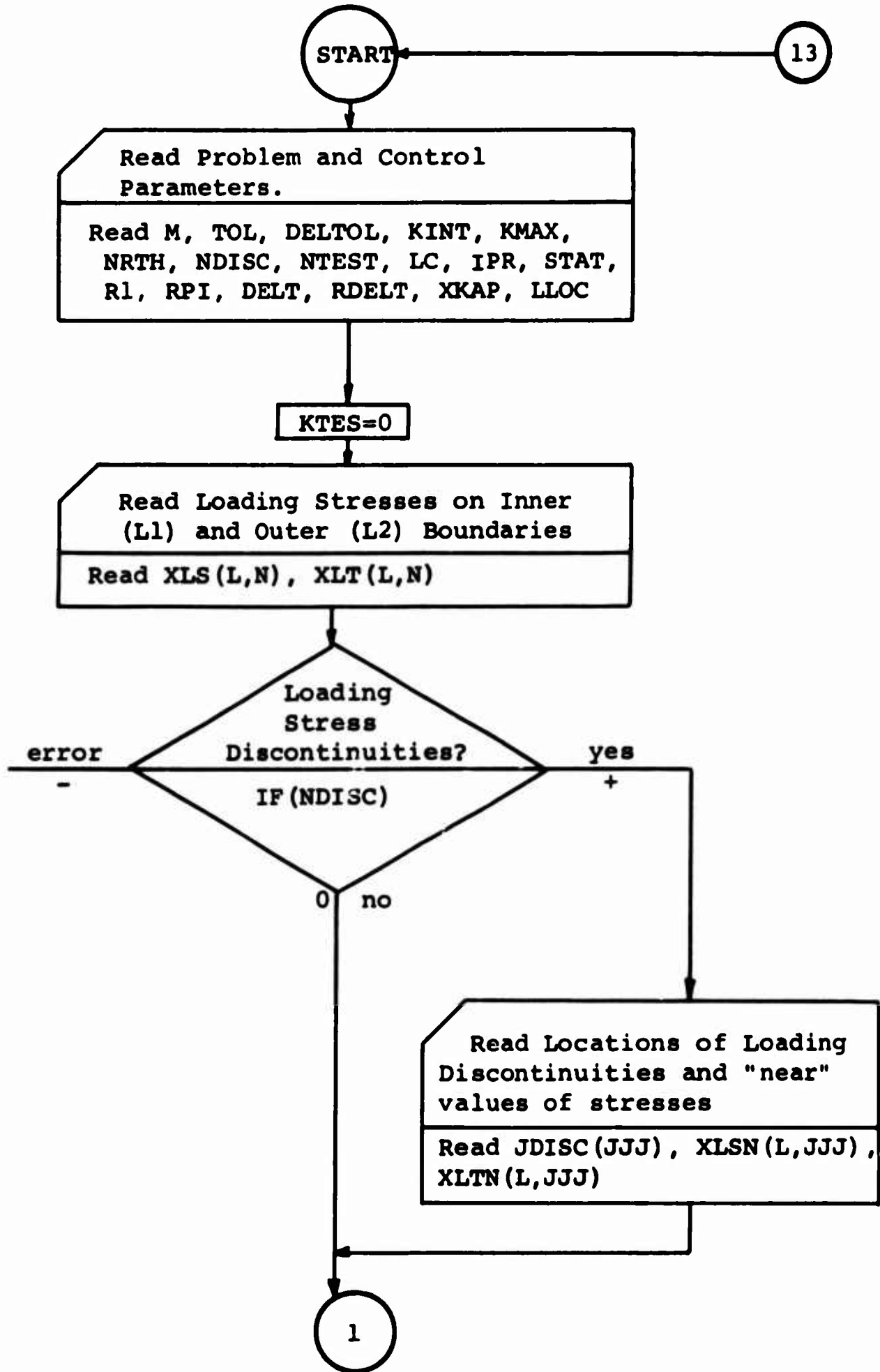
Initially the problem and control parameters are read in. then the loading stresses on both boundaries ("far" points) are entered. If any discontinuities exist, the "near" values of the stresses at all discontinuity points are read in. Next the locations at which stresses and displacements are to be computed are read. Certain boundary points are designated test points at which locations the computed radial and shear stresses must match the corresponding loading stresses within a certain tolerance--this is the fundamental criterion upon which is based the decision to proceed with more computation or to consider the problem solved and print results. The final data input is a table of sines and cosines of the angle for each division point.

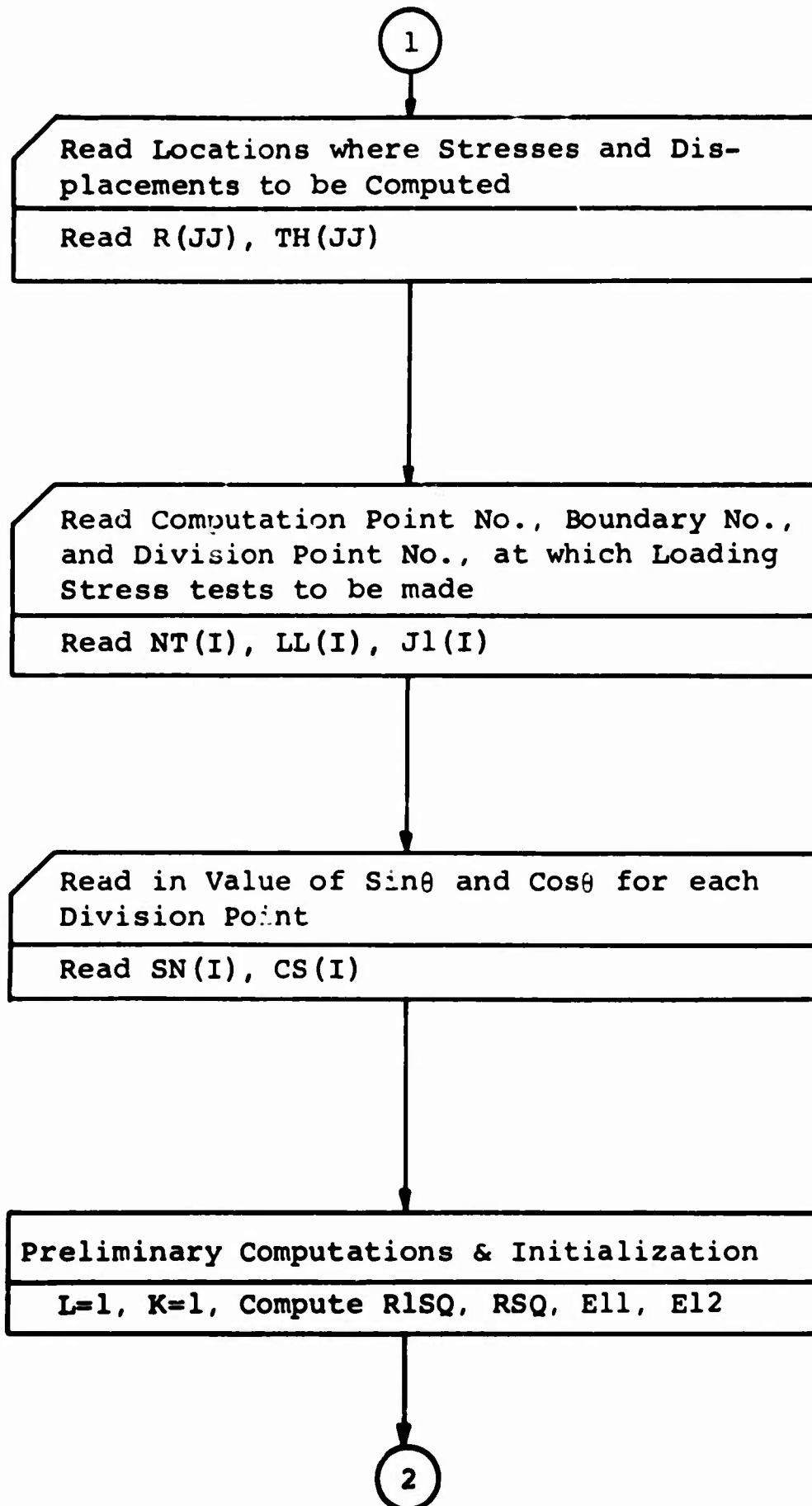
In case only one boundary is loaded, certain loading coefficients are zero. When such a loading condition exists, those loading coefficients are set to zero to avoid wasted computation time.

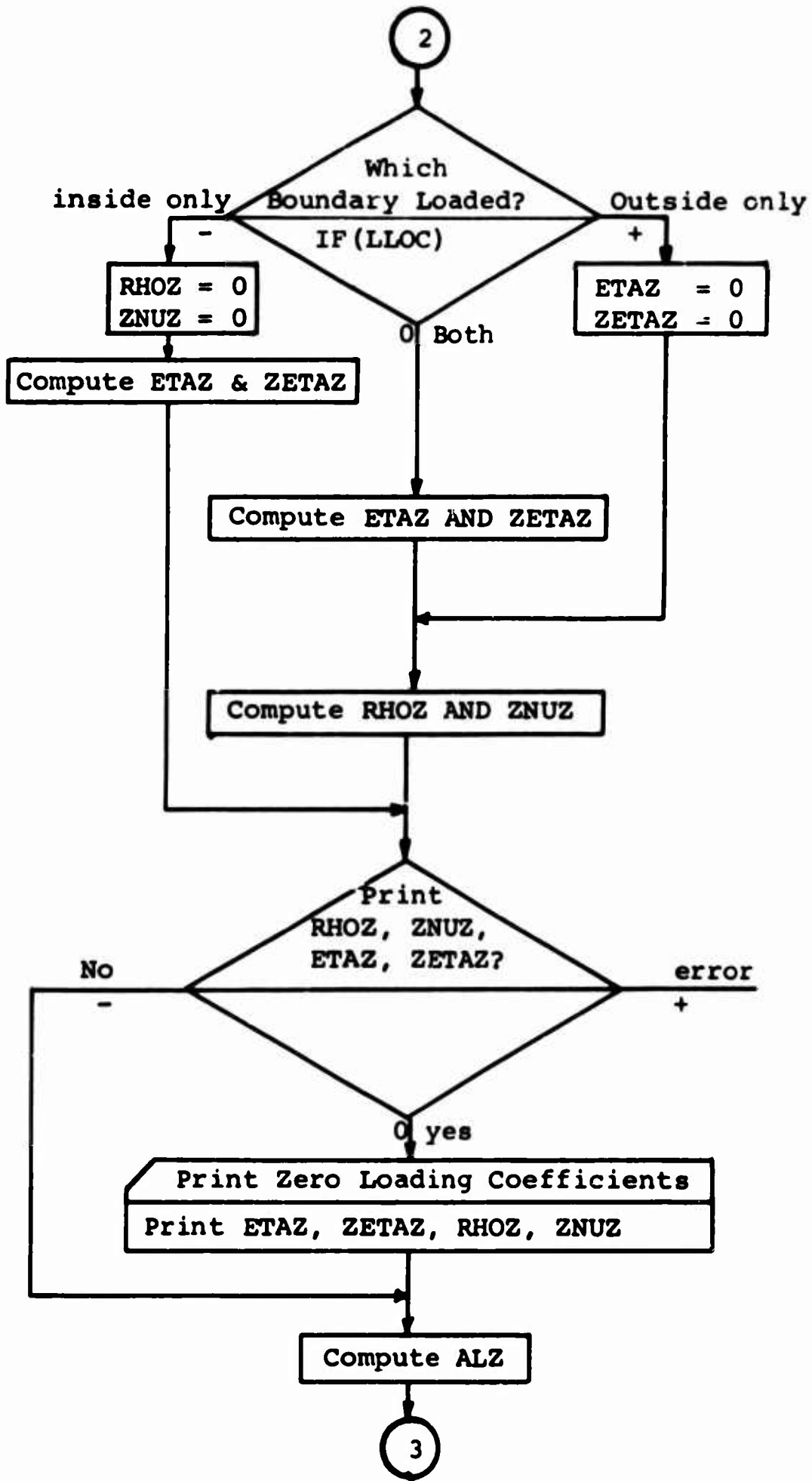
Since the entire method is based on static equilibrium of the shell, checks are made for this condition. If the shell is not in equilibrium, the program pauses and prints such a message. These static checks are made after the loading coefficients for $k = 0$ (moment check) and $k = 1$ (force check) are computed. Thus, very little time is wasted if static equilibrium does not exist.

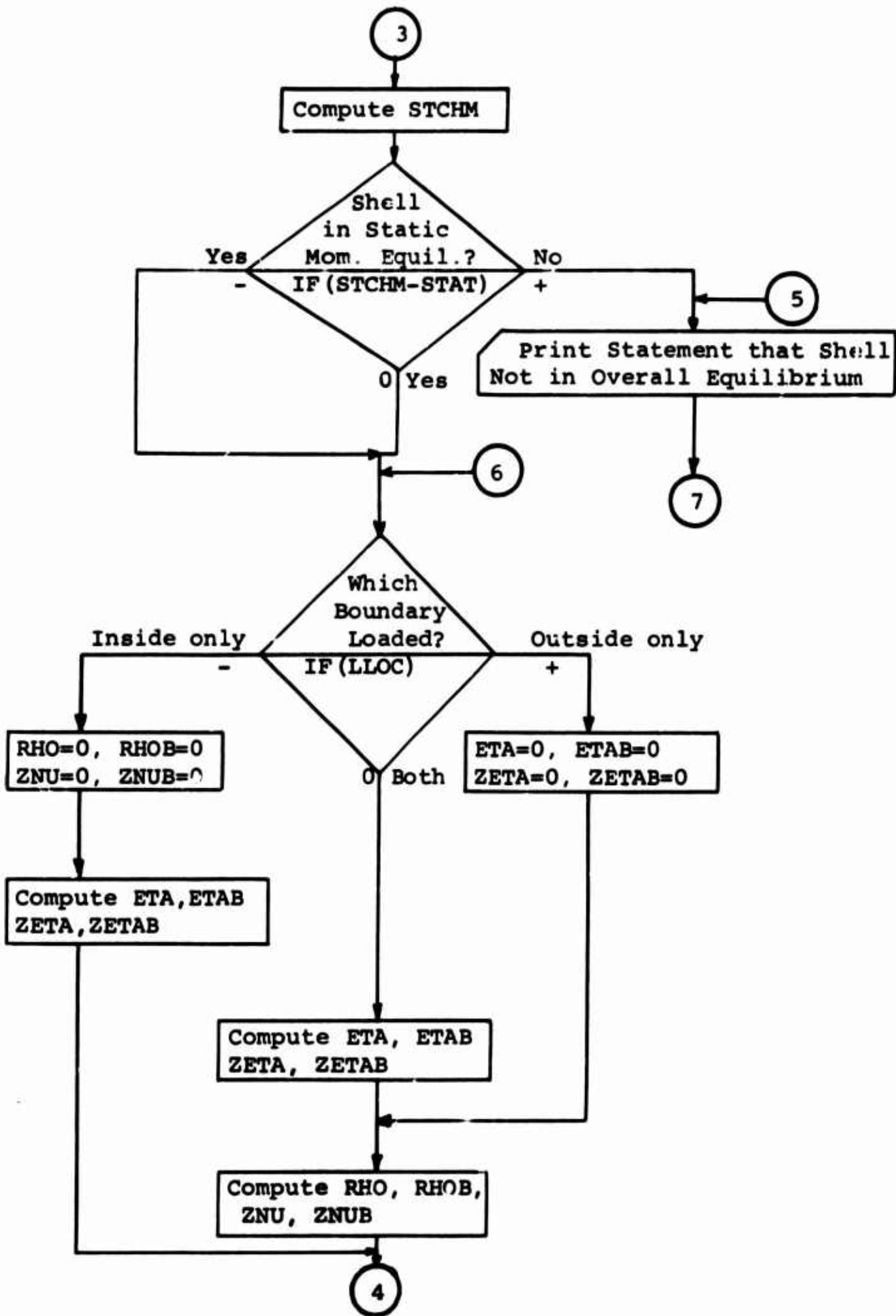
As soon as a set of loading coefficients is computed for any $k \geq 1$, complete use is made of this set of coefficients and they are never used again. Then the next set of loading coefficients are stored in the same locations. The contributions to stresses and displacements by each set of loading coefficients are accumulated, so we have a running set of results at all times. This scheme has both advantages and disadvantages. The disadvantage is that stresses and displacements can be found only for that set of computation points originally read in. The advantage is that, since only eight storage locations are used for the loading coefficients (for $k \geq 1$), there is no limit as to the number of terms (value of k) that can be used to solve a problem having complicated loading stress distributions. Computer storage will, of course, limit the number of computation points; but this usually will not be a problem. If results at more points are desired, run the program again for the new points.

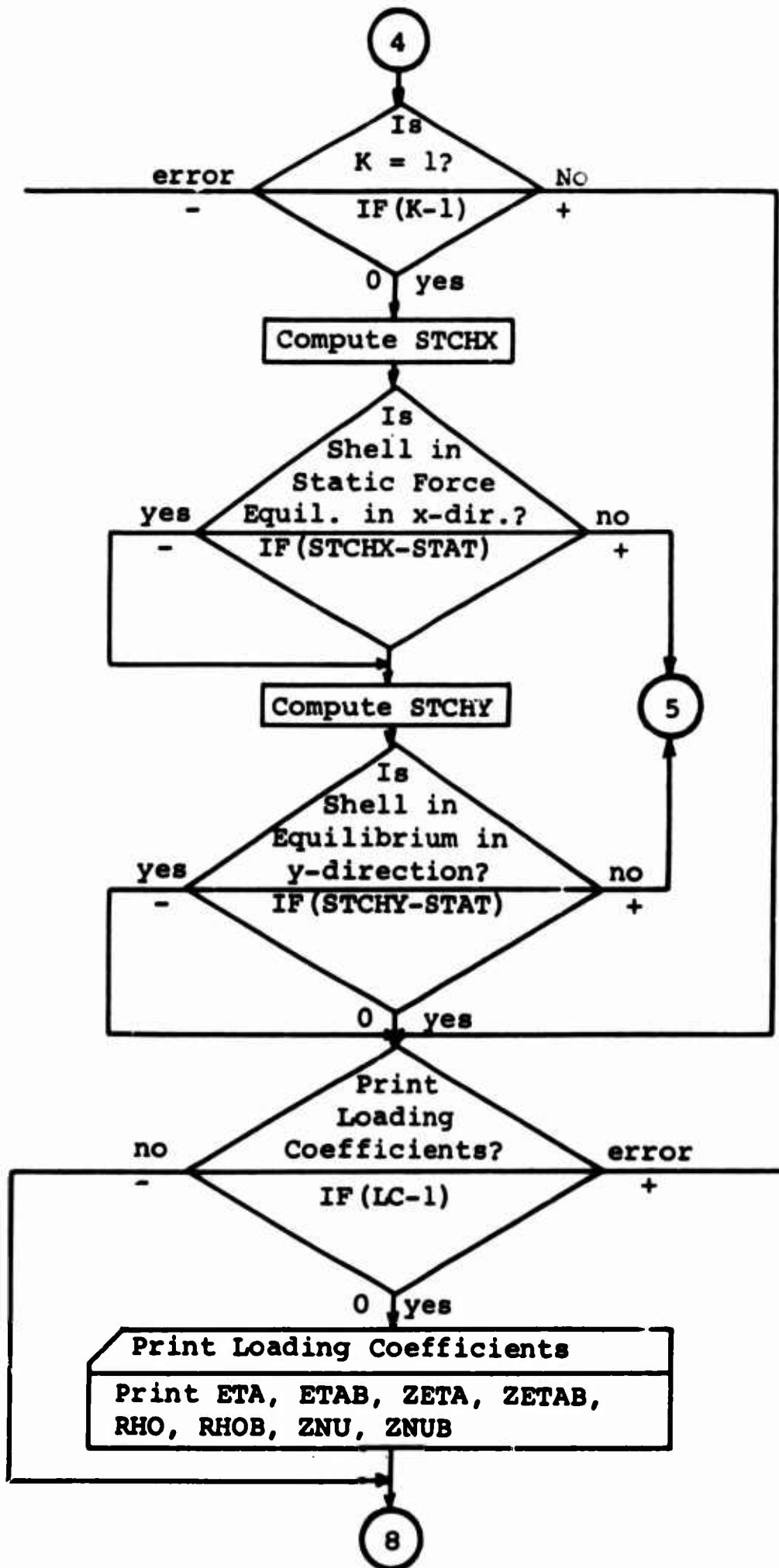
The Flow Chart

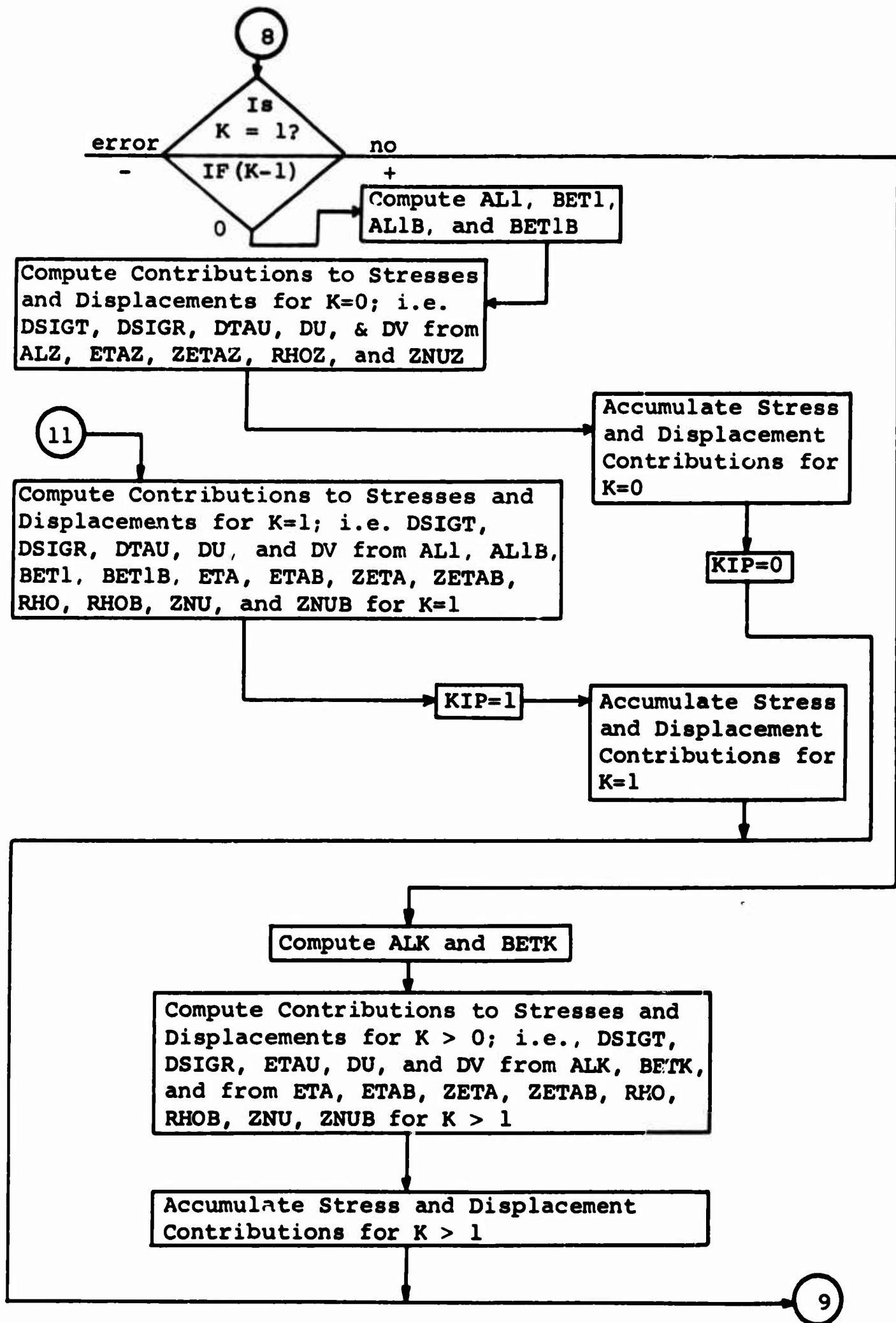


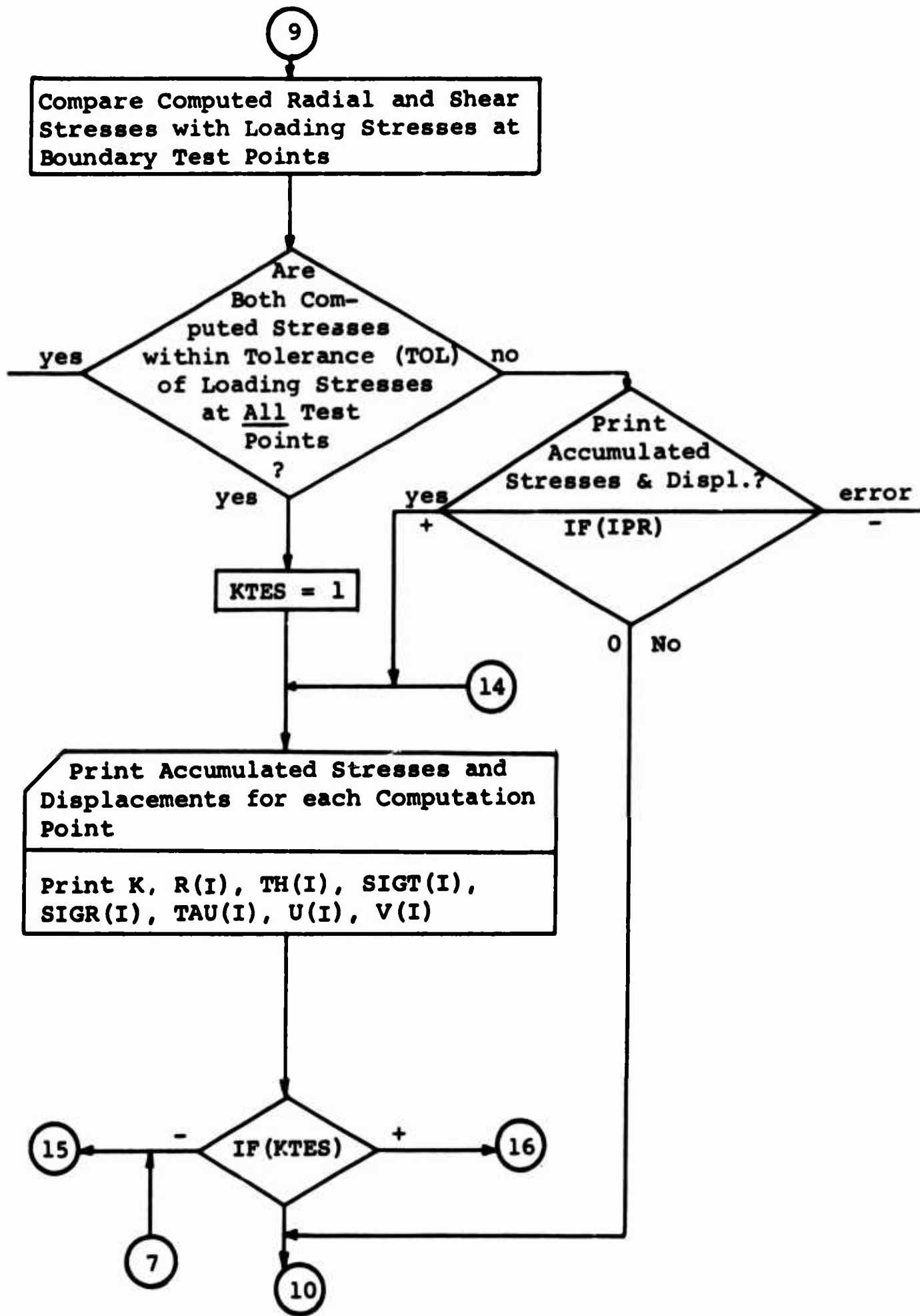


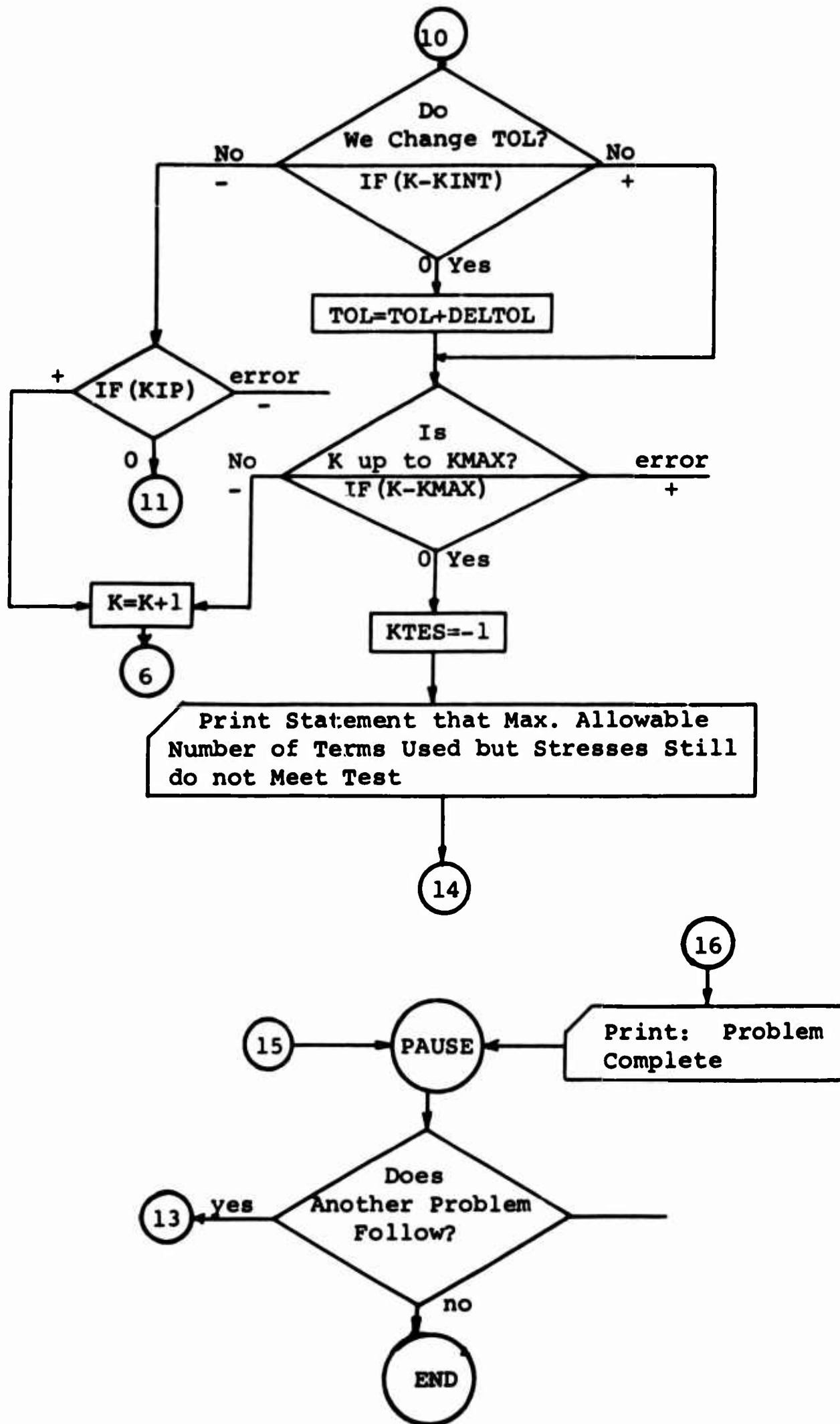












```

DIMENSION XLS(2,102),XLT(12,102),SN(102),CS(102),JDISC(4),XLSN(2,4)
1,XLTN(2,4),NT(12),R(12),TH(12),SIGR(12),SIGT(12),TAU(12),U(12),V(1
22),LL(12),J1(12)
6   FORMAT(20X,2F20.0)
1   FORMAT(13,2X,2F6.0,3I6,4I4,F6.0, / 5F15.0,3X,I2)
63  READ1,M,TOL,DELTOI,KINT,KMAX,NRTH,NDISC,NTEST,LC,IPR,STAT,R1,RPI,D
1ELT,RDELT,XKAP,LLOC
   READ1111,UF
1111 FORMAT(11H UNDERFLOW=,F4.0)
   MP1=M+1
   XTES=0
   MP2=M+2
   REAC2,((XLS(L,N),XLT(L,N),N=1,MP2),L=1,2)
   FORMAT(25X,2F20.0)
   FORMAT(15,5X,2F10.0)
   IF(NDISC)91,92,91
91  READ3,((JDISC(JJJ),XLSN(L,JJJ),XLTN(L,JJJ),JJJ=1,NDISC),L=1,2)
4   FORMAT(4E20,14)
5   FORMAT(13,2F8.5,3F10.6,2F15.13)
92  READ302,(R(JJ),TH(JJ),JJ=1,NRTH)
302  FORMAT(25X,2F20.0)
7   FORMAT(3I5)
   READ7,(NT(I),LL(I),J1(I),I=1,NTEST)
8   FORMAT(78H K R THETA SIG THET SIGMA R TAU
1U  V
9   FORMAT(55H THIS PROBLEM COMPLETE RESTART IF OTHER PROBLEM FOLLOWS)
   READ6,(SN(I),CS(I),I=1,MP2)
18  FORMAT(48H MAX NUMBER TERMS COMPUTED BUT DID NOT MEET TEST)
41  FORMAT(13,2H=K,62H THE NEXT 8 NUMBERS ARE ETA,ETAB,ZETA,ZETAB,RHO
1,RHOB,ZNU,ZNUH)
411  FORMAT(51H THE NEXT FOUR NUMBERS ARE ETAZ,ZETAZ,RHOZ,AND ZNUZ)
C   PRELIMINARY COMPUTATIONS AND INITIALIZATIONS
   R1SQ=R1*R1
   RSQ=1.-R1SQ
   E11=1.-R1SQ*R1SQ

```

```

E12=(1.+RISO)*(XKAP+1.)
L=1
K=1
IF(LLOC)25,25,200
COMPUTATION OF LOADING COEFFICIENTS FOR K=0
C 25 SAA=0.
SBB=0.
SAA=0.
SB=0.
SC=0.
SD=0.
DO2ON=1,M
SAA=SAA+XLT(L,N)
SA=SA+XLS(L,N)
IF(NDISC)12,12,11
11 DO21JJJ=1,NDISC
SBB=SBB+XLTN(L,JJJ)
SB=SB+XLSN(L,JJJ)
NMN=JDISC(JJJ)
SC=SC+XLS(L,NMN)
SD=SD+XLT(L,NMN)
21 E1=DELTA*.25*RPI*(SA+SA+SB-SC)
12 E2=-DELTA*.25*RPI*(SAA+SAA+SBB-SD)
22 IF(L-2)22,23,23
ETAZ=E1
ZETAZ=E2
200 L=2
IF(LLOC)201,25,203
201 RMOZ=0.
ZNUZ=0.
GOTO202
203 ETAZ=0.
ZETAZ=0.
GOTO25
23 RMOZ=E1

```

```

ZNUZ=E2
202 IF(LC-1)51,50,53
50 PRINT411
C PRINT4,ETAZ,ZETAZ,RHOZ,ZNUZ
51 COMPUTE ALPHA ZERO (BETA ZERO = 0)
ALZ=.5*(RHOZ-RISQ*ETAZ)/RSQ
STCHM=ZETA7*RISQ-ZNUZ
IF(ABS (STCHM)-STAT)154,154,52
52 PUNCH24
PRINT24
24 FORMAT(45H LOADING STRESSES NOT IN OVERALL EQUILIBRIUM)
PAUSE
GOTO83
C COMPUTE LOADING COEFFICIENTS FOR K NOT = ZERO
154 IF(LLDC)54,54,205
54 L=1
55 SUME=0.
SUMF=0.
SUMG=0.
SUMH=0.
JJJ=1
34 DO31N=2,MP1
C COMPUTE NET ARGUMENT FOR LOOKUP OF STORED SIN AND COS
XK=K
XNM1=N-1
XM=M
AREV=K*(N-1)/M
TARG=XK*XNM1/XM
NA=(TARG-AREV)*XM+1.5
C INSTRUCTIONS FROM HERE THRU 29+4 TAKE CARE OF DISCONTINUITIES
N1=N-1
N2=N+1
BA=XLS(L,N2)
BB=XLTL(L,N2)
IF(NDISC)53,29,94

```

```

94  IF(JJJ-NDISC)101,101,29
101  IF(JDISC(JJJ)-N)13,37,13
37  IF(JJJ-NDISC)100,13,53
100  IF(JDISC(JJJ+1)-N2)16,27,16
27  BA=XLSN(L,JJJ+1)
    BB=XLTN(L,JJJ+1)
    GOTO25
13  IF(JDISC(JJJ)-N2)16,14,16
14  BA=XLSN(L,JJJ)
    BB=XLTN(L,JJJ)
16  IF(JDISC(JJJ)-N)29,26,29
26  AB=XLSN(L,JJJ)+XLS(L,N)-XLS(L,N1)-BA
    AC=XLTN(L,JJJ)+XLT(L,N)-XLT(L,N1)-BB
    AD=XLSN(L,JJJ)-XLS(L,N)
    AE=XLTN(L,JJJ)-XLT(L,N)
    JJJ=JJJ+1
    GOTO30
29  AB=XLS(L,N)+XLS(L,N)-XLS(L,N1)-BA
    AC=XLT(L,N)+XLT(L,N)-XLT(L,N1)-BB
    AD=0.
    AE=0.
30  FAC=.5*RPI/XK
    RKAD=RDELT/XK
    SUME=SUME+FAC*(AD*SN(NA)+AB*CS(NA)+RKAD)
    SUMF=SUMF+FAC*(AE*CS(NA)-AC*SN(NA)+RKAD)
    SUMG=SUMG-FAC*(AE*SN(NA)+AC*CS(NA)+RKAD)
    SUMH=SUMH+FAC*(AD*CS(NA)-AB*SN(NA)+RKAD)
31  IF(L-2)32,33,53
32  ETA=SUME+SUMF
    ETAB=SUME-SUMF
    ZETA=SUMG+SUMH
    ZETAB=SUMG-SUMH
205  L=2
    IF(LLOC)207,55,206
206  ETA=0.

```

```

ETAB=0.
ZETA=0.
ZETAB=0.
GOTO55
207 RMO=0.
    RHOB=0.
    ZNU=0.
    ZNUB=0.
    GOTO208
33  RMO=SUME+SUMF
    RHOB=SUME-SUMF
    ZNU=SUMG+SUMH
    ZNUB=SUMG-SUMH
208 IF(K-1)53,15,10
15  STCHX=RMO-K1*ZETA
    IF(ABS (STCHX)-STAT)17,17,52
17  STCHY=ZNU-R1*ZETA
    IF(ABS (STCHY)-STAT)10,10,52
10  IF(1-C-1)36,35,53
35  PUNCH41,K
    PUNCH4,ETA,ETAB,ZETA,ZETAB,RMO,RHOB,ZNU,ZNUB
    PRINT41,K
36  PRINT4,ETA,ETAB,ZETA,ZETA,ZETAB,RMO,RHOB,ZNU,ZNUB
    :F(K-1)53,38,39
C   COMPUTE ALPHA ONE,BETA ONE,ALPHA ONE BAR,AND BETA ONE BAR
38  AL1=(RHOB-R1*RISQ*ETAB)/E11-(ETA+ETA)*R1/E12
    BET1=(-ZNUB+R1*RISQ*ZETAB)/E11-(ZETA+ZETA)*R1/E12
    AL1B=ETA*R1/(XKAP+1.)
    BET1B=-ZETA*R1/(XKAP+1.)
    GCTO63
39  E13=1.+XK
    E14=XK-1.
    IF(K-1)53,63,64
C   INITIALIZE STRESS AND DISPLACEMENT SUMS
63  DC60I=1,NRTH

```

```

SIGT(I)=0.
SIGR(I)=0.
TAU(I)=0.
U(I)=0.
V(I)=0.
60  COMPUTE ZERO TERMS FOR STRESSES AND DISPLACEMENTS
      C
      DO61JJ=1,NRTH
      E20=2.*ALZ
      E21=R1SQ*(RMOZ-ETAZ)
      E19=R1SQ*(ZNUZ-ZETAZ)
      E22=R(JJ)**(-2)
      E23=RSQ*R(JJ)
      DSIGT=E20+E21+E22/RSQ
      DSIGR=E20-E21+E22/RSQ
      DTAU=R1SQ*(ZNUZ-ZETAZ)*E22/RSQ
      DU=ALZ*(XKAP-1.)*R(JJ)+E21/E23
      DV=-E19/E23
      SIGT(JJ)=SIGT(JJ)+DSIGT
      SIGR(JJ)=SIGR(JJ)+DSIGR
      TAU(JJ)=TAU(JJ)+DTAU
      U(JJ)=U(JJ)+DU
      V(JJ)=V(JJ)+DV
      KIP=0
      GOTO66
      COMPUTE TERMS OF STRESSES AND DISPLACEMENTS FOR K=1
      KIP=1
      DO62JJ=1,NRTH
      E24=R(JJ)**(-3)
      E25=SIN (TH(JJ))
      E26=COS (TH(JJ))
      E27=R(JJ)+2.
      E28=1.+XKAP
      E29=R(JJ)**(-2)
      E30=XKAP+2.
      E32=R(JJ)

```

60
C

61

C 271

```

E33=1./E32
E34=E28/E32
E35=E32-E24
F36=3./E32
E37=R1SQ/R1SQ/E24
E38=ALOG(R(JJ))
E99=XKAP-2.
DSIGT=(13.*E32+E24)*AL1+(E33+E24+E24)*AL1B-XKAP*R1*ETA/(E28
1*E32)-RHOB*E24)*E26+(-13.*E32+E24)*BET1+(E33+E24+E24)*BET1B+XKAP
2*R1*ZETA/E34-ZNUB*E24)*E25
DSIGR=(E35*AL1+(E36-E24-E24)*AL1B+XKAP*R1*ETA/E34+RHOB*E2
14)*E26+(-E35*HET1+(E36-E24-E24)*BET1B-XKAP*R1*ZETA/E34+ZNUB*E24)*
2E25
DTAU=(E32-E37)*BET1+(-E33+2.*R1SQ*E24)*BET1B-XKAP*R1*ZETA/E34-R1S
1Q*R1*ZETAB*E24)*E26+(E32-E37)*AL1+(E33-2.*R1SQ*E24)*AL1B-XKAP*R1*
2ETA/E34-R1*R1SQ*ETAB*E24)*E25
DU=(XKAP*AL1B+XKAP*ETA*R1/E28)*E38-AL1B+(AL1B+AL1B+AL1-RHOB)*.5*
1E29+E32*E39*AL1*.5)*E26+((XKAP*BET1B-XKAP*ZETA*R1/E28)*E36-BET
21B-(BET1B+BET1B-BET1-ZNUB)*.5*E29-E32*E39*BET1*.5)*E25
DV=((XKAP*BET1B-XKAP*ZETA*R1/E28)*E38+BET1B+E32*E30*BET1*.5-(-
12.*BET1B-BET1-ZNUB)*.5*E29)*E26+(-(XKAP*AL1B+XKAP*ETA*R1/E28)*E38-
3A
?L1B+E32*E30*AL1*.5+(AL1B+AL1B+AL1-RHOB)*.5*E29)*E25
SIGT(JJ)=SIGT(JJ)+DSIGT
SIGR(JJ)=SIGR(JJ)+DSIGR
TAU(JJ)=TAU(JJ)+DTAU
U(JJ)=U(JJ)+DU
V(JJ)=V(JJ)+DV
GOTO66
62
C COMPUTE TERMS OF STRESSES AND DISPLACEMENTS FOR K GREATER THAN ONE
DO65JJ=1,NRTH
E29=R(JJ)*(-2)
E32=R(JJ)
E33=1./E32
E34=ALOG10(R1)

```

```

E38=ALOG10(E32)
E41=R1*(-2)
IF(XK+E38+UF)210,210,211
E44=0
GOTO212
E44=R(JJ)*K
211
212 IF(XK+XK-2.)E38+UF)213,213,214
213 E45=0
GOTO215
E45=R(JJ)*K+K-2)
214
215 E46=COS(XK*TH(JJ))
E47=SIN(XK*TH(JJ))
IF(XK-1.)E38+UF)216,216,217
E48=0
GOTO218
E48=R(JJ)*K-1)
217
218 IF(XK+E34+UF)219,219,220
219 F49=0
GOTO221
E49=R1*K
220
221 IF(XK+XK)*F34+UF)222,222,223
222 E50=0
GOTO224
E50=E49+E49
223
224 IF(XK+XK-2.)E34+UF)225,225,226
225 E51=0
GOTO227
E51=E50+E41
226
227 IF(XK-2.)E34+UF)228,228,229
228 E53=0
GOTO230
E53=E49+E41
229
230 IF(XK-4.)E34+UF)231,231,232
231 E54=0
GOTO233

```

232 E54=E53*E41
 233 Q=R1/R(JJ)
 QL=ALOG10(Q)
 IF(XK*QL+UF)234,234,235
 234 QK=0
 GOT0236
 235 QK=J*QK
 236 IF(1XK+2.1*QL+UF)237,237,238
 237 QK2=0
 GOTC239
 238 QK2=Q*(K+2)
 239 T1=E13-E13*R1SQ
 T2=-E14+E14*R1SQ
 XM=XK*XK*(2.*R1SQ+E11-2.)*R1SQ*(E50-2.)
 T3=2.*XK-E14*E29
 T4=2.*XK+E13*E29+E45
 T9=1./(1.+XH*E51)
 T10=XK-E29*E14
 T11=E13*E29-XK-E45
 T12=E32*(XKAP-E13)/E13+E33
 T13=E32*(XKAP+E14)/E14-E33+E32*E45/E14
 T14=E32*(XKAP+E13)/E13-E33
 IF(XK*QL+(XK-2.)*E34+UF)240,240,241
 W1=0
 GOT0242
 241 W1=QK*E53
 242 IF(XK*QL+(XK*XK)*E34+UF)243,243,244
 243 W2=0
 GOT0245
 244 W2=GK*E50
 245 IF(XK*QL+(XK*XK+XK)*E34+UF)246,246,247
 246 W3=0
 GOT0248
 247 W3=QK*E49*E50
 248 IF(1XK+2.)*QL+(XK-4.)*E34+UF)249,249,250

```

249 W4=0
    GOT0251
250 W4=QK2*E54
251 IF((XK+2.)*OL+(XK+XK-2.)*E34+UF)252,252,253
252 W5=0
    GOTC254
253 W5=QK2*E51
254 T5=(W1*(T2*RHOB-RHO)-W2*(T2*ETAB+R1SQ*ETA)+QK*ETA+W3*RHO)*T9
    T6=(W4*(T1*RHO-RHOB)-XH*RHOB)-QK2*E41*ETA*T1-QK2*ETAB+W5*ETAB)*T9
    T7=(W1*(T2*ZNUB+ZNU)+W2*(ZETA*R1SQ-T2*ZETAB)-QK*ZETA-W3*ZNU)*T9
    T8=(W4*(ZNUB-T1*ZNU-XH*ZNUB)-QK2*E41*T1*ZETA+QK2*ZETAB-W5*ZETAB)*T
19
255 IF((XK+XK+XK)*E34+UF)255,255,256
    W6=0
    GOT0257
256 W6=E4)*E50
257 ALK=T9*(E51*(T1*RHO-RHOB)-E49*(T1*ETA+R1SQ*ETAB)+W6*ETAB+RHOB)
    BETK=T9*(E51*(T1*ZNU+ZNUB)+E49*(R1SQ*ZETAB-T1*ZETA)-W6*ZETAB-ZNUB)
    BUG=1.E-30
258 IF(ABS(ALK)-BUG)258,258,259
    ALK=0
    GOT0260
259 AL=ALOG10(ABS(ALK))
    IF(XK+E38+AL+UF)260,260,261
260 W7=0
    GOT0262
261 W7=E44*ALK
262 IF(ABS(BETK)-BUG)263,263,264
263 BETK=0
    GOT0265
264 BL=ALOG10(ABS(BETK))
    IF(XK+E38+BL+UF)265,265,266
265 W8=0
    GOT0267
266 W8=E44*BF TK

```

```

10ZNU+E29+T7*(4.-T4)-T8)*E47
DTAU=(W8*T10-E44+E29*ZNU+T11*T7+T8)*E46+(W7*T10-E44+E29*RHO-T11
10T5-T6)*E47
DU=(W7*T12-T13+T5+E48*RHO/E14+E32*T6/E13)*E46+(-W8*T12-T13+T7-E48
10ZNU/E14+E32*T8/E13)*E47
DV=(W8*T14+T7*(T13-2.*E32*XKAP/E14)-E48*ZNU/E14-E32*T8/E13)*E46+(
1W7*T14-T5*(T13-2.*E32*XKAP/E14)-E48*RHO/E14+E32*T6/E13)*E47
SIGT(JJ)=SIGT(JJ)+DSIGT
SIGR(JJ) = SIGR(JJ) + DSIGR
TAU(JJ) = TAU(JJ) + DTAU
U(JJ) = U(JJ) + DU
V(JJ) = V(JJ) + DV
65 COMPARE COMPUTED RADIAL AND SHEAR STRESSES AT TEST POINTS WITH LOA
C
C
66 DING STRESSES
DC 71 I = 1, NTEST
JJ = NT(I)
L = LL(I)
JJJ = J1(I)
70 IF(ABS (SIGR(JJ)-XLS(L,JJJ))-TOL)70,70,73
71 IF(ABS (TAU(JJ)-XLT(L,JJJ))-TOL)71,71,73
CCONTINUE
KTES = 1
80 PRINT 8
DC 74 I = 1, NRTH
75 IF(KIP)53,76,303
76 PRINT5,KIP,R(I), TH(I),SIGT(I),SIGR(I),TAU(I),U(I),V(I)
GOTO74
303 PRINT5,K,R(I),TH(I),SIGT(I),SIGR(I),TAU(I),U(I),V(I)
74 CCONTINUE
81 IF(KTES)81,270,81
PRINT 9
PAUSE

```

```

73      GO TO 83
270     IF(IPR)53,270,80
277     IF(K-KINT)77,78,79
272     IF(KIP)53,271,272
      K=K+1
      GCTO154
78     TOL = TOL + DELTOL
79     IF(K-KMAX)77,84,53
84     KTES = -1
      PRINT 18
      PUNCH 18
      GO TO 80
53     PRINT 82
82     FORMAT(41H LOGIC ERRORS SEE 23+2,31+1,33+4,10,36,79)
      PAUSE
      GCTO83
      END

```

INPUT PARAMETERS AND DATA

Definition of the Numbers in the Dimension Statement

XLS(A,B), XLT(A,B): A = 2 (two boundaries)
 B = M + 2

SN(A), CS(A): A = M + 2

JDISC(A): A = NDISC (number of discontinuities)

XLSN(A,B), XLTN(A,B): A = 2 (two boundaries)
 B = Number of discontinuities

NT(A), LL(A), JI(A): A = NTEST (number of test points)

R(A), TH(A), SIGR(A),
SIGT(A), TAU(A), U(A),
V(A): A = NRTH (number of computation points)

Definition of Problem and Control Parameters

M --number of equal sectors into which ring is divided, must be divisible by 4.

TOL --tolerance within which all computed stresses must match loading stresses at test points.

DELTOL--increase in tolerance after KINT terms of Fourier series representing loading stresses have been used.

KINT --number of terms at which TOL will be increased by DELTOL.

KMAX --maximum number of terms the program will be allowed to run.

NRTH --the number of computation points; that is, the total number of locations at which stresses and displacements are to be computed including the test points on boundaries.

NDISC --number of division points at which there is a loading stress discontinuity of any kind on either boundary. Even if only one stress on one boundary has a discontinuity at a given division point, it counts as one of NDISC.

NTEST --number of test points. Test points are those locations on the boundaries at which loading and computed stresses are compared. The test points are included in the computation points.

LC --if LC = 0, we do not print loading coefficients;
 if LC = 1, we do print loading coefficients.

IPR --if IPR = 0, we do not print accumulated stresses and dis-
 placements; if IPR = 1, we do print them.

STAT --amount within which the computed checks for static equili-
 brium must fall. Since there are various unavoidable
 inaccuracies, STAT must not be zero, or the program will
 always stop because of apparent non-equilibrium. Judge-
 ment in choosing STAT must be based on total forces and
 moments on the ring. Perhaps .1% of absolute area under
 loading stress curves might be tried. If a problem has
 symmetric loading, use a rather small STAT--this gives a
 check on data entry error.

R1 --radius of inner boundary (for outer boundary = 1). R1 is
 the ratio of inner to outer radius in the actual problem.

RPI = $1/\pi$

DELT = $2\pi/M$, the angle in radians between division points.

RDELT = $1/DELT$

XKAP = κ = a Lamé' constant. $\kappa = 3-4\sigma$ for plane stress. $\kappa = \frac{3-\sigma}{1+\sigma}$
 for plane strain, where σ = Poisson's ratio.

LLOC --if LLOC = -1, inner boundary only is loaded;
 if LLOC = 0, both boundaries are loaded;
 if LLOC = +1, outer boundary only is loaded.

UF --underflow control parameter. If certain numbers become
 less than 10^{-UF} , we set that number to zero to avoid an
 underflow; of course, the test is made before computation.
 UF = 20. has been used with IBM 7040 (which underflows at
 10^{-30}), but the characteristics of the machine being used
 should govern.

Loading Stresses and Their Specification

The loading stress notation is shown for radial stress on the
 outer boundary. Similar notation is used for the other three load-
 ing stresses. The division point numbering starts with 1 at $\theta = 0$
 because a subscript cannot be zero in a Fortran subscripted variable.
 Shown in Fig. 16 are the radial stresses at several points with no
 discontinuities and one point at which a discontinuity exists.
 Only one value for each of the four loading stresses is read in if
 there are no discontinuities at that division point in any of the
 four stresses. However, if one or more of the four stresses has a

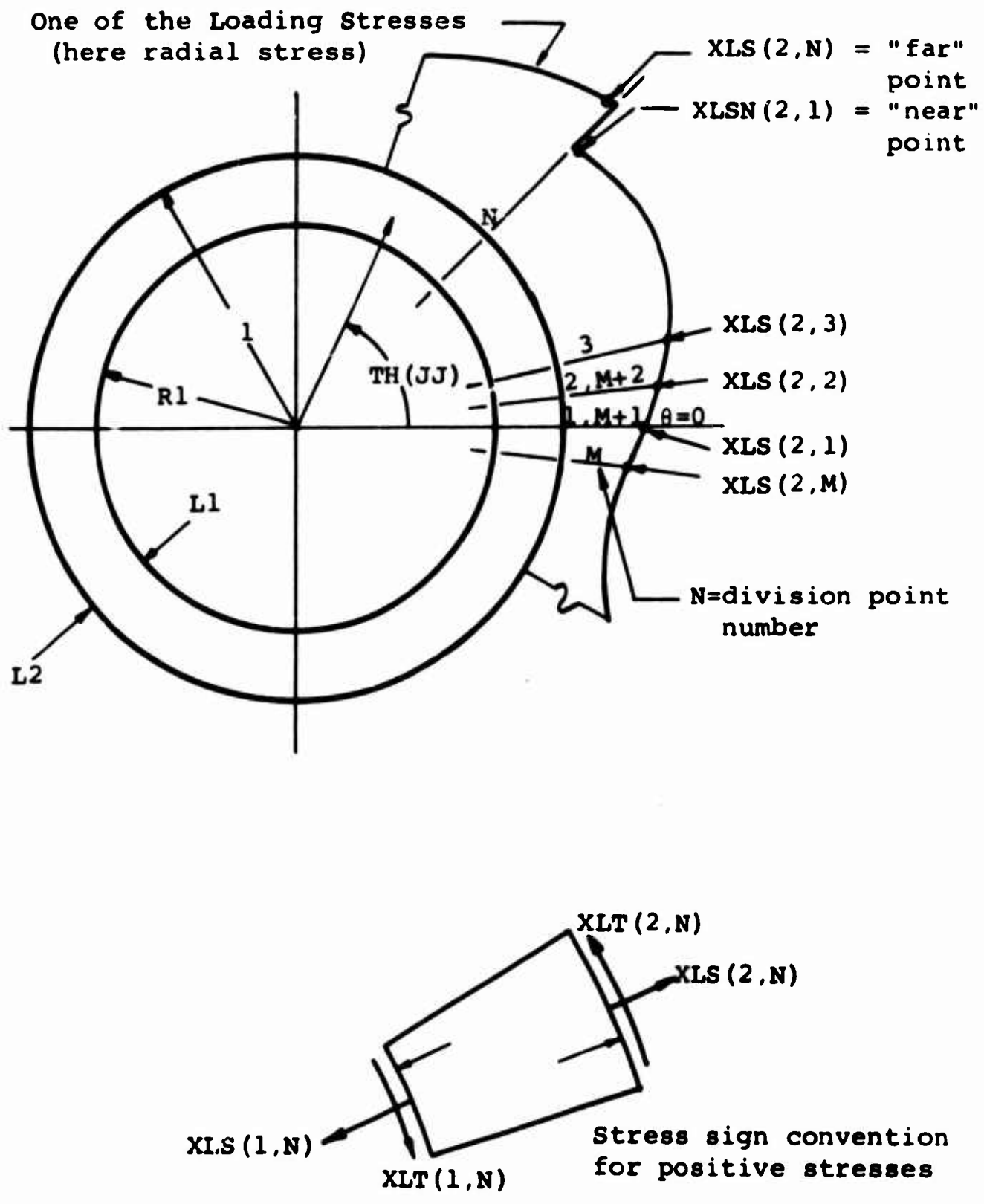


Figure 16. Notation used with loading stresses.

discontinuity at a given division point, all four stresses are considered to be discontinuous, and two values are read in for each stress (even though the two values may be identical for some of the stresses). Definitions for loading stresses follow:

- XLS(L,N) --radial loading stress (σ_r) on boundary L at division point N. If there is a discontinuity at this division point, XLS(L,N) is the "far" point as shown in Fig. 16.
- XLT(L,N) --shear boundary stress ($\tau_{r\theta}$) on boundary L at division point N. Again, this is "far" point if there is a discontinuity.
- N --division point number starting with 1 and proceeding through M + 2. This overlap of two on the numbering was necessary because of starting and ending some of the series'.
- L --boundary identification. L = 1 signifies inner boundary; L = 2 means outer boundary.
- XLSN(L,JJJ) --"near" value of radial loading stress at a discontinuity on boundary L. JJJ is the serial number of the discontinuity starting with 1 for the first discontinuity and running through NDISC for the last.
- XLTN(L,JJJ) --"near" value of shear loading stress at a discontinuity on boundary L. JJJ same as above.
- JDISC(JJJ) --division point number at which discontinuity serial number JJJ occurs.

Computation Point Identification

- R(JJ) --radius of computation point serial number JJ. JJ starts with 1 and runs through NRTH.
- TH(JJ) --angle measured from $\theta = 0$ of computation point serial number JJ.

See Fig. 17 for sketch of computation point numbering system.

Test Point Identification

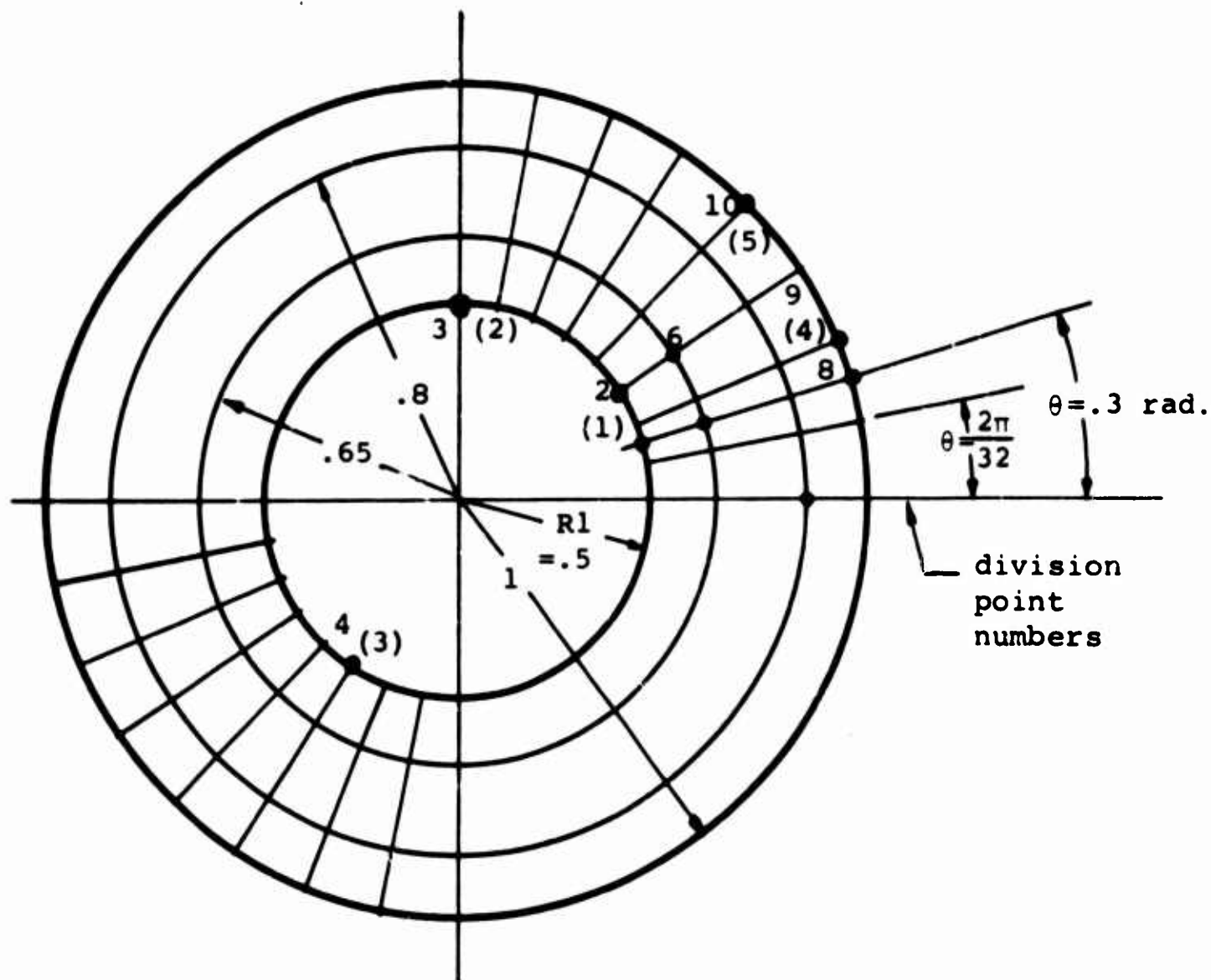
- NT(I) --computation point number of the test point having serial number I. I starts with 1 and runs through NTEST.

LL(I)--boundary identification of test point having serial number I.
 LL(I) = 1 for inner boundary; LL(I) = 2 for outer boundary.

J1(I)--division point number of test point having serial number I.

Figure 17 shows the numbering scheme for computation points and test points. We start with computation point number 1 at the smallest angle and the smallest radius at which stress and displacement computations are to be made. Then we proceed counter-clockwise at this same radius until all computation points on that circle are numbered. Next we move to the next larger radius at which any computations are to be made and again proceed counter-clockwise until all computation points at this radius are numbered. This process continues until all computation points are numbered serially from 1 through NRTH. Computation points will be used as test points--thus computation point 8 may be test point 2. Test points must lie on division points in order to have a stress to compare with. Test points must not be points of discontinuity. As an example, for $M = 32$, we will locate on Fig. 17 the computation and test points indicated in the following table:

Comp. Pt. No. (JJ)	Test Pt. No. (I)	Radius (R(JJ)=fract. of R1)	Angle (TH(JJ) in radians)
1	---	.5	.3
2	(1)	.5	$\frac{6\pi}{32}$
3	(2)	.5	$\frac{16\pi}{32}$
4	(3)	.5	$\frac{42\pi}{32}$
5	---	.65	.3
6	---	.65	$\frac{6\pi}{32}$
7	---	.8	0
8	---	1.0	.3
9	(4)	1.0	$\frac{4\pi}{32}$
10	(5)	1.0	$\frac{8\pi}{32}$



1, 2, ... 10 are computation point numbers
 (1), (2), ... (5) are test point numbers

Figure 17. Example of numbering system for computation points and test points

Table of Sines and Cosines

In much of the program, sines and cosines of the division point angles are used many times. Since there are only $M+2$ of these angles, the values of $\sin\theta = SN(I)$ and $\cos\theta = CS(I)$ are

computed by a preliminary program; these values are then read in as data. This procedure makes the program run considerably faster than it would if sines and cosines were determined as functions.

SN(I)--sine of the angle whose division point number is I. I starts at 1 for $\theta = 0$, is M for $\theta = 2\pi - \text{DELT}$, is M+1 for $\theta = 2\pi$ and ends at M+2 for $\theta = 2\pi + \text{DELT}$.

CS(I)--cosine of the angle whose division point number is I.

OUTPUT RESULTS

The outputs are nearly self explanatory in that they will all have header symbols above. However, for clarity let us discuss briefly each of the outputs.

Stresses and Displacements at Computation Points

These, of course, are the results that the entire program is designed to produce. These results may be printed only once, after the computed stresses match the loading stresses at all test points; if this is desired set IPR = 0. Another choice is to print these results after the stress and displacement accumulations are made for each value of k; if this is desired, set IPR = +1. The latter mode enables one to observe rate of convergence, proximity of computed to test stresses, etc. Following is an example of the form for these results:

K	R	THETA	SIG THET	SIGMA R	TAU	U	V
38	.65	1.45	1.7	.8	-.9	.1	-.2

K = 38 --38 Fourier terms of loading stress representation have been computed and their contributions to stresses and displacements accumulated.

R = .65 --this computation point has radius = .65.

THETA = 1.45 --this computation point located at angle 1.45 rad.

SIG THET = 1.7 --transverse stress (σ_{ρ}) accumulated to date is 1.7.

SIGMA R = .8 --radial stress accumulated to date is .8.

TAU = -0.9 --shear stress ($\tau_{r\theta}$) accumulated to date is -.9.

U = .1 --radial displacement (u) accumulated to date is $u = U/2\mu = .1/2\mu$, where μ = the second Lamé' constant (μ = shear modulus).

V = -.2 --transverse displacement accumulated is $v = V/2\mu = -.2/2\mu$.

Note that the above example gives output for only one computation point; if more points were computed, the heading would not be repeated for each point.

Loading Coefficients

It may be desired to observe the values of the loading coefficients ETA, --- ZNUB after each k to see how convergence is progressing. These loading coefficients are not simply the Fourier coefficients of the loading stress functions, but are simple combinations of them. If it is not desired to print these coefficients after each k, set LC = 0; if printing is desired, set LC = +1. This output is of the following form:

THE NEXT 8 NUMBERS ARE ETA, ETAB, ZETA, ZETAB, RHO, RHOB,
ZNU, ZNUB

0.1	0.2	0.	0.
-0.3	0.	0.25	-0.2

Here we have ETA=0.1, ETAB=0.2, ZETA=0., ZETAB=0., RHO=-0.3, RHOB=0., ZNU=0.25, and ZNUB=-0.2.

Static Equilibrium Check

In case the absolute value of any of STCHX, STCHY, or STCHM is greater than STAT, the following statement will be printed and punched:

| LOADING STRESSES NOT IN OVERALL EQUILIBRIUM |

After this statement is punched and printed, the computer will pause. Restart if another problem follows.

If a careful check of the loading stresses reveals no error, the above statement may merely mean that the value of STAT was chosen too small for the inherent errors and approximations made.

Insufficient Terms Used

In case the maximum desired number of terms (KMAX) has been reached by k and the computed stresses at the test points have still not come within tolerance (TOL + DELTOL), the following statement will be printed and punched:

| MAX NUMBER TERMS COMPUTED BUT DID NOT MEET TEST |

After the above statement is punched and printed, the stresses and displacements accumulated to date will be printed after which will be printed the end-of-problem statement described in the next paragraph.

End of Problem Statement

If the problem is terminated because of successful solution or because of k reaching KMAX the following statement will be printed:

| THIS PROBLEM COMPLETE RESTART IF OTHER PROBLEM FOLLOWS |

The above statement will not be printed if the problem is terminated because of failure to meet static equilibrium.

After the above statement is printed, the machine will pause and should be restarted if another problem follows.

Logic Errors

In case some control number is set to a meaningless value accidentally the following statement will be printed:

| LOGIC ERRORS CHECK CONTROL PARAMETERS |

If this statement is printed, examine KINT, KMAX, LC, IPR, LLOC.

EXAMPLE PROBLEM

Actual Problem

A cylinder is loaded in plane strain conditions by compressive radial stresses of 5000 psi over two small arcs on the outer boundary as shown in the figure. The outside radius is 100 inches; the inside radius is 50 inches. Poisson's ratio of the material is 0.3 and the shear modulus is 2×10^6 psi. The loaded small arcs are $4\pi/100$ radians. See Example Figure 18.

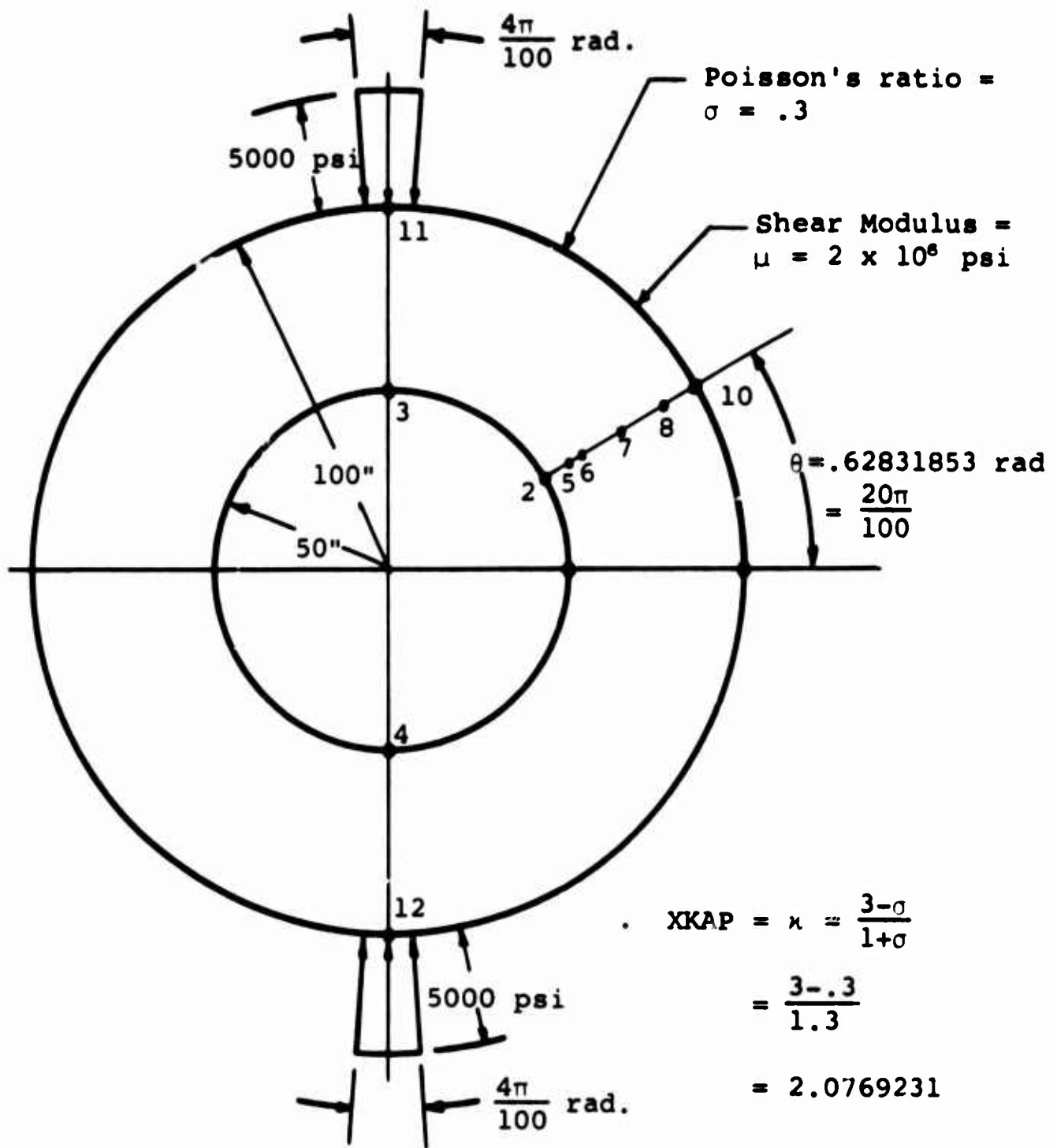
Program Problem (See Example Figure 19)

Desire to compute answers at indicated locations:

No.	r (inches)	θ (rad)
1	50	0
2	50	.62831853
3	50	1.5707963
4	50	4.7123890
5	60	.62831853
6	62.5	.62831853
7	75	.62831853
8	85	.62831853
9	100	0.0
10	100	.62831853
11	100	1.5707963
12	100	4.7123890

Input Data

1. DIMENSION XLS(2,102), XLT(2,102), SN(102), CS(102), JDISC(4), XLSN(2,4), XLTN(2,4), NT(6), R(12), TH(12), SIGR(12), SIGT(12), TAU(12), U(12), V(12), LL(6), J1(6)



Example Figure 18. Loading stresses on actual shell

2. READ 1, M, TOL, DELTOL, KINT, KMAX, NRTH, NDISC, NTEST, LC,
IPR, STAT, R1, RPI, DELT, RDEL'T, XKAP, LLOC

2 cards:

Remarks:

M =	100	shell divided into 100 equal segments
TOL =	.03	
DELTOL =	.1	
KINT =	10	increase TOL by DELTOL when K = KINT
KMAX =	100	end problem if K = KMAX
NRTH =	12	there are 12 computation points
NDISC =	4	there are 4 discontinuities
NTEST =	6	there are 6 test points
LC =	1	print loading coefficients
IPR =	1	print accumulated stresses and displacements after each K
STAT =	.001	symmetric problem should allow small STAT
R1 =	.5	
RPI =	.31830990	reciprocal of π
DELT =	.06283185	2π radians divided by 100
RDEL'T =	15.9154943	reciprocal of DELT
XKAP =	2.0769231	$\kappa = \frac{3-\sigma}{1+\sigma}$ for plane strain, and $\sigma =$ Poisson's ratio = .3
LLOC =	+1	loading stresses on outside boundary only

3. READ 1111, UF

UF = 20.

4. READ 2, ((XLS(L,N), XLT(L,N), N = 1, MP2), L = 1, 2) Note:
MP2 = M+2 = 102

204 cards:

102 blank cards for unloaded inner boundary, L = 1.

24 blank cards for L = 2 and N = 1, 2, ... 24.

2 cards XLS(2,N) XLT(2,N):

-1.0	0.0	N = 25
-1.0	0.0	N = 26

48 blank cards for L = 2 and N = 27, 28, ... 74

2 cards XLS(2,N)	XLT(2,N):	
-1.0	0.0	N = 75
-1.0	0.0	N = 76

26 blank cards for L = 2 and N = 77, 78, ... 102.

5. READ 3, ((JDISC(JJJ), XLSN(L,JJJ), XLTN(L,JJJ), JJJ = 1, NDISC), L = 1, 2)

8 cards:			Re. :ks:		
JDISC(JJJ)	XLSN(L,JJJ)	XLTN(L,JJJ)	L	JJJ	
25	0.	0.	1	1	
27	0.	0.	1	2	
75	0.	0.	1	3	
77	0.	0.	1	4	NDISC = 4
25	0.	0.	2	1	
27	-1.0	0.	2	2	
75	0.	0.	2	3	
77	-1.0	0.	2	4	NDISC = 4

Note: These cards contain the "far" point loading stresses at the four discontinuities. See Example Figure 19.

6. READ 2, (R(JJ), TH(JJ), JJ = 1, NRTH)

12 cards:		Remarks:
R(JJ)	TH(JJ)	JJ
0.5	0.	1 also test pt. #1
0.5	.62831853	2
0.5	1.5707963	3 also test pt. #2
0.5	4.7123890	4 also test pt. #3
0.6	.62831853	5
0.625	.62831853	6
0.75	.62831853	7
0.85	.62831853	8

1.0	0.	9 also test pt. #4
1.0	.62831853	10
1.0	1.5707963	11 also test pt. #5
1.0	4.7123890	12 also test pt. #6

NRTH = 12

See Example Fig. 19 for location of these computation points. These numbers are not in parentheses.

7. READ 7, (NT(I), LL(I), J1(I), I = 1, NTEST)

6 cards:

Remarks:

NT(I)	LL(I)	J1(I)	I	
1	1	1	(1)	
3	1	26	(2)	
4	1	76	(3)	
9	2	1	(4)	
11	2	26	(5)	
12	2	76	(6)	NTEST = 6

See Example Fig. 19 for location of these test points. Test point numbers are in parentheses; e.g. (4).

Output Results

An example of the output for $k = 1$ is included here to show the actual format. Such intermediate results do not need to be printed. Also the printing of ETA, ... ZNUB need not be printed.

l=K THE NEXT 8 NUMBERS ARE ETA, ETAB, ZETA, ZETAB, RHO, RHOB, ZNU, ZNUB

0.	0.	0.	0.
0.	0.	-0.	-0.

K.	R	THETA	SIG THET	SIGMA R	TAU	U	V
1	0.50000	0.	-0.106667	0.000000	-0.	-0.041025642	0.
1	0.50000	0.62832	-0.106667	0.000000	-0.	-0.041025742	0.
1	0.50000	1.57080	-0.106667	0.000000	-0.	-0.041025742	0.
1	0.50000	4.71239	-0.106667	0.000000	-0.	-0.041025642	0.
1	0.60000	0.62832	-0.090370	-0.016296	-0.	-0.039452992	0.

1	0.62500	0.62832	-0.087467	-0.019200	-0.	-0.039202052	0.
1	0.75000	0.62832	-0.077037	-0.029630	-0.	-0.039316240	0.
1	0.85000	0.62832	-0.071788	-0.034879	-0.	-0.040096532	0.
1	1.00000	0.	-0.066667	-0.040000	-0.	-0.042051283	0.
1	1.00000	0.62832	-0.066667	-0.040000	-0.	-0.042051283	0.
1	1.00000	1.57080	-0.066667	-0.040000	-0.	-0.042051283	0.
1	1.00000	4.71239	-0.066667	-0.040000	-0.	-0.042051283	0.

Conversion of Results Back to Original Problem

From dimensional analysis we find that we can obtain a given stress by the following relation:

$$\left\{ \frac{S}{S_{\max}} \right\}_{\text{actual shell}} = \left\{ \frac{S}{S_{\max}} \right\}_{\text{program shell}}$$

$$\therefore S_{\text{act}} = \frac{(S_{\max})_{\text{act.}}}{(S_{\max})_{\text{prog.}}} \times S_{\text{prog.}}$$

where

S_{act} = any stress in actual shell.

S_{prog} = corresponding stress in program shell.

$(S_{\max})_{\text{act}}$ = maximum absolute value of any loading stress on actual shell.

$(S_{\max})_{\text{prog}}$ = maximum absolute value of any loading stress of program shell.

For our example, $\frac{(S_{\max})_{\text{act}}}{(S_{\max})_{\text{prog}}} = \frac{5000}{1} = 5000$

Thus any stress in the actual shell can be obtained by multiplying its counterpart in the program shell by 5000.

Also, we find from dimensional analysis the following relation for displacements:

$$\left\{ \frac{d}{R_s} \right\}_{\text{actual shell}} = \left\{ \frac{d}{R_s} \right\}_{\text{program shell}}$$

$$\therefore d_{\text{act}} = \frac{R_{s \text{ act}}}{R_{s \text{ prog}}} \times d_{\text{prog}}$$

where

d_{act} = either displacement, u or v , in actual shell.

d_{prog} = corresponding displacement in program shell.

R_{act} = radius of outer boundary of actual shell.

$R_{prog} = 1$ = radius of the outer boundary of program shell.

For our example problem, $R_{act} = 100$ ". Thus, any displacement of the actual shell may be found by multiplying the corresponding displacement in the program shell by 100.

Of course, the usual similitude requirements must be met before the above conversion relations are valid. The shells must be geometrically similar, the points under consideration must be located geometrically similarly, the elastic constants must be the same, and loading stresses must be similar throughout. All these requirements are met by our problem procedure.

REFERENCES

1. I. N. Muskhelishvili, Some Basic Problems of the Mathematical Theory of Elasticity. (Translated by J. R. M. Radok)
P. Noordhoff Ltd., Groningen, Holland, 1953.

SECTION III

STRESSES IN THICK-WALLED CYLINDERS WITH CAPPED ENDS

CHAPTER 1

INTRODUCTION

This section is concerned with static stresses in thick-walled cylinders with end caps. The cylinders are assumed to be loaded axisymmetrically; thus the general problem is to solve axisymmetric elasticity problems involving a difficult geometry.

The specific problems considered are axisymmetrically loaded thick-walled cylinders with: (1) one end closed with a flat cap; (2) one end closed with a hemispherical cap; and (3) both ends closed with either flat or hemispherical end caps.

Axisymmetric problems are mathematically two dimensional, involving the area which when rotated about an axis of revolution generates the solid of revolution comprising the region of the problem. Since the geometry of capped thick-walled cylinders precludes an exact solution, an approximate numerical solution was considered.

Of the numerical methods considered the finite difference method in conjunction with Southwell stress functions was used¹. This method is well suited to machine computation and can be organized such that most of the tedious labor is delegated to the computer. The axisymmetric problem is essentially solved when Southwell stress functions φ and ψ are obtained over the generating area of the solid of revolution of interest.

Assuming the z axis to be an axis of revolution, the Southwell stress functions φ and ψ over the generating area are governed in cylindrical coordinates by the equations:

$$\frac{\partial^2 \varphi}{\partial r^2} - \frac{1}{r} \frac{\partial \varphi}{\partial r} + \frac{\partial^2 \varphi}{\partial z^2} = 0 \quad (3-1a)$$

$$\frac{\partial^2 \psi}{\partial r^2} - \frac{1}{r} \frac{\partial \psi}{\partial r} + \frac{\partial^2 \psi}{\partial z^2} = \frac{\partial^2 \varphi}{\partial z^2} \quad (3-1b)$$

Stresses for the axisymmetric problem are defined in terms of φ and ψ as:

$$\sigma_r = \frac{1}{r} \left[\frac{\partial \varphi}{\partial r} + \frac{\partial \psi}{\partial r} \right] - \frac{1}{r^2} \left[\psi + (1-\nu)\varphi \right] \quad (3-2a)$$

$$\sigma_\theta = \frac{\nu}{r} \left[\frac{\partial \varphi}{\partial r} \right] + \frac{1}{r^2} \left[\psi + (1-\nu)\varphi \right] \quad (3-2b)$$

$$\sigma_z = -\frac{1}{r} \frac{\partial \psi}{\partial r} \quad (3-2c)$$

$$\tau_{zr} = \frac{1}{r} \frac{\partial \psi}{\partial z} \quad (3-2d)$$

Allen has shown that boundary conditions are satisfied if φ and ψ satisfy equations equivalent to the following on the boundary of the generating area: [See Ref. 1, pg. 139]

$$\frac{\partial \psi}{\partial s} = -r\sigma_{pz} \quad (3-3a)$$

$$\frac{\partial \psi}{\partial n} + \left\{ \frac{\partial \varphi}{\partial r} - \frac{1}{r} \left[\psi + (1-\nu)\varphi \right] \right\} \cos \alpha = r\sigma_{pr} \quad (3-3b)$$

In summary of the Southwell Stress Functions; Functions φ and ψ must be found such that Eqs.(3-1) are satisfied over the generating area, and Eqs.(3-3) are satisfied on the boundary of the generating area. Stresses may then be obtained with Eqs.(3-2).

CHAPTER 2

THE FINITE DIFFERENCE METHOD AND SOUTHWELL STRESS FUNCTIONS

Difference Equations in Cylindrical Coordinates

Finite Difference Methods are among the more frequently encountered approximate methods for solving differential equations. The literature on this subject is extensive. Frequent references are made in this study to the book by Forsythe and Wasow².

In the finite difference method the region of interest is covered by a mesh or grid. The intersections of the grid lines are referred to as nodal points and are classified as boundary points, adjacent points, or interior points according to proximity to the boundary. All differential equations are approximated by algebraic difference equations which involve the representative values of the unknown functions φ and ψ at the nodal points. Sufficient difference equations must be written to solve for all φ and ψ values associated with the nodal points over the region. This involves approximating Eqs.(3-1) and (3-3) by difference equations, and applying the equations to the appropriate nodal points. Stresses may then be obtained from the solved values of φ and ψ by difference equations approximating Eqs.(3-2).

Where possible, well known central difference equations were used to approximate differential equations [See Ref. 2, pg. 187]. Figure 20 shows the notation employed. Thus, for example,

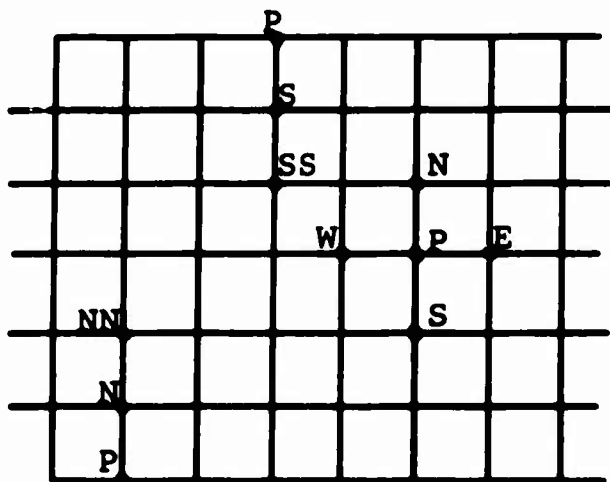


Figure 20. Notation for nodal points.

$$\frac{\partial(\quad)}{\partial r} \approx \frac{1}{2h} [(\quad)_N - (\quad)_S]$$

$$\frac{\partial^2(\quad)}{\partial r^2} \approx \frac{1}{h^2} [(\quad)_N - 2(\quad)_P + (\quad)_S]$$

For a square mesh, which was used in the rectangular generating areas, the difference equations equivalent to Eqs.(3-1) are respectively:

$$\varphi_E + (1 - \frac{h}{2r})\varphi_N + \varphi_W + (1 + \frac{h}{2r})\varphi_S - 4\varphi_P = 0 \quad (3-4a)$$

$$\psi_E + (1 - \frac{h}{2r})\psi_N + \psi_W + (1 + \frac{h}{2r})\psi_S - 4\psi_P = \varphi_E + \varphi_W - 2\varphi_P \quad (3-4b)$$

On the boundary central difference equations equivalent to Eqs.(3-2) involve nodal points outside of the region, i.e. "fictitious" nodal points. Accordingly a backward difference equation using the first three terms of Newton's backward interpolating formula is employed there³. On an outer boundary for example:

$$\frac{\partial}{\partial r} \approx \frac{1}{2h} [3(\quad)_P - 4(\quad)_S + (\quad)_{SS}] \quad (3-5a)$$

and on an inner boundary,

$$\frac{\partial}{\partial r} \approx -\frac{1}{2h} [3(\quad)_P - 4(\quad)_N + (\quad)_{NN}] \quad (3-5b)$$

Similar equations can be written in the z direction.

Using Eqs.(3-5) and central difference equations where possible to represent Eqs.(3-2) yields the difference equations for calculating normal stresses on the boundary surfaces of a cylindrical region.

On an outer surface parallel to the z axis:

$$\sigma_r \approx \frac{1}{2rh} \left\{ \left[3 - \frac{2h}{r}(1-\nu) \right] \varphi_P - 4\varphi_S + \varphi_{AA} + \left[3 - \frac{2h}{r} \right] \psi_P - 4\psi_S + \psi_{SS} \right\} \quad (3-6a)$$

$$\sigma_{\theta} \approx \frac{1}{2rh} \left\{ \left[3 + \frac{2h}{rv}(1-\nu) \right] \varphi_P - 4\varphi_S + \varphi_{SS} + \frac{2h}{rv} \psi_P \right\} \quad (3-6b)$$

$$\sigma_z \approx \frac{1}{2rh} \left[3\psi_P - 4\psi_S + \psi_{SS} \right] \quad (3-6c)$$

A similar equation can be written for an inner boundary, using the second of Eqs.(3-5) for the derivative in the r direction.

On a boundary parallel to the r axis:

$$\sigma_r \approx \frac{1}{2rh} \left[\varphi_N - \varphi_S + \psi_N - \psi_S \right] - \frac{1}{r^2} \left[\psi_P + (1-\nu)\varphi_P \right] \quad (3-7a)$$

$$\sigma_{\theta} \approx \frac{\nu}{2rh} \left[\varphi_N - \varphi_S \right] + \frac{1}{r^2} \left[\psi_P + (1-\nu)\varphi_P \right] \quad (3-7b)$$

$$\sigma_z \approx -\frac{1}{2rh} \left[\psi_N - \psi_S \right] \quad (3-7c)$$

Boundary Conditions for Cylindrical Regions

In general it is always possible to integrate Eq.(3-3a) around the boundary of the region to obtain ψ on the boundary. To apply Eq.(3-3b) it is necessary to combine its difference equation equivalent with difference equations approximating Eqs.(3-1) in such a way that "fictitious" nodal points are eliminated. Allen discusses in detail how this is accomplished for a special case of loading¹. More general boundary equations can be obtained in the same way. These equations are referred to as governing φ equations on the boundary, since φ must be determined there. All boundaries are assumed parallel to either the z or r axis.

On an outer boundary,

$$\begin{aligned} \varphi_S - \left[1 - \frac{h}{r} \left(1 - \frac{h}{2r} \right) (1-\nu) \right] \varphi_P + \psi_S - \left[1 - \frac{h}{r} \left(1 - \frac{h}{2r} \right) \right] \psi_P \\ = rh \left[\left(\frac{h}{2} \right) \frac{\partial \sigma_{pz}}{\partial z} - \left(1 - \frac{h}{2r} \right) \sigma_{pr} \right] \end{aligned} \quad (3-8a)$$

On an inner boundary,

$$\begin{aligned} \varphi_N - \left[1 + \frac{h}{r} \left(1 + \frac{h}{2r} \right) (1-\nu) \right] \varphi_P + \psi_N - \left[1 + \frac{h}{r} \left(1 + \frac{h}{2r} \right) \right] \psi_P \\ = rh \left[\left(\frac{h}{2} \right) \frac{\partial \sigma_{pz}}{\partial z} + \left(1 + \frac{h}{2r} \right) \sigma_{pr} \right] \end{aligned} \quad (3-8b)$$

On a right boundary,

$$\begin{aligned} \left(1 - \frac{h}{2r} \right) \varphi_N + \left(1 + \frac{h}{2r} \right) \varphi_S - 2\varphi_P + 2\psi_W - 2\psi_P \\ = r \left[h^2 \frac{\partial \sigma_{pz}}{\partial r} - 2h \sigma_{pr} \right] \end{aligned} \quad (3-8c)$$

On a left boundary,

$$\begin{aligned} \left(1 - \frac{h}{2r} \right) \varphi_N + \left(1 + \frac{h}{2r} \right) \varphi_S - 2\varphi_P + 2\psi_E - 2\psi_P \\ = r \left[h^2 \frac{\partial \sigma_{pz}}{\partial r} + 2h \sigma_{pr} \right] \end{aligned} \quad (3-8d)$$

For cylindrical regions not touching the z axis and with boundaries parallel to the r and z axis, Eqs. (3-4), (3-3a), and (3-8) are sufficient to obtain φ and ψ everywhere, providing the boundary conditions are in terms of axisymmetric stresses. However, regions that have end-caps and hence touch the z axis are of particular interest in this report.

Conditions on the Axis of Revolution

For solids of revolution that touch the axis of revolution the governing Eqs. (3-4) become undefined in their present form. Allen has pointed out it is necessary to apply L'Hospital's rule to obtain for these equations on the z axis the limiting forms:

$$\frac{\partial^2 \varphi}{\partial z^2} = \frac{\partial^2 \psi}{\partial z^2} = 0 \quad (3-9)$$

which implies φ and ψ are linear functions along the z axis. Furthermore the displacement u in the r direction relates φ and ψ by the general equation [See Ref. 1, pg. 196]

$$\psi + (1-\nu)\varphi = \left(\frac{Er}{1+\nu}\right)u$$

Thus along the z axis where r and u are zero,

$$\varphi = -\frac{\psi}{(1-\nu)} \quad (3-10)$$

It follows if ψ is known on the left and right boundaries of a region at the axis of revolution, then ψ and φ can be obtained all along the axis of revolution (z axis).

In the calculation of ψ on the boundary by integration of Eq.(3-3a), the initial value of ψ at the starting point of integration is arbitrary. Assume that the starting point of the integration is always the left intersection of the z -axis with the generating area, and the initial value of ψ there, hereafter denoted as ψ_L , is set to zero. Then ψ , denoted by ψ_R , at the right intersection of the z axis with the generating area is,

$$\psi_R = \int_L^R -r\sigma_{pz} ds \equiv 0 \quad (3-11)$$

where the integration is around the boundary of the generating area from the left to the right intersection of the z axis with the solid of revolution. That the integral vanishes identically follows from static equilibrium in the z direction of any sector of an axisymmetrically loaded solid of revolution, i.e.,

$$\int_L^R \sigma_{pz} (r\Delta\theta) ds \equiv 0$$

Note $\Delta\theta$ is arbitrary because of axial symmetry.

It may be concluded from Eqs.(3-9), (3-10), and (3-11) that for ψ_L set equal to zero, φ and ψ will be zero all along the axis of revolution.

With the values of φ and ψ established along the z axis, Eqs.(3-4), (3-3a), and (3-8) are sufficient to handle cylindrical

regions that touch the z axis, but which do not have interior cavities. Problems that can be solved include cylinders with one end open, since they may be classified as having a singly-connected region. Cylinders with both ends capped involve doubly-connected regions, and will be discussed in Chapter 4.

By Eqs. (3-2a,b) the definitions of σ_r and σ_θ in terms of φ and ψ also become undefined as r goes to zero. The limiting values of these equations are:

$$\sigma_r = \sigma_\theta = \frac{1}{2} \left[\frac{\partial^2 \psi}{\partial r^2} + (1+\nu) \frac{\partial^2 \varphi}{\partial r^2} \right]$$

Employing symmetry about the z axis and letting $\varphi = \psi = 0$ on the z axis the equivalent difference equation is,

$$\left[\sigma_r = \sigma_\theta \right]_{r=0} = (1+\nu) (\varphi_N) + \psi_N \quad (3-12)$$

Difference Equations in Spherical Coordinates

For cylinders with hemispherical end-caps it is possible to employ a square grid in the rectangular generating area and a polar coordinate grid in the quarter ring which generates the end-cap. The two coordinate systems must be coupled together at the juncture of the end-cap and cylinder as will be discussed later.

In the quarter ring generating area Eqs. (3-1), (3-2), and (3-3) must be transformed to spherical coordinates (which reduce to polar coordinates for axial symmetry) and equivalent difference equations written. Again, central difference equations were employed where possible⁴. Appendix A includes the somewhat lengthy derivation of the difference equations applying in the quarter ring generating area. The following equations perform the same function in the generating rectangular and quarter ring areas respectively: Eqs. (3-4) and (A-3), (3-6) and (A-15), and Eqs. (3-8) and (A-12, A-13).

The procedure is identical for the cylindrical and spherical regions. Of particular interest is a problem involving both regions coupled together at the juncture of the cylinder and cap.

Juncture of Cylindrical and Hemispherical Regions

Figure 21 shows the generating area in the neighborhood of the juncture of a cylinder and hemispherical end cap. As stated in Appendix A, the stress functions ϕ and ψ will be invariant under coordinate transformation from physical considerations. Coupling of the coordinate systems may thus be accomplished by considering the values of the functions along the interface at points P1 through P to be common to both regions.

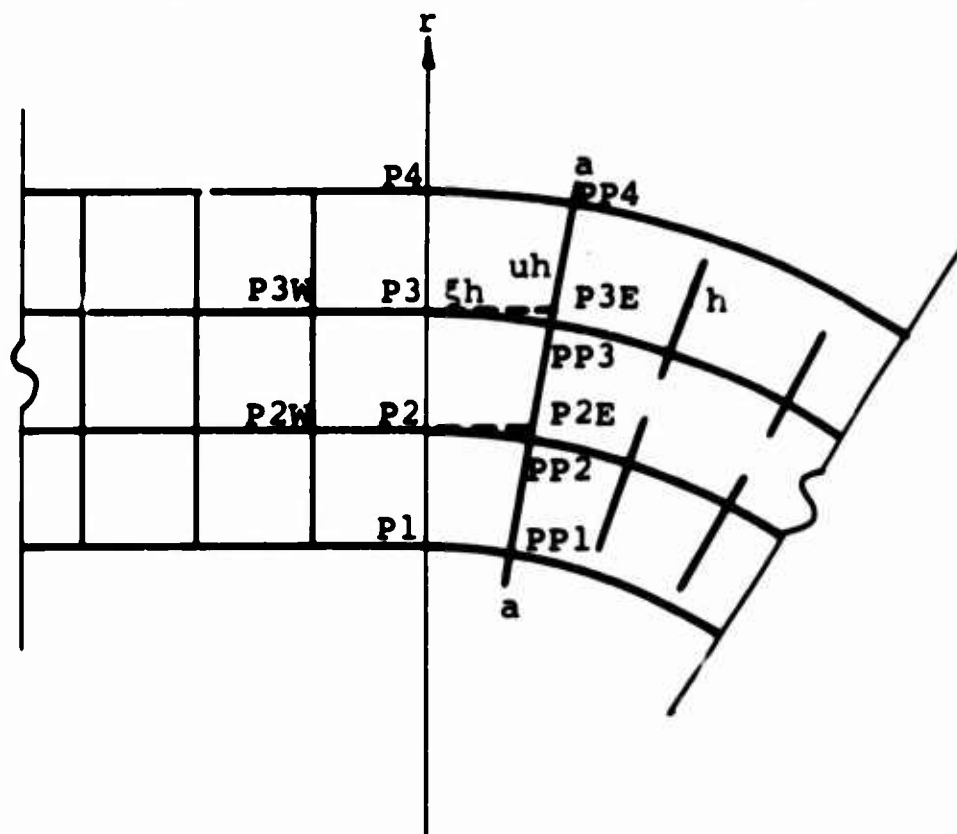


Figure 21. Juncture of cylinder and end cap.

In Fig. 21, functions at points P1 through P4 are assumed to be governed by difference equations in rectangular coordinates. The horizontal grid lines are extended into the polar regions intersecting radius a-a at points P2E and P3E. It is not necessary to extend the grid lines from P1 or P4, since the rectangular difference equations there involve only P1, P2 and P3, P4 respectively.

Governing difference equations equivalent to Eqs.(3-1) can be written for points P2 and P3 by using equivalent difference expressions for the second derivative in the z direction with unequal intervals [See Ref. 1, pg.67]. Considering point P3 of Fig. 21 for example:

$$\left[\frac{\partial^2 (\quad)}{\partial z^2} \right]_{P3} \approx \frac{2}{h^2 (1+\xi)} \left[\frac{1}{\xi} (\quad)_{P3E} + (\quad)_{P3W} - \frac{1+\xi}{\xi} (\quad)_{P3} \right] \quad (3-13)$$

Using the above equation in Eq. (3-1a) yields for the governing φ equation at P3:

$$\left[\frac{2}{(\xi)(1+\xi)} \right] \varphi_{P3E} + \left(1 - \frac{h}{2r}\right) \varphi_{P4} + \left(\frac{2}{1+\xi}\right) \varphi_{P3W} + \left(1 + \frac{h}{2r}\right) \varphi_{P2} - 2 \left(\frac{1+\xi}{\xi}\right) \varphi_{P3} = 0 \quad (3-14)$$

The value of the function at point P3E in the above equation can be expressed in terms of values at points PP4, PP3, and PP2 by interpolation along the radius a-a. Using the first three terms of Newton's forward interpolating formula [See Ref. 3, pg. 64],

$$\begin{aligned} (\quad)_{P3E} &\approx \frac{1}{2} \left[(2-3u+u^2) (\quad)_{PP4} + (2u)(2-u) (\quad)_{PP3} - (u)(1-u) \right. \\ &\left. (\quad)_{PP2} \right] \end{aligned} \quad (3-15)$$

Substituting Eq. (3-15) into (3-14) yields the governing φ equation at point P3.

$$\begin{aligned} &\frac{1}{(\xi)(1+\xi)} \left[(2-3u+u^2) \varphi_{PP4} + (2u)(2-u) \varphi_{PP3} - (u)(1-u) \varphi_{PP2} \right] \\ &+ \left(1 - \frac{h}{2r}\right) \varphi_{P4} + \left(\frac{2}{1+\xi}\right) \varphi_{P3W} + \left(1 + \frac{h}{2r}\right) \varphi_{P2} - 2 \left(\frac{1+\xi}{\xi}\right) \varphi_{P3} = 0 \end{aligned} \quad (3-16)$$

A similar equation can be written at point P2 by using the appropriate nodal points and u and ξ values.

The governing equations for ψ at point P3 can be found by combining the operators of Eqs. (3-1) and (3-13).

$$\begin{aligned} &\frac{1}{(\xi)(1+\xi)} \left[(2-3u+u^2) \psi_{PP4} + (2u)(2-u) \psi_{PP3} - (u)(1-u) \psi_{PP2} \right] \\ &+ \left(1 - \frac{h}{2r}\right) \psi_{P4} + \left(\frac{2}{1+\xi}\right) \psi_{P3W} + \left(1 + \frac{h}{2r}\right) \psi_{P2} - 2 \left(\frac{1+\xi}{\xi}\right) \psi_{P3} \\ &- \frac{1}{\xi(1+\xi)} \left[(2-3u+u^2) \varphi_{PP4} + (2u)(2-u) \varphi_{PP3} - u(1-u) \varphi_{PP2} \right] \\ &- \left(\frac{2}{1+\xi}\right) \varphi_{P3W} + \left(\frac{2}{\xi}\right) \varphi_{P3} = 0 \end{aligned} \quad (3-17)$$

A similar governing ψ equation can be written for point P2, again using the appropriate nodal points and values of u and ξ .

The functions along the radius a-a at points PP1, PP2, etc. are assumed to be governed by appropriate equations developed in Appendix A for spherical regions. The difference equations at those points will involve points P1 through P4 without any modifications being necessary. Likewise points P2W and P3W will be governed by unmodified rectangular difference equations and will involve points P2 and P3. Thus a sufficient number of equations are available to solve for all unknown values of φ and ψ in the neighborhood of the juncture of the cylinder and hemispherical cap.

CHAPTER 3

APPLICATIONS TO CYLINDERS WITH ONE END CAPPED

Cylinder with a Flat Cap

Figure 22 shows the generating area for an example problem with a flat cap. The loading considered was a unit normal pressure p on the outer surface. Normal stresses obtained on the boundaries by the finite difference method and Southwell stress functions are also shown.

An indication of the error in the solution on the boundaries parallel to the z axis can be obtained by comparing the σ_r values calculated from the φ and ψ functions to the known applied normal boundary stress. The error is obviously greatest at the re-entrant corner, where the boundary was rounded off to avoid a singularity. The nodal point there is considered to be an interior node, but the error inherent in representing a rapidly changing geometry by a set of discrete points is apparent. Grading the mesh around the corner would hopefully reduce the error there, but would require more hand labor and machine storage. A stress concentration obviously exists at the corner which cannot be found directly by the finite difference method, but hopefully could be approached with a closer spacing of nodal points. The solution approaches the Lamé' solution quite rapidly as z increases beyond the neighborhood of the end cap.

In obtaining the solution for the example problem computer programs were designed and used for: (1) generating most of the coefficients in the matrix of coefficients for the unknown φ and ψ values at interior nodal points; (2) solving by an iteration procedure for φ and ψ from the complete matrix of coefficients and constants vector; and (3) calculating normal stresses on boundaries parallel to the z axis. These programs are included in Appendix B. Program B-1 employs Eqs.(3-4), while program B-3 employs Eqs.(3-6).

The generation of the coefficients for boundary points of a rectangular generating area must be done by hand using Eqs.(3-8). It is also necessary to modify the coefficients in the equations for the points adjacent to the boundary by inserting appropriate boundary coefficients or constants according to Eqs.(3-4). The constants vector is derived from applying Eqs.(3-8) and (3-4).

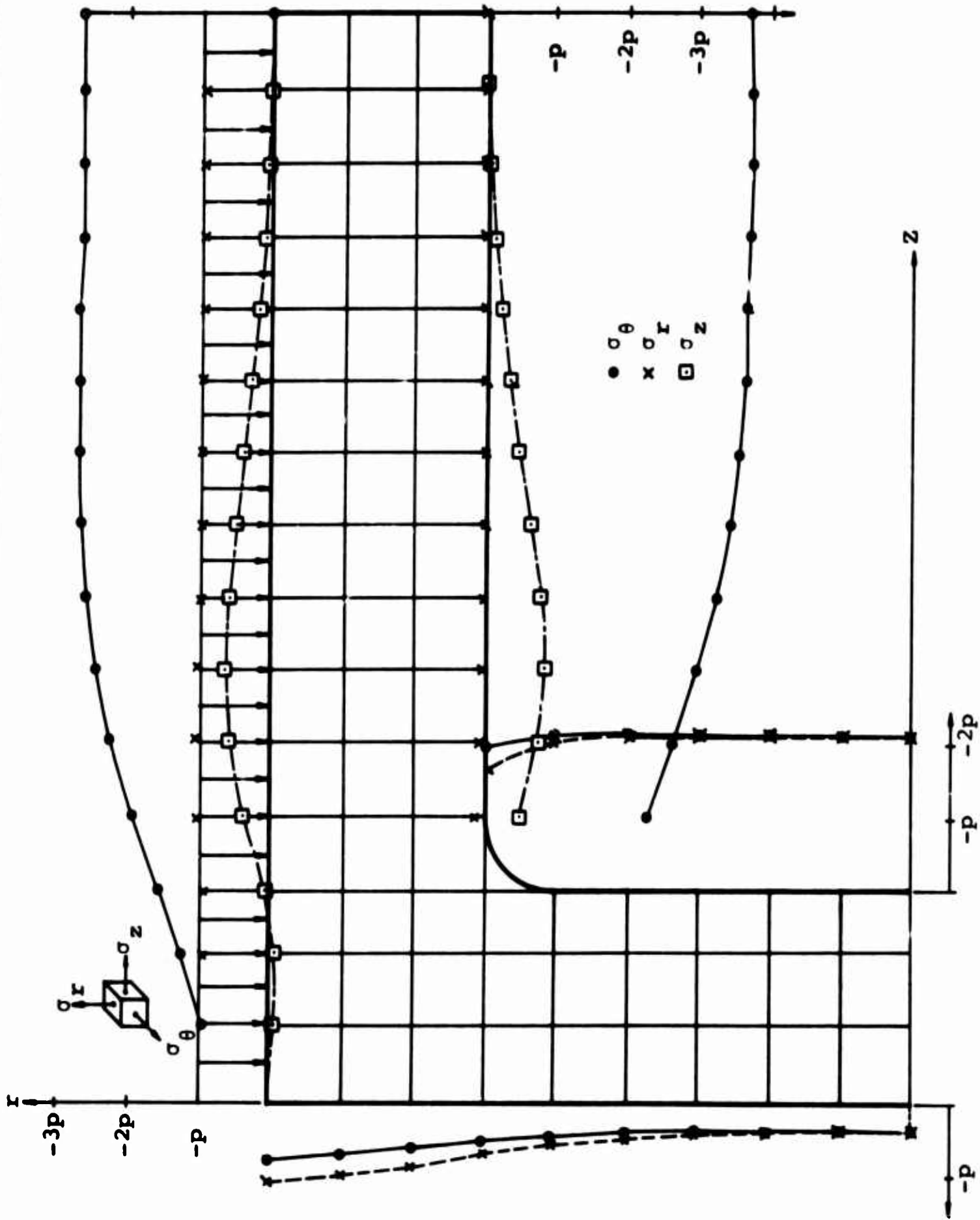


Figure 22. Stresses in an open cylinder with flat cap.

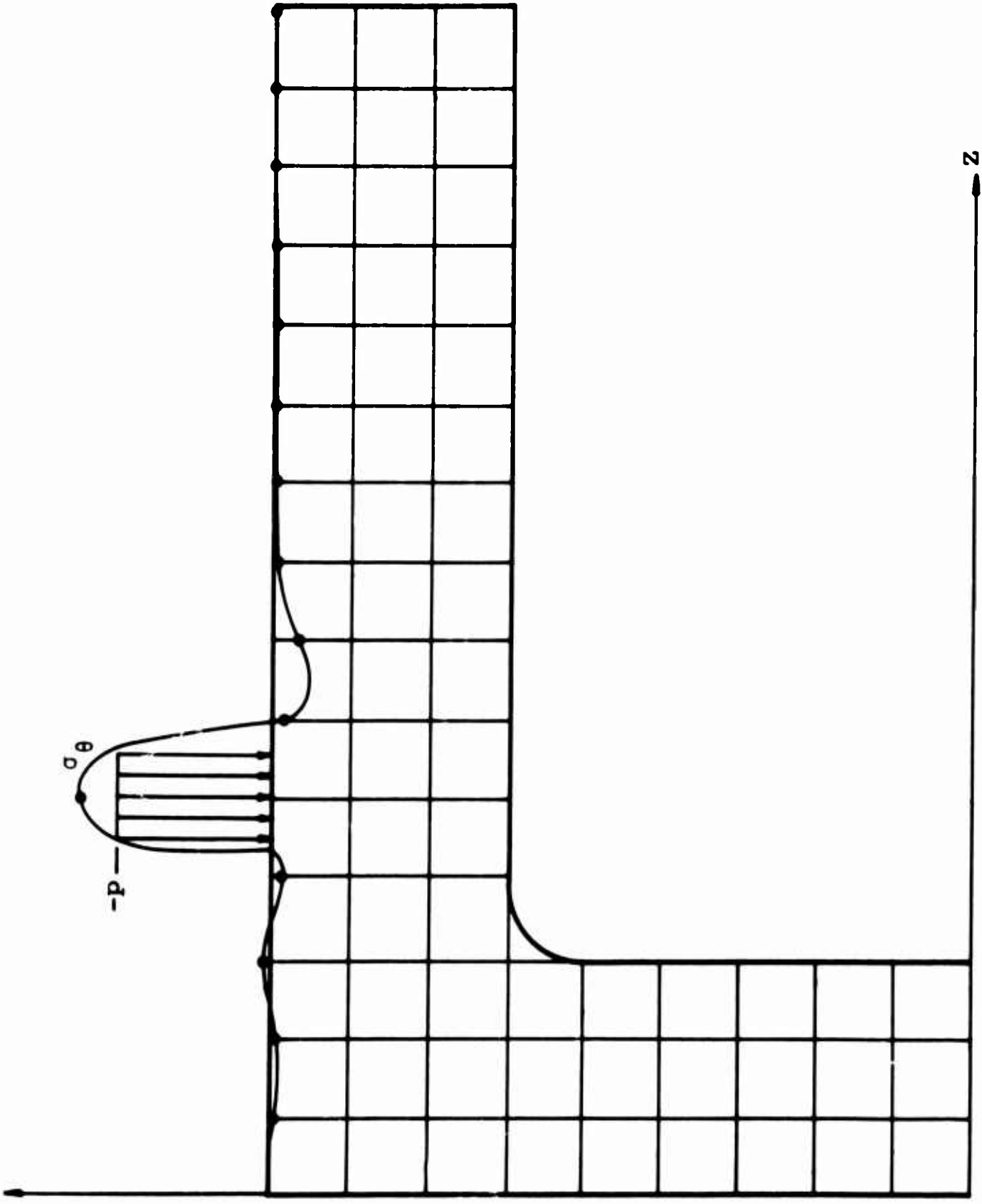


Figure 23. Hoop stress on the outer surface of a cylinder due to a band of pressure.

The iteration procedure for solving the difference equations and the program for calculating normal stresses on the boundary may be used without hand modification.

In the second example problem, a unit ring of pressure was applied at a particular location. Figure 23 shows the hoop stress on the outside boundary. The main objective of this example was to study how rapidly the stress decays away from the point of load application. The stress apparently decays quite rapidly, implying the effect of the end caps also decays rapidly as z increases beyond the neighborhood of the end.

Cylinders with a Hemispherical Cap

Figure 24 shows the generating area for an example problem with hemispherical cap. The loading considered was a unit pressure on the outer cylindrical portion of the solid of revolution. Normal stresses on the boundaries are also shown.

Again an indication of the error involved may be obtained by comparing the calculated value of stress normal to the boundary to the applied stress. As might be anticipated, the maximum error occurs near the juncture of the two regions. Again, as in the case of a re-entrant corner, grading the mesh near the juncture would probably reduce the error there. Additional study of the coupling of two coordinate systems for a finite difference solution would be desirable.

In obtaining the solution for the cylinder with a hemispherical end cap the three computer programs described in the previous sub-section were used. In addition programs were written and used for: (4) generating the coefficients in the matrix of coefficients for all points in the quarter-ring generating area; and (5) calculating normal stresses on the inner and outer surfaces of the hemispherical cap. These programs are included in Appendix B. Program B-4 employs Eqs. (A-5), (A-6), (A-12) and (A-13). Program B-5 employs Eqs. (A-15) and (A-16).

Generation of the matrix of coefficients corresponding to Fig. 24 requires the use of programs B-1 and B-4. In addition, for nodal points on and adjacent to the boundaries of the rectangular generating area the procedure described in the last sub-article which involves hand modification must be used. For the interior nodal points along the interface of the two regions equations similar to Eqs. (3-16) and (3-17) must be applied by

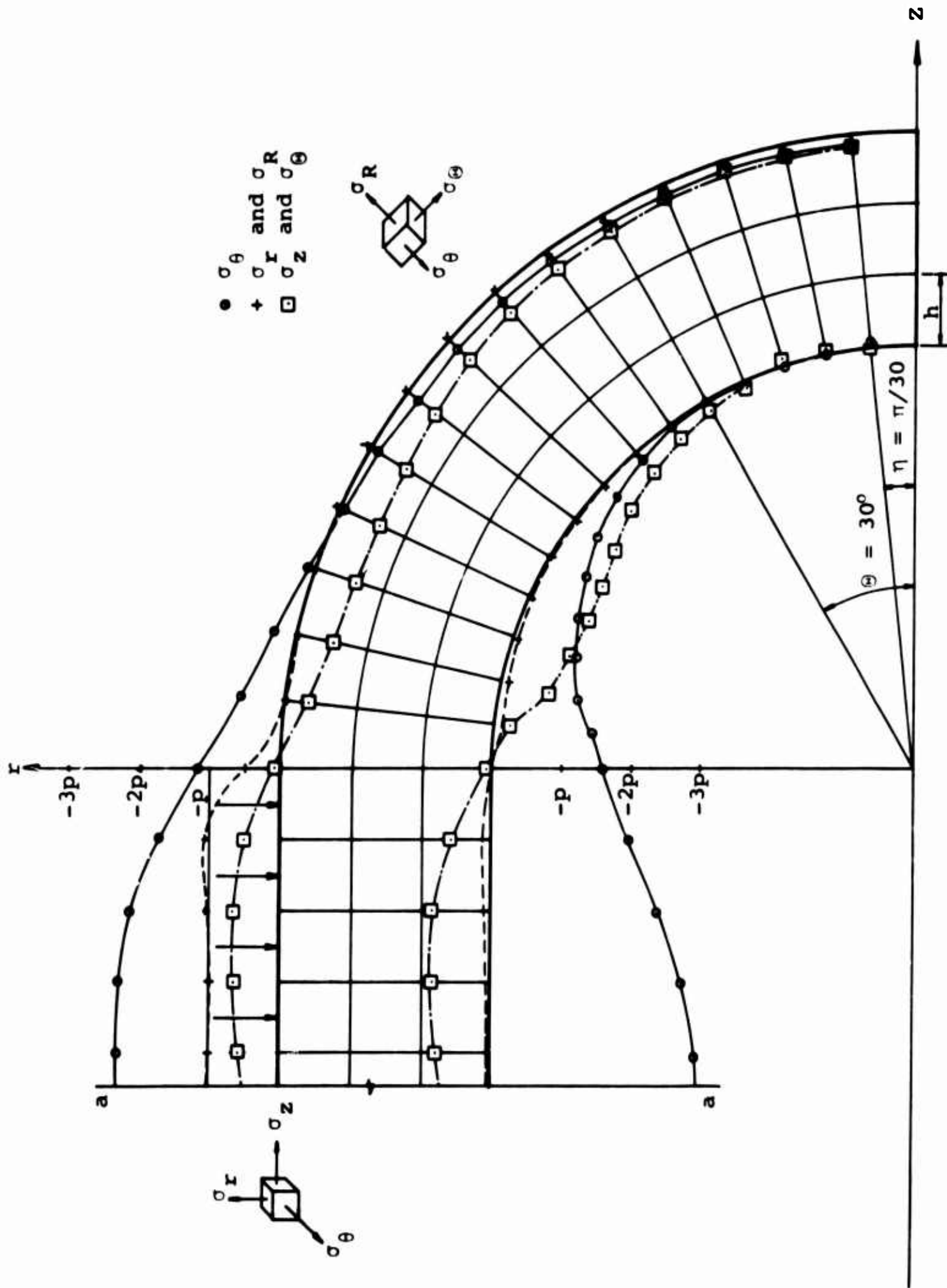


Figure 24. Stresses in a cylinder with hemispherical cap.

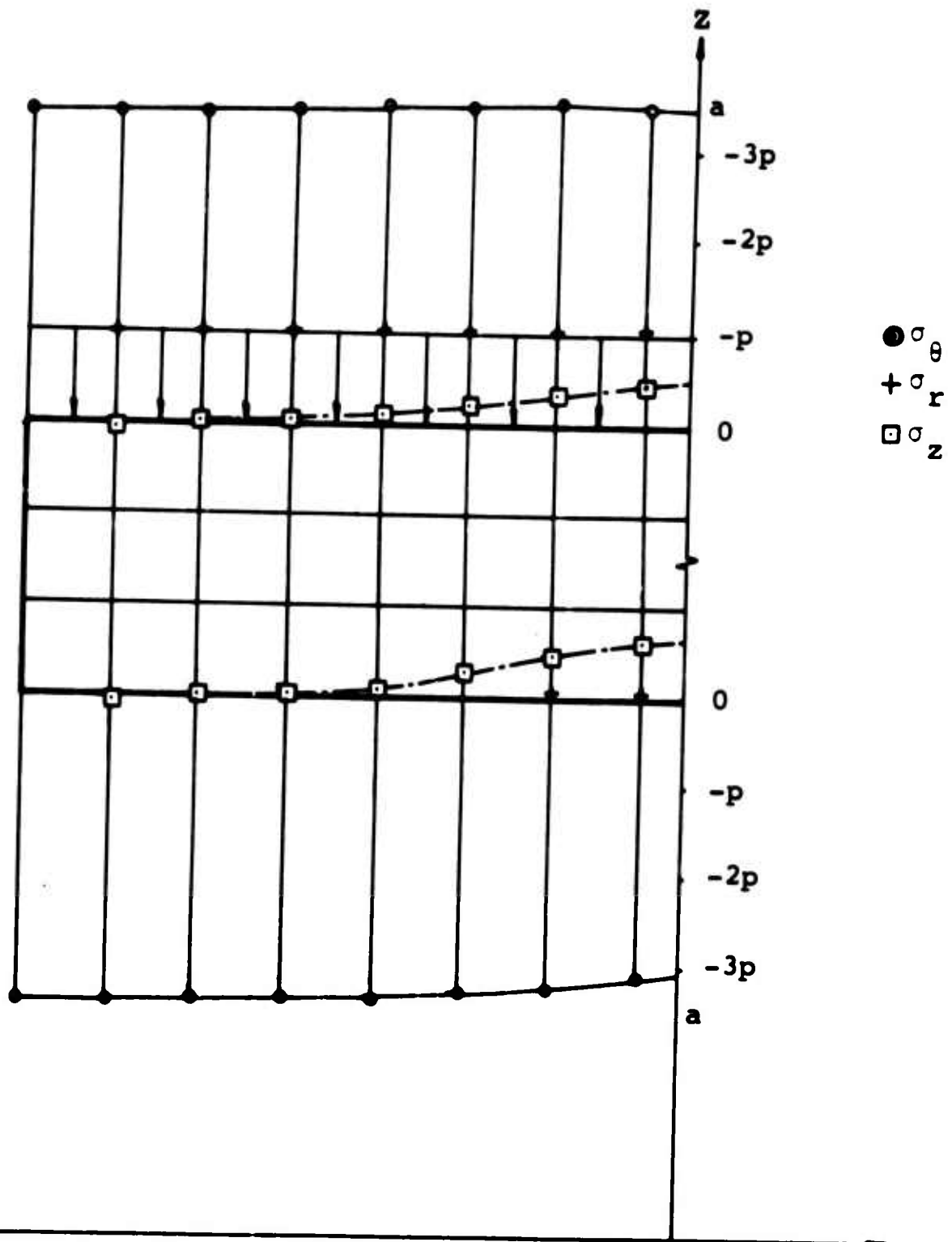


Figure 25. Continuation of Figure 24.

hand. The final matrix of coefficients must be in a form acceptable to the iteration procedure program, B-2. Obviously there should be no duplication of numbering of unknowns over the two regions comprising the total generating area. Programs B-3 and B-5 will scan the total output of the solution by program B-2, and calculate the appropriate stresses.

The hand labor involved for this problem comes about mainly from hand applications of difference equations to the boundary points of the rectangular generating area and to points along the interface between the two areas. The time expended in machine calculations is spent mainly in obtaining the solutions to the difference equations.

CHAPTER 4

ANALYSIS OF CYLINDERS WITH BOTH ENDS CAPPED

Cavities in Axisymmetric Solids

Allen has discussed the solution for axisymmetric solids with a cavity [see Ref. 1, pp. 195-198]. He shows that for any axisymmetric body single valuedness of displacement, v , in the z direction is insured by the equation

$$\oint_C \frac{\partial v}{\partial s} ds = \iint \left[\left(\frac{\partial^2 \psi}{\partial r^2} - \frac{1}{r} \frac{\partial \psi}{\partial r} + \frac{\partial^2 \psi}{\partial z^2} - \frac{\partial^2 \varphi}{\partial z^2} \right) + v \left(\frac{\partial^2 \varphi}{\partial r^2} - \frac{1}{r} \frac{\partial \varphi}{\partial r} + \frac{\partial^2 \varphi}{\partial z^2} \right) \right] dr dz = 0 \quad (3-18)$$

where C is any closed curve in the generating area. For any curve not enclosing a cavity, the above integral equation requirement is equivalent to Eqs.(3-1). However for solids with cavities not touching the axis of revolution, the above equation applied around the inner boundary can be used to determine the no longer arbitrary initial value of ψ there. For if the initial value of ψ on the exterior boundary is selected to be arbitrary, then the initial value of ψ on the inner boundary is not.

For an axisymmetric solid with a cavity touching the axis of revolution the above equation yields no information about ψ when applied around the inner boundary. In this case it is not possible to return to the starting point of integration because of the "gap" along the z axis. If an integration is performed in the negative r region, then the integral all around the axisymmetric cavity correctly vanishes identically since this is essentially a re-tracing in the opposite direction of the integral in the generating area above the z axis. Another method must be used to determine the initial value of ψ on an inner cavity.

Determination of ψ on an Inner Boundary

Consider the solid of revolution shown in Fig. 26. From a previous discussion in chapter 2 the values of ψ and φ will be

related constants along the z axis. The behavior of ψ on an inner boundary, denoted by ψ_I along $r = \rho$, as ρ approaches zero, is of particular interest.

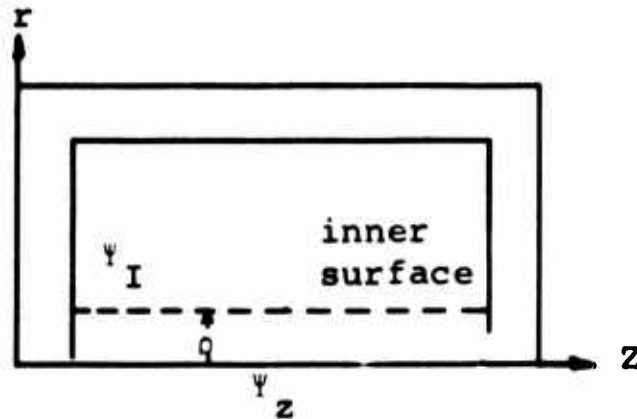


Figure 26. Determination of ψ_I on the inner surface of a closed cylinder.

It will be argued that ψ_I approaches the value of ψ on the z axis, denoted by ψ_z , as ρ approaches zero. Thus, the initial value of ψ on an inner boundary at the axis of revolution is equal to the arbitrary initial value of ψ on an outer boundary at the axis of revolution.

Consider the physical effect of making ρ ever smaller. As ρ decreases σ_z in the central "core" of material along the z axis will increase, but at a decreasing rate. For as ρ is made smaller the central core will carry less of the load that ties the ends together. This force is distributed to the cylinder walls, which are theoretically capable of carrying any load. Furthermore the elongation of the core in the z direction will remain small, and will become essentially constant as ρ approaches zero. The latter statement is true because the displacement of the cylinder ends in the direction of the z axis is affected to an ever smaller extent by the decreasing of ρ after the cylinder walls are carrying almost all of the load formerly carried by the core of the cylinder. It follows the strain and hence the stress on the core for small values of ρ remains defined and essentially constant as ρ becomes smaller.

Recall that

$$\sigma_z = - \frac{1}{r} \frac{\partial \psi}{\partial r},$$

and along the z axis,

$$\sigma_z = - \frac{\partial^2 \psi}{\partial r^2}.$$

Thus if σ_z remains defined throughout the core as ρ becomes small, then $\frac{\partial \psi}{\partial r}$ throughout the core and $\frac{\partial^2 \psi}{\partial r^2}$ on the z axis remain defined. This implies that ψ_I approaches ψ_z as ρ approaches zero.

It is therefore possible to set $\psi = 0$ on the inner boundary at the z axis, if the initial value of ψ on the external boundary at the z axis is also set to zero. If the cylinder is subject to internal loads on the inner cavity, then ψ will vary there according to Eq. (3-3a).

The initial value of ψ on the interior surface of a thick walled cylinder with both ends capped may be found by the above analysis. The solution otherwise is identical to the solution for a cylinder with an open end.

Figure 27 shows normal stresses in a closed flat-end cylinder. The cylinder was loaded by a uniform pressure over the ends. The analysis discussed above was used in the determination of the initial value of ψ on the inner boundary of the cylinder. Values of σ_r and σ_z were not plotted at the reentrant corner as it was felt the values obtained there were unrealistic due to the rapidly changing geometry and the relatively coarse mesh employed.

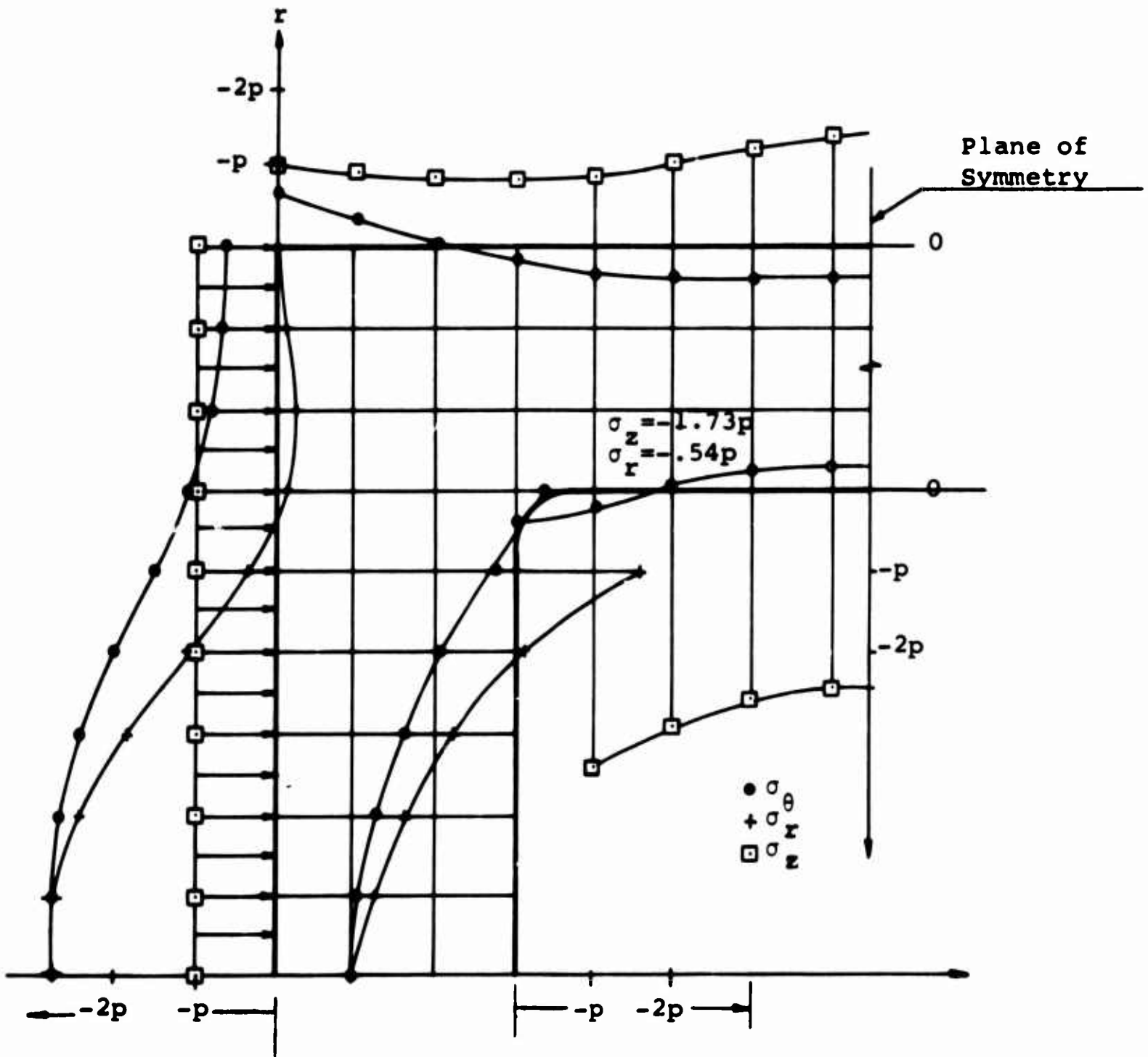


Figure 27. Stresses in a closed cylinder.

CHAPTER 5

SUMMARY

A method has been presented for the determination of stresses in axially loaded thick walled cylinders with one end capped. The end cap may be either flat or hemispherical. Computer programs have been designed to handle most of the tedious labor associated with the finite difference technique. Example problems of cylinders with both types of end caps are presented.

The maximum error in the example problems considered occurs in the neighborhood of reentrant corners and at the juncture of the cylinders and end caps. Additional refinement of the grid would probably reduce the error in these locations, but would require additional hand work to obtain the corresponding difference equations.

An analysis of thick walled cylinders with both ends capped has been made. It is shown that on the axis of revolution the initial value of the Southwell stress function ψ on an inner surface may be set equal to ψ on the outer surface. An example problem employing the above analysis is presented for a cylinder with both ends capped by flat caps.

Of additional interest would be: (1) the effect of refining the grid at the reentrant corners, (2) a more effective coupling together of the two coordinate systems at the juncture of the cylinders and hemispherical end caps, and (3) cylinders with end caps that are not complete hemispheres.

REFERENCES

1. Allen, D. N. de G., Relaxation Methods in Engineering and Science, 1954, McGraw-Hill, N.Y.
2. Forsythe, G. E., and Wasow, W. R., Finite-Difference Methods for Partial Differential Equations, 1960, John Wiley and Sons, N. Y.
3. Nielsen, K. L., Methods in Numerical Analysis, 1956, MacMillan Co., N.Y.
4. Salvadori and Baron, Numerical Methods in Engineering, 1961, Second Edition, Prentice-Hall, Englewood Cliffs, New Jersey.

APPENDIX A
DEVELOPMENT OF FINITE DIFFERENCE EQUATIONS FOR
SOUTHWELL STRESS FUNCTIONS IN SPHERICAL REGIONS

As noted previously axisymmetric elasticity problems are mathematically two dimensional and involve the generating area of a solid of revolution. Thus for spherical regions the problem involves a generating area which can most readily be described by the coordinates (R, θ) as shown in Fig. 28.

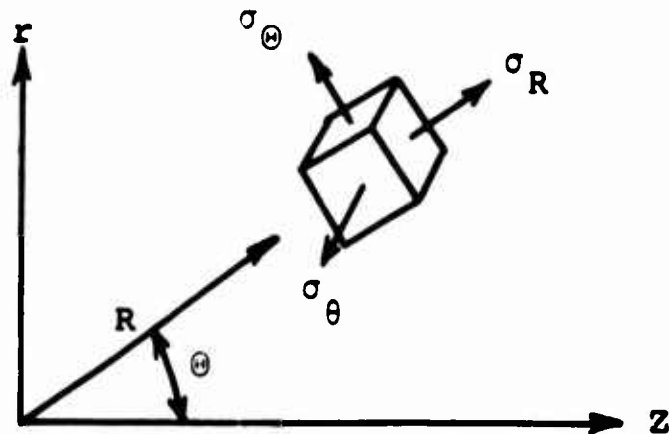


Figure 28. Coordinate system and notation.

Since the differential equations governing the Southwell stress functions are of second order it is feasible to transform them into the coordinates (R, θ) and use appropriate polar coordinate finite difference representations. From physical considerations the stress functions ψ and φ will be invariant under coordinate transformations. The equations defining the stresses σ_r , σ_θ , σ_z and τ_{zr} become in the (R, θ) coordinates:

$$\sigma_r = \frac{1}{R \sin\theta} \left\{ \sin\theta \frac{\partial(\varphi+\psi)}{\partial R} + \frac{\cos\theta}{R} \frac{(\varphi+\psi)}{\partial\theta} - \frac{1}{R \sin\theta} [\psi + (1-\nu)\varphi] \right\} \quad (a) \quad (A-1)$$

$$\sigma_\theta = \frac{\nu}{R \sin\theta} \left\{ \left[\sin\theta \frac{\partial\varphi}{\partial R} + \frac{\cos\theta}{R} \frac{\partial\varphi}{\partial\theta} \right] + \frac{1}{\nu R \sin\theta} [\psi(1+\nu)\varphi] \right\} \quad (b)$$

$$\sigma_z = -\frac{1}{R \sin\theta} \left[\sin\theta \frac{\partial \psi}{\partial R} + \frac{\cos\theta}{R} \frac{\partial \psi}{\partial \theta} \right] \quad (c)$$

(A-1)

$$\tau_{zr} = \frac{1}{R \sin\theta} \left[\cos\theta \frac{\partial \psi}{\partial R} - \frac{\sin\theta}{R} \frac{\partial \psi}{\partial \theta} \right] \quad (d)$$

The normal stresses σ_R and σ_θ can be found by stress transformations of the type involving direction Cosines l, m, and n:

$$\sigma_R = \sigma_z l^2 + \sigma_r m^2 + 2lm \tau_{zr}.$$

Substituting Eqs. (A-1) in the stress transformation equations yields σ_R and σ_θ .

$$\sigma_R = \frac{1}{R \sin\theta} \left\{ \sin\theta \left(\frac{\partial \psi}{\partial R} \right) - \frac{\cos\theta}{R} \left(\frac{\partial \psi}{\partial \theta} \right) + \sin^2\theta \left[\left[\sin\theta \frac{\partial \varphi}{\partial R} + \frac{\cos\theta}{R} \frac{\partial \varphi}{\partial \theta} \right] - \frac{1}{R \sin\theta} [\psi + (1-\nu)\varphi] \right] \right\}. \quad (a)$$

(A-2)

$$\sigma_\theta = \frac{1}{R \sin\theta} \left\{ -\sin\theta \left(\frac{\partial \psi}{\partial R} \right) + \frac{\cos\theta}{R} \left(\frac{\partial \psi}{\partial \theta} \right) + \cos^2\theta \left(\sin\theta \frac{\partial \varphi}{\partial R} + \frac{\cos\theta}{R} \frac{\partial \varphi}{\partial \theta} \right) - \frac{\cos^2\theta}{R \sin\theta} [\psi + (1-\nu)\varphi] \right\}. \quad (b)$$

The governing equations for the Southwell Stress Functions φ and ψ in the coordinates (R, θ) are:

$$\frac{\partial^2 \varphi}{\partial R^2} - \frac{1}{R^2} \left[\cos\theta \frac{\partial \varphi}{\partial \theta} - \frac{\partial^2 \varphi}{\partial \theta^2} \right] = 0, \quad (a)$$

$$\frac{\partial^2 \psi}{\partial R^2} - \frac{1}{R^2} \left[\cot\theta \frac{\partial \psi}{\partial \theta} - \frac{\partial^2 \psi}{\partial \theta^2} \right] = \frac{\partial^2 \varphi}{\partial R^2} \cos^2\theta - 2 \frac{\partial^2 \varphi}{\partial \theta \partial R} \frac{\sin\theta \cos\theta}{R} \quad (A-3)$$

$$+ \frac{\partial \varphi}{\partial R} \frac{\sin^2\theta}{R} + 2 \frac{\partial \varphi}{\partial \theta} \frac{\sin\theta \cos\theta}{R^2} + \frac{\partial^2 \varphi}{\partial \theta^2} \frac{\sin^2\theta}{R^2}. \quad (b)$$

For a circular boundary, $\frac{\partial}{\partial \eta} = \frac{\partial}{\partial R}$, $\alpha = (90^\circ - \theta)$. The boundary conditions for the Southwell Stress Functions may then be written in terms of (R, θ) as:

$$\frac{\partial \psi}{\partial S} = -r \sigma_{pz} \quad (a)$$

and

$$\frac{\partial \psi}{\partial R} + \left\{ \frac{\partial \varphi}{\partial R} \sin \theta + \frac{\partial \varphi}{\partial \theta} \frac{\cos \theta}{R} - \frac{1}{R \sin \theta} [\psi + (1-\nu)\varphi] \right\} \sin \theta \quad (A-4)$$

$$= R \sin \theta \sigma_{pr} \quad (b)$$

The resulting problem in a hollow hemispherical region can be solved by finite difference techniques in a fashion similar to that for the hollow cylindrical region. Functions φ and ψ must be found that satisfy Eqs. (A-3) over the region and the boundary conditions (A-4) on the boundary of the region. To accomplish this central difference equations in polar coordinates will be employed.⁴

The notation shown in Fig. 29 will be used in the development of finite difference equations in the coordinates (R, θ) .

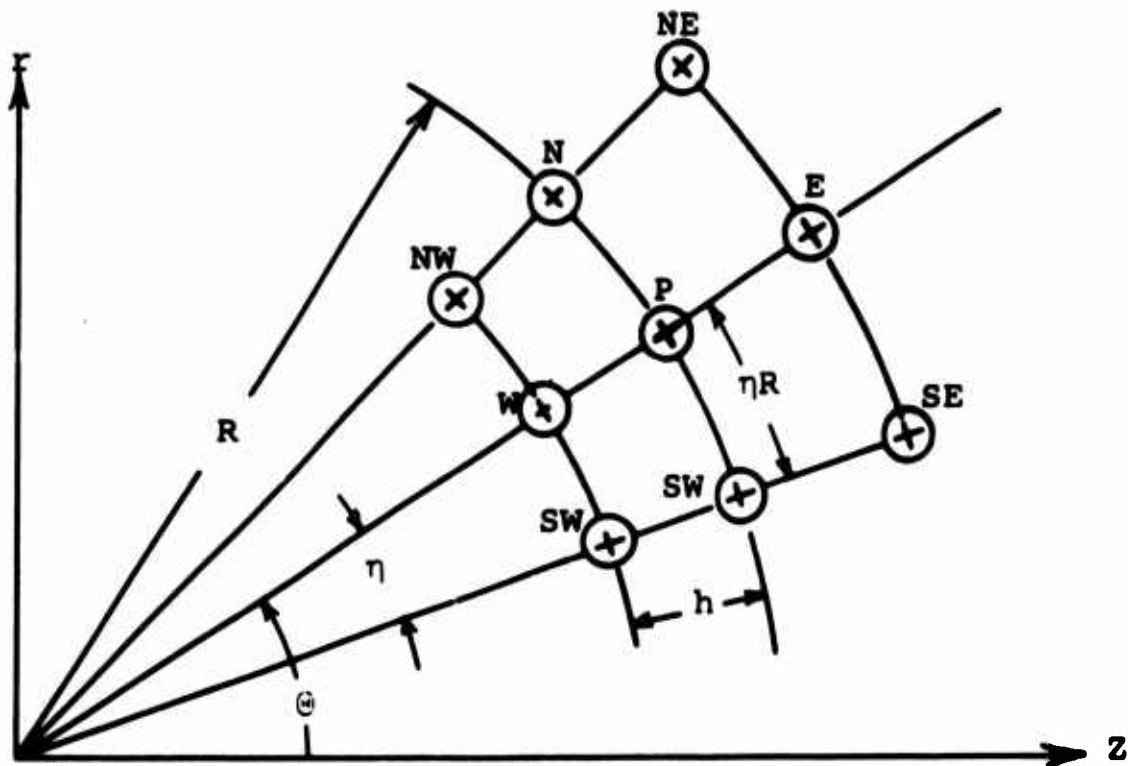


Figure 29. Notation for nodal points in polar coordinates.

Only equal intervals in the radial direction will be considered. The incremental angles η shall likewise be equal. The "compass" notation is used to identify the unknown values of φ and ψ at the nodal points labeled as shown above.

The finite difference equations corresponding to Eqs. (A-3a) and (A-3b) are respectively:

$$\varphi_E + \left(\frac{h}{\eta R}\right)^2 \left[1 - \eta \frac{\text{Cot}\theta}{2}\right] \varphi_N + \varphi_W + \left(\frac{h}{\eta R}\right)^2 \left[1 + \eta \frac{\text{Cot}\theta}{2}\right] \varphi_S - 2 \left[1 + \left(\frac{h}{\eta R}\right)^2\right] \varphi_P = 0 \quad (\text{A-5})$$

and

$$\begin{aligned} \psi_E + \left(\frac{h}{\eta R}\right)^2 \left[1 - \frac{\eta \text{Cot}\theta}{2}\right] \psi_N + \psi_W + \left(\frac{h}{\eta R}\right)^2 \left[1 + \eta \frac{\text{Cot}\theta}{2}\right] \psi_S - 2 \left[1 + \left(\frac{h}{\eta R}\right)^2\right] \psi_P \\ - \left[\text{Cos}^2\theta + \frac{h}{2R} \text{Sin}^2\theta\right] \varphi_E + \left[\frac{h}{2\eta R} \text{Sin}\theta \text{Cos}\theta\right] \varphi_{NE} - \left(\frac{h}{\eta R}\right)^2 \text{Sin}\theta \\ \left[\text{Sin}\theta + \eta \text{Cos}\theta\right] \varphi_N - \left(\frac{h}{2\eta R}\right) \left[\text{Sin}\theta \text{Cos}\theta\right] \varphi_{NW} - \left[\text{Cos}^2\theta - \frac{h}{2R} \text{Sin}^2\theta\right] \varphi_W \\ + \left(\frac{h}{2\eta R}\right) \left[\text{Sin}\theta \text{Cos}\theta\right] \varphi_{SW} - \left(\frac{h}{\eta R}\right)^2 \text{Sin}\theta \left[\text{Sin}\theta - \eta \text{Cos}\theta\right] \varphi_S \\ - \left(\frac{h}{2\eta R}\right) \left[\text{Sin}\theta \text{Cos}\theta\right] \varphi_{SE} = 0 \quad (\text{A-6}) \end{aligned}$$

As might be anticipated the boundary conditions are more complex in the (R, θ) coordinates than in the (r, z) coordinates. The equation (A-4a) may be integrated around the boundary to obtain ψ on the boundary, as was done for the (r, z) coordinates. The equation (A-4b) has for its finite difference equivalent:

$$\begin{aligned} \text{Sin}^2\theta \varphi_E + \left(\frac{h}{\eta R}\right) \text{Sin}\theta \text{Cos}\theta \varphi_N - \text{Sin}^2\theta \varphi_W - \left(\frac{h}{\eta R}\right) \text{Sin}\theta \text{Cos}\theta \varphi_S \\ - \left(\frac{2h}{R}\right) (1-\nu) \varphi_P + \psi_E - \psi_W - \frac{2h}{R} \psi_P = 2hR \text{Sin}\theta \sigma_{pr}. \quad (\text{A-7}) \end{aligned}$$

The "east" or "west" values will be regarded as "fictitious" values to be eliminated according to whether the equation is applied on the outer or inner boundary of the region.

Consider for example the development of the boundary equation governing φ on the outer boundary of the polar generating area. Note again that ψ is known on the boundaries from Eq. (A-4a).

To apply Eq. (A-7) on the outer boundary the φ_E and ψ_E terms must be eliminated by combining Eqs. (A-5), (A-6) and (A-7).

Equation (A-5) is multiplied by $(-\sin^2\theta)$ and added to Eq. (A-7) to yield an equation free of φ_E , i.e.

$$\begin{aligned} & \left[-\sin^2\theta \left(\frac{h}{\eta R}\right)^2 (1-\eta \frac{\cot\theta}{2}) + \left(\frac{h}{\eta R}\right) \sin\theta \cos\theta \right] \varphi_N - 2 \left[\sin^2\theta \right] \varphi_W \\ & \left[-\sin^2\theta \left(\frac{h}{\eta R}\right)^2 (1+\eta \frac{\cot\theta}{2}) - \left(\frac{h}{\eta R}\right) \sin\theta \cos\theta \right] \varphi_S + 2 \left[\sin^2\theta \right. \\ & \left. \left[1 + \left(\frac{h}{\eta R}\right)^2 \right] - \frac{h}{R} (1-\nu) \right] \varphi_P + \psi_E - \psi_W - \frac{2h}{R} \psi_P = 2hR \sin\theta \sigma_{pr} \end{aligned} \quad (A-8)$$

To eliminate ψ_E from the above Eq. (A-8) it is necessary to obtain a second equation free of φ_E . A combination of Eqs. (A-5) and a modified form of Eq. (A-6) will yield an appropriate equation.

The modified form of Eq. (A-6) employs a backward difference representation of the cross derivative of φ in Eq. (A-3b). This is necessary to eliminate the fictitious values of φ_{NE} and φ_{SE} in Eq. (A-6), for there is no possibility of otherwise handling these terms. The backward difference formulas used on the outer and inner boundaries for the cross derivative were respectively:

$$\frac{\partial^2 \varphi}{\partial \theta \partial R} \cong \frac{1}{2\eta h} \left[\varphi_N - \varphi_{NW} + \varphi_{SW} - \varphi_S \right] \quad (A-9)$$

$$\frac{\partial^2 \varphi}{\partial \theta \partial R} \cong \frac{1}{2\eta h} \left[\varphi_{NE} - \varphi_N + \varphi_S - \varphi_{SE} \right]$$

Using the first of Eqs. (A-9) in the representation of Eq. (A-3b) yields:

$$\begin{aligned} & \psi_E + \left(\frac{h}{\eta R}\right)^2 \left[1 - \frac{\eta \cot\theta}{2} \right] \psi_N + \psi_W + \left(\frac{h}{\eta R}\right)^2 \left[1 + \frac{\eta \cot\theta}{2} \right] \psi_S - 2 \left[1 + \left(\frac{h}{\eta R}\right)^2 \right] \psi_P \\ & - \left[\cos^2\theta + \frac{h}{2R} \sin^2\theta \right] \varphi_E - \left(\frac{h}{\eta R}\right) \sin\theta \left[\cos\theta \left(\frac{h}{R} - 1\right) + \frac{h}{\eta R} \sin\theta \right] \varphi_N \\ & - \left(\frac{h}{\eta R}\right) \left[\sin\theta \cos\theta \right] \varphi_{NW} - \left[\cos^2\theta - \frac{h}{2R} \sin^2\theta \right] \varphi_W + \left(\frac{h}{\eta R}\right) \left[\sin\theta \cos\theta \right] \varphi_{SW} \end{aligned}$$

$$+ \left(\frac{h}{\eta R}\right) \sin\theta \left[\cos\theta \left(\frac{h}{R} - 1\right) - \frac{h}{\eta R} \sin\theta \right] \varphi_S = 0 \quad (\text{A-10})$$

Multiplying Eq. (A-5) by $\left[\cos^2\theta + \frac{h}{2R} \sin^2\theta \right]$ and adding to the above equation yields a second equation free of φ_E .

$$\begin{aligned} & \psi_E + \left(\frac{h}{\eta R}\right)^2 \left[1 - \frac{\eta \cot\theta}{2} \right] \psi_N + \psi_W + \left(\frac{h}{\eta R}\right)^2 \left[1 + \frac{\eta \cot\theta}{2} \right] \psi_S - 2 \left[1 + \left(\frac{h}{\eta R}\right)^2 \right] \psi_P \\ & + \varphi_E + \left\{ \left(\frac{h}{\eta R}\right)^2 \left[1 - \frac{\eta \cot\theta}{2} \right] \left[\cos^2\theta + \frac{h}{2R} \sin^2\theta \right] - \left[\frac{h}{\eta R} \sin\theta \right] \left[\cos\theta \left(\frac{h}{R} - 1\right) \right. \right. \\ & \left. \left. + \frac{h}{\eta R} \sin\theta \right] \right\} \varphi_N - \left(\frac{h}{\eta R}\right) \left[\sin\theta \cos\theta \right] \varphi_{NW} + \left(\frac{h}{R}\right) \left[\sin^2\theta \right] \varphi_W + \left(\frac{h}{\eta R}\right) \\ & \left[\sin\theta \cos\theta \right] \varphi_{SW} + \left\{ \left(\frac{h}{\eta R}\right)^2 \left[1 + \frac{\eta \cos\theta}{2} \right] \left[\cos^2\theta + \frac{h}{2R} \sin^2\theta \right] \right. \\ & \left. + \left[\frac{h}{\eta R} \sin\theta \right] \left[\cos\theta \left(\frac{h}{R} - 1\right) - \frac{h}{\eta R} \sin\theta \right] \right\} \varphi_S = 0 \quad (\text{A-11}) \end{aligned}$$

Subtracting Eq. (A-8) from Eq. (A-11) yields a boundary equation for φ on an outer boundary free of all fictitious values.

$$\begin{aligned} & \left(\frac{h}{\eta R}\right)^2 \left\{ \left[1 - \frac{\eta \cot\theta}{2} \right] \left[1 + \frac{h}{2R} \sin^2\theta \right] - \left[\sin^2\theta \right] - \left[\eta \sin\theta \cos\theta \right] \right\} \varphi_N \\ & - \left(\frac{h}{\eta R}\right) \left[\sin\theta \cos\theta \right] \varphi_{NW} + \left(\sin^2\theta \right) \left[2 + \frac{h}{R} \right] \varphi_W + \left(\frac{h}{\eta R}\right) \left[\sin\theta \cos\theta \right] \varphi_{SW} \\ & + \left(\frac{h}{\eta R}\right)^2 \left\{ \left[1 + \frac{\eta \cot\theta}{2} \right] \left[1 + \frac{h}{2R} \sin^2\theta \right] - \left[\sin^2\theta \right] + \left[\eta \sin\theta \cos\theta \right] \right\} \varphi_S \\ & - 2 \left(\frac{h}{\eta R}\right)^2 \left\{ 1 - \left[\left(\frac{\eta R}{h}\right)^2 \left(\frac{h}{R}\right) (1-\nu) \right] - \sin^2\theta \left[1 - \left(\frac{\eta R}{h}\right)^2 - \frac{h}{2R} \left[\left(\frac{\eta R}{h}\right)^2 + 1 \right] \right] \right\} \varphi_P \\ & + \left(\frac{h}{\eta R}\right)^2 \left[1 - \frac{\eta \cot\theta}{2} \right] \psi_N + 2\psi_W \\ & + \left(\frac{h}{\eta R}\right)^2 \left[1 + \frac{\eta \cot\theta}{2} \right] \psi_S - 2 \left[1 - \frac{h}{R} + \left(\frac{h}{\eta R}\right)^2 \right] \psi_P = -2hr \sin\theta \sigma_{pr} \end{aligned}$$

Note that in the above equations ψ_N , ψ_S , and ψ_P will be known values on the boundary. The above equation is the difference equation for φ_P on an outer boundary, $R = \text{constant}$.

In a similar fashion the governing equation for φ_p on an inner boundary may be obtained. It is necessary in this case to use the second of Eqs. (A-9) in the difference representation of the cross derivative in Eq. (A-3b). The resulting governing φ equation is:

$$\begin{aligned}
 & \left[\sin^2 \theta \left(2 - \frac{h}{R} \right) \right] \varphi_E + \left(\frac{h}{\eta R} \right) \left[\sin \theta \cos \theta \right] \varphi_{NE} + \left(\frac{h}{\eta R} \right)^2 \left\{ \left[1 - \frac{\eta \cot \theta}{2} \right] \right. \\
 & \left. \left[1 - \frac{h}{2R} \sin^2 \theta \right] - \left[\sin^2 \theta \right] - \left[\eta \sin \theta \cos \theta \right] \right\} \varphi_N + \left(\frac{h}{\eta R} \right)^2 \left\{ \left[1 + \frac{\eta \cot \theta}{2} \right] \right. \\
 & \left. \left[1 - \frac{h}{2R} \sin^2 \theta \right] - \left[\sin^2 \theta \right] + \left[\eta \sin \theta \cos \theta \right] \right\} \varphi_S - \left(\frac{h}{\eta R} \right) \left[\sin \theta \cos \theta \right] \varphi_{SE} \\
 & - 2 \left(\frac{h}{\eta R} \right)^2 \left\{ 1 + \left[\left(\frac{\eta R}{h} \right)^2 \left(\frac{h}{R} \right) (1-\nu) \right] - \sin^2 \theta \left[1 - \left(\frac{\eta R}{h} \right)^2 + \frac{h}{2R} \left(\frac{\eta R}{h} \right)^2 + 1 \right] \right\} \varphi_P \\
 & + 2 \psi_E + \left(\frac{h}{\eta R} \right)^2 \left[1 - \frac{\eta \cot \theta}{2} \right] \psi_N + \left(\frac{h}{\eta R} \right)^2 \left[1 + \frac{\eta \cot \theta}{2} \right] \psi_S - 2 \left[1 + \frac{h}{R} + \left(\frac{h}{\eta R} \right)^2 \right] \psi_P \\
 & = 2hR \sin \theta \sigma_{pr}
 \end{aligned}$$

In the above equation (as in A-12) the values of ψ_N , ψ_S , and ψ_P are known.

If only hollow hemispherical regions joined to cylindrical regions are studied as in this report, then Eqs. (A-5), (A-6), (A-12), and (A-13) are sufficient to obtain φ and ψ over the circular area generating the hemispherical region. The value of φ will be known along $\theta = 0$ in general, and the values of φ along $\theta = \pi/2$ are assumed to be determined by appropriate difference equations written for the adjoining rectangular area generating the cylindrical region. More detail on this final statement is given in the main body of the report.

The values of φ and ψ obtained by the above equations may then be substituted into the difference equation representation of Eqs. (A-1b,d) and Eqs. (A-2) to yield values of σ_θ , τ_{zr} , σ_R and σ_θ .

Since the values of φ and ψ are solved on the boundary and in the interior of the region, it is necessary to use a backward difference formula for $\frac{\partial}{\partial R}$. The first three terms of Newton's backward interpolating formula for the first derivative may be

used here.³ On the outer boundary the radial derivative operator is represented by:

$$\frac{\partial(\quad)}{\partial R} \cong \frac{1}{2h} \left[3(\quad)_P - 4(\quad)_W + (\quad)_{WW} \right]$$

and on the inner boundary,

(A-14)

$$\frac{\partial(\quad)}{\partial R} \cong -\frac{1}{2h} \left[3(\quad)_P - 4(\quad)_E + (\quad)_{EE} \right]$$

The double subscript implies the value of the function at the next node beyond the west or east nodal point in the radial direction.

Using Eqs. (A-14) and central difference equations for the angular derivatives in Eqs. (A-1b) and (A-2) yields the difference equation relations for normal stress on an outer boundary.

$$\begin{aligned} \sigma_{\theta} \cong & \frac{\nu}{2hR} \left\{ \left(\frac{h}{\eta R} \right) [\cot \theta] \varphi_N + \varphi_{WW} - 4\varphi_W - \left(\frac{h}{\eta R} \right) [\cot \theta] \varphi_S + \left[3 + \frac{2h(1-\nu)}{\nu R \sin^2 \theta} \right] \varphi_P \right. \\ & \left. + \left[\frac{2h}{\nu R \sin^2 \theta} \right] \psi_P \right\} \quad (a) \end{aligned}$$

$$\begin{aligned} \sigma_R \cong & \frac{1}{2hR} \left\{ \sin^2 \theta \left[\left(\frac{h}{\eta R} \right) [\cot \theta] \varphi_N + \varphi_{WW} - 4\varphi_W - \left(\frac{h}{\eta R} \right) [\cot \theta] \varphi_S \right. \right. \\ & \left. \left. + \left[3 - \frac{2h(1-\nu)}{R \sin^2 \theta} \right] \varphi_P \right] - \left(\frac{h}{\eta R} \right) [\cot \theta] \psi_N + \psi_{WW} - 4\psi_W \right. \\ & \left. + \left(\frac{h}{\eta R} \right) [\cot \theta] \psi_S + \left[3 - \frac{2h}{R} \right] \psi_P \right\} \quad (b) \end{aligned} \quad (A-15)$$

$$\begin{aligned} \sigma_{\theta} \cong & \frac{1}{2hR} \left\{ \cos^2 \theta \left[\left(\frac{h}{\eta R} \right) [\cot \theta] \varphi_N + \varphi_{WW} - 4\varphi_W - \left(\frac{h}{\eta R} \right) [\cot \theta] \varphi_S \right. \right. \\ & \left. \left. + \left[3 - \frac{2h(1-\nu)}{R \sin^2 \theta} \right] \varphi_P \right] + \left(\frac{h}{\eta R} \right) [\cot \theta] \psi_N - \psi_{WW} + 4\psi_W \right. \\ & \left. - \left(\frac{h}{\eta R} \right) [\cot \theta] \psi_S - \left[3 + \frac{2h}{R} (\cot \theta)^2 \right] \psi_P \right\} \quad (c) \end{aligned}$$

On an inner boundary the difference equations which are used to determine the normal stresses are:

$$\sigma_{\theta} \approx \frac{\nu}{2hR} \left\{ -\varphi_{EE} + 4\varphi_E + \left(\frac{h}{\eta R}\right) [\cot\theta] \varphi_N - \left(\frac{h}{\eta R}\right) [\cot\theta] \varphi_S \right. \\ \left. - \left[3 - \frac{2(1-\nu)}{\nu R \sin^2\theta} \right] \varphi_P + \left[\frac{2h}{\nu R \sin^2\theta} \right] \psi_P \right\} \quad (a)$$

$$\sigma_R \approx \frac{1}{2hR} \left\{ \sin^2\theta \left[-\varphi_{EE} + 4\varphi_E + \left(\frac{h}{\eta R}\right) [\cot\theta] \varphi_N - \left(\frac{h}{\eta R}\right) [\cot\theta] \varphi_S \right. \right. \\ \left. - \left[3 + \frac{2h(1-\nu)}{R \sin^2\theta} \right] \varphi_P \right] - \psi_{EE} + 4\psi_E - \left(\frac{h}{\eta R}\right) [\cot\theta] \psi_N \\ \left. + \left(\frac{h}{\eta R}\right) [\cot\theta] \psi_S - \left[3 + \frac{2h}{R} \right] \psi_P \right\} \quad (b) \quad (A-16)$$

$$\sigma_{\theta} \approx \frac{1}{2hR} \left\{ \cos^2\theta \left[-\varphi_{EE} + 4\varphi_E + \left(\frac{h}{\eta R}\right) [\cot\theta] \varphi_N - \left(\frac{h}{\eta R}\right) [\cot\theta] \varphi_S \right. \right. \\ \left. - \left[3 + \frac{2h(1-\nu)}{R \sin^2\theta} \right] \varphi_P \right] + \psi_{EE} - 4\psi_E + \left(\frac{h}{\eta R}\right) [\cot\theta] \psi_N \\ \left. - \left(\frac{h}{\eta R}\right) [\cot\theta] \psi_S + \left[3 - \frac{2h}{R} (\cot\theta)^2 \right] \psi_P \right\} \quad (c)$$

FOREWORD TO APPENDIX B

Computer Programs

The programs described were written in Fortran II for the IBM 1620. In certain programs, such as the coefficients generator program B-1, the use of cards is implied. It is convenient to remove certain machine generated "flagged" cards by sorting and to replace them with hand written cards according to the special situation encountered.

Descriptions of programs, flow charts, and source deck listings are included. The stress calculation program, B-5, applying to hemispherical end caps is highly specialized and serves primarily as an example program which can be modified for problems other than the example solution shown in Fig. 24. A table of contents for Appendix B follows for convenience in locating a specific program.

<u>Program</u>	<u>Page</u>
B-1. Coefficients Generator for Southwell Stress Functions in Rectangular Coordinates	173
B-2. Equations-solver Program by Iteration	185
B-3. Calculation of Normal Stresses on Boundaries Parallel to the Axis of Revolution	197
B-4. Coefficients Generator for Southwell Stress Functions in Polar Coordinates	209
B-5. Calculation of Normal Stresses on Boundaries of a Hemispherical Cap	224

APPENDIX B
COMPUTER PROGRAMS

Program 1.--Coefficients Generator for Southwell Stress Functions
in Rectangular (r,z) Coordinates.

This program essentially generates a matrix of coefficients corresponding to linear algebraic equations derived by finite difference techniques and the use of Southwell Stress Functions. It generates the matrix of coefficients of the unknown values of ϕ and ψ occurring at interior nodal points of a square grid covering the regions of interest. For a complete solution of any problem the coefficients generated here must be supplemented by coefficients obtained by hand for boundary points and interior points adjacent to the boundary. This program will flag unknown boundary values affecting nodal points adjacent to the boundary as JW1, JW2, JE1, etc., which must then be inserted by hand. The resulting output is in a form suitable for input to the iteration program included in this study.

Definitions of input parameters which describe the region of interest and identify the unknowns follow.

K = last row number in the region, obtained as distance measured in grid intervals h from the z axis to the furthest parallel grid line in the region.

J = number associated with the initial unknown ϕ value which is assumed to occur at the left end of the initial row. All unknowns are numbered sequentially from left to right and in the increasing r direction, through the ϕ and then ψ unknowns.

I_{init} = first row number in the region, obtained as distance between the z axis and the nearest parallel grid line.

Limits of Rows = distances measured in grid intervals h from a common r axis to the first and last nodal points respectively of rows first through last.

Input--(fixed point throughout)

1. Parameter Card

Cols 1-5	K
Cols 6-10	J
Cols 11-15	I_{init}

2. Limits of Rows Cards--(Rows I_{init} through K in sequence, one card per row)

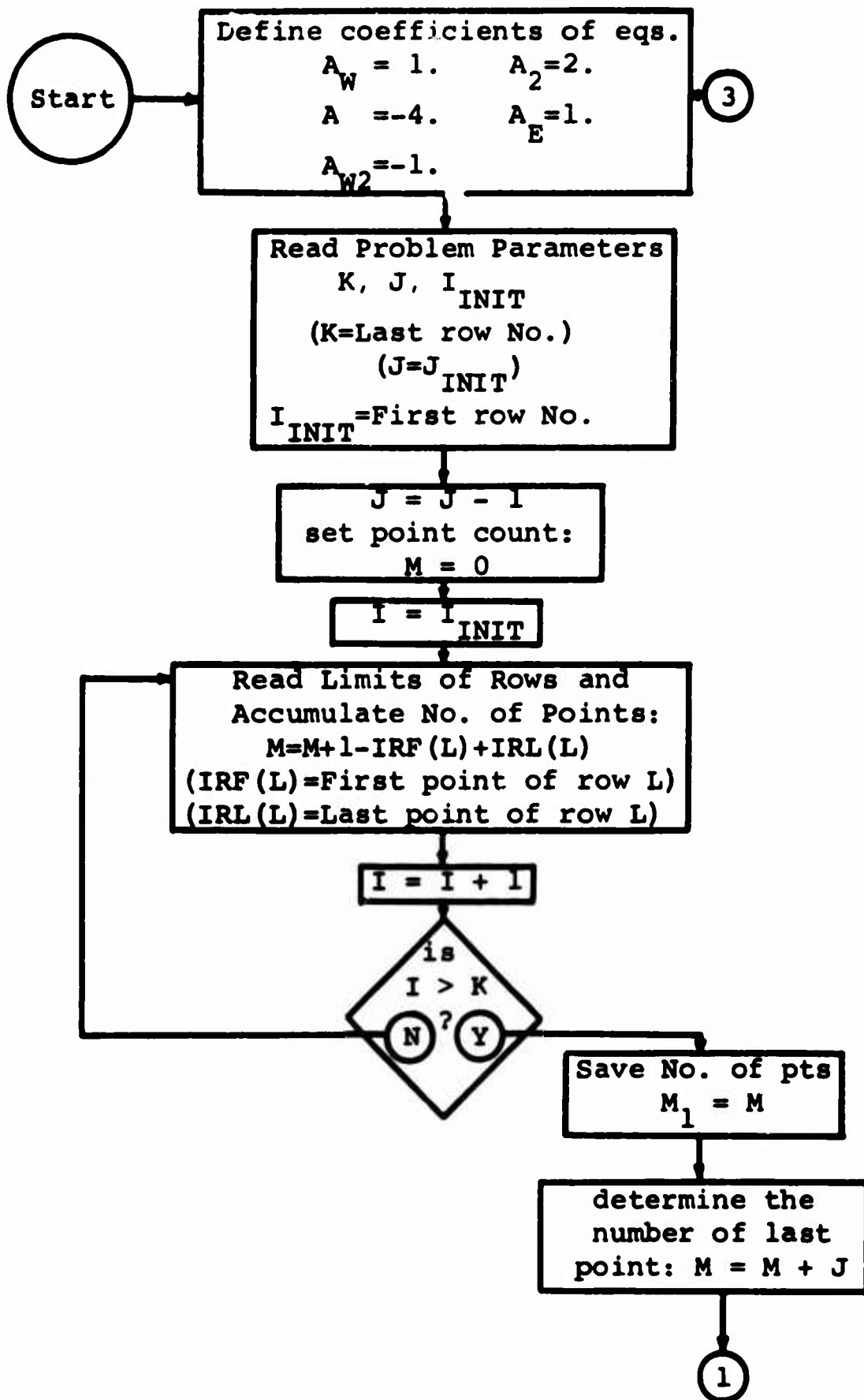
Cols 1-5	Row No.
Cols 6-10	Distance to first nodal point in row
Cols 11-15	Distance to last nodal point in row

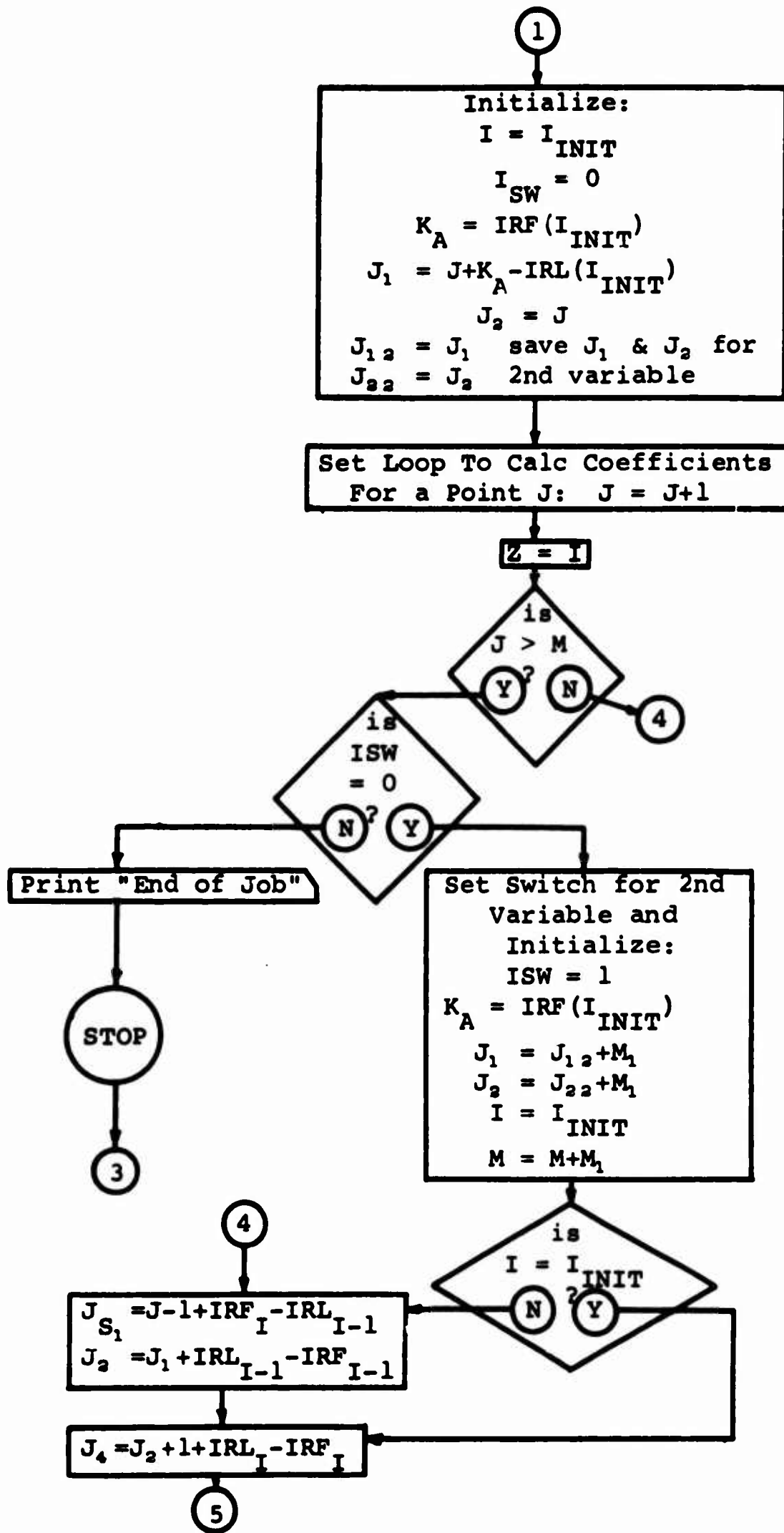
Output

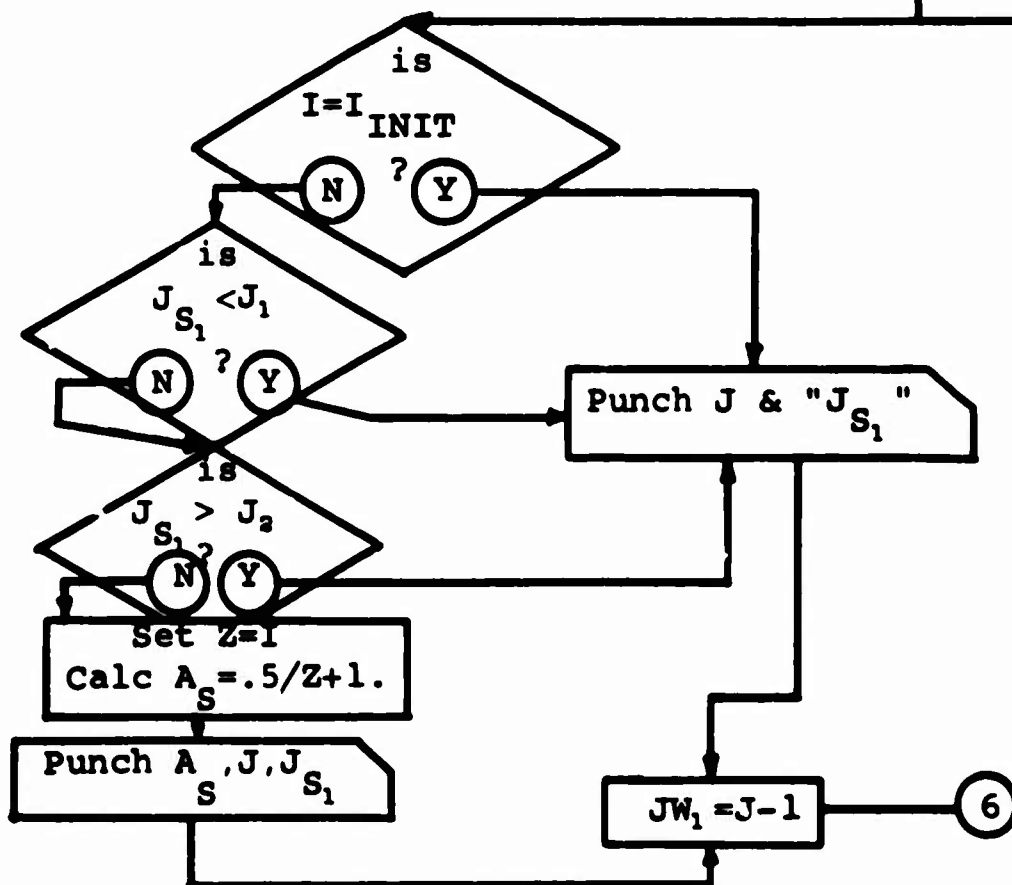
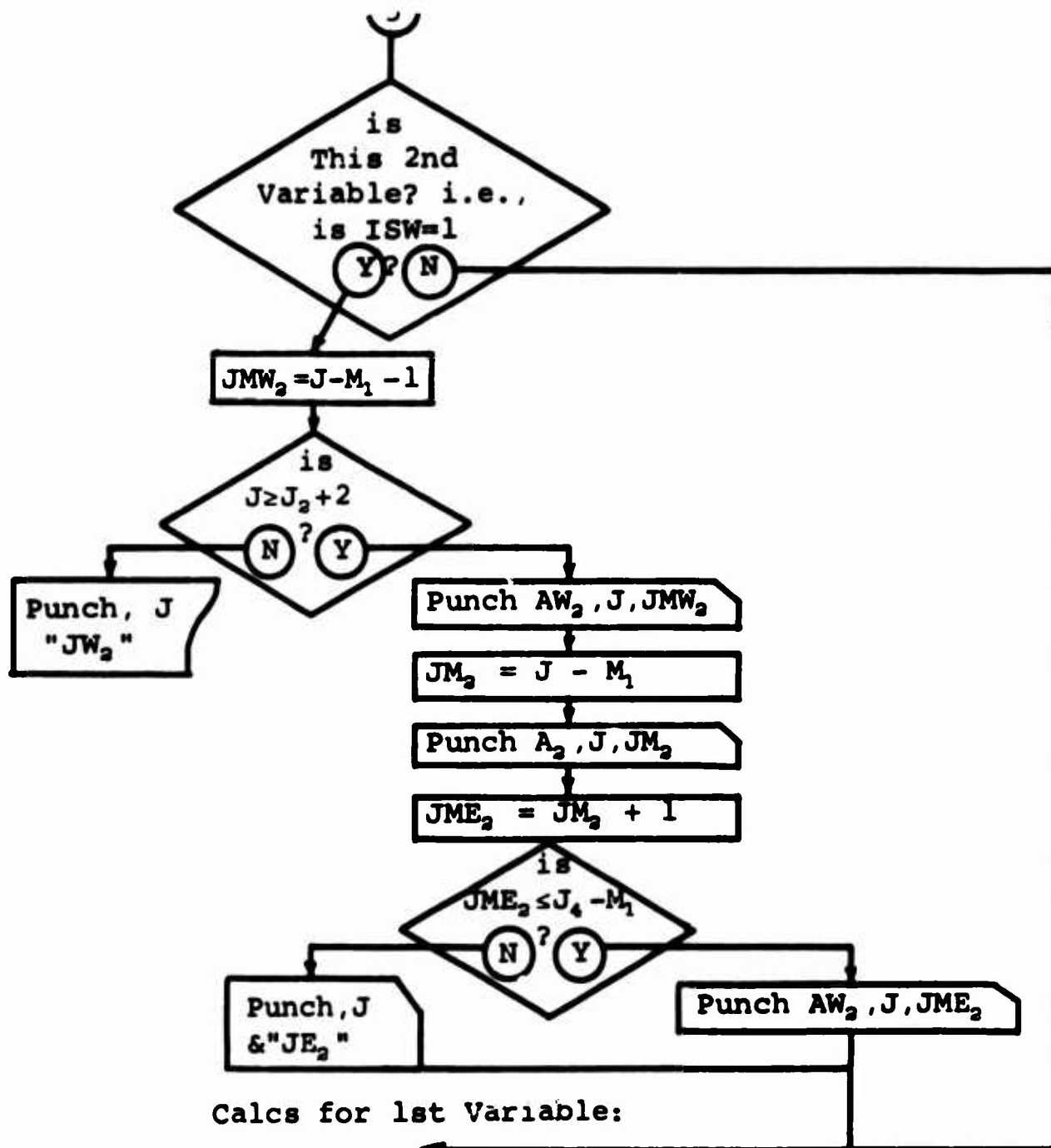
Cols 1-10	Coefficients of Unknowns
Cols 11-15	Rows of Unknowns
Cols 16-20	Cols of Unknowns

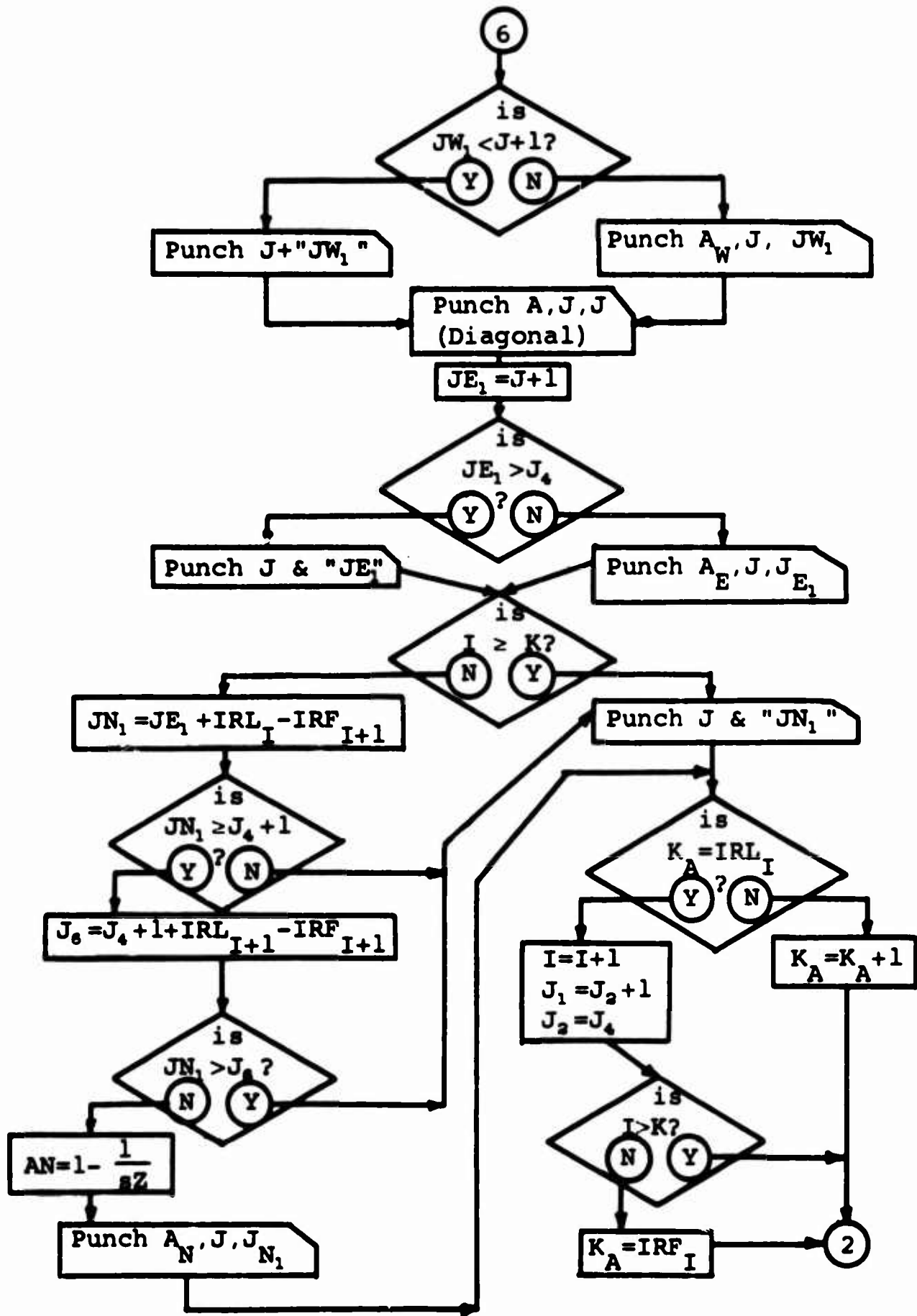
An additional comment should be made that does not deal directly with this program. Before writing by hand the equations involving the boundary nodal points the map of the grid covering the region should be drawn to avoid error. Note the unknowns on the boundaries parallel to the z axis should be numbered from left to right, as this is required by the stress calculation program B-3.

COEFFICIENTS GENERATOR IN RECTANGULAR COORDINATES









```

C C 1306-53008 EQUATION GENERATOR
AM=1.
A=-4.
A2=2.
AE=1.
AM2=-1.
K=LAST ROW NO.
J=INITIAL VALUE OF J
IINIT = FIRST ROW NO.
READ100,K,J,IINIT
J=J-1
M=0
DIMENSION IRF(100),IRL(100)
READ LIMITS OF ROWS AND ACCUMULATE NO. OF POINTS
DO21=IINIT,K
READ100,L,IRF(L),IRL(L)
M=M+1-IRF(L)+IRL(L)
M1=M
DETERMINE NUMBER OF LAST POINT
M=M+J
INITIALIZE
I=IINIT
ISW=0
KA=IRF(IINIT)
J1=J+KA-IRL(IINIT)
J2=J
C SAVE J1 AND J2 FOR SECOND VARIABLE
J12=J1
J22=J2
C ENTER LOOP TO CALC. COEFFICIENTS FOR A POINT J
J=J+1
Z=1
IF(J-M)7,7,4
IF(ISW)5,6,5
PRINT102
PAUSE
GOTO1

```

C SET SWITCH FOR 2ND VARIABLE AND INITIALIZE

```

6 ISW=1
  KA=IRF(IINIT)
  J1=J12+M1
  J2=J22+M1
  I=IINIT
  M=M+M1
7 IF(I-IINIT)0,00,0
8 JS1=J-1+IRF(I)-IRL(I-1)
  J2=J1+IRL(I-1)-IRF(I-1)
80 J4=J2+1+IRL(I)-IRF(I)
C IF 2ND VARIABLE, WRITE EXTRA ELEMENTS
  IF(ISW)33,33,24
24 JMW2=J-M1-1
  IF(J-J2-2)26,27,27
26 PUNCH108,J
  GOT020
27 PUNCH104,AM2,J,JMW2
28 JM2=J-M1
  PUNCH104,A2,J,JM2
29 JME2=JM2+1
30 IF(JME2-J4+M1)32,32,31
31 PUNCH109,J
  GOT033
32 PUNCH104,AM2,J,JME2
C CALCS. FOR FIRST VARIABLE
33 IF(I-IINIT)330,10,330
330 IF(JS1-J1)10,9,9
  IF(JS1-J2)11,11,10
  PUNCH103,J
  GOT012
11 Z=I
  AS=.5/Z+1.
  PUNCH104,AS,J,J51
12 JWI=J-1
  IF(JWI-J2-1)13,14,14
13 PUNCH105,J

```

```

14 GOTO15
15 PUNCH104, AM, J, JN1
PUNCH104, A, J, J
JN1=J+1
IF(JN1-J4)17,17,16
16 PUNCH106, J
GOTO18
17 PUNCH104, AE, J, JN1
18 IF(L-K)19,22,22
19 JN1=JN1+IRL(I)-IRF(I+1)
IF(JN1-J4-1)22,20,20
20 J6=J4+1+IRL(I+1)-IRF(I+1)
IF(JN1-J6)21,21,22
21 AN=1-.5/Z
PUNCH104, AM, J, JN1
GOTO23
22 PUNCH107, J
23 IF(KA-IRL(I))35,34,35
34 I=I+1
JI=J2+1
J2=J4
IF(I-K)36,36,3
36 KA=IRF(I)
GOTO3
35 KA=KA+1
GOTO3
100 FORMAT(3I5)
102 FORMAT(10HEND OF JOB)
103 FORMAT(115,2X,3HJS1)
104 FORMAT(F10.6,2I5)
105 FORMAT(115,2X,3HJW1)
106 FORMAT(115,2X,3HJE1)
107 FORMAT(115,2X,3HJN1)
108 FORMAT(115,2X,3HJW2)
109 FORMAT(115,2X,3HJE2)
END

```

Program 2.--Equations-Solver Program by Iteration

The program described in the following pages involves an iteration procedure which reduces to Gauss Seidel iteration if the incorporated over-relaxation factor is set to one. This was done for most of the problems of this study, as the equations resulting from the finite difference method in conjunction with Southwell stress functions tended to diverge or show little benefit from the use of an over-relaxation factor other than one.

The program is described in terms of general x unknowns. For this study the x unknowns represent the Southwell stress functions ϕ and ψ . Thus two unknowns exist at each interior nodal point of a region and one at each boundary nodal point.

Immediately following the source deck listing of this program is a brief conversion program that converts the output from any cycle of iteration to a form suitable for input of initial "guesses" of the unknowns for a following cycle of iteration. In this way the solution can be interrupted at the end of any cycle of iteration and then continued at a later time.

Young-Frankel Iteration Program for Solution of Sparsely Populated Matrices.

The purpose of this program is to solve a very large number of simultaneous equations by the Young-Frankel over-relaxation procedure [See ref. 2, p. 242]. The size of the system that may be processed is determined only by the number of non-zero coefficients and constants. In solving various types of differential equations by finite difference methods, a system of linear equations is obtained. The resulting matrix of coefficient terms is usually sparsely populated and the distribution may or may not follow a pattern. Ordinary elimination techniques are impractical where the coefficients are randomly distributed, because a large amount of intermediate computer storage may be required. Iterative techniques are usually more time-consuming, but the storage requirements may be kept to a minimum. Instead of storing the coefficient array in its usual two-dimensional array, where most of the elements are zero, two one-dimensional arrays are stored; one is the list of non-zero coefficients and constants arranged in order, the second is an index matrix giving the relative position of the corresponding element in the coefficient and constant matrix. The ordering of the elements of both matrices can be illustrated in the example shown below:

$$\begin{array}{rcl} a_{11} x_1 + & & a_{13} x_3 = C_1 \\ & a_{22} x_2 + a_{23} x_3 = & 0 \\ a_{31} x_1 & & + a_{33} x_3 = C_3 \end{array}$$

<u>Order</u>	<u>List of Coefficients</u>	<u>Index Matrix</u>
1	a_{11}	1
2	a_{13}	3
3	a_{22}	5
4	a_{23}	6
5	a_{31}	7
6	a_{33}	9
7	C_1	1
8	C_3	3

For a system of n equations, an additional set of n locations is used for intermediate approximations of the unknowns, which can be set at the discretion of the operator. As each

new x is computed, the next approximation is taken according to the following equation, which forms the basis of the Young-Frankel method:

$$x_i^{(k+1)} = x_i^{(k)} + r_i (x_i' - x_i^{(k)})$$

where

$x_i^{(k+1)}$ = next approximation to x_i (corrected)

$x_i^{(k)}$ = preceding approximation

r_i = relaxation factor for the i^{th} equation

x_i' = next approximation to x_i (uncorrected)

Note that if the relaxation factor = 1, then

$$x^{(k+1)} = x_i'$$

which is the Gauss-Seidel procedure. It has been demonstrated that the rate of convergence may be greatly accelerated by choosing a factor other than 1 in the correction step. A definite optimum may exist which will give the maximum convergence rate. For a given problem, however, this factor must be determined, usually by trial based on previous experience. The program is arranged to allow a different relaxation factor for each equation, if desired.

Additional features of the program include multiple-processing of constant vectors without re-entry of the coefficient list, and intermediate output of results which may be obtained at any time during processing. Since initial approximations may be entered, the program may be stopped at any time by output of intermediate results which may then be re-entered as approximations. A check routine is included to ascertain whether all diagonal elements of the coefficients matrix have been entered. A maximum value of the total allowable relative error in the solution vector may be specified; at any time that the sum is less than that given the program will give the results and halt. A maximum number of iterations may also be given; when this number has been completed, the program stops and the results to that point are given as output.

Input

Type:

1. Parameter card

Cols 1-10

TOLR, maximum allowable relative error
(fixed point)

Cols 11-15	No. of equations (fixed point)
Cols 16-20	Maximum No. of iterations (fixed point)
Cols 21-48	Problem identification (any alphameric data)

2. Coefficient cards (one card per element)
- | | |
|------------|--------------------------|
| Cols 1-10 | Element (floating point) |
| Cols 11-15 | Row No. (fixed point) |
| Cols 16-20 | Column No. (fixed point) |

(No zero coefficient is permitted as input)

(The row and column numbers are understood to give the position of the element in the original two-dimensional array)

(Cards must be sorted in order Cols 11-20)

3. One blank card.

4. Relaxation factors (as many cards as desired--minimum of one, maximum of n)

Cols 1-10	Factor
Cols 11-15	Highest row No. for which this factor is to be used.

If one factor is used then the Cols 11-15 must contain No. of equation.

If more than one factor is used, then these cards must be sorted in order by Cols 11-15.

5. One blank card.

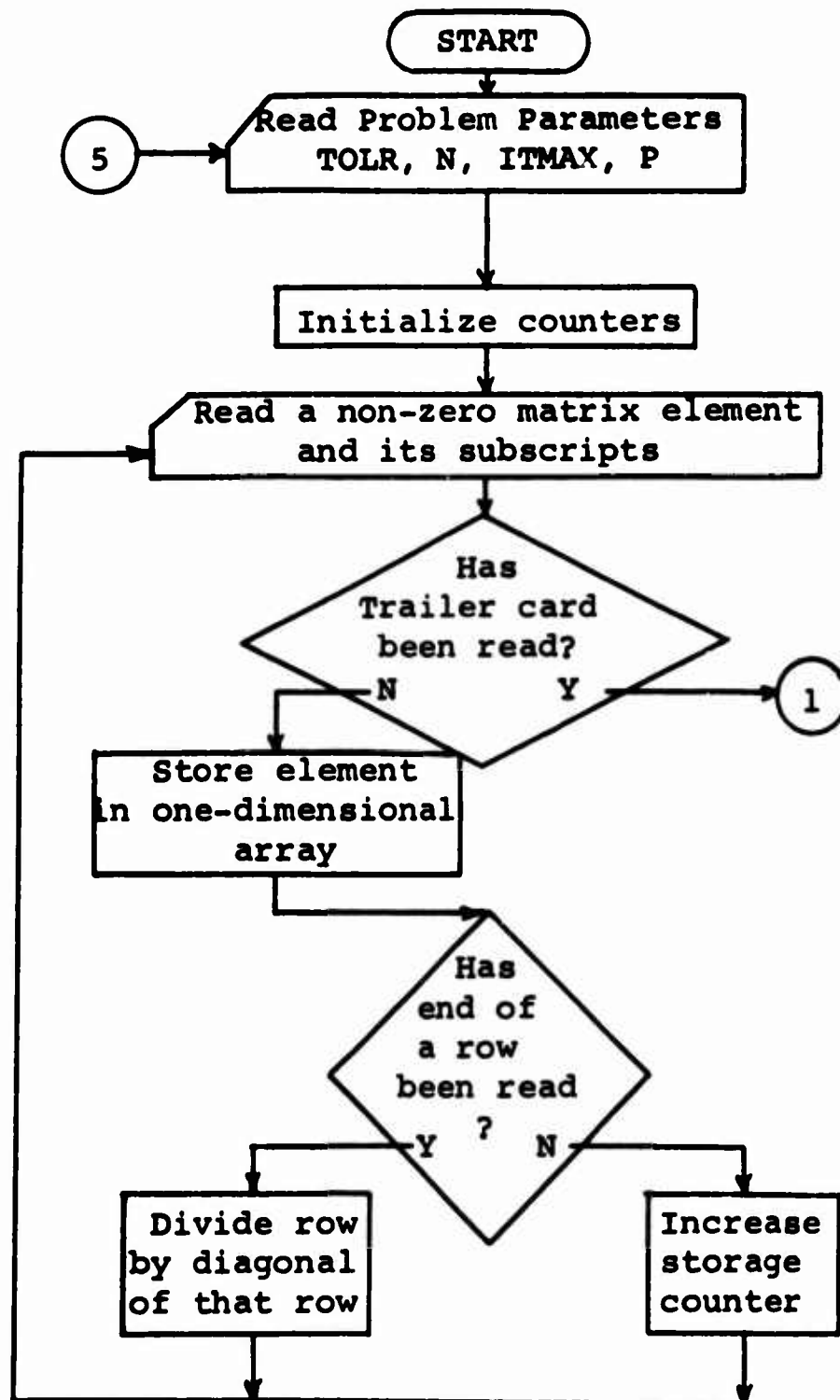
6. Initial approximations (as many cards as desired--minimum none, maximum of n--all others assumed zero)

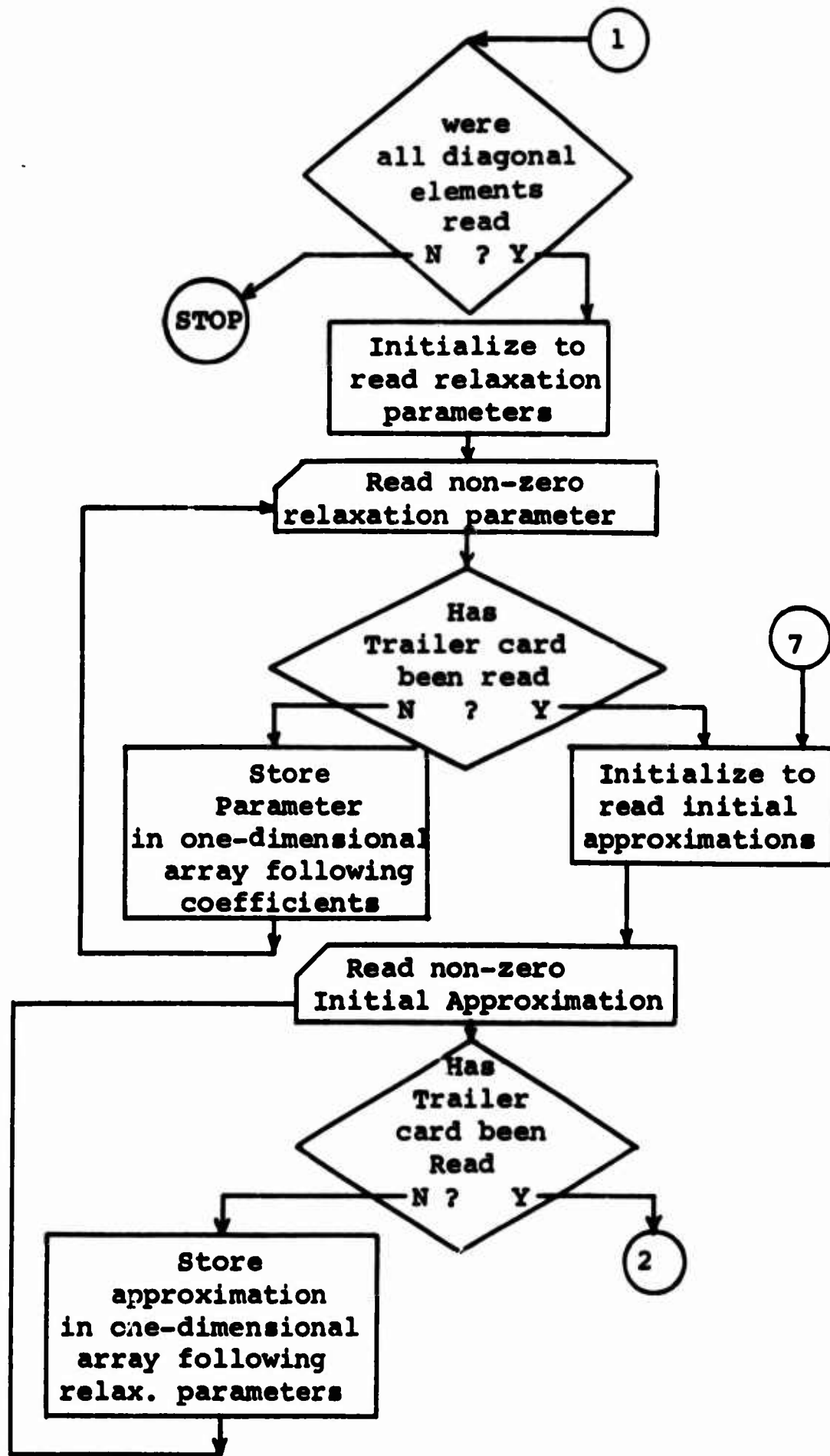
Cols 1-10	Initial approximation
Cols 11-15	Position of corresponding x element in solution vector.

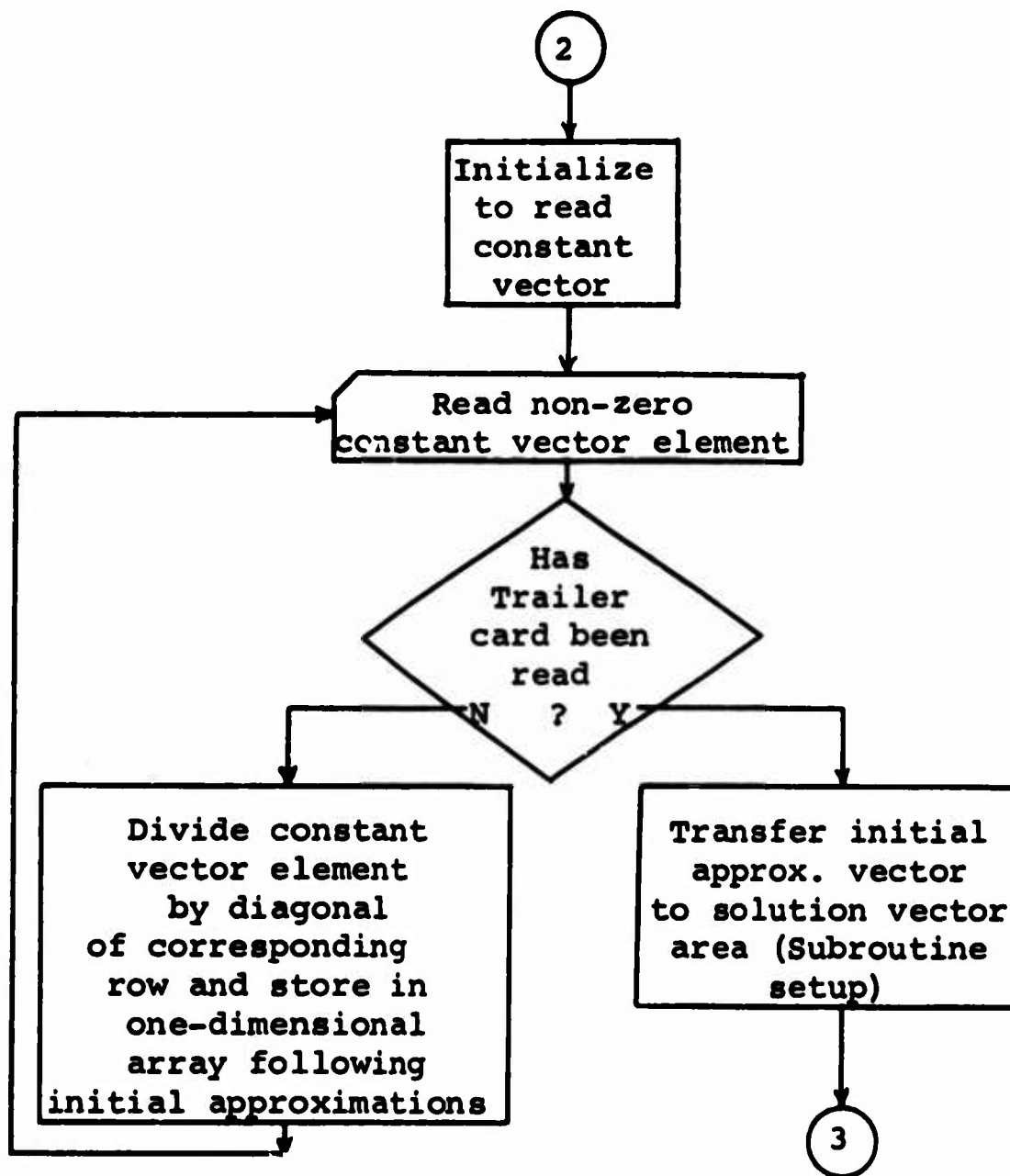
Cards must be sorted by Cols 11-15.

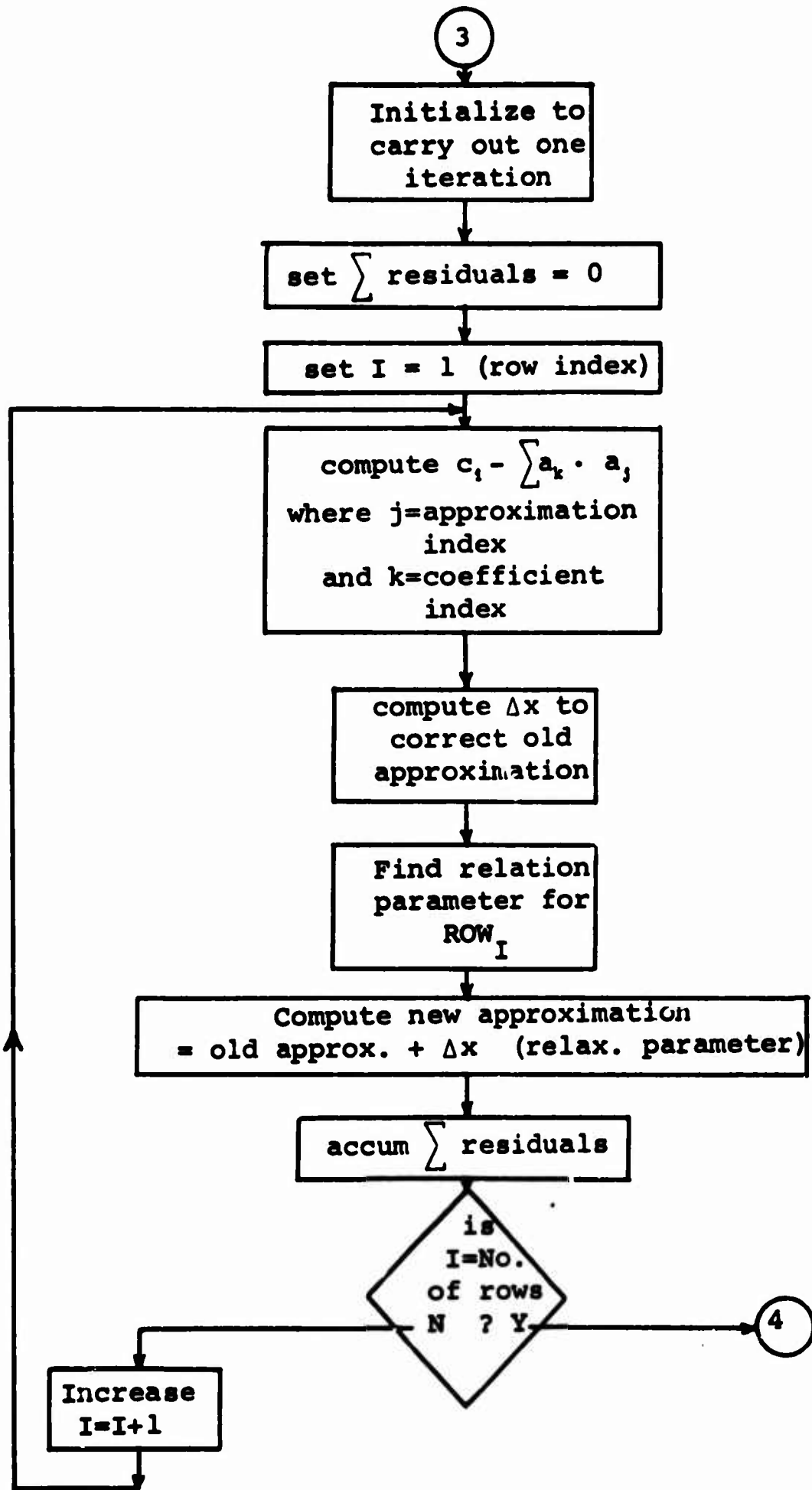
7. One blank card.

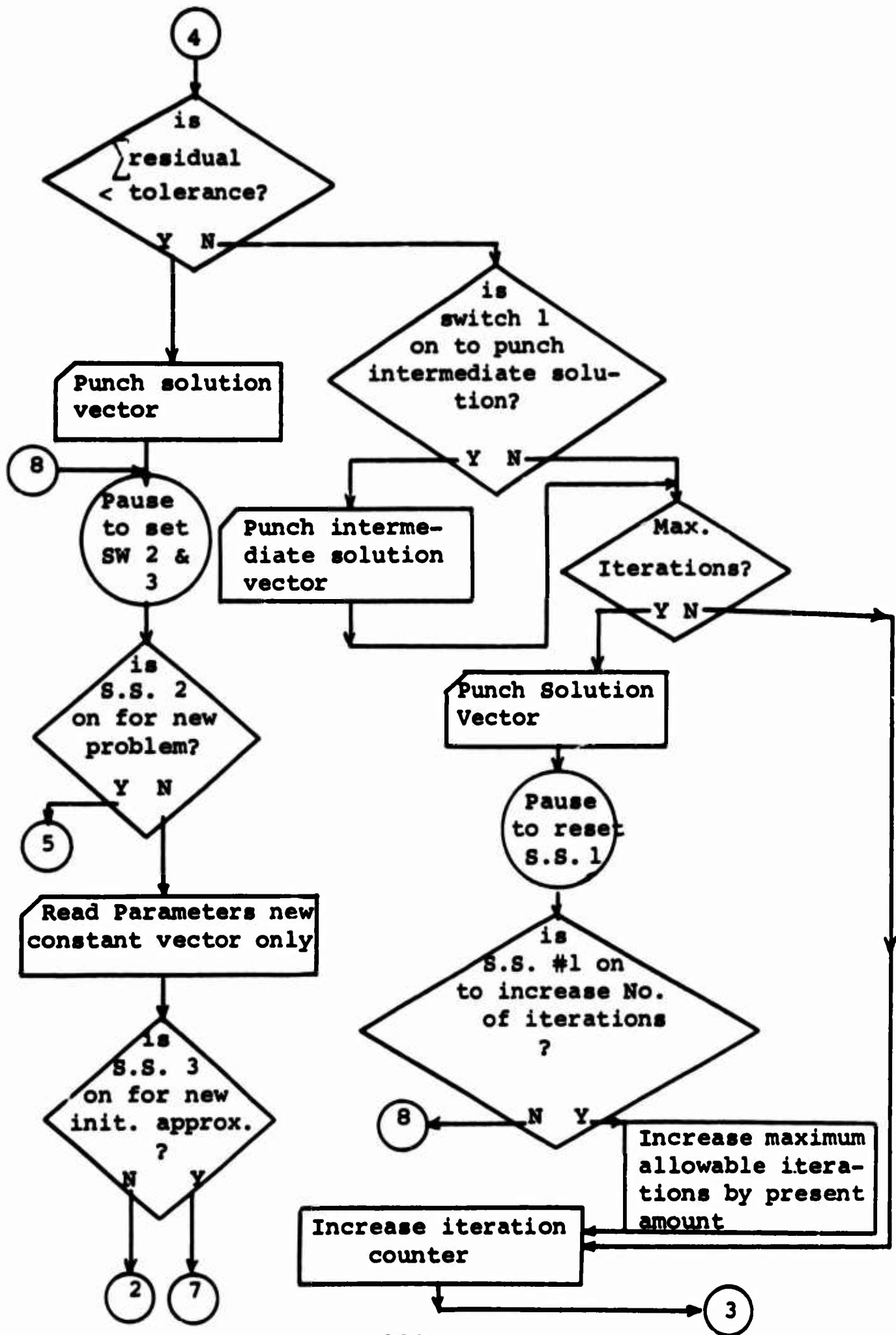
Young-Frankel Iteration Program
for Solution of Sparsely Populated Matrices












```

C 24 IF(IJ)35,30,35
C 26 IF(IJ)50,28,50
C 28 ID=ID+1
    IDIAG=K
    GOT050
    IDSAV=K
    ID=ID+1
    IF(ID-N)35,31,35
C 31 IDIAG=K
C 35 II = II + 1
C 36 IF(II - IDIAG) 36,37,36
    A(LI) = A(II) / A(IDIAG)
C 37 IF(M(K) - I2)38,39,38
C 38 IF(M(II+1) - I2) 35,35,40
C 39 IF( M(II) - I2) 35,40,35
C 40 I2 = I2 + N
    IF(IJ)50,42,50
    IDIAG=IDSAV
    K=K+1
    GOT020
C 60 IF(ID-N)70,80,70
    PRINT01
    PAUSE
    GO TO 10
    FORMAT(16HDIAGONAL MISSING)
C 801 READ RELAXATION PARAMETERS, INITIAL
    APPROXIMATIONS, AND CONSTANT VECTOR
    SAVE PARAM. ADDRESS
C
C
C

```

```

00029
00030
00031
00032
00033
00034
00035
00036
00037
00038
00039
00040
00041
00042
00043
00044
00045
00046
00047
00048
00049
00050
00051
00052
00053
00054
00055
00056
00057
00058
00059
00060
00061
00062
00063
00064
00065

```

```

TEST IF DIAGONAL WAS READ
INCREMENT DIAG. INDEX
SAVE DIAGONAL ADDRESS
INCREASE ARRAY INDEX
TEST IF ELEMENT IS A DIAGONAL
DIVIDE NON-DIAGONAL ELEMENT BY DIAGONAL
TESTS TO END DIVIDE LOOP
INCREASE STORAGE COUNTER FOR CONTINUATION OF
TEST IF ANY DIAG.=0, IF SO START OVER

```

```

00066
00067
00068
00069
00070
00071
00072
00073
00074
00075
00076
00077
00078
00079
00080
00081
00082
00083
00084
00085
00086
00087
00088
00089
00090
00091
00092
00093
00094
00095
00096
00097
00098
00099
00100
00101
00102

      IF=K
      ISW=0
      ID=M
      READ(800),E,I
      TEST IF LAST CARD
      IF(E)100,110,100
      MMK)=I
      IF(ISW)111,111,112
      AMK)=E
      GO TO 116
      TEST SWITCH(IMS) FOR TYPE OF NEXT INPUT
      DIV. VECTOR BY DIAG.
      SAVE INIT APP ADDRESS
      SET SW TO READ INIT APP., THEN CONST VECTOR
      SAVE CONST VECTOR ADDRESS
      SET SW TO READ CONST VECTOR, THEN EXIT LOOP
      REARRANGE INITIAL APPROXIMATION INTO SOLUTION
      VECTOR
      SOLVE BY ITERATION
      FINAL PART
      TEST RESIDUAL SUM AND NO. OF ITERATIONS

80  C      IF=K
      C      ISW=0
      C      ID=M
      C      READ(800),E,I
      C      TEST IF LAST CARD
      C      IF(E)100,110,100
      C      MMK)=I
      C      IF(ISW)111,111,112
      C      AMK)=E
      C      GO TO 116
      C      TEST SWITCH(IMS) FOR TYPE OF NEXT INPUT
      C      DIV. VECTOR BY DIAG.
      C      SAVE INIT APP ADDRESS
      C      SET SW TO READ INIT APP., THEN CONST VECTOR
      C      SAVE CONST VECTOR ADDRESS
      C      SET SW TO READ CONST VECTOR, THEN EXIT LOOP
      C      REARRANGE INITIAL APPROXIMATION INTO SOLUTION
      C      VECTOR
      C      SOLVE BY ITERATION
      C      FINAL PART
      C      TEST RESIDUAL SUM AND NO. OF ITERATIONS

100 C      IF(E)100,110,100
      C      MMK)=I
      C      IF(ISW)111,111,112
      C      AMK)=E
      C      GO TO 116

110 C      IF(ISW)130,120,140
      C      II=(I-1)*NI+1
      C      ID=ID+1
      C      IF(M(ID)-II)115,114,115
      C      AMK)=E/A(ID)
      C      K=K+1
      C      GO TO 90

120 C      IA=K
      C      ISW=-1
      C      GO TO 90

130 C      IV=K
      C      ISW=1
      C      GO TO 90

140 C      CALL SETUP
      C      CALL SOLVE

160 C
      C

```

```

170 IF(RSUM-TOLR)170,180,180
    CALL OUT
    GO TO 240
180 CALL SSWTCH(1,J)
    GO TO (190,200),J
190 CALL OUT
200 IF(ITER-ITMAX)230,210,230
210 CALL OUT
    CALL SSWTCH (1,J)
    GO TO (220,175),J
220 ITMAX=ITMAX+MAX
230 ITER=ITER+1
    GO TO 160
C
C
240 CALL SSWTCH (1,J)
    GO TO (10,250),J
C
C
250 READ800,TOLR,N,ITMAX,P
    CALL SSWTCH (1,J)
    GO TO (260,270),J
260 K=IA
    GOTO121
270 K=IV
    GO TO 90
175 CALL EXIT
    END
$1BFTC SETUP  NODECK
SUBROUTINE SETUP
DIMENSIONA(2500),M(2500)
DIMENSION P(7)
COMMON A,M
COMMON P
COMMON CORR,D,E,RSUM,SUM,TOLR,ITMAX,ID,I,IF,ISW,IA,IV,IX,ITER
COMMON ISN,IFA,II,IE,IT,J,K,N,NI
J=IA

```

00103
00104
00108

00110
00111
00112

00117
00118
00119
00120
00121

00123
00124
00125

00127
00128
00129
00130

00131

00133
00001
00002
00003
00004
00005
00006
00134

SW2 ON FOR NEW PROB.. OFF FOR NEW CONST
VECT OR APPROX.

SW3 ON FOR NEW VECTOR AND APPROX. OFF
FOR NEW VECTOR ONLY

```

ISN=1
D0330K=1,N
IF(IV-IA)300,310,300
300 IF(M(J)-K)310,320,310
320 A(ISN)=A(J)
J=J+1
GO TO 330
310 A(ISN1)=0.
330 ISN=ISN+1
ITER=1
RETURN
END

$IBFTC OUT N0DECK
SUBROUTINE OUT
DIMENSIONA(2500),M(2500)
DIMENSION P(7)
COMMON A,M
COMMON P
COMMON CORR,D,E,RSUM,SUM,TOLR,ITMAX,IA,IV,IX,ITER
COMMON ISN,IFA,II,IE,IT,J,K,N,N1
PUNCH#008,P
PUNCH#006,ITER,RSUM
PUNCH#007
PUNCH#004,(I,A(I),I=1,N)
RETURN
806 FORMAT(//14H ITERATION NO.,I4,4X14HRESIDUAL SUM =,F10.6//)
808 FORMAT(//1X,8HPR0B NO.,7A4)
804 FORMAT(4(I4,1X,E12.5,3X))
807 FORMAT(4(2X1M15X4HX(17X))//)
END

$IBFTC SOLVE N0DECK
SUBROUTINE SOLVE
DIMENSIONA(2500),M(2500)
DIMENSION P(7)
COMMON A,M
COMMON P
COMMON CORR,D,E,RSUM,SUM,TOLR,ITMAX,IA,IV,IX,ITER

```

```

00135
00136
00137
00138
00139
00140
00141
00142
00143
00146
00147
00148

00150
00001
00002
00003
00004
00005
00006
00151
00152
00153
00154
00155
00156
00157
00158
00159
00160

00162
00001
00002
00003
00004
00005

```



```

540 IE=IE+1
550 IF(IE-I)560,560,570
560 J=J+1
      GOT0500
C 570 D=SUM-A(ISN)
      GET NEW X AND DELTA X
C 580 IF(M(IFA)-I)440,450,440
      FIND RELAXATION PARAMETER
440 FAC=A(IFA)
      GO TO 460
450 IFA=IFA+1
460 CORR=FAC*D
      A(ISN)=A(ISN)+CORR
      IF(A(ISN))465,466,465
465 RSUM=ABS(CORR/A(ISN))+RSUM
466 IF(I-N)470,480,480
470 I=I+1
      ID=ID+NI
      II=II+N
      ISN=ISN+1
      GOT0400
480 RETURN
      END

```

```

00201
00202
00203
00204
00205
00206
00207
00208
00209
00210
00211
00212
00213
00214
00216
00217
00218
00219
00220
00221
00222
00223

```

Converter Program

```
1   READ100,I,A,J,B,K,C,L,D
100  FORMAT(4(I4,E13.5,3X))
     PUNCH101,A,I,B,J,C,K,D,L
101  FORMAT(F10.5,I5)
     GO TO 1
     END
```

Program 3.--Calculation of Normal Stresses on Boundaries Parallel to the Axis of Revolution.

This program calculates normal stresses on boundaries parallel to the z axis according to Eqs.(3-6). It employs the output from any cycle of iteration of the equation solver Program B-2. To use the output of Program B-2 the identifying preliminary cards must be removed from the particular output being used.

The equations (3-6) are applied from left to right along the boundaries. This program assumes unknowns will be numbered sequentially from left to right, however there may be gaps in numbering between rows. The Equation Generator, B-1, numbers interior points from left to right, but care must be taken to number boundary points also from left to right. Known values of ψ from left to right on the boundaries must be read in sequentially after each data card. If ψ is constant on the boundary, then only one ψ card is required and the sense switch 1 must be turned on.

Definitions of Input Terms.

- KEQUA = number of equations in input data from program B-2.
- PR = Poisson's ratio of material
- KEEP = identifying number of first unknown at left end of boundary. See Fig. 30.
- L2 = identifying number of unknown ϕ value at first interior point. See Fig. 30.
- L3 = identifying number of unknown ψ value at first interior point. See Fig. 30.
- L4 = identifying number of unknown ϕ value at second interior nodal point.
- L5 = identifying number of unknown ψ value at second interior nodal point.
- LAST = identifying number of last unknown at right end of boundary.
- R = distance to boundary in terms of grid spacing H.
- H = grid spacing. This number is 1.0 for all work done in this study. In general it depends on the units in which the original difference equations are written.

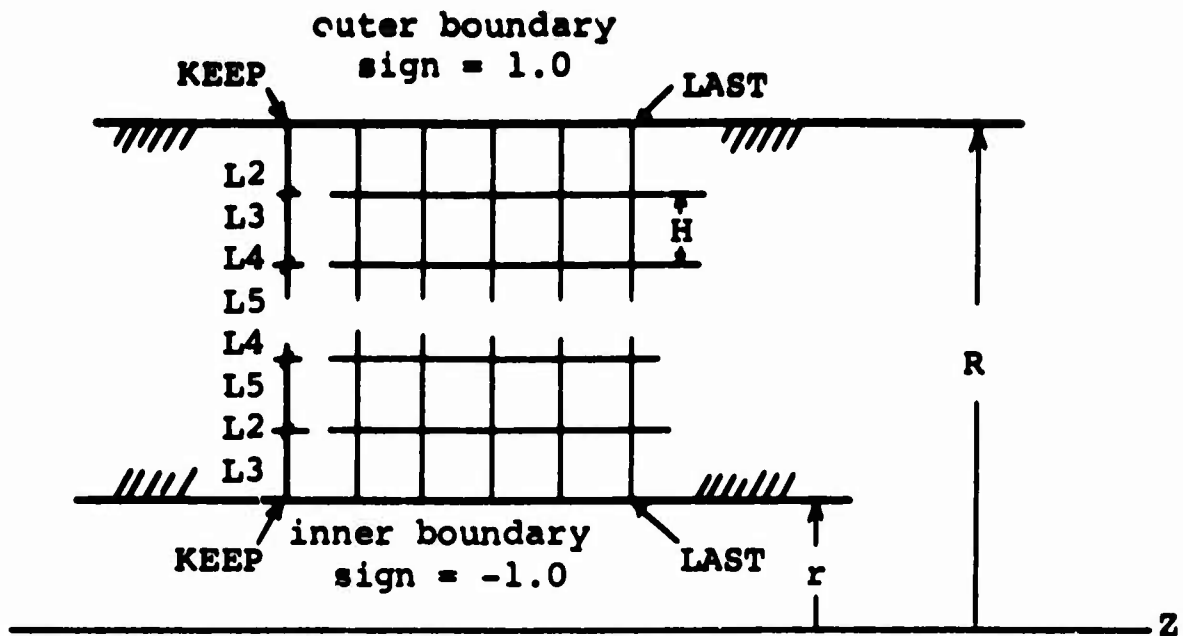


Figure 30. Notation for program 3.

SIGN = +1.0 for outer boundary calculations, -1.0 for inner boundary calculations.

PSI = value of the second Southwell stress function ψ at boundary points at which normal stresses are calculated.

PSIC = constant value of ψ at boundary points.

Input

1. Header Card

Cols 1-4	KEQUA, Right Justified Integer (Fixed Pt.)
Cols 11-20	PR, Floating Point
2. Solutions Cards--Output from Program B-2.
3. Data Cards

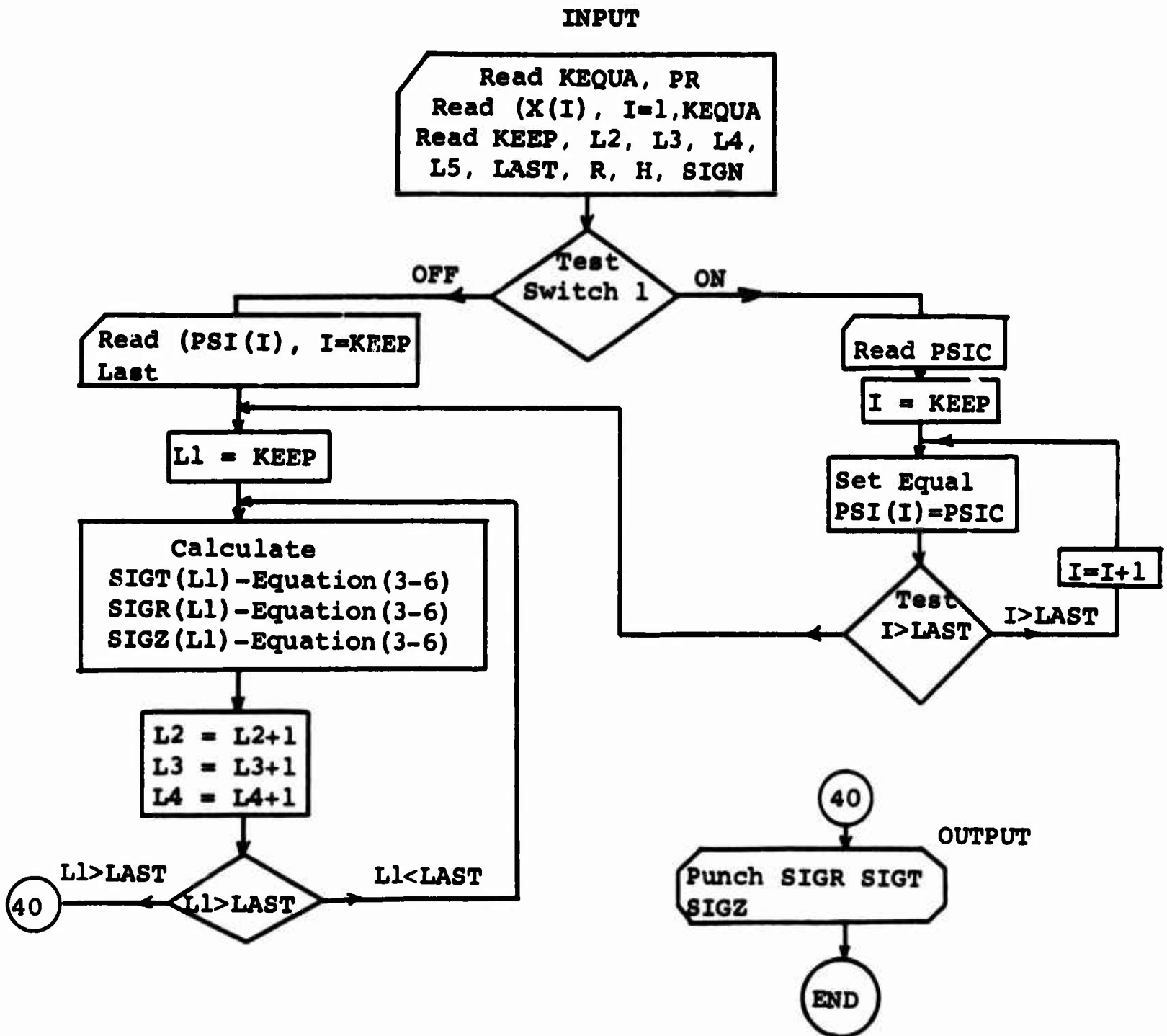
Cols: 1-3	KEEP, Right Justified Integer (Fixed Pt.)
4-6	L2, Right Justified Integer (Fixed Pt.)
7-9	L3, Right Justified Integer (Fixed Pt.)
10-12	L4, Right Justified Integer (Fixed Pt.)
13-15	L5, Right Justified Integer (Fixed Pt.)
16-18	LAST, Right Justified Integer (Fixed Pt.)
19-28	R, Floating Point
29-38	H, Floating Point
39-48	SIGN, Floating Point
4. PSIC Card (S.S. 1 on), or PSI Cards (S.S. 1 off)

Cols 1-10	PSIC or PSI
-----------	-------------

Output

Sigma R = values of normal stress at point in r direction.
Sigma Theta = values of normal stress at point in θ direction.
Sigma z = values of normal stress at point in z direction.

Calculation of Normal Stresses on Boundaries of a Thick-walled Cylinder



```

1 DIMENSION X(500), SIGR(500), SIGT(500), SIGZ(500), PSI(500)
2 READ 10, KEQUA, PR
3 READ 1, (X(I), I=1, KEQUA)
4 FORMAT(4(5X, E12.5, 3X))
5 READ 3, KBEP, L2, L3, L4, L5, LAST, R, H, SIGN
6 FORMAT(6I3, 3F10.6)
7 IF(SENSE SWITCH 1) 4, 7
8 READ 5, PSIC
9 FORMAT(10F8.3)
10 DO 6 I=KBEP, LAST
11 PSI(I)=PSIC
12 GO TO 8
13 READ 5, (PSI(I), I=KEEP, LAST)
14 PUNCH 11
15 CON1=(1./(2.*H*R))*SIGN
16 CON2=PR*CON1
17 CON3=2.*H/R
18 CON4=CON3/PR
19 CON5=1.-PR
20 P1=(3.+CON4*CON5*SIGN)*CON2
21 P2=1./(R*R)
22 P3=-4.*CON2
23 Y1=13.-CON3*CON5*SIGN*CON1
24 Y2=(3.-CON3*SIGN)*CON1
25 Y3=-4.*CON1
26 DO 9 L1=KEEP, LAST
27 SIGT(L1)=P1*X(L1)+P2*PSI(L1)+P3*X(L2)+CON2*X(L4)
28 SIGR(L1)=Y1*X(L1)+Y2*PSI(L1)+X(L2)+X(L3)+Y3*(X(L4)+X(L5))*CON1
29 SIGZ(L1)=(-3.*PSI(L1)+4.*X(L3)-X(L5))*CON1
30 L2=L2+1
31 L3=L3+1
32 L4=L4+1
33 L5=L5+1
34 PUNCH 10, (I, SIGR(I), SIGT(I), SIGZ(I), I=KEEP, LAST)
35 FORMAT(14, 3X, 3E16.8, 25X)
36 FORMAT(52HPOINT          SIGMA R          SIGMA THETA          SIGMA Z)

```

GO TO 2
END

**Program 4.--Coefficients Generator for Southwell Stress Functions
in Polar (R,θ) Coordinates.**

This program generates the matrix of coefficients corresponding to the linear algebraic equations derived by finite difference techniques and Southwell stress functions. It essentially applies Eqs.(A-13), (A-5), (A-12), and (A-6) to a quarter-ring which, when rotated, generates a hemispherical solid.

With reference to Figure 31, this program will generate the entire matrix of coefficients for the generating ring area, except for the coefficients of the unknowns along $\theta = \pi/2$. These unknowns lie on the interface between the end cap and cylinder, and equations applying here must be written by hand according to Eqs.(3-16) and (3-17). Note however that this program will write the complete equations for points adjacent to the interface, and therefore the unknowns along the interface must be numbered. There must be no duplication in numbering of unknowns anywhere over the ring and subsequently coupled rectangular area. The output of this program is in a form similar to that of Program B-1, and can be combined with it as input to the equation solver Program B-2.

Referring to Figure 31 the equations of Appendix A are applied in the following order: (1) Eq.(A-13) on the inner boundary starting at point "MIKE" and moving in the increasing θ direction, (2) Eq.(A-5) to interior points in the increasing θ and then R

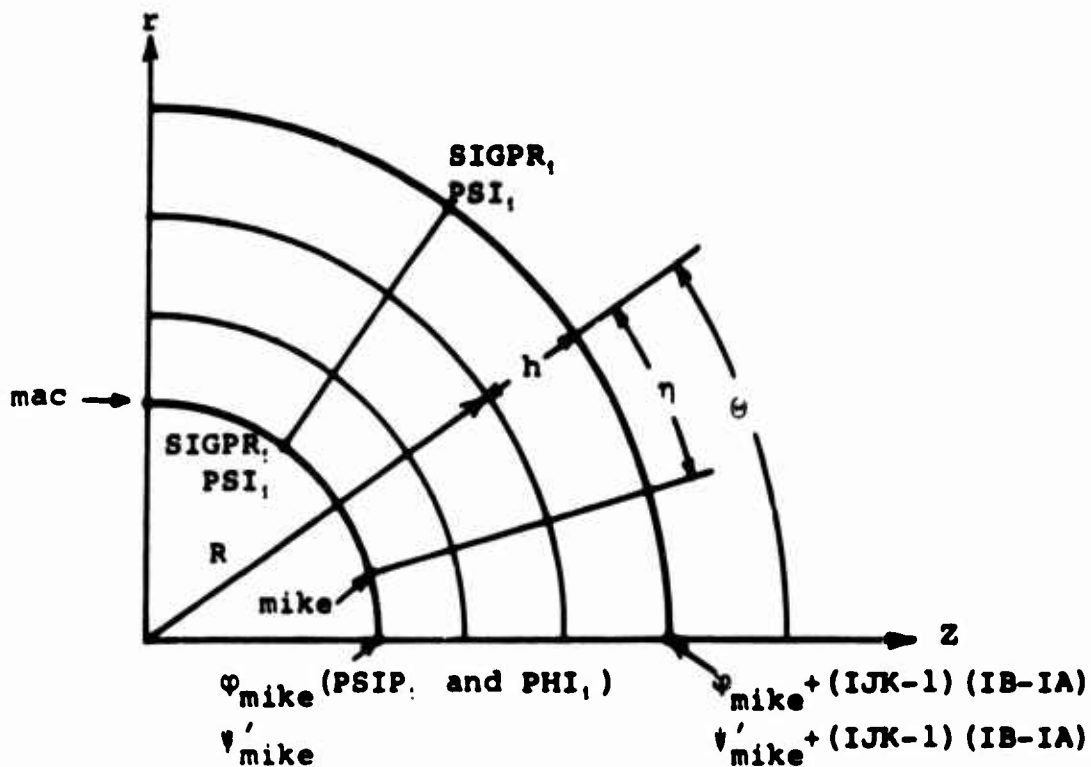


Figure 31. Notation for program 4.

directions, (3) Eq.(A-12) on the outer boundary in the increasing θ direction, and (4) Eq.(A-6) to interior points in the increasing θ and then R directions. The first three steps involve φ unknowns at the inner boundary, interior, and outer boundary nodal points respectively. The last step involves ψ unknowns at interior nodal points.

Definitions of Input parameters and symbols used in the program follow.

- IA = Interior radius, an integer in terms of h, the grid spacing in the R direction, > 0
- IB = Exterior radius, an integer in terms of h, $> IA+1$.
- IJK = Number of angular subdivisions of one quadrant, ≥ 3 .
- MIKE = Identifying number associated with the unknown φ value on the inner boundary at the initial point of the ring. See Figure 31.
- MAC = Identifying number associated with the unknown φ value on the inner boundary at the initial point of the juncture of the ring with the cylinder. See Figure 3.
- PR = $(1-\nu)$, one minus Poisson's ratio of the material.
- PHI = Input values of φ along the inner and outer boundaries.
- SIGPR = σ_{pr} = Input values of applied stress in r direction along inner and outer boundaries.
- ETA = Increment of angle in polar grid.
- THETA = Polar angle at location of equation application. See Fig. 31.
- X1,X2,etc. = Varying coefficients of φ and ψ values appearing in Eqs.(A-13), (A-5), etc.
- CONST = Constant coefficients of φ and ψ values appearing in Eqs.(A-13), (A-5), etc.
- CONH = Constant term of an equation that appears in the constants vector. It is made up of input boundary values of ψ and boundary stress σ_{pr} according to Eqs.(A-13), (A-5), etc.

Input

1. First Data Card

Cols 1-3	IA	A right justified integer (Fixed Pt.)
Cols 4-6	IB	A right justified integer (Fixed Pt.)
Cols 7-9	IJK	A right justified integer (Fixed Pt.)

Cols 10-12	MIKE	A right justified integer (Fixed Pt.)
Cols 13-15	MAC	A right justified integer (Fixed Pt.)
Cols 16-30	PR	Floating Point.

2. Additional Data Cards--Use floating point numbers, 8 per card, 10 cols. per number, blank cards read as zeros. Data is sequential, and no spaces must be left unless they represent zeros. Example Input data is listed:

Inner Boundary Terms:

ψ [mike]' σ [pr mike]' ψ [mike+1]' σ [pr mike+1]' ... ψ [mike+IJK-2],

Outer Boundary Terms: (follow above data with no spaces)

ψ [mike+(IJK-1)(IB-IA)]' σ [pr (same pt.)]' ψ [mike+(IJK-1)(IB-IA)+1]

σ [pr same pt.]' ... ψ [mike+(IJK-1)(IB-IA+1)-1]' σ [pr same]

Horizontal Boundary Terms: (follow above data with no spaces)

φ [mike]' ψ '[mike]' φ [mike+IJL]' ψ '[mike+IJL]' φ [mike+2(IJL)]'

ψ '[same]' ... φ [mike+(IJK-1)(IB-IA)], ψ '[same]'

Lower Point on Vertical Boundary: (follows above data with no spaces)

ψ [mike+IJK-1]

Top Point on Vertical Boundary: (follows above data with no spaces)

ψ [mike+(IB-IA+1)(IJK-1)]

Output

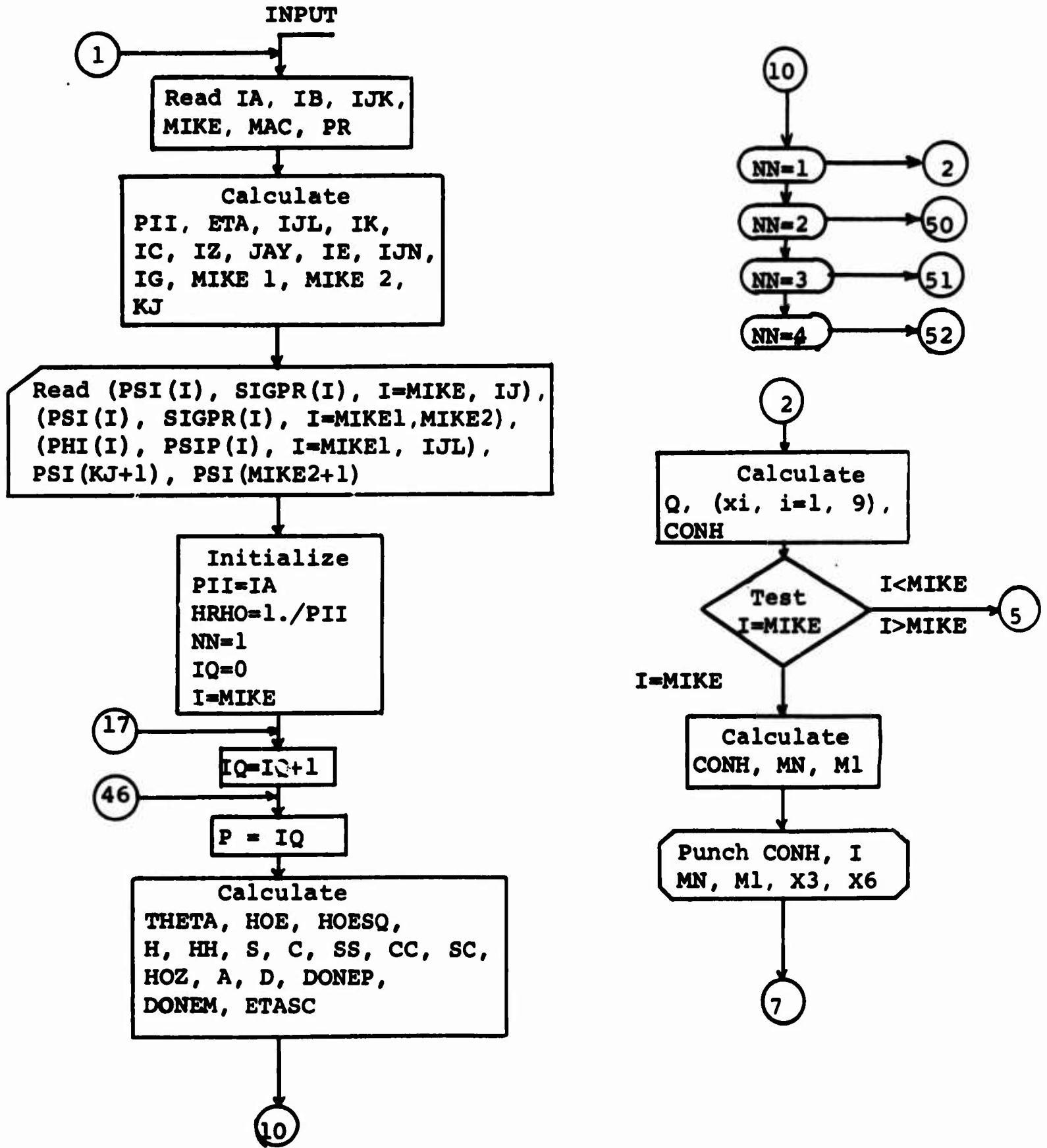
Coefficients Cards

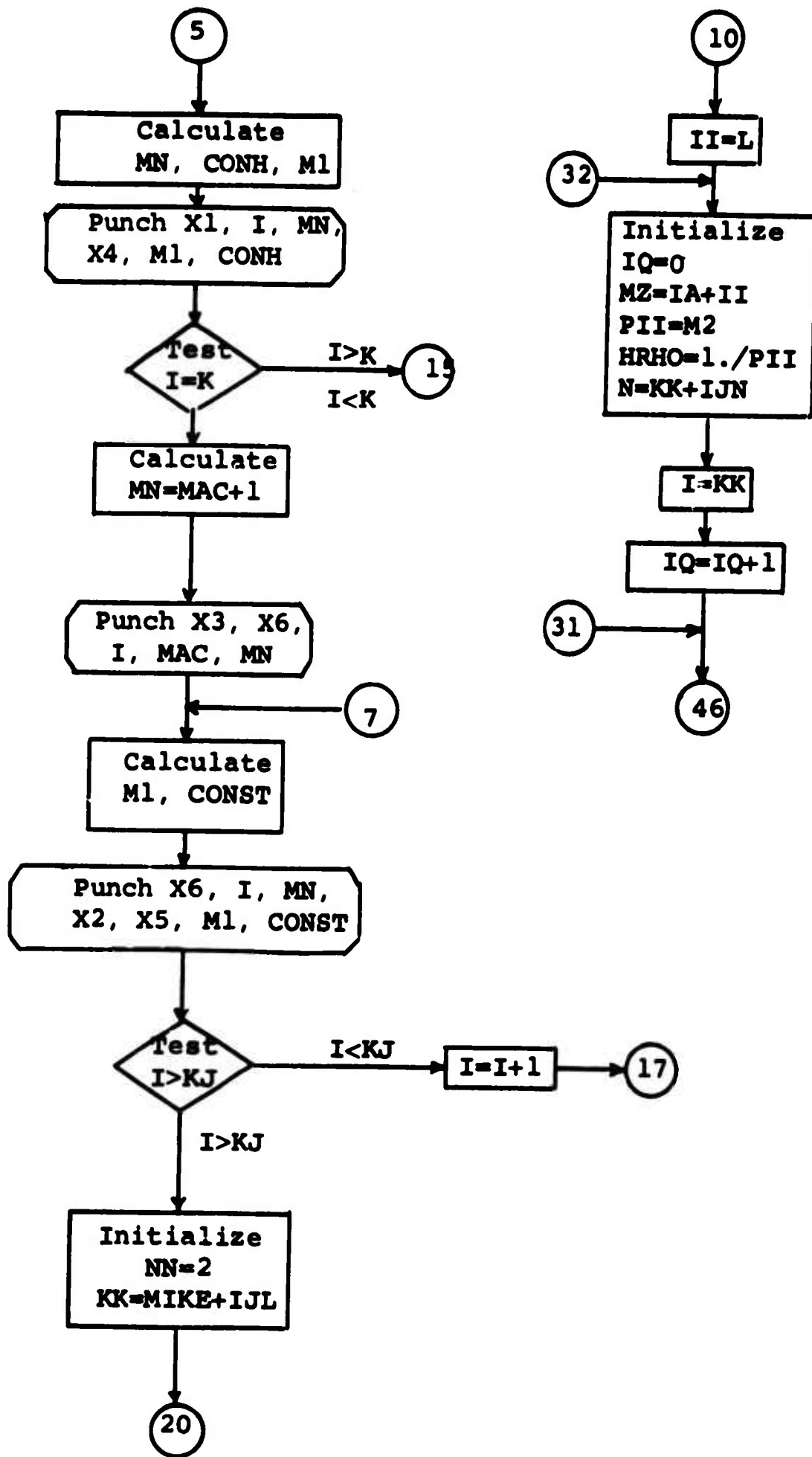
Cols 1-10	Coefficients in Floating Point
Cols 11-15	Row number of Coefficients
Cols 16-20	Column Number of Coefficients

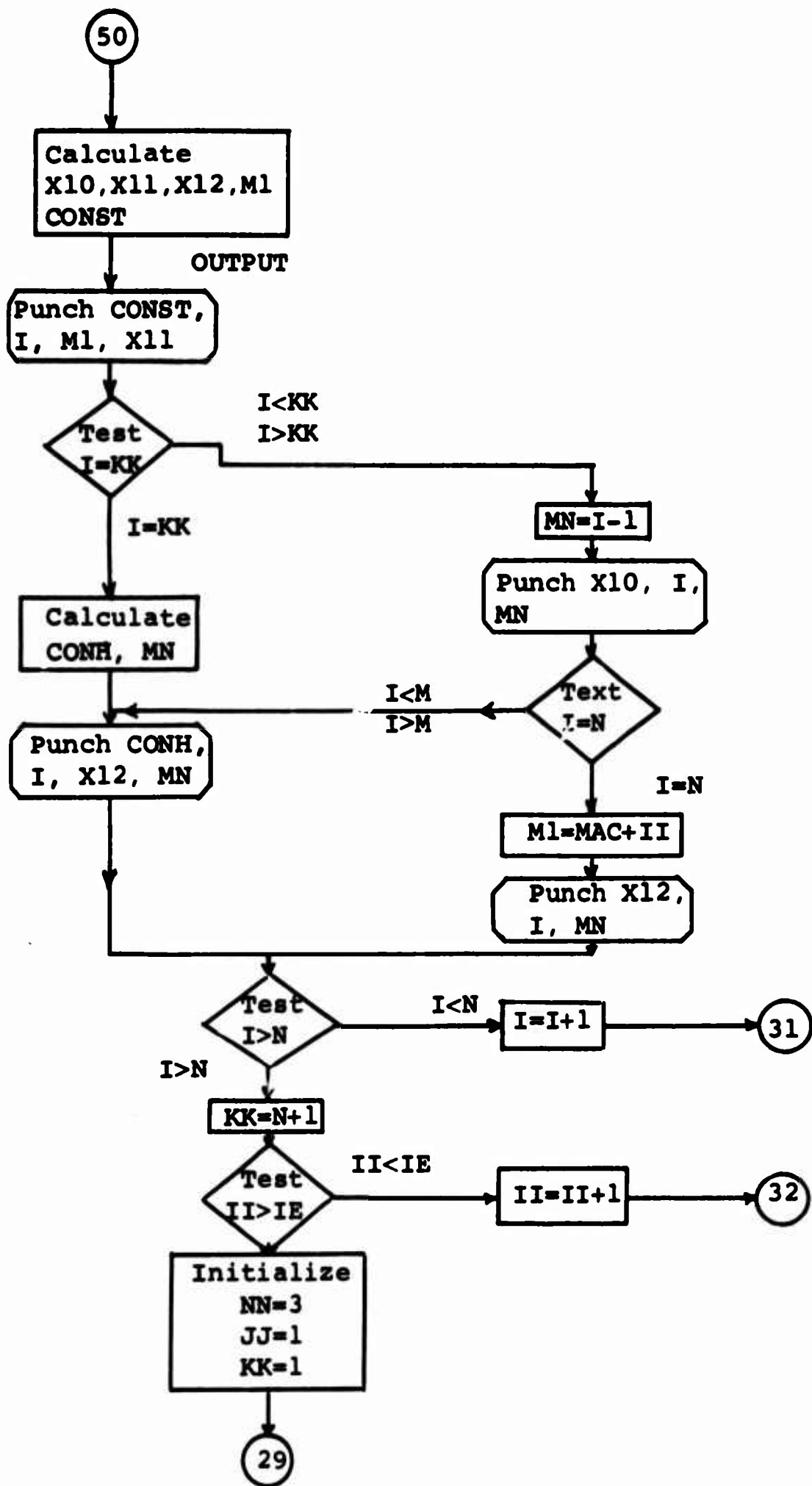
Constants Cards

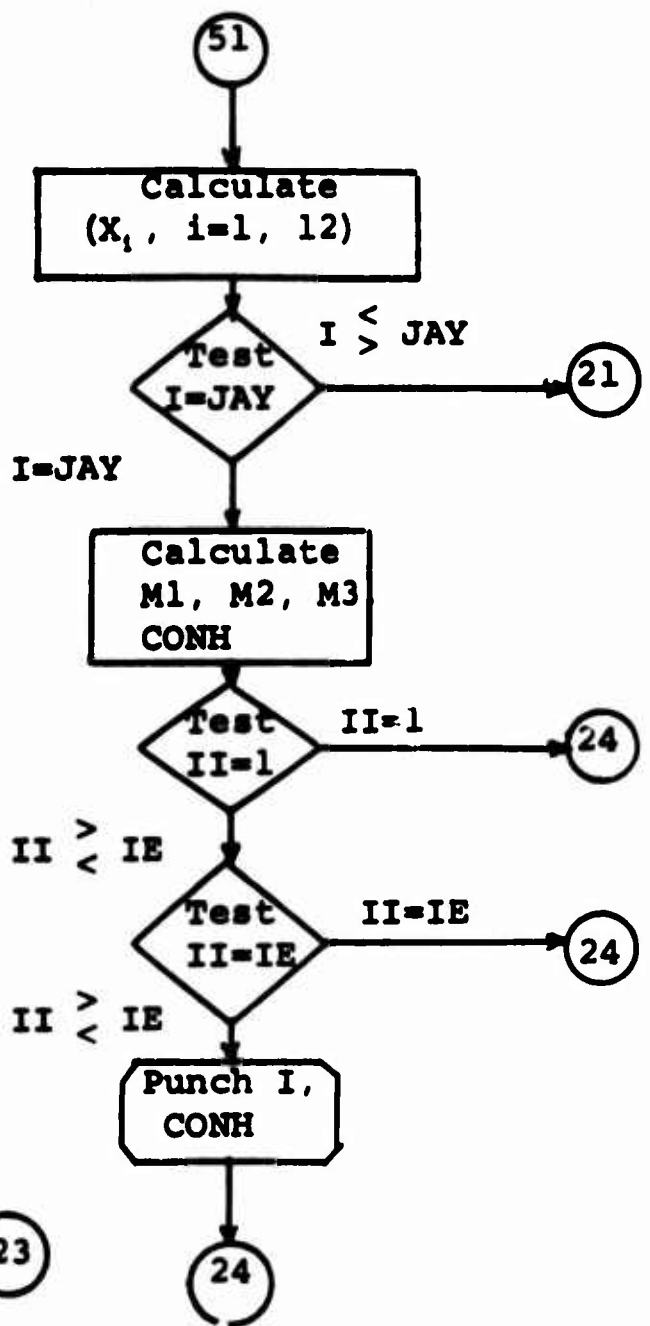
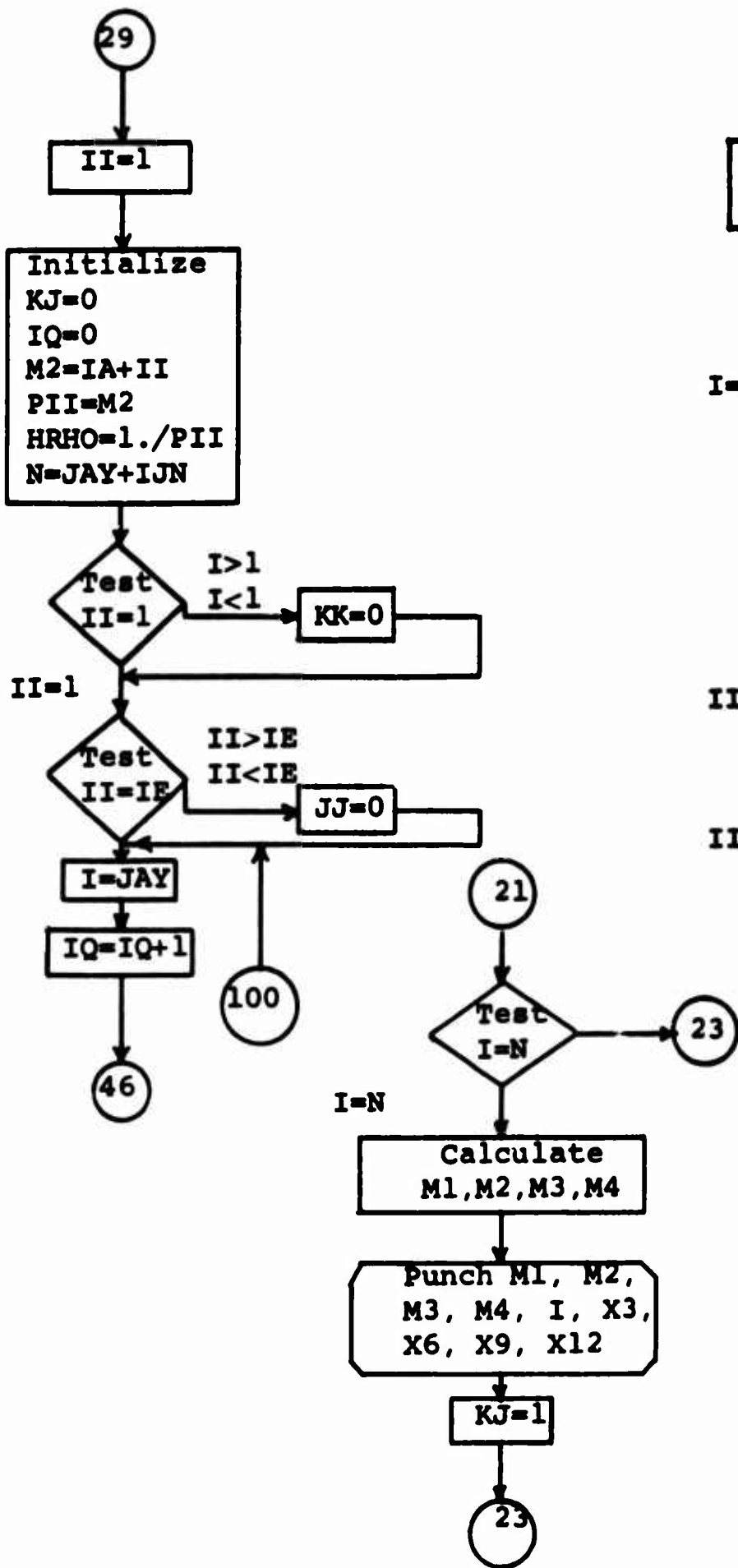
Cols 1-10	Constants in Floating Point
Cols 11-15	Corresponding Row Number of Constant

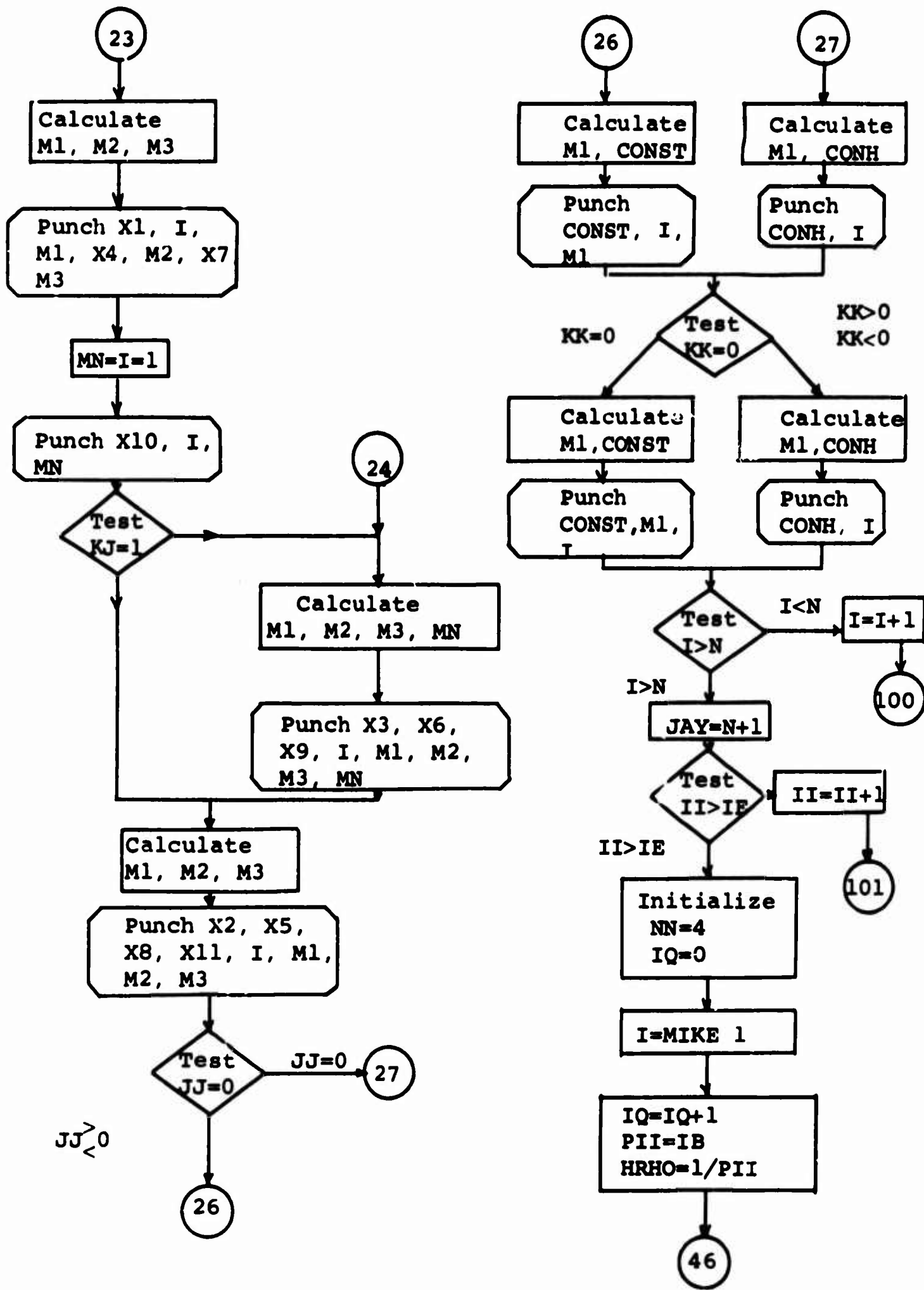
Coefficients Generator in Polar Coordinates

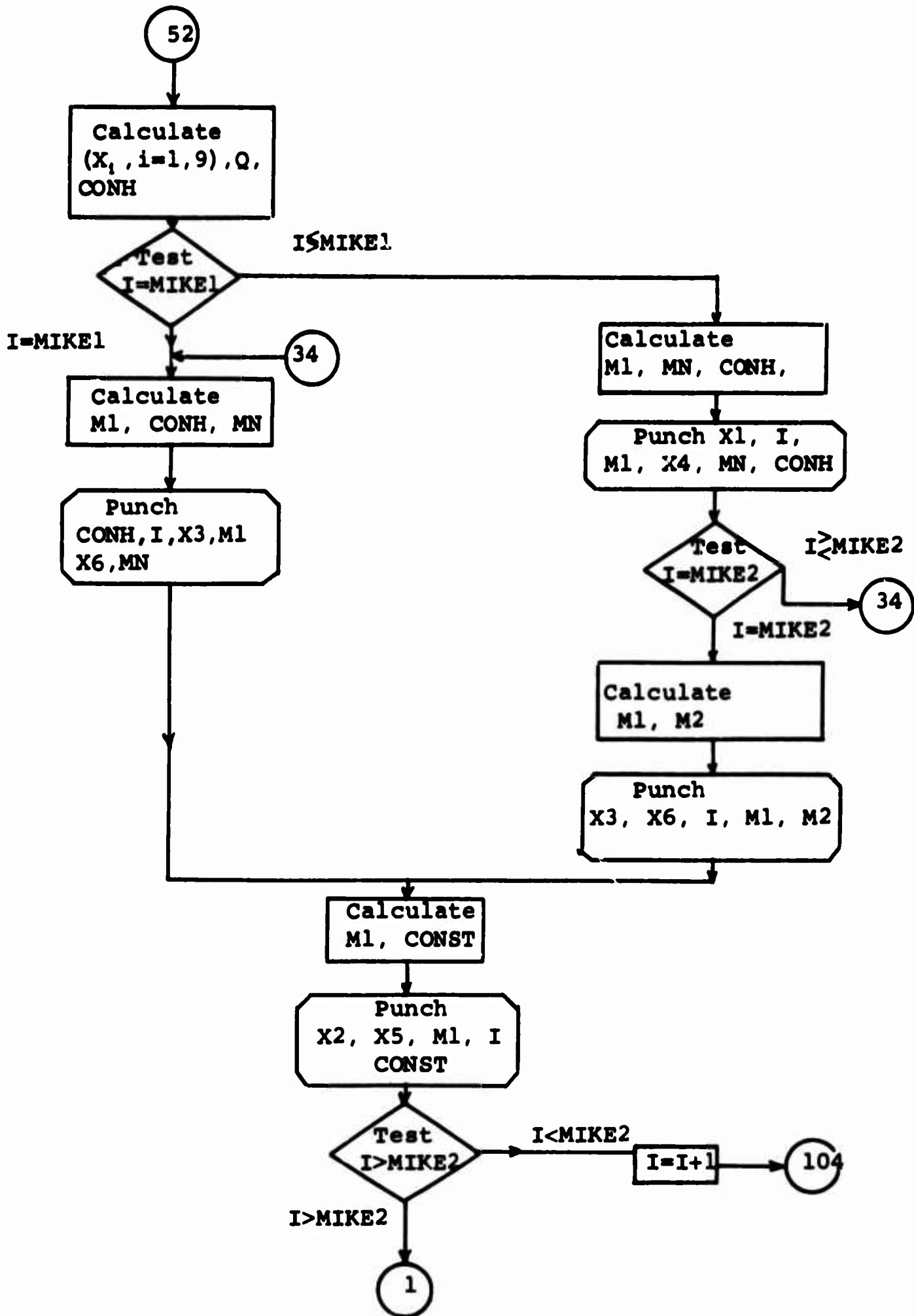












```

C EQUATION GENERATOR, FOR ONE QUADRANT OF A CYLINDRICAL SECTION
C IJK, THE NO. OF DIVISIONS OF ONE QUADRANT, MUST BE AT LEAST 3.
C THERE MUST BE AT LEAST ONE INTERIOR LINE.
C DUE TO SPACE LIMITATIONS, NO SUBSCRIPT SHOULD BE GREATER THAN 812.
1 DIMENSION PHI(812), PSI(812), PSIP(812), SIGPR(812)
READ 47, IA, IB, IJK, MIKE, MAC, PR
PII=IJK
ETA=1.5707963/PII
IJL=IJK-1
ID=IB-IA
IC=ID+1
IZ=IJL*IC
C JAY IS THE FIRST PSI SUBSCRIPT.
JAY=MIKE+IZ
C IE IS THE NUMBER OF INTERIOR LINES.
IE=ID-1
LJN=IJK-2
C ADD IG TO PHI SUBSCRIPT TO GET PSI AT ANY INTERIOR POINT.
IG=IJL*ID
MIKE1=MIKE+IG
MIKE2=MIKE+IZ-1
KJ=MIKE+IJN
OREAD 48, (PSI(I), SIGPR(I), I=MIKE, KJ), (PSI(I), SIGPR(I), I=MIKE1, MIKE2)
1 , (PHI(I), PSIP(I), I=MIKE, MIKE1, IJL), PSI(KJ+1), PSI(MIKE2+1)
C BEGIN WRITING EQUATIONS FOR POINTS ALONG INNER BOUNDARY
PII=IA
HRHO=1./PII
NN=1
IQ=0
DOBI=MIKE, KJ
IQ=IQ+1
P=IQ
THETA=ETA*P
HCE=HRHO/ETA
HOESQ=HOE*HOE
H=1./HOESQ
HM=H*HRHO*PR

```

46

```

S=SINF(THETA)
C=COSF(THETA)
SS=S*S
CC=C*C
SC=S*C
MO2=HRHO*.5
A=2.*HRHO
D=ETA*C*.5/S
DONEP=1.*D
DONEM=1.-D
ETASC=ETA*SC
GOTO12,50,51,52),MN
Q=1.-MO2*SS
X1=(DONEP*Q-SS+ETASC)*HOESQ
X2=-1-(1.+H)*MO2+1.-H)*SS+1.*HH)*2.*HOESQ
X3=(DONEM*Q-SS-ETASC)*HOESQ
X4=-HOE*SC
X5=(2.-HRHO)*SS
X6=-X4
X7=DONEP*HOESQ
X8=-11.*HRHO*HOESQ)*2.
X9=DONEM*HOESQ
CONH=2.*PII*S*SIGPR(I)
IF(I-MIKE)5,3,5
M1=I+I*JL
CONH=-X1*PHI(I)-X4*PHI(M1)-X7*PSIP(I)-X8*PSI(I)-X9*PSI(I+1)+CONH
PUNCH40,CONH,I
MN=I+1
PUNCH40,X3,I,MN
M1=I+I*JK
PUNCH40,X6,I,M1
GOTO7
MN=I-1
PUNCH40,X1,I,MN
M1=I+I*JN
PUNCH40,X4,I,M1
CONH=-PSI(I-1)*X7-PSI(I)*X8-PSI(I+1)*X9+CONH

```

2

3

4

5

```

PUNCH40, CONH, I
IF(I-KJ)4,6,4
PUNCH40, X3, I, MAC
MN=MAC+I
PUNCH40, X6, I, MN
PUNCH40, X2, I, I
M1=I+I*JL
PUNCH40, X5, I, M1
M1=I+I*Z
CONST =2.
PUNCH40, CONST, I, M1
C THROUGH WITH INNER BOUNDARY
C BEGIN WRITING EQUATIONS FOR INTERIOR PHI POINTS
NN=2
NK=MIKE+I*JL
DOL5II=I, IE
IQ=0
M2=IA+II
PII=M2
HRHO=1./PII
N=KK+I*JN
DOL4I=KK, N
IQ=IQ+I
GOTO46
50 X10=DDNEP+HOESQ
X11=(I-1.-HOESQ)*2.
X12=DDNEM+HOESQ
M1=I-I*JL
CONST =1.
PUNCH40, CONST, I, M1
PUNCH40, X11, I, I
M1=I+I*JL
CONST =1.
PUNCH40, CONST, I, M1
IF(I-KK)10,9,10
CONH=-X10*PHI(I)
PUNCH40, CONH, I
9

```

```

10  GOT013
    MN=I-1
    PUNCH40,X10,I,MN
    IF(I-N)13,12,13
12  M1=MAC+II
    PUNCH40,X12,I,M1
    GOT014
13  MN=I+1
    PUNCH40,X12,I,MN
14  CONTINUE
15  MK=N+1
    THROUGH WITH INTERIOR PHI POINTS
    BEGIN WRITING EQUATIONS FOR INTERIOR PSI POINTS
    NN=3
    JJ=1
    KK=1
    DO32II=1,IE
    KJ=0
    IQ=0
    M2=IA+II
    PII=M2
    HRMO=1./PII
    N=JAY+IJM
    IF(I-I-1)16,17,16
    KK=0
16  IF(II-IE)19,18,19
17  JJ=0
18  DO31I=JAY,N
19  IQ=IQ+1
    GOT046
51  X1=HOE*.5*SC
    X2=-CC+MO2*SS
    X3=-X1
    X4=(ETASC-SS)*HOESQ
    X5=(SS*HOESQ+CC)*2.
    X6=(ETASC+SS)*(-HOESQ)
    X7=X3

```

```

X6=-CC-H02*SS
X9=X1
X10=DONEP*HOESQ
X11=(-1.-HOESQ)*2.
X12=DONEM*HOESQ
CONH=0.
IF(I-JAY)21,20,21
M1=I-IZ
M2=M1+I JL
M3=M2+I JL
CONH=-X1*PHI(M1)-X4*PHI(M2)-X7*PHI(M3)-X10*PSIP(M2)+CONH
IF(II-1)11,24,11
IF(II-IE)39,24,39
PUNCH40,CONH,I
GOTO24
IF(I-N)23,22,23
M1=MAC+I I
M2=M1+I
M3=M1-I
M4=M1+I D
PUNCH40,X3,I,M3
PUNCH40,X6,I,M1
PUNCH40,X9,I,M2
PUNCH40,X12,I,M4
KJ=1
M1=I-IZ-1
M2=M1+I JL
M3=M2+I JL
PUNCH40,X1,I,M1
PUNCH40,X4,I,M2
PUNCH40,X7,I,M3
MN=I-1
PUNCH40,X10,I,MN
IF(KJ-1)24,25,24
M1=I-IZ+1
M2=M1+I JL
M3=M2+I JL

```

20

11
39

21
22

23

24

```

PUNCH40,X3,I,M1
PUNCH40,X6,I,M2
PUNCH40,X9,I,M3
MN=I+1
PUNCH40,X12,I,MN
M1=I-IZ
M2=M1+IJL
M3=M2+IJL
PUNCH40,X2,I,M1
PUNCH40,X5,I,M2
PUNCH40,X8,I,M3
PUNCH40,X11,I,I
IF(IJJ)26,27,26
M1=I+IJL
CONST =1.
PUNCH40,CONST,I,M1
GOTO28
M1=I-IG+IJL
CONH=-PSI(M1)+CONH
PUNCH40,CONH,I
IF(KK)30,29,30
M1=I-IJL
CONST =1.
PUNCH40,CONST,I,M1
GOTO31
M1=I-IZ
CONH=-PSI(M1)+CONH
PUNCH40,CONH,I
CONTINUE
JAY=N+1
THROUGH WITH INTERIOR PSI POINTS
BEGIN WRITING EQUATIONS FOR POINTS ALONG OUTER BOUNDARY
NN=4
IQ=0
D0381=MIKE1,MIKE2
IQ=IQ+1
PII=IR

```

25

26

27

28
29

30

31
32

C
C

```

HRHD=1./PII
GOTO46
52 Q=1.+HO2=SS
X1=HOE*SC
X2=SS*A
X3=-X1
X4=(DONEP*Q-SS+ETASC)*HOESQ
X5=-((1.-H-(1.+H)*HO2)*SS+1.-HM)*2.*HOESQ
X6=(DONEM*Q-SS-ETASC)*HOESQ
X7=DONEP*HOESQ
X8=(HRHD-HOESQ-1.)*2.
X9=DONEM*HOESQ
CONH=-2.*PII*S*SIGPR(I)
IF(I-MIKE1)35,33,35
33 M1=I-IJL
OCONH=-X1*PHI(M1)-X4*PHI(I)-X7*PSIP(I)-X8*PSI(I)-X9*PSI(I+1)+
ICONH
PUNCH40,CONH,I
34 M1=I-IJN
PUNCH40,X3,I,M1
MN=I+I
PUNCH40,X6,I,MN
GOTO37
35 M1=I-IJK
PUNCH40,X1,I,M1
MN=I-I
PUNCH40,X4,I,MN
CONH=-X7*PSI(I-1)-X8*PSI(I)-X9*PSI(I+1)+CONH
PUNCH40,CONH,I
IF(I-MIKE2)34,36,34
36 M1=MAC+IE
M2=MAC+ID
PUNCH40,X3,I,M1
PUNCH40,X6,I,M2
37 M1=I-IJL
PUNCH40,X2,I,M1
PUNCH40,X5,I,I

```

```
MI=I-IJL+IG
CONST =2.
PUNCH#0,CONST,I,M1
FORMAT(F10.4,2I5)
FORMAT(5I3,E15.8)
FORMAT(8F10.4)
GOTO1
END
```

```
38
40
47
48
```

12045	15707963E+01
12050	00001
12055	00002
12065	10000000E+01
12070	00000
12080	50000000E+00
12090	20000000E+01
12095	00003
12105	00000000E--99
12110	00004
12115	0001
12125	0047
12135	0048
12140	0008
12145	0046
12150	0002
12155	0050
12160	0051
12165	0052
12170	0005
12175	0003
12185	0040
12190	0004
12195	0007
12200	0006
12205	0015
12210	0014
12215	0010
12220	0009
12225	0013
12230	0012
12235	0032
12240	0016
12245	0017
12250	0019
12255	0018
12260	0031

12265	0021	20475
12270	0020	28595
12275	0011	36715
12280	0024	44835
12285	0039	
12290	0023	
12295	0022	
12300	0025	
12305	0026	
12310	0027	
12315	0028	
12320	0030	
12325	0029	
12330	0038	
12335	0035	
12340	0033	
12345	0034	
12350	0037	
12355	0036	
12365	PHI	
20485	PSI	
28605	PSIP	
36725	SIGPR	
44840	IA	
44845	ID	
44850	IJM	
44855	MIKE	
44860	MAC	
44870	PR	
44880	PII	
44890	ETA	
44895	IJL	
44900	ID	
44905	IC	
44910	IZ	
44915	JAY	
44920	IE	

44925	IJN
44930	IG
44935	MIKE1
44940	MIKE2
44945	KJ
44950	I
44960	HRHO
44965	NN
44970	IQ
44980	P
44990	THETA
45000	HOE
45010	HOESQ
45020	H
45030	HH
45040	S
45050	C
45060	SS
45070	CC
45080	SC
45090	HO2
45100	A
45110	D
45120	DONEP
45130	DONEM
45140	ETASC
45150	Q
45160	X1
45170	X2
45180	X3
45190	X4
45200	X5
45210	X6
45220	X7
45230	X8
45240	X9
45250	CONH

45255	M1
45260	MM
45270	CONST
45275	KK
45280	II
45285	M2
45290	N
45300	X10
45310	X11
45320	X12
45325	JJ
45330	M3
45335	M4

Program 5.--Calculation of Normal Stresses on Boundaries of a Hemispherical End Cap.

This program calculates values of normal stress on the boundaries of hemispherical regions according to Eqs.(A-15) and (A-16). As the program is now written it is specialized for the generating quarter ring area shown in Fig. 24. Thus $\eta = \pi/30$ in the equations (A-15) and (A-16). However this program could be easily modified to a more general form.

Definitions of input parameters follow:

- L Number identifying first unknown in the output of program B-2 (lowest row No. in the matrix of coefficients for φ and ψ).
- N Number identifying last unknown in output of program B-2.
- K Integer multiplying η such that $\Theta = K\eta$, see Fig. 32.
- JJ=2 Defines location in terms of K of initial point at which stress is calculated on inner boundary.
- IK=13 Defines location in terms of K of final point at which stress is calculated on inner boundary.
- MM Subscript of φ at IK from map of region. (See Fig. 32).
- MK Subscript of φ at initial point at which stress is calculated on the outer boundary.
- NK Subscript of φ at final point at which stress is calculated on the outer boundary
- II=L+70=71 Subscript of φ at initial point on inner boundary for the example problem shown in Fig. 24. This number should be changed for a different numbering of the initial point. This requires a modification of the program, i.e., number of 70 must be changed.
- KK=N-78=82 Subscript of φ at point preceding final point on inner boundary at which stress is calculated. Special case for Fig. 3-5, number of 78 must be changed for different problem.

Input--Fixed Point

1. First Card

Cols. 1-5	L
Cols. 6-10	N
Cols. 11-15	K
Cols. 16-20	JJ
Cols. 21-25	IK
Cols. 26-30	MM
Cols. 31-35	MK
Cols. 36-40	NK

2. Data Cards

Output of Program B-2, all preliminary cards removed.

3. Output

Values of Sigma Theta = σ_{θ} , Sigma Nor = σ_R , Sigma Tan = σ_{θ} , versus K. Note $K\eta = \theta$.

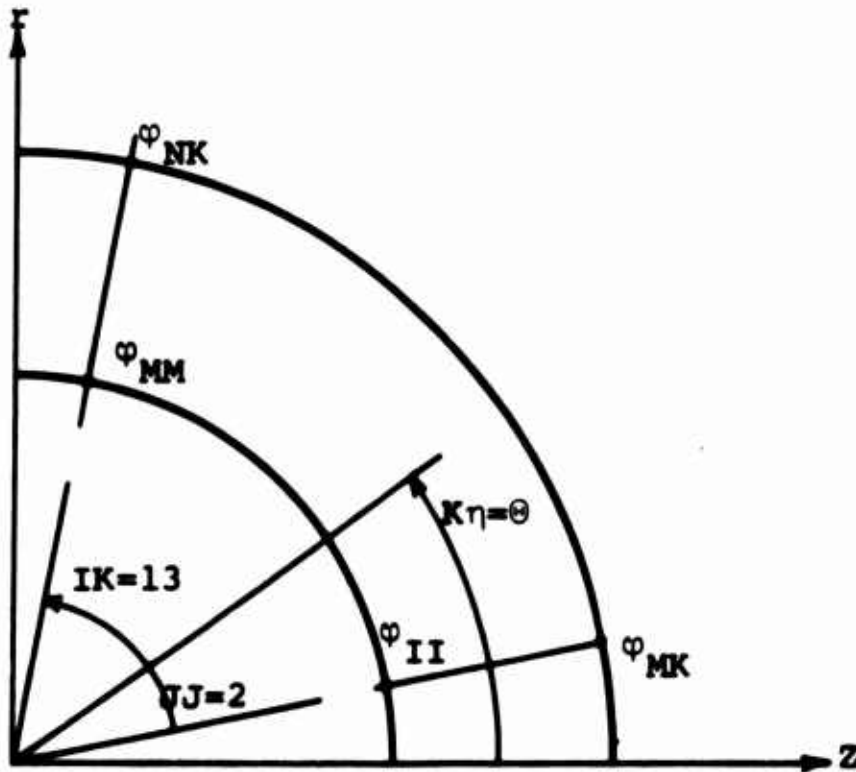
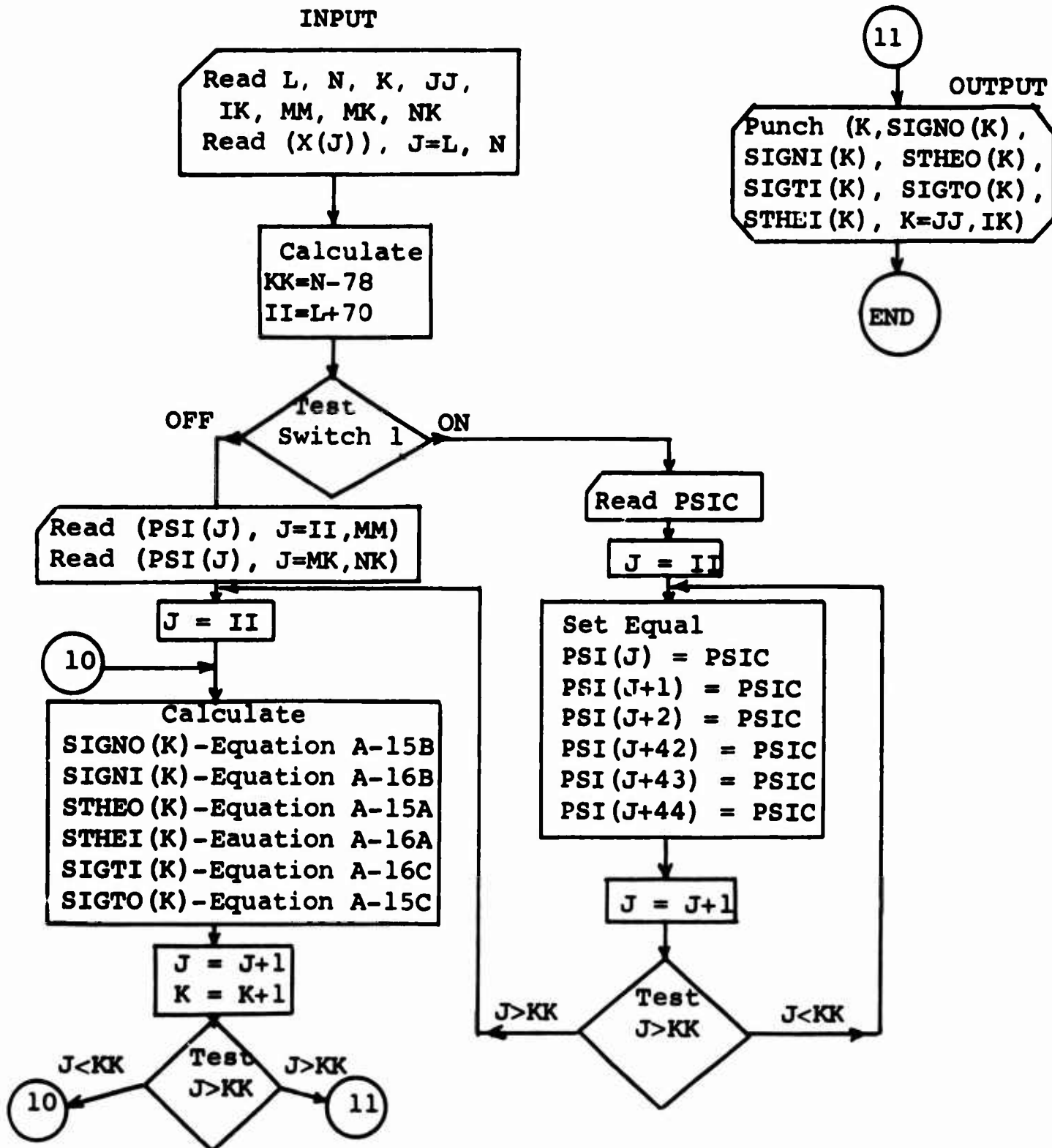


Figure 32. Notation for program 5.

**Calculation of Normal Stresses
on Boundaries of a Hemispherical End-Cap**



```

DIMENSION STHEI(13), SIGNI(13), SIGTI(13), PSI(127)
17 READ17,L,M,K,JJ,IK,MM,MK,NK
   FORMAT(8I5)
100 READ100,(X(J),J=L,N)
   FORMAT(14(1X,E13.0,3X))
   NK=N-78
   I1=L+70
   Z=3.1415927*.3
   E=3.1415927/5.
   IF(SENSE SWITCH 1)4,7
4   READ5,PSIC
5   FORMAT(10F8.3)
   DO14J=11,NK
   PSI(J)=PSIC
   PS14J+1)=PSIC
   PS1(J+2)=PSIC
   PS1(J+42)=PSIC
   PS1(J+43)=PSIC
   PS1(J+44)=PSIC
14  GO TO 12
7   READ5,(PSI(J),J=11,MM)
   READ5,(PSI(J),J=MM,NK)
12  DO10J=11,NK
   PK=K
   B=COSF(PK*3.1415927/30.)
   A=SINF(PK*3.1415927/30.)
   C=A*A
   D=A**3
123 G=8**8
   H=8**3
   AK=-X(J)+X(J+2)
   BK=4.*X(J+15)-X(J+29)
   CK=-3.*A+1./A
   DK=2./(1.5*A)
   ZK=B*C*AK/E
141 RK=PSI(J+2)-PSI(J)
   UK=(-3.*A-A/3.)*PSI(J+1)

```

```

TK=B*RK/E
SK=X(J+1)*(-3.*D-.25*A)
YK=A*(4.*X(J+57)-X(J+71))
XK=D*BK
214 RC=H*AK/E
YC=X(J+1)*(-3.*G*A-G*.25/A)
XC=(3.*A-G/(3.*A))*PSI(J+1)
SC=G*A*BK
RB=X(J+44)-X(J+42)
SB=X(J+15)-4.*X(J+29)
182 TB=3.*A+1./(1.5*A)
AB=2./(2.25*A)*PSI(J+43)
RD=8*C*RB/Z
SD=D*SB
TD=A*(X(J+57)-4.*X(J+71))
XD=X(J+43)*(3.*D-A/6.)
ZD=PSI(J+44)-PSI(J+42)
YD=-B/Z*ZD
UD=(3.*A-A/4.5)*PSI(J+43)
85 RG=M/Z*RB
ZG=PSI(J+43)*(-3.*A-G/(4.5*A))
SG=G*A*SR
XG=X(J+43)*(3.*G*A-G/(6.*A))
SIGNO(K)=1./(18.*A)*(RD+SD+TD+XD+YD+UD)
STHEO(K)=.25/(18.*A)*(B/Z*RB+A*SB+X(J+43)*TB+AB)
SIGNI(K)=1./(12.*A)*(ZK+YK+XK+SK+TK+UK)
SIGTI(K)=1./(12.*A)*(RC+SC-YK+YC+TK+XC)
SIGTO(K)=1./(18.*A)*(RG+SG+XG-TD-YD+ZG)
STHEI(K)=.25/(12.*A)*(B*AK/E+A*BK+X(J+1)*CK+DK*PSI(J+1))
K=K+1
10 CONTINUE
PUNCH21
21 FORMAT(28X,15HINSIDE BOUNDARY)
PUNCH20,(K,STHEI(K),SIGNI(K),SIGTI(K),K=JJ,IK)
20 FORMAT(/4X,1HK,9X,11HSIGMA THETA,11X,9HSIGMA NOM,11X,9HSIGMA TAN/(
115,3F20.5))
PUNCH22

```

22 FORMAT(1/27X,16HOUTSIDE BOUNDARY)
 PUNCH20.(K,STHEO(K),SIGNO(K),SIGTO(K),K=JJ,IK)
 STOP
 END
 DIMENSION STHEO(13),SIGNO(13),SIGTO(13),X(160)